A Theoretical study of Elastic Electron Positronium Scattering and Photo-absorption by the Positronium Negative Ion.

A thesis submitted for the degree of

Doctor of Philosophy

in

the University of London

Sandra June Ward, B.Sc. (London)

October 1986

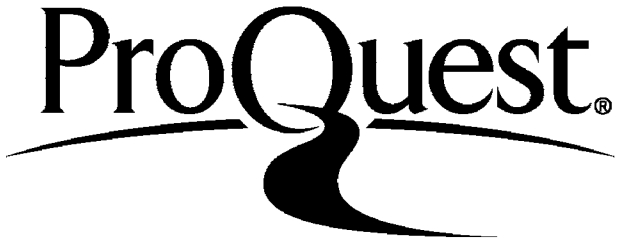

Abstract

This thesis describes both a theoretical study of low-energy electron scattering by positronium (Ps), below the n=2 threshold and the photodetachment of the positronium negative ion (Ps^-.)

$$e^{\pm} + Ps(1s) \rightarrow e^{\pm} + Ps(1s)$$

$$Ps^- + h\nu \rightarrow Ps(1s) + e^-$$

The importance of the photodetachment of Ps^- was recognized by Mills (in 1981) since it can be used as a possible mechanism of producing a slow monoenergetic Ps beam.

Accurate $^{1,3}S$ and $^{1,3}P$ phase shifts were evaluated by the Kohn and inverse Kohn variational methods in which very flexible trial functions were used. Higher order phase shifts were determined by the static exchange and adiabatic exchange models in order to obtain the total elastic, momentum-transfer, ortho-para conversion and elastic differential cross sections for the scattering process. In the variational calculation, the lowest ^1S, ^1P and the two lowest ^3P resonances, which lie just below the n=2 threshold were revealed. The scattering results for e^--Ps were compared with those for e^--H.

Using a variational bound-state wave function, which contained 95 linear and 2 non-linear parameters, and a p-wave continuum function, which contained 220-linear and 3 non-linear parameters, the photodetachment cross section was calculated in both the length and velocity formulation. The agreement between the length and velocity forms was to better than 1.6% for $\lambda \leq 27.5 \times 10^3 \mathring{A}$, and the sum-rule was satisfied to within 2%. By systematically improving both the bound-state and continuum wave functions separately, the reliability of the cross section was determined. A comparison of the photodetachment of Ps^- was made with the corresponding atomic ion, H^-.

Acknowlegments.

I am deeply grateful to Professor M.R.C. McDowell for suggesting this project and for his continued guidance and support.

I am indebted to Dr. J.W. Humberston for the tremendous help which he has given me both on the variational calculation and at the time of writing this thesis.

I am also grateful to Dr. K.T. Taylor for his interest in this work and for his advice. This work has greatly benefited from useful discussions with Dr. A. Bhatia, Dr. R.J. Drachman, Professor C.H. Greene and Dr. Y.K. Ho. I would like to express my appreciation to Professor P.G. Burke, for bringing to my attention at the start of this project, a corresponding problem in nuclear physics. Thanks are also due to Professor G. Ferrante for a brief stay at the University of Palermo.

I appreciate the discussions which I have had with Dr. O'Mahony and Dr. C. Whelan, here at Royal Holloway and Bedford New College, and with the experimental positron group at University College London.

The use of the London university computer facilities and the award of a research studentship from the Science Engineering Research Council is gratefully acknowledged.

"Our fears for today, our worries about tomorrow, or where we are, high above the sky, or in the deepest ocean nothing will ever be able to separate us from the love of God demonstrated by our Lord Jesus Christ when he died for us."

Romans 8:38b

Contents

Page No.

Chapter 1

Introduction

The subject of positron interactions with matter has grown extensively, both experimentally and theoretically, over the last fifteen years. One of the main reasons for this is due to the development of slow monoenergetic positron beams. It was found (Costello, et al 1972) that fast positrons could be moderated by passing them through a suitable foil, leading to the re-emission of positrons of energies about (1.0 ± 0.5)eV. The fast positrons are obtained from either a radioactive source, a favourite being ^{22}Na, or from an accelerator (Griffith and Heyland ,1978).

Various types of materials have been investigated as possible moderators in order to increase the conversion efficiency: the number of slow positrons to the number of original fast positrons. Coleman et al (1973) obtained an efficiency of 1 in 10^6 by using a gold lined cylinder as moderator with ^{22}Na as the positron source. A suitable moderator was obtained by Canter et al (1972) by coating a gold lined cylinder with a fine layer of MgO which had a conversion efficiency of 1 in 10^5.

A lot of research is still being undertaken to increase the moderator efficiency, the activity of the source and to improve the beam optics, in the hope of achieving a greater intensity, slow monoenergetic positron beam. At the present time, the best moderators in common use are the clean single crystals of copper and nickel. Gullikson, working with Mills, is examining the possibility of using the solid rare gases as moderators. In 1986, Gullikson (1986) reported a conversion efficiency of 0.56% for solid Ne on ^{22}Na. Beling et al (1986) is investigating the possibility of using electric fields to increase the efficiency of a moderator. Using a silicon crystal and a ^{22}Na source, they hope to achieve efficiency of 10%. Further advances in the subject of positron collisions is expected over the next few years with the advent of the new intense positron beam at Brookhaven (Lynn et al, 1986). This beam has an energy of about 1.0eV, an energy spread of 75meV and at present, the intensity is $4 \times 10^7 positrons\ s^{-1}$. It is expected that the intensity of this beam will be increased by at least an order of magnitude, for instance by making use of the brightness enhancement concept described by Mills (1980). A single crystal of ^{64}Cu and ^{63}Cu is used as the positron source and self-moderator. This crystal is

formed by radiating a very pure copper pellet in a high flux reactor and evaporating the pellet onto a W(110) crystal substrate where Cu(111) is grown epitaxially. The conversion efficiency is of the order 1 in 10^4. A more complete discussion on the development of slow positron beams, together with their application, can be found in articles by Massey (1976, 82), Griffith and Heyland (1978), Mills (1983) and Charlton (1985).

Theoretical development in the study of positron collisions have been stimulated by the experiments made possible by the availability of slow intense positron beams. Positron collisions with atoms and molecules have recently been reviewed by Humberston (1986), Ghosh et et al.(1982), Humberston (1979) and earlier by Fraser (1968), Bransden (1969), Massey (1971) and Drachman (1972, 1982a). For low energy positron scattering from hydrogen and from helium the variational approach has been used (see Humberston (1986) and references within), and for scattering from the noble gases, the polarized orbital approach seems successful (McEachran and Stauffer, 1986). Experimentally and theoretically, positron scattering by the alkali-atoms seems to be very interesting, and recently Stein et al. (1985) reported some results on positron-potassium scattering.

The significance of positrons in astrophysics has been discussed by Massey (1982), Drachman (1982a,b), Burns et al (1983), McKinley (1985), Leventhal et al (1985), Leventhal and MacCallum (1986), Leventhal and Brown (1986) and McKinley (1986). In the laboratory, positrons have been used to study surfaces and the bulk properties of the solid. The basic method for doing this consists in measuring the shift in energy or angle of the gamma rays produced by positron annihilation (with respect to those produced in the e^- - e^+ Centre of Mass frame) or from life-time studies (Heyland et al, 1982). The role of positrons in surface studies is discussed by Nieminen (1984).

Although positron collisions in many respects are similar to electron- collisions, different processes can occur. Exchange is absent in positron-collision, but the possibility of forming positronium exists. (Positronium (Ps) is the bound-state of an electron and positron). With e^+-scattering, annihilation may occur. As discussed by Massey (1982), in any perturbation series, for instance that obtained for the scattering amplitude or interative potential, the odd terms must differ in sign

between electrons and positrons due to the difference in sign of their charge. Thus, by studying both positron and electron-collisions from the same target atom or molecule, much more information can be extracted then if just one at the projection was used.

With the arrival of more intense positron beams, it is hoped that Ps beams can be produced which will be monoenergetic and sufficiently intense as to make it worthwhile to perform Ps-diffraction experiments to study surfaces. Ps is a useful probe since it is mainly sensitive to the outer surface layers (Canter, 1984), and thus has a similar role to that of He. Ps scattering by atoms is of interest in view of the e^--Ps, Ps-H resonances reported by Drachman (1982a) and from the fact that Ps^- is a purely leptonic system and this can be used in tests of quantum electrodynamics. A comparison of elastic and inelastic cross-sections for Ps-scattering by a gas will be useful in the interpretation of data obtained from Ps-formation experiments. Also a knowledge of Ps break-up cross-section σ_b, for the process,

$$Ps + A \rightarrow e^+ + e^- + A$$

is valuable in the understanding of e^- slowing down fluorescence. Recently, intense, energetic, monoenergetic Ps beams have been produced by:

(a) the beam-foil technique demonstrated by Mills and Crane (1985).

(b) by forming Ps from scattering e^+'s of an Al(110) surface at glancing angles as low as 6° with respect to the surface (Gidley et al, 1986).

(c) by the charge-exchange process where positrons are transmitted through a gas cell of a low-density gas such as He, or Ar (Brown 1986, Berko et al. 1986 and Larrichia et al. 1986).

Another possible mechanism for producing a monoenergetic beam of Ps of controllable energy has been suggested by Mills (1981a), namely producing a positronium negative ion (Ps^-), accelerating it to the desired energy, and then photodetaching the electron. (The positronium negative ion is the bound-state of two electrons and a positron). The aim of this present work was to determine theoretically the photodetachment cross-section of Ps^- which would be useful as a guide to the experimentalists. We have restricted our attention to low-energy photons, so

that the residual Ps-atom will be left in its ground-state, and we have treated the problem non-relativistically.

Although Ps^- was theoretically predicted in 1946 by Wheeler (1946), it was not experimentally verified until 1981 by Mills (1981a). The possible role Ps^- play in astrophysics has been described by Sivaram and Krishan (1982). Over the last twenty years there has been much interest to determine the properties of this ion which is purely leptonic system. Ps^- has some properties similar to the hydrogen negative ion H^-. Both ions consist of two electrons and a positive particle of charge +e. Like H^-, Ps^- has only one bound-state. The best value for the binding energy of Ps^- was determined by Bhatia and Drachman (1983), who obtained a value of 0.024010113 Ryd which is approximately equal to that for H^-, scaled by the reduced mass of positronium which is one half. When fine structure effects are neglected, the energy levels of Ps correspond to those of H, scaled by one-half. Both Ps and H excited states are degenerate. Some of the resonance structure which is known to exist for H^- due to the ns-np dipole coupling of the degenerate states, has been theoretically predicted for Ps^- (Ho 1979,84, Botero and Greene 1985,6 Ward et al 1985,6).

However, some features which occur in H^- are absent in Ps^- and vice versa. For instance, the calculation by Mills (1981b) and Bhatia and Drachman (1983) show that the $^3P^e$ metastable state which exist in H^- probably does not occur in Ps^-. One significant difference between Ps^- and H^- is that annihilation of the positron in Ps^- can occur. A very fine experiment was performed by Mills (1983) to measure the decay rate of Ps^-, giving a value of $(2.09 \pm 0.09)ns^{-1}$. The decay rate has been very accurately determined by Bhatia and Drachman (1983) and their value agrees with experiment. Independent calculations have been performed by Ho (1983) and Ferrante (1968) to determine the two-photon annihilation rate and angular correlation function. Ho (1985) has also evaluated two-photon annihilation rates for some $^1S^e$ doubly excited states of Ps^-.

The photodetachment cross-section, like the decay rate Γ, is very sensitive to the details of the wave function describing the Ps^- system. To evaluate this cross-section, both the bound-state and p-wave component of the continuum wave function of Ps^- is required. This latter is equivalent to the elastic scattering of

low-energy p-wave electrons by positronium, below the n=2 threshold. Since e^--Ps scattering is of interest in itself, we have evaluated other partial waves in order to determine various cross-sections: momentum-transfer, total elastic, ortho-para conversion and elastic differential cross-sections. Measurement of e^+ - Ps and e^- - Ps scattering cross-sections can be used to test charge conjugation in the leptonic system. These cross-sections will also be valuable in view of the Ps-formation experiments where positrons are passed through a gas cell (Larrichia et al, 1986).

At the start of this present work, there were no reliable calculations available on the continuum properties of Ps^-, or its photodetachment. However, the corresponding system, e^--H, has been extensively studied; H^- ions being the dominant source of opacity in the solar atmospheres (Wildt, 1939). Therefore, we investigated those methods which proved successful for e^--H scattering, below the n=2 threshold, and applied them to the e^--Ps system, with suitable modifications. Great emphasis has been placed in this thesis in comparing the results of e^-- Ps with those obtained for e^--H.

Outline of Thesis.

In chapter 2, an investigation is made of the suitability of the static- exchange (S.E.) and adiabatic-exchange (A.E.) methods to electron scattering by hydrogen, below the n=2 threshold. The static-exchange method was then applied to the problem of e^--Ps scattering below the n=2 threshold. For the e^--Ps system, it was essential to work in the centre of mass frame. In order to determine the reliability of the S.E. results, it was felt necessary to perform an accurate variational calculation for the s- and p-waves.

The s-wave calculation which was performed using the Kohn and inverse Kohn variational methods is described in chapter 3. Our best s-wave trial function contained 3 non-linear and 70 linear parameters for the singlet, 50 linear parameters for the triplet. This wave function was very flexible; the interelectronic separation r_{12} was included explicitly by terms of the form $r_{12}^p e^{-\gamma r_{12}}$ (where p is an integer) and we were able to locate the lowest $^1S^e$ resonance. Our values for the resonance parameters agree well with those determined by Ho(1979,84) and Botero and Greene (1985). Singlet and triplet s-wave phase shifts and scattering lengths for the e^--

Ps system are given for energies below the 1^{st} excitation level of Ps. Using the short-range correlation part of the full wave function we predicted a value for the binding energy of Ps^- which agreed to within 0.004% of the best value to date (Bhatia and Drachman, 1983). This bound-state wave function was used in our photodetachment calculation.

In chapter 4, a description is given of the p-wave variational wave function which contained 3 non-linear and 220 linear parameters. The singlet and triplet phase shifts were determined by using the Kohn and inverse Kohn variational methods. With this wave function, we were able to detect possible $^{1,3}P$ resonances. A comparison is made of the resonance parameters for the lowest ^1P resonance with that obtained by Botero and Greene (1986). The singlet p-wave function, with suitable normalization, was used in the evaluation of the photodetachment cross-section. A discussion is also given in this chapter of possible long-range terms which can be added to the s- and p-wave trial functions to improve convergence with respect to the number of parameters at very low energies and at energies close to the n= 2 threshold.

A polarization term, with suitable cut-off function, was added to the static-exchange integro-differential equation for the radial wave function, in order to make some allowance for the distortion of the positronium atom. This method, known as the adiabatic-exchange approximation, is described in chapter 5, where the results are presented. The singlet and triplet phase shifts obtained in the various models: S.E., A.E. and variational, are compared. A detail comparison is made of the e^- -Ps results with the results of the e^- -H system. By using the l=0,1 phase shifts determined by the variational method, higher order phase shifts determined by the A.E. method and then by the Born-polarization term, we were able to calculate the various cross-sections for e^--Ps scattering below the n=2 threshold, namely: total elastic, momentum-transfer, ortho-para conversion and elastic differential cross-sections.

In chapter 6, the photodetachment cross-section of Ps^- evaluated in both the length and velocity forms is given. The bound-state wave function contained 2 non-linear and 95 linear parameters, and the p-wave function contained 3 non-linear and 220 linear parameters. As a check, the sum-rule S_{-1} was calculated. Finally,

in chapter 7, a summary is given of this thesis, the conclusions reached and the feasibility of experimental work in this area.

Chapter 2

Static-exchange method applied to e^--H and e^--Ps scattering

2.1 Introduction

The principle aim of this present work was to determine the photo detachment cross section of Ps^- which requires a knowledge of the initial bound state wave function and the p-wave component of the continuum wave function. This later is equivalent to the wave function describing the scattering of p-wave slow electrons by positronium. However, since the scattering process is of interest in itself, we have also evaluated the other partial waves in order to determine the total and differential cross sections for scattering below the n=2 threshold of positronium. We have treated this problem non-relativistically which means that within the approximation e^+-Ps scattering is identical to e^--Ps.

Experiments to measure various cross sections for electron and positron scattering by positronium would be of fundamental importance since they could be used to provide a test of charge-conjugation in the leptonic systems (e^+, e^-, e^-) or (e^-, e^+, e^+). If σ_+ is the cross section for positron impact on Ps (for any process) and σ_- is that for electron impact, then if charge conjugation holds

$$\eta = \sigma_+ - \sigma_- = 0.$$

An actual experiment will set a bound and our predicted theoretical cross sections should be of use as a guide to the experimentalists. Also, with the recent interest in positron scattering experiments to form positronium, it is advisable to know the cross section for e^+-Ps scattering since scattering by any stray positrons might have serious consequence on the results.

The static-exchange method provides a simple description of the scattering problem and has the advantage over many other methods in that all partial waves can be readily evaluated. Allowance for the polarization of the target was made by using the approximation in which the polarization potential, with suitable cut-off, is included in the integro- differential equation derived from the static-exchange

method. As we are considering scattering below the n=2 threshold, only a few partial waves ($l = 0 \rightarrow 4$) are important, the s and p-waves being the dominant contribution to the cross sections. The s and p-waves were later determined very accurately from a variational calculation. Thus, by using the $l = 0, 1$ phase shifts calculated by the variational method, the $l = 2 - 5$ phaseshifts evaluated by either the static- exchange or adiabatic-exchange methods and the higher-order phase-shift by the Born-polarization term, we were able to calculate accurate total elastic cross sections and (less accurately) elastic differential cross sections in the energy range from zero to 5.102eV.

Our main motivation in applying the static-exchange and adiabatic- exchange methods to the problem of scattering of low-energy electrons by positronium below the n=2 threshold was that these methods proved to be successful in the corresponding problem e^--H scattering. The computer program for the e^--H system (McDowell et al. 1973,4) was readily available for us to use. As explained in the introduction chapter, the e^--Ps and e^--H systems are very similar; both consist of two electrons and a positive particle of charge +e. Each system has only one bound state, the Ps^- ion is more diffuse than the H^- and is less tightly bound.

This chapter begins with a description of the static-exchange and adiabatic-exchange methods (§2.2). These methods are then applied to the e^--H problem, and in §(2.3) the results for this system are discussed. In §(2.4) the static-exchange treatment is applied to the e^--Ps system and in §(2.5) details of the static-exchange analysis are given. The tests performed to check the analysis and numerical work are explained in §2.6. In §2.7, the results for the e^--Ps system are presented, discussed and compared to the results of the e^--H system. A brief discussion is given of the need to allow for the polarization of the target positronium atom, but this is discussed more fully in chapter 5. The conclusions are presented in §2.8.

The calculations were performed on the R.H.B.N.C VAX system for the e^--H system and for the $l = 0, 1$ phase shifts of the e^--Ps system. Higher order phase-shifts for the e^--Ps system were calculated on the ULCC CRAY1s.

2.2 The static-exchange and adiabatic-exchange methods and their application to e^--H scattering.

The wave function to describe the scattering of an electron from a target must asymptotically be equal to the product of the electron wave function (with respect to the target) and the target wave function. In accordance with the Pauli exclusion principle, the wave function must be symmetric with respect to exchange of any two electrons for the singlet and anti-symmetrical for the triplet state. For the scattering of low-energy electrons from a hydrogenic target, where the nucleus is assumed to be 'infinitively' heavy, a very simple wave function which satisfies the above two requirements is of the form:

$$\Psi^{\pm}(\mathbf{r}_1,\mathbf{r}_2) \;=\; 2^{-\frac{1}{2}}\left\{\phi_0(\mathbf{r}_1)F^{\pm}(\mathbf{r}_2) \pm \phi_0(\mathbf{r}_2)F^{\pm}(\mathbf{r}_1)\right\} \qquad (2.1)$$

where $\mathbf{r}_1, \mathbf{r}_2$ are the positron vectors of the two electrons with respect to the nucleus which is assumed to be at rest. The (+) sign refers to the singlet, the (-) for the triplet. In this wave function, $\phi_0(\mathbf{r}_1)$ is the wave function of the ground state target atom and $F^{\pm}(\mathbf{r}_2)$ is the wave function of the free electron. This wave function eqn.(2.1) is known as the static-exchange wave function. It is of the same form as the Hartree-Fock wave functions for bound states. The static-exchange wave function does not allow for the polarization of the target and has no explicit terms depending on $|\mathbf{r}_1 - \mathbf{r}_2|$ describing electron correlation. Both these effects are important at very low energies. Although this wave function only includes the elastic scattering channel (the target atom being in the ground state) and should strictly be used only for scattering below the first inelastic threshold, it has been fairly successful in describing elastic scattering at energies as high as 200eV.

It is important to state that for the scattering of electrons from a hydrogenic target, the 'infinitely' heavy nucleus approximation has been used, so that the centre of mass and laboratory frames are considered to coincide.

The free electron wave function $F^{\pm}(\mathbf{r})$ is determined from the condition that the projection of the Schrodinger equation $((H-E)\Psi)$ onto the ground state wave function of the target must vanish. For simplicity in deriving the equation for the

radial wave function, the target atom is assumed to be hydrogen. Thus,

$$\int \phi_0^*(\mathrm{r}_2)[H - E]\Psi^{\pm}(\mathrm{r}_1, \mathrm{r}_2)\, d\mathrm{r}_2 = 0 \tag{2.2}$$

$$\int \phi_0^* \left[-\frac{1}{2}\nabla_{r_1}^2 - \frac{1}{2}\nabla_{r_2}^2 - \frac{1}{r_1} - \frac{1}{r_2} + \frac{1}{|r_1 - r_2|} - E_{tot} \right] \times \left\{ \phi_0(r_1) F^{\pm}(r_2) \pm \phi_0(r_2) F^{\pm}(r_1) \right\} dr_2 = 0 \tag{2.3}$$

where $E_{tot} = E_1 + \frac{k^2}{2}$ $a.u$, E_1 being the ground state energy of the hydrogen atom and $\frac{k^2}{2}$ the energy of the scattering electron. We note that since $F^{\pm}(\mathrm{r})$ is determined from equ.(2.3), the static exchange wave function is a variational wave function, although very simple. This means that the phase shifts should provide a 'bound' on the true phase shifts, see next chapter where there is a discussion on minimum principles. By using the Schroedinger equation for the ground-state hydrogen atom, namely:

$$\left[-\frac{1}{2}\nabla_{r_1}^2 - \frac{1}{r_1} \right] \phi_0(r_1) = E_1\, \phi_0(r_1) \tag{2.4}$$

this equation reduces to:

$$\left(\nabla_1^2 + k^2\right) F^{\pm}(r_1) = 2\, V_{1s,1s}(r_1)\, F^{\pm}(r_1) \pm 2 \int K(r_1, r_2)\, F^{\pm}(r_2)\, dr_2 \tag{2.5}$$

where $V_{1s,1s}(\mathrm{r}_1)$ is the direct-potential and $K(\mathrm{r}_1, \mathrm{r}_2)$ is the exchange potential which is non-local, (Bransden and Joachain, 1983, p.505, Bransden, 1983. p,202). The

direct potential is given by:

$$V_{1s,1s}(\underline{r}_1) = \int \phi_0^* \left(-\frac{1}{r_1} + \frac{1}{|\underline{r}_1 - \underline{r}_2|} \right) \phi_0(\underline{r}_2)\, d\underline{r}_2$$

$$= -\left(1 + \frac{1}{r_1}\right) e^{-2r_1} \qquad (2.6)$$

and the exchange potential by

$$K(\underline{r}_1, \underline{r}_2) = \phi_0^*(\underline{r}_1)\phi_0(\underline{r}_2)\left[\frac{1}{|\underline{r}_1 - \underline{r}_2|} - (E_{tot} - 2E_1) \right] \qquad (2.7)$$

Expanding $F^{\pm}(\mathbf{r})$ in partial waves, in the usual way,

$$F^{\pm}(\underline{r}) = \sum_{l=0}^{\infty} a_l^{\pm} \frac{u_l^{\pm}(k,r)}{r} P_l(\cos\theta) \qquad (2.8)$$

where $a_l^{\pm}$ is a normalization constant, and the radial wave function $u_l^{\pm}(k,r)$ satisfies the boundary conditions

$$u_l^{\pm}(k,0) = 0 \qquad (2.9)$$

$$u_l^{\pm}(k,r) \underset{r\to\infty}{\sim} k^{-1/2} \sin\left(kr - \frac{1}{2}l\pi + \delta_l^{\pm}\right)$$

yields the integro differential equation

$$\left(\frac{d^2}{dr_1^2} - \frac{l(l+1)}{r_1^2} + k^2 \right) u_l^{\pm}(k,r_1) = 2V_{1s,1s}(r_1)\, u_l^{\pm}(k,r_1)$$

$$\pm 2 \int_0^{\infty} K_l(r_1, r_2)\, u_l^{\pm}(k,r_2)\, dr_2 \qquad (2.10)$$

where

$$K_l(r_1, r_2) = \frac{4 r_1 r_2 e^{-(r_1 + r_2)}}{(2l+1)} \left[\frac{r_<^l}{r_>^{l+1}} - \delta_{l0}(E_{tot} - 2E_1) \right] \qquad (2.11)$$

and $r_<, r_>$ being the lesser and greater of r_1, r_2 respectively.

Temkin and Lamkin (1961), later modified by Drachman and Temkin (1972), have obtained a polarization potential with suitable cut-off terms to protect the region near the origin. This polarization potential, which is attractive, is added to the integro differential equation for $u_l^{\pm}(k,r)$, equation (2.10), to obtain what is known as the adiabatic-exchange approximation;

$$\left(\frac{d^2}{dr_1^2} - \frac{l(l+1)}{r_1^2} + k^2\right) U_l^{\pm}(k,r) = 2\,V_{1s,1s}(r_1)\,U_l^{\pm}(k,r_1) + 2\,V_{pol}(r_1)\,U_l^{\pm}(k,r_1) \pm 2\int_0^{\infty} K_l(r_1,r_2)\,U_l^{\pm}(k,r_2)\,dr_2 \qquad (2.12a)$$

where

$$V_{pol}(r) = -\frac{9}{4r^4}\left[1 - e^{-2r}\left(1+2r+2r^2+\frac{4}{3}r^3+\frac{2}{3}r^4 + \frac{4}{27}r^5\right)\right]$$

$$= -\frac{\beta(r)}{2r^4} \qquad (2.12b)$$

In the adiabatic-exchange approximation, the polarization is neglected for the exchange terms, and this is where this method differs from the polarized orbital approach (Bransden, 1983, pg.218).

The method of solution is due to Marriott and Percival (Marriott, 1958), see for example Burke et al (1983), and is described fully in the papers by McDowell et al (1973,4). I shall describe it here only very briefly for completness, but the reader should refer to the papers by McDowell et al, loc.cit.

The integro-differential equation (2.12) is converted into a pair of coupled

differential equation by making use of the Hartree-function $Y_l(k,r)$,

$$\frac{d^2 U_l^{\pm}(k,r)}{dr^2} = f_l(k,r) U_l^{\pm}(k,r) + g_l(r) Y_l(k,r) + \delta_{l,0} I(k,r) \qquad (2.13)$$

$$\frac{d^2 Y_l(k,r)}{dr^2} = \frac{l(l+1)}{r^2} Y_l(k,r) - (2l+1) e^{-r} U_l^{\pm}(k,r)$$

where

$$f_l(k,r) = -k^2 - 2\left(1 + \frac{1}{r}\right) e^{-2r} + \frac{l(l+1)}{r^2} - \frac{\beta(r)}{r^4}$$

$$g_l(r) = \frac{(-1)^{s+1} 8 e^{-r}}{(2l+1)} \qquad (2.14)$$

$$I(k,r) = -(-1)^{s+1} 4r e^{-r}(1+k^2) \int_0^{\infty} e^{-x} x U_0^{\pm}(k,x)\, dx,$$

and s = 0(1) refers to the singlet (triplet) state. These equations (2.13) are homogenous for $l \neq 0$ and the boundary conditions are:

$$U_l^{\pm}(k,r) \longrightarrow 0, \qquad Y_l(k,r) \underset{r \to 0}{\to} 0 \qquad (2.15)$$

$$U_l^{\pm}(k,r) \underset{r \to \infty}{\longrightarrow} k^{-1/2} \sin\left(kr - \frac{1}{2}l\pi + \delta_l^{\pm}\right), \quad Y_l(k,r) \underset{r \to \infty}{\to} 0$$

A starting solution (power series r) is used to generate the wave function near the origin and to ensure that it has the correct form. By using Numerov's method (Burke et al 1983, pg 60), the coupled differential equations are replaced by finite difference equations. The radial wave function at further distances from the origin is generated by knowing the wave function in the vicinity of the origin and by making use of these finite difference equations. This procedure of generating

the radial wave function is continued until the asymptotic region is reached and the solution is of the form:

$$U_l^{\pm}(k,r) \underset{r\to\infty}{\sim} A \sin(kr - \tfrac{1}{2}l\pi + \delta_l^{\pm}) \qquad (2.16)$$

where A is constant and was determined by normalizing the wave function according to the asymptotic boundary condition equation (2.15).

The mesh used in the finite difference equations was chosen so that it is much finer near the origin then for large values of r. This was done by doubling the mesh size at radial distances r_1, r_2, r_3 given by

$$\begin{aligned} r_1 &= (N1)H, \\ r_2 &= (N2 - N1)2H + r_1, \\ r_3 &= (N3 - N2)4H + r_2 \end{aligned} \qquad (2.17a)$$

where H is the original mesh size used near the origin and $N1, N2, N3$ are integers which are input parameters for the programme. The total range R which is given by:

$$R = (N4 - N3)8H + r_3, \qquad (2.17b)$$

where $N4$ is an input parameter and R is the distance from the origin to somewhere within the asymptotic region. Up to this distance R, the Numerov procedure is used to generate the radial wavefunction, after this distance R the asymptotic form of the radial wave functions is used.

We varied R to ensure that the asympotic region was indeed reached. For a given R, we varied $N4, N3, N2, N1, H$ to check that the results, phase shifts and cross sections, were independent on the choice of mesh. From a knowledge of the phase shifts, the total elastic and differential cross sections were readily obtained. As we increased l for a given k the adiabatic-exchange results became in closer agreement to the Born-polarization results evaluated from the term.

$$tan\,\delta_l^{\pm} = \frac{\pi\alpha k^2}{(2l-1)(2l+1)(2l+3)} \qquad (2.18),$$

When this agreement, was to less than 10^{-4}, born-polarization term was used to calculate the phase-shifts from this value of l up to l_{max}, where $l \approx 300$.

2.3 Results obtained from the static- and adiabatic-exchange methods for e^--H scattering.

We found that for energies from 20 eV to 400 eV a suitable mesh for the static- exchange calculation is given by: R=46, N4 = N3 = 6000, N2 = 400, N1 = 200 and H = 0.0020. For this range R, the phase shifts and cross sections were stable to at least 4 figures as we varied the mesh parameters N4,N3,N2,N1 and H. At lower energies, a longer range R was required since the asymptotic region is determined by the value of kr. We chose for the adiabatic-exchange case, and for energies less than 20 eV the mesh given by : R = 186.00, N4 = N3 = 8000, N2 = 400, H = 0.0060, although this value of R is larger than what is really required.

In figs. 2.1, 2.2a,b, 2.3 the static- and adiabatic- exchange results are compared with the variational results of Schwartz(1961), for l=0 (fig 2.1), Armstead (1968), for l = 1 (fig 2.2a,b) and Register and Poe (1975), for l = 2 (fig. 2.3) for scattering below the n = 2 threshold.

The s-wave phase shifts, singlet and triplet, tend to π as k tends to zero. From Levinson's theorem, we would expect the singlet phase shifts to tend to π since there exists one bound state of H^- which is a singlet state. However, Levinson's theorem breaks down for the triplet state, since according to this theorem we would expect the triplet phase shift to tend to zero as k tends to zero. The failure of Levinson's theorem is due to the existence of a bounded solution of equation (2.10), which vanishes at large r but does not correspond to a bound-state (Bransden, 1983, pg.204). We see from equation (2.1) that the wave function is identically zero when

$$F^{\pm}(\mathbf{r}) = \phi_0(r)$$

and thus a solution equation (2.5) is:

$$u^{\pm}(r) = r\phi_0(r).$$

Levinson's theorem breaks down for non-local potentials.

From fig.2.1, it is clear that for the s-wave, both the static-exchange and adiabatic-exchange methods produce phase shifts which are in close agreement with the accurate variational results. The static exchange phase shifts are somewhat

lower than the variational results. However, the triplet adiabatic-exchange phase shifts are an over estimate, but the singlet are an under estimate of the variational results. Since the static exchange wave function is derived from the variational principle, see equation (2.3), the phase shifts will satisfy the 'bound' principle: they will be lower than the 'exact' true phase shifts. The accurate variational results are obtained from a very flexible wave function, and thus we would expect them to lie above the static exchange phase shifts. However, the adiabatic-exchange results do not obey the bound principle since an 'ad-hoc' polarization term has been added to the integro-differential equation.

In fig. 2.2a,b, we see that as k tends to zero, the singlet and triplet p-wave phase shifts, correctly tend to zero. Polarization effects are important in the p-wave, especially at low energies, consequently the adiabatic- exchange phase shifts are in closer agreement with the accurate variational results than are the static- exchange. Except for the static exchange singlet results, the p-wave results are positive at very low energies. Also at very low energies, where polarization is the dominant potential, the singlet and triplet results are comparable in magnitude. However, over most of the energy-range, the static- exchange phase-shifts do give reasonable agreement with the variational results and show the correct trend. This is somewhat surprizing considering the simplicity of the state-exchange wave function. As with the s-wave results, the adiabatic-exchange phase shifts are in close agreement with the variational results, although they are over-estimates.

We note from fig.2.3 that the d-wave adiabatic-exchange phase shifts are in good agreement with the variational results, especially at low energies. In this energy region, $k < 0.3a_0^{-1}$, the singlet and triplet phase shifts which are positive, are comparable in magnitude. The effect of polarization extends over a wider range of energy than is the case for the p-wave. At about $k = 0.3a_0^{-1}$, the effects of exchange become increasingly important.

We calculated the scattering lengths in the adiabatic- exchange case, by extrapolating $\tan\delta_0^{\pm}/k$ to zero k. The adiabatic exchange approximation gives electron hydrogen singlet and triplet scattering lengths $a^+ = 6.325a_0$ and $a^- = 1.675a_0$ compared with the accurate variational values of $5.965a_0$ and $1.769a_0$ respectively (Schwartz, 1961), which we regard as entirely satisfactory agreement.

Using the static exchange phase shifts and the adiabatic exchange phase shifts together with the phase shifts calculated from the Born polarization term, equation (2.15), we determined the total elastic momentum transfer and elastic differential cross section for energies up to 200eV. For the higher energies, it was obviously necessary to include more partial waves in the determination of the cross section than is the case at lower energies. The differential cross section provides a more sensitive test of the reliability of method than the total cross section. In fig. 2.4 we compare the differential cross sections at 100eV calculated by the static-exchange and adiabatic-exchange methods with the E.B.S and U.E.B.S. values (Byron et al, 1982). The adiabatic-exchange results, as opposed to the static-exchange results, shows the forward peak for low angles. Considering that the static-exchange (adiabatic-exchange) wave function only includes the n=1 channel and neglects the other channels; excitation and ionization, which are all open, the agreement is quite astonishing. Also, the static-exchange wave function makes no explicit allowance for electron correlation or distortion of the target. Although I have not shown the total elastic cross section results here, it is suffice to say that the agreement with more elaborate calculations and with experiment is good.

2.4 Static-exchange method applied to low energy e^--Ps scattering, below the n=2 threshold

We saw in the last section that for the problem of electron- hydrogen scattering, below the n=2 threshold, that the static-exchange and adiabatic-exchange results agree reasonably well with the accurate variational results for the l=0,1,2 partial waves. Therefore, it is reasonable to apply the static-exchange method to the related problem of e^--Ps scattering, below the n=2 threshold for a first attempt at this problem. A fundamental difference does, however, exist between the e^--H and e^--Ps systems, in that for e^--Ps the centre of mass does not coincide with any particle. It is therefore essential that we separate out the centre of mass motion and work in the centre of mass frame. The natural relative co-ordinates for this problem are the Jacobi co ordinates (fig. 2.5) $\mathbf{r}_2, \rho$, where $\mathbf{r}_2$ is the position of the bound electron to the positron, and ρ is the positron vector of the free electron to the centre of mass of the positronium. In this co-ordinate system, the non-relativistic relative hamiltonian is:

$$H = -\frac{1}{2\mu_{Ps^-}}\nabla_\rho^2 - \frac{1}{2\mu_{Ps}}\nabla_{\mathbf{r}_2}^2 - \frac{1}{r_1} - \frac{1}{r_2} + \frac{1}{r_3}\ a.u. \tag{2.19}$$

where $r_1 = |\rho + \frac{1}{2}\mathbf{r}_2|$, $r_3 = |\rho - \frac{1}{2}\mathbf{r}_2|$, and $\mu_{Ps^-} = \frac{2}{3}$, $\mu_{Ps} = \frac{1}{2}\ a.u.$. The Schroedinger equation for the relative motion is:

$$H\Psi^{\pm}(\mathbf{r}_2, \rho) = E\Psi^{\pm}(\mathbf{r}_2, \rho) \tag{2.20}$$

where $E = E_{Ps} + \frac{k^2}{2\mu_{Ps^-}}$, $E_{Ps} = -\frac{1}{4}a.u.$, the +(-) sign refers to the singlet (triplet) state.

As discussed in section 2.2, the static-exchange wave function is the product of the target wave function and the wave function of the free electron with respect to the target, suitably (anti-) symmetrized. In this co-ordinate system, the static-exchange wave function is written as:

$$\Psi^{\pm}(\mathbf{r}_2, \rho) = 2^{-\frac{1}{2}}\left\{\phi_{Ps}(r_2)F^{\pm}(\rho) \pm \phi_{Ps}(|\rho + \frac{1}{2}\mathbf{r}_2|)F^{\pm}(\frac{3}{4}\mathbf{r}_2 - \frac{1}{2}\rho)\right\} \tag{2.21}.$$

Although this wave function is (anti-) symmetrical with respect to the interchange of the two electrons, this is difficult to see when the wave function is written in

terms of the $(\mathbf{r}_2, \rho)$ co-ordinate system. However, this symmetry is more readily seen when the wave function is written in terms of the $(\mathbf{r}_1, \mathbf{r}_2)$ co-ordinate system (fig. 2.5), where $\mathbf{r}_i (i = 1, 2)$ are the position vectors of the two electrons with respect to the positron. In terms of the $(\mathbf{r}_1, \mathbf{r}_2)$ co-ordinate system, the wave function is re-written as:

$$\Psi^{\pm}(\mathbf{r}_1, \mathbf{r}_2) = 2^{-\frac{1}{2}} \left\{ \phi_{Ps}(r_2) F^{\pm}(\mathbf{r}_1 - \frac{1}{2}\mathbf{r}_2) \pm \phi_{Ps}(r_1) F^{\pm}(\mathbf{r}_2 - \frac{1}{2}\mathbf{r}_1) \right\} \tag{2.22}$$

and the hamiltonian is written as:

$$H = -\frac{1}{2\mu_{Ps}} \nabla^2_{\mathbf{r}_1} - \frac{1}{2\mu_{Ps}} \nabla^2_{\mathbf{r}_2} - \frac{\nabla_{\mathbf{r}_1} . \nabla_{\mathbf{r}_2}}{m} - \frac{1}{r_1} - \frac{1}{r_2} + \frac{1}{r_3} \tag{2.23}$$

where $\frac{\nabla_{\mathbf{r}_1} . \nabla_{\mathbf{r}_2}}{m}$ is the mass-polarization term (Bethe and Salpeter, 1957 pg.168; Bransden and Joachain, 1983, pg.250), and $m = 1 a.u.$, $r_3 = |\mathbf{r}_1 - \mathbf{r}_2|$. Using the $(\mathbf{r}_1, \mathbf{r}_2)$ co-ordinate system, the kinetic-energy operator is more complicated and the potential-energy term is simplier than when the $(\mathbf{r}_2, \rho)$ co-ordinate system is used.

(a) Simplified static-exchange and adiabatic-exchange methods.

As we wanted to make maximum use of the static-exchange, adiabatic- exchange analysis and computer program which we used for the e^--H system which has been thoroughly tested, in our first treatment of the e^--Ps program we simplified the true static-exchange wave function (equations (2.21), (2.22)) by making the approximation $|\mathbf{r}_1 - \frac{1}{2}\mathbf{r}_2| \approx |\mathbf{r}_1|$. This approximation, at least superticially, seems reasonable since the form of the static-exchange wave function is that which is suitable when the free electron is at large distances from the target, i.e. as $r_1 \to \infty$. The distance of the bound-electron from the positron, r_2, is of the order at 2 bohr. Making this approximation, the wave function (2.22) reduces to:

$$\Psi^{\pm}_{S.E.1}(\mathbf{r}_1, \mathbf{r}_2) = 2^{-\frac{1}{2}} \left\{ \phi_{Ps}(r_2) F^{\pm}(\mathbf{r}_1) \pm \phi_{Ps}(r_1) F^{\pm}(\mathbf{r}_2) \right\} \tag{2.24}$$

and this allows us to use the static-exchange program used for e^--H with only minor alterations. This method we denoted by S.E.1. (Ward et al 1985) and when

a polarization potential is inserted into the integro differential equation, the method is referred to as A.E.1. (Ward and McDowell, 1984).

Using the wave function of the form (2.24), the hamiltonian (2.23), and projecting out according to

$$\int \phi^*_{Ps}(\mathbf{r}_2)[H - E]\Psi^{\pm}_{S.E.1.}(\mathbf{r}_1, \mathbf{r}_2)\, d\mathbf{r}_2 \; = 0 \qquad (2.25)$$

and then expanding the function $F^{\pm}(\mathbf{r})$ in partial waves we obtain the integro differential equation,

$$\left(\frac{d^2}{dr_1^2} - \frac{l(l+1)}{r_1^2} + K^2\right) u_l^{\pm}(K, r) = 2\mu_{Ps} V_{1s,1s}(r_1)\, u_l^{\pm}(K, r_1)$$
$$\pm 2\mu_{Ps} \int_0^{\infty} K_l(r_1, r_2)\, u_l^{\pm}(K, r_2)\, dr_2 \pm \frac{\mu_{Ps}}{12} r_1 e^{-\frac{1}{2}r_1} \int_0^{\infty} r_2\, u_l^{\pm}(K, r) e^{-\frac{1}{2}r_2}\, dr_2\, \delta_{l1}$$

(2.26)

In equation (2.26)

$$K^2 = \mu_{Ps} k^2 / \mu_{Ps}.$$

the direct-potential $V_{11}(r_1)$ is given by:

$$V_{1s,1s}(r_1) = -\left(\frac{1}{r_1} + \frac{1}{2}\right) e^{-r_1} \qquad (2.27)$$

the exchange kernel being:

$$K_l(r_1, r_2) = \left[\frac{r_1 r_2}{2(2l+1)}\right] e^{-\frac{1}{2}(r_1 + r_2)} \left[\frac{(r_<)^l}{(r_>)^{l+1}} - \delta_{l0}(E - 2\epsilon_{Ps})\right]$$

(2.28)

where $r_<, r_>$ being the lesser and greater of r_1 and r_2 respectively.

The radial wave function $u_l^{\pm}(\kappa, r)$ for equation (2.26) has the asympotic form

$$u_l^{\pm}(\kappa, r) \underset{r \to \infty}{\sim} \kappa^{-\frac{1}{2}} \sin(\kappa r - \frac{1}{2} l\pi + \eta_l^{\pm}) \qquad (2.29)$$

and the third term on the right-hand side of equation (2.26) arises from the mass-polarization term. More details of this analysis can be found in Ward and McDowell (1984) and Ward et al (1985).

To allow for the polarization of the target, we added a polarization potential $V_{pol}(r)$, of the form given by equation (2.12b), multiplied by the reduced mass μ_{Ps} into the integro differential equation. The polarizability of positronium (α_{Ps}) is eight times that of hydrogen. We modified the cut-off function slightly to allow for the reduced mass of the positronium so that the polarization potential which we used took the form:

$$V_{pol}(r) = -\frac{\alpha_{Ps}}{2x^4}[1 - e^{-2x}(1 + 2x + 2x^2 + \frac{4}{3}x^3 + \frac{2}{3}x^4 + \frac{4}{27}x^5)]\mu_{Ps} \quad (2.30)$$

where $\alpha_{Ps} = 36a_0^3$ and $x = \mu_{Ps}r$.

As with the integro-differential equation of e^--H, the method of solution was to convert the integro differential equation (2.26) into a pair of coupled differential equations (Marriot (1958)). We found that the range R, discussed in the previous section needed to be longer for the e^--Ps system. This is reasonable since the e^--Ps system is more diffuse than the e^--H system. For the static exchange case, we took R=69.0 and for the adiabatic-exchange case, R=304.5. Within these ranges, we checked that the phase shifts were independent of the choice of mesh.

Although these particular methods, S.E.1. and A.E.1. have the advantage that they are easy to use and that the partial waves and their corresponding phase shifts can be easily evaluated, they do suffer from three major disadvantages, namely:

(1) There should be no static potential since the e^--Ps potential is anti symmetric about the centre of mass, and the charge density of the ground state vanishes (Drachman 1984).

(2) The radial solution of the integro differential equation (2.26) has the asymptotic form:

$$u_l^{\pm}(\kappa, r) \sim \kappa^{-\frac{1}{2}} sin(\kappa r - \frac{1}{2}l\pi + \eta_l^{\pm}) \quad (2.31)$$

rather than the true asymptotic form:

$$u_l^{\pm}(k, \rho) \sim k^{-\frac{1}{2}} sin(k\rho - \frac{1}{2}l\pi + \delta_l^{\pm}) \quad (2.32).$$

(It is possible for us to modify our asymptotic form to obtain the correct form by using a translation operator as described by Fels and Mittleman (1967).)

(3) Since we have modified the true static-exchange wave function, our phase shifts do not obey the bound principle.

These three disadvantages prevents us from determining the reliability of our results. We therefore, thought it necessary to perform the full static-exchange treatment (S.E.) and to use the Jacobi co-ordinate system since this is more appropriate for the scattering problem In the next section we describe this full static-exchange model for the e^--Ps system. and in §2.7, we compare the s-wave phase shifts from the S.E.1 and A.E.1 models with the S.E. phase-shifts.

(b) The full static-exchange treatment applied to e^--Ps scattering below the n=2 threshold.

The Schroedinger equation for the e^--Ps system is:

$$H\Psi^{\pm}(\mathbf{r}_2,\rho) = E\Psi^{\pm}(\mathbf{r}_2,\rho) \tag{2.33}$$

where in terms of Jacobi co-ordinates $(\mathbf{r}_2,\rho)$ (fig. 2.5) the hamiltonian is:

$$H = -\frac{1}{2\mu_{Ps^-}}\nabla^2_{\rho} - \frac{1}{2\mu_{Ps}}\nabla^2_{\mathbf{r}_2} - \frac{1}{r_1} - \frac{1}{r_2} + \frac{1}{r_3}\ a.u. \tag{2.34}$$

where $r_1 = |\rho + \frac{1}{2}\mathbf{r}_2|$, $r_3 = |\rho - \frac{1}{2}\mathbf{r}_2|$ and the static-exchange wave function is:

$$\Psi^{\pm}(\mathbf{r}_2,\rho) = 2^{-\frac{1}{2}}\left\{\phi_{Ps}(\mathbf{r}_2)F^{\pm}(\rho) \pm \phi_{Ps}(\mathbf{r}_1)F^{\pm}(\acute{\rho})\right\} \tag{2.35}$$

where $\acute{\rho} = \frac{3}{4}\mathbf{r}_2 - \frac{1}{2}\rho$. The analysis required to solve (2.33) is very similar to that used by Buckingham and Massey (1941) for the corresponding problem in nuclear physics of neutron-deutron (n-d) scattering. Since the n-d system, like e^--Ps, consist of three particles of equal mass, the kinetic-energy operator is the same. Our problem of e^--Ps scattering is somewhat simplier than the n-d problem since the atomic potential energy and target wave function are known. The potential energy is the coulomb potential. Further investigations of the n-d problem have been performed by Burke and Roberton (1957), Haas and Roberton (1959) and Humberston (1964) using different models for the nuclear potential.

To obtain an equation for $F^{\pm}(\rho)$ by solving (2.33) we make use of the following:

(a) The kinetic energy operator,

$$T = -\frac{\nabla_{\rho}^2}{2\mu_{Ps^-}} - \frac{\nabla_{r_2}^2}{2\mu_{Ps}} \qquad (2.36)$$

can be written in an alternative form, in terms of (r_1, ρ), which is equivalent,

$$T = -\frac{\nabla_{\rho'}^2}{2\mu_{Ps^-}} - \frac{\nabla_{r_1}^2}{2\mu_{Ps}} \qquad (2.37)$$

(b) The Schoedinger equation for the ground-state positronium atom,

$$\left[-\frac{\nabla_{r_2}^2}{2\mu_{Ps}} - \frac{1}{r_2}\right]\phi_{Ps}(r_2) = E_{Ps}\,\phi_{Ps}(r_2) \qquad (2.38)$$

for when electron (2) is bound, and

$$\left[-\frac{\nabla_{r_1}^2}{2\mu_{Ps}} - \frac{1}{r_1}\right]\phi_{Ps}(r_1) = E_{Ps}\,\phi_{Ps}(r_1) \qquad (2.39)$$

when electron (1) is bound.

Using (2.33), and projecting out on the ground state wave function $\phi_{Ps}(r_2)$ we obtain:

$$(\nabla_{\rho}^2 + k^2)F^{\pm}(\rho) = \pm 2\mu_{Ps^-}\int \phi_{Ps}^*(r_2)\left[-\frac{1}{2\mu_{Ps^-}}\nabla_{\rho}^2 - \frac{1}{2\mu_{Ps}}\nabla_{r_2}^2\right]\phi_{Ps}(r_1)F^{\pm}(\rho')\,dr_2$$

$$\pm 2\mu_{Ps^-}\int \phi_{Ps}^*(r_2)\left[-\frac{1}{r_1} - \frac{1}{r_2} + \frac{1}{r_3}\right]\phi_{Ps}(r_1)F^{\pm}(\rho')\,dr_2$$

$$\pm 2\mu_{Ps^-}\left(-E_{Ps} - \frac{k^2}{2\mu_{Ps^-}}\right)\int \phi_{Ps}^*(r_2)\,\phi_{Ps}(r_1)\,F^{\pm}(\rho')\,dr_2 \qquad (2.40)$$

where we note that the direct potential vanishes.

Consider the integral I_1,

$$I_1 = 2\mu_{Ps^-} \int \phi_{Ps}(\underline{r}_2)\left[-\frac{1}{2\mu_{Ps^-}}\nabla^2_{\underline{\rho}} - \frac{1}{2\mu_{Ps}}\nabla^2_{\underline{r}_2}\right]\phi_{Ps}(\underline{r}_1)F^{\pm}(\underline{\rho}')\,d\underline{r}_2 \qquad (2.41)$$

$$= \left(\frac{4}{3}\right)^3 \left\{ 2\mu_{Ps^-} \int \phi_{Ps}(r_2)\left[E_{Ps} + \frac{1}{r_1}\right]\phi_{Ps}(r_1)F^{\pm}(\rho')\,d\rho' \right.$$

$$\left. - \int \left\{\nabla^2_{\rho'}\,\phi_{Ps}(r_1)\,\phi_{Ps}(r_2)\right\} F^{\pm}(\rho')\,d\rho' \right\} \qquad (2.42)$$

where we have used (2.37), (2.39), Green's Theorem and have replaced the variable integration from $\mathbf{r}_2$ to ρ. Now,

$$\nabla^2_{\rho'}\,\phi_{Ps}(r_1)\,\phi_{Ps}(r_2) = \frac{16}{9}\,\phi_{Ps}(r_1)\,\nabla^2_{\underline{r}_2}\phi_{Ps}(r_2) + \frac{4}{9}\,\phi_{Ps}(r_2)\,\nabla^2_{\underline{r}_1}\phi_{Ps}(r_1)$$

$$+ \frac{16}{9}\,\frac{\underline{r}_1 \cdot \underline{r}_2}{r_1 r_2}\,\phi'_{Ps}(r_1)\,\phi'_{Ps}(r_2)$$

$$= \frac{4}{9}\,\phi_{Ps}(r_1)\,\phi_{Ps}(r_2)\left[-5E_{Ps} - \frac{1}{r_1} - \frac{4}{r_2}\right], \qquad (2.43)$$

$$+ \frac{16}{9}\,\frac{\underline{r}_1 \cdot \underline{r}_2}{r_1 r_2}\,\phi'_{Ps}(r_1)\,\phi'_{Ps}(r_2)$$

where (2.38) and (2.39) have been used. Substituting (2.43) into (2.42), then from

(2.40) we obtain:

$$(\nabla_\rho^2 + k^2) F^{\pm}(\rho) = \int \left\{ Q^{\pm}(\rho,\rho') + P^{\pm}(\rho,\rho') + \left(\frac{E_R}{E_{P_3}} - \frac{5}{3}\right) N^{\pm}(\rho,\rho') \right\} F^{\pm}(\rho')\, d\rho' \qquad (2.44)$$

where $E_R = \frac{3k^2}{4} a.u.$,

$$Q^{\pm}(\rho,\rho') = \pm\left(\frac{4}{3}\right)^4 \phi_{P_3}(r_1)\, \frac{1}{r_3}\, \phi_{P_3}(r_2)$$

$$P^{\pm}(\rho,\rho') = \pm\frac{1}{3}\left(\frac{4}{3}\right)^4 \left\{ \phi_{P_3}(r_1)\left[\frac{r_1}{r_1} + \frac{1}{r_2}\right] \phi_{P_3}(r_2) - 4\, \phi'_{P_3}(r_1)\, \phi'_{P_3}(r_2)\, \frac{\underline{r}_1 \cdot \underline{r}_2}{r_1 r_2} \right\}$$

$$N^{\pm}(\rho,\rho') = \mp\left(\frac{4}{3}\right)^4 E_{P_3}\, \phi_{P_3}(r_1)\, \phi_{P_3}(r_2)$$

(2.45)

and $$\phi'_{P_3}(r) = \frac{d}{dr}\, \phi_{P_3}(r).$$

To obtain the equation for the radial wave function, $F^{\pm}(\rho)$ and the kernels

$Q^{\pm}(\rho,\acute{\rho}), P^{\pm}(\rho,\acute{\rho}), N^{\pm}(\rho,\acute{\rho})$ are expanded in Legendre polynomials,

$$F^{\pm}(\rho) = \sum_{l=0}^{\infty} \frac{u_l^{\pm}(k,\rho)}{\rho} P_l(\cos\theta), \qquad (2.46)$$

$$\left.\begin{matrix} Q^{\pm}(\rho,\rho') \\ P^{\pm}(\rho,\rho') \\ N^{\pm}(\rho,\rho') \end{matrix}\right\} = \sum_{s=0}^{\infty} \frac{(2s+1)}{4\pi\rho\rho'} P_s(\cos\acute{\theta}) \left\{\begin{matrix} q_s^{\pm}(\rho,\rho') \\ p_s^{\pm}(\rho,\rho') \\ n_s^{\pm}(\rho,\rho') \end{matrix}\right. \qquad (2.47a)$$

where

$$\left.\begin{matrix} q_s^{\pm}(\rho,\rho') \\ p_s^{\pm}(\rho,\rho') \\ n_s^{\pm}(\rho,\rho') \end{matrix}\right\} = 2\pi\rho\rho' \int_0^{\pi} P_s(\cos\acute{\theta})\sin\acute{\theta}\, d\acute{\theta} \left\{\begin{matrix} Q^{\pm}(\rho,\rho') \\ P^{\pm}(\rho,\rho') \\ N^{\pm}(\rho,\rho') \end{matrix}\right. \qquad (2.47b)$$

and $cos\acute{\theta} = \frac{\rho\cdot\acute{\rho}}{\rho\acute{\rho}}$ and θ is the polar angle of ρ (w.r.t z-axis).

From equations (2.44), (2.46), (2.48) and using the orthogonal properties of the legendre polynomials we obtain:

$$\left(\frac{d^2}{d\rho^2} + k^2 - \frac{l(l+1)}{\rho^2}\right) u_l^{\pm}(k,\rho) = \int_0^{\infty} k_l^{\pm}(\rho,\rho')\, u_l^{\pm}(k,\rho')\, d\rho' \qquad (2.48)$$

where

$$k_l^{\pm}(\rho,\rho') = \pm\left\{q_l(\rho,\rho') + p_l(\rho,\rho') + \left(\frac{\epsilon_R}{\epsilon_{R_2}} - \frac{s}{3}\right) n_l(\rho,\rho')\right\} \qquad (2.49)$$

and the radial function $u_l^{\pm}(k,\rho)$ is required to satisfy the bounday conditions:

$$u_l^{\pm}(k,0) = 0,\ u_l^{\pm}(k,\rho) \underset{\rho\to\infty}{\sim} k^{-\frac{1}{2}} sin(k\rho - \frac{1}{2}l\pi + \delta_l^{\pm}) \qquad (2.50)$$

2.5 Method of solution of the integro-differential equation for e^--Ps scattering.

(i) Evaluation of the kernels.

The kernels can be written in terms of the integrals $T_l, F_l(1,0), F_l(0,1), F_l(0,0), G_l$, such that:

$$q_l(\rho,\acute{\rho}) = bT_l,$$

$$p_l(\rho,\acute{\rho}) = e\{F_l(1,0) + F_l(0,1)\} + hG_l, \tag{2.51}$$

$$n_l(\rho,\acute{\rho}) = aF_l(0,0)$$

where $a = \left(\frac{2}{3}\right)^4, b = \frac{2^5}{3^3}, e = 2\left(\frac{2}{3}\right)^4, h = -2\left(\frac{2}{3}\right)^5$. The integrals are given by:

$$T_l = \int_{-1}^{+1} EX(l)(\rho^2 + \acute{\rho}^2 - 2\rho\acute{\rho}x)^{-\frac{1}{2}}\, dx$$

$$F_l(n,m) = \int_{-1}^{+1} EX(l)X(\rho,\acute{\rho})^{-n}X(\acute{\rho},\rho)^{-m}\, dx \tag{2.52}$$

$$G_l = \int_{-1}^{+1} EX(l)(2\acute{\rho}^2 + 2\rho^2 + 5\rho\acute{\rho}x)X(\rho,\acute{\rho})^{-1}X(\acute{\rho},\rho)^{-1}\, dx$$

where

$$X(\rho,\acute{\rho}) = (\rho^2 + 4\acute{\rho}^2 + 4\rho\acute{\rho}x)^{\frac{1}{2}},$$

$$EX(l) = \rho\acute{\rho}exp[-\frac{1}{3}(X(\rho,\acute{\rho}) + X(\acute{\rho},\rho))]P_l(x) \tag{2.53}$$

and $P_l(x)$ is the l^{th} order legendre polynomial of the first kind.

Since the kernels are symmetric, i.e. $k^{\pm}(\rho,\acute{\rho}) = k^{\pm}(\acute{\rho},\rho)$, we only need to consider $\rho \geq \acute{\rho}$. The integral T_l has a singularity at the upper limit of integration when $\rho = \acute{\rho}$. This singularity is removed by making the substitution $Z^2 = \rho^2 + \acute{\rho}^2 - 2\rho\acute{\rho}x$. We remove the singularity which appears in $F_l(1,0), G_l$ at the lower integration point when $\rho = 2\acute{\rho}$ by using the substitution $y^2 = \rho^2 + 4\acute{\rho}^2 + 4\rho\acute{\rho}x$.

All of the integrals $(T_l, F_l(1,0), F_l(0,1), F_l(0,0), G_l)$ were performed numerically by using Gauss-Legendre quadrature. The nag library (mark 11, 1983) routines (D01BBF (D01BAZ)) were used and the kernels were tabulated as a function of $\rho, \acute{\rho}$. In §2.6, the convergence of the kernel with respect to the number of integration points is discussed.

(ii) Solving the integro-differential equation.

The method of solving (2.48) has been described in detail by Robertson (1956), Haas and Roberton (1959) and Humberston (1964).

As the kernel $k_l^{\pm}(\rho,\acute{\rho})$ decreases very rapidly with increasing $\rho,\acute{\rho}$, it is possible to replace the upper limit by some finite value R. Equation (2.48) can therefore be written as:

$$(\frac{d^2}{d\rho^2}+D)u_l^{\pm}(k,\rho)=\int_0^R k_l^{\pm}(\rho,\acute{\rho})u_l^{\pm}(k,\acute{\rho})\,d\acute{\rho} \tag{2.54}$$

where

$$D=k^2-\frac{l(l+1)}{\rho^2}.$$

For small values of $\rho(or\acute{\rho})$ the wave function $u_l^{\pm}(k,\rho)$ varies rapidly with ρ whereas for large ρ, the variation, which is of form (2.50), is much more slowly varying. This means that when we split the ρ range of integration into a set of mesh points, it is important to have a small mesh spacing when ρ is small. However, since we also require a large value for R, we can chose a slightly larger mesh spacing H for ρ in the intermediate range and in the asymptotic region. Our choice of mesh for the ρ (and $\acute{\rho}$) range of integration is according to:

$$R=N1H+(N2-N1)2H+(N3-N2)4H+(N4-N3)8H \tag{2.55}$$

where $N1,N2,N3,N4$ are integers and H is the initial mesh spacing. The mesh parameters (N4,N3,N2,N1,H) are input parameters of the program.

Obviously it is important to check that the results are independent of the choice of mesh and that the range R is sufficiently large. Care is taken at the positions where the mesh spacing is doubled. Roberton (1956) divided the $\rho,\acute{\rho}$ range of integration into equal intervals. This was perfectly acceptable since the nuclear potentials have much shorter range than the atomic.

The equation (2.54) was re-written by replacing the second derivative by its central difference representation and the integral was replaced by a summation in which Simpson's rule was used. To reduce the error which arises from using the central differences representation of the second derivative, and is of the order H^2, we followed Fox and Goodwin (1949) by operating on the whole equation by

$\left\{1 + \frac{1}{12}\delta^2\right\}$. δ is the central difference operator (see Fröberg, 1979). After this procedure, equation (2.54) becomes:

$$\left(1 + \frac{1}{12}(Hr)^2 D_{n-1}\right) U_{n-1} - \left(2 - \frac{10}{12}(Hr)^2 D_n\right) U_n$$
$$+\left(1 + \frac{1}{12}(Hr)^2 D_{n+1}\right) U_{n+1} = \frac{1}{12}(Hr)^2 \sum_{m=0}^{N} (K_{n-1,m} + 10K_{n,m} + K_{n+1,m}) T_m U_m \qquad (2.56)$$

where we have ignored the correction term and T_m are the weights obtained from Simpson's rule.$K_{n,m}$ is the kernel evaluated at point (n, m).

In equation (2.56).

$$(Hr) = Hfor 0 \leq \rho \leq (N1 - 1)H,$$
$$(Hr) = 2Hfor\ N1H + 2H \leq \rho \leq (N2 - 1 - N1)2H + N1H,$$
$$(Hr) = 4Hfor(N2 - N1)2H + N1H + 4H \leq \rho \leq$$
$$(N3 - 1 - N2)4H + (N2 - N1)2H + N1H$$
$$(Hr) = 8Hfor(N3 - N2)4H + (N2 - N1)2H + N1H + 8H \leq \rho \leq$$
$$(N4 - N3)8H + (N3 - N2)4H + (N2 - N1)2H + N1H - 8H.$$

When $\rho = \rho_1, \rho_2, \rho_3$, where $\rho_1 = N_1 H$, $\rho_2 = (N2 - N1)2H + N1H$, $\rho_3 = (N3 - N2)4H + (N2 - N1)2H + N1H$, the point (n-1) has to be replaced by (n-2) in order to obtain the correct spacing. Apart from this change, equation (2.56) can be used.

Equation (2.56) can be written in the alternative form:

$$\sum_{m=2}^{N} B_{nm} u_m = -B_{n1} u_1 - B_{n0} u_0 \ (n = 1, 2, \ldots, N-1) \qquad (2.57)$$

where

$$B_{nm} = T_m (K_{n-1,m} + 10K_{nm} + K_{n+1,m}) \frac{(Hr)^2}{12} \qquad (2.57b)$$
$$-\left(1 + \frac{1}{12}(Hr)^2 D_{n-1}\right) \delta_{n-1,m} + \left(2 - \frac{10}{12}(Hr)^2 D_n\right) \delta_{n,m} - \left(1 + \frac{1}{12}(Hr)^2 D_{n+1}\right) \delta_{n+1,m}$$

The boundary condition at the origin requires that $u_0 = 0$ and since the equation is homogeneous we chose $u_1 = 1$.

As ρ tends to zero, the term $B_{n0}u_l(0)$ is non-zero if $n=1$ and $l=1$. This can be seen by expanding the wave function for small ρ in a power series about the origin,

$$u_l(\rho) = a_{0l}\rho^{l+1} + a_{1l}\rho^{l+2} + a_{2l}\rho^{l+3} + \ldots \tag{2.58}$$

$$\lim_{\rho\to 0} B_{n0}u_l(\rho) = \left\{-\left(1+\frac{1}{12}H^2D_{n-1}\right)\delta_{n-1,0} + \left(2-\frac{10}{12}H^2D_n\right)\delta_{n,0} - \left(1+\frac{1}{12}H^2D_{n+1}\right)\delta_{n+1,0}\right\}\left(a_{0l}\rho^{l+1} + a_{1l}\rho^{l+2} + \ldots\right)$$

if n=1

$$\lim_{\rho\to 0} B_{10}u_l(0) = \frac{1}{12}H^2(l+1)\left(a_{0l}\rho^{l-1} + a_{1l}\rho^{l} + \ldots\right) \tag{2.59}$$

which is non-zero if $l=1$, and equals $\frac{1}{12}H^2 2a_{01}$. The constant a_{01} is obtained by neglecting all but the first term in (2.58) giving $a_{01} = H^{-2}$. Thus, equation (2.57a) becomes

$$\sum_{m=2}^{N} B_{nm}u_m = -(B_{n1} + \frac{1}{6}\delta_{n1}\delta_{l1}) \tag{2.60}$$

or in matrix form

$$Bu = A \tag{2.61}$$

Equation (2.61) was solved using the NAG library, . (mark11,1983), and the normalization was obtained by matching the solution at large ρ with the asymptotic form.

$$u_l^{\pm}(k,\rho) = k^{-\frac{1}{2}}sin(k\rho - \frac{1}{2}l\pi + \delta_l^{\pm})$$

which enables us to determine the phase shift.

Since the individual kernels $p_l^{\pm}(\rho,\acute{\rho}), q_l^{\pm}(\rho,\acute{\rho}), n_l^{\pm}(\rho,\acute{\rho})$ are energy independent, they were evaluation in a separate program from that required to solve the integro differential equation. The kernels were tabulated at the mesh points $\rho,\acute{\rho}$ in a data file. A separate program read in the kernels, multiplied the $n_l^{\pm}(\rho,\acute{\rho})$ kernel by the energy dependent term, and then solved the integro- differential equation in the manner just described. We ran the programs on the R.H.B.N.C. VAX,

2.6 Tests performed to check the analysis and computer program for the solution of the integro-differential equation.

(a) Convergence of the kernels.

We used 8,16,32,64 integration points (NI) in the evaluation of the kernels to check the convergence of the integrals performed by Gauss-Legendre quardrature. The convergence was rapid; the agreement in the kernels as NI was increased from 32 to 64 points were mainly to at least 7 figures. This corresponded to a change in the 4 figure of $\tan\delta_0^+(k=0.3)$, (see Table .2). The agreement in the radial function for $l=0$ and $k=0.3$ was mainly to at least 4 figures. We tested the convergence for higher order partial waves and the convergence was good. Our choice of NI was 64.

(b) Solution of integro-differential equation for a test kernel.

We needed to know the accuracy of the numerical solution $u_l(\rho)$ determined from the matrix equation (2.61). Therefore, we used a test kernel in which it was possible to obtain an analytical solution of (2.48). The analytical solution was compared with the numerical solution calculated by using (2.61) together with the test kernel. This provided a check on our coding of equation (2.61) and whether the representation of the second differential by the central difference formula was adequate. Obviously it was important to chose a test kernel which was of the same form of the true kernal for the scattering problem.

A suitable test kernel is given by

$$\mathrm{K}_0^t(\rho,\acute{\rho}) = (A\rho\acute{\rho} - B)e^{-\beta(\rho+\acute{\rho})} \tag{2.62}$$

where A, B, β are constants.

We considered just the $l=0$ case so that the integro-differential equation (2.48) is of the form:

$$\left\{\frac{d^2}{d\rho^2}+k^2\right\} f_0^t(\rho) = \int_0^\infty \mathrm{K}_0^t(\rho,\acute{\rho}) f_0^t(\acute{\rho})\, d\acute{\rho} \qquad . \tag{2.63.}$$

It is clear that the solution is of sinusoidal form. We solved (2.63) by applying the Laplace transform to the whole equation. The solution is:

$$f_0^t(\rho) = \frac{AC}{(\beta^2+k^2)}\left\{\frac{1}{(\beta^2+k^2)}\left\{-2\beta\cos k\rho + \left(\frac{\beta^2}{k} - k\right)\sin k\rho\right.\right.$$

$$\left.\left. + 2\beta e^{-\beta\rho} + \rho e^{-\beta\rho}\right\} - \frac{BD}{(\beta^2+k^2)}\left\{e^{-\beta\rho}\cos k\rho + \frac{\beta}{k}\sin k\rho\right\}\right.$$

$$+ \frac{f_0^t(H)}{H}\frac{\sin k\rho}{k} \qquad (2.64)$$

where $C = C(\beta, k)$ and $D = D(\beta, k)$. (Full details given in Appendix A1).

As with the numerical solution, we took

$$f_0^t(H) = 1.0. \qquad (2.65)$$

Details of how this equation is obtained, the values for A, B, β and the expression for C and D are given in Appendix A1. The agreement between the numerical and analytical solution $f_0^t(\rho)$ was to better than 6 figures for $k = 0.1a_0^{-1}$, to mainly 6 figures for $k = 0.2a_0^{-1}$ and mainly to 5 figures for $k = 0.3a_0^{-1}$. This agreement is very good and gives us confidence in the numerical method of solving equation (2.48). By varying the mesh parameters $(N1, N2, N3, N4, H)$ we checked that the solution was independent of the choice of mesh. We found that $R = 7.9$ was adequate and $H = 0.01$ was sufficiently small.

(c) Numerical Integration.

Simpsons rule was used for the numerical integration of the integrals on the right hand side of equation (2.63). We repeated this integration by using the trapezoidal rule and the agreement in the numerical solution was very good. A further check on the integration was provided by varying the mesh and checking that the solution remained stationary.

(d) Stability of Mesh.

Since we were confident in the numerical method used to solve the integro-differential equation, we could now use the true kernel for the e^--Ps scattering

problem (2.48,2.49). We investigated the effect of changing the value of R, H and the other mesh parameters had on the phase shifts and numerical solution. The range R needs to be sufficiently large so that the integral from R to ∞ of equation (2.48) can justificably be neglected. Also, H needs to be sufficiently small so that the error term arising from using the central difference representation of the second differential is negligibly small. As a guide, ten mesh points per half cycle is reasonable. Thus,

$$10\Delta(k,\rho) = \pi$$

and for a given k

$$H = \frac{\pi}{10k}.$$

Since $k = 0.5a_0^{-1}$, the value of k at the n=2 threshold, is the largest value of k we need to consider, we should ensure $H \leq 0.6$.

Both the program to evaluate the kernal and the program to solve the integro-differential equation were run on the R.H.B.N.C VAX. We found that the limitation was not so much the memory space but the CPU time. The time limit on a medium batch job was 15 minutes. This meant restricting N4 = 250 when the numbers of integration points in the evaluation of the kernels (NI) was 32 and N4 = 180 when NI = 64. With N4 = 180 and 250, we investigated suitable values for R and H. Since a sufficiently large value of R and sufficiently small value of H could be obtained with N4 = 180, we decided to use NI = 64, for added accuracy. With R fixed, we varied the other mesh parameters (N4, N3, N2 N1, H) to check that both the solution and phase shift were independent of the choice of mesh parameters. In choosing the mesh spacing H, we ran the program with zero kernel for l = 0. The solution of equation (2.48) which satisfies the boundary conditions (2.50) is:

$$u_0^{\pm}(k,\rho) = k^{-\frac{1}{2}} sin k\rho.$$

With N4 = 180, R = 31, H = 0.025, the agreement between the analytical and numerical solution was to better than 6 figures for 155 of the mesh points and to 5 figures for the remaining mesh points. When N4 = 90, R = 31, H = 0.05, the agreement was to better than 6 figures for 55 of the mesh points and to 5 figures for the remaining points. Thus H = 0.05 is sufficiently small, although it is preferable

to take H =0.025. With the true kernel we checked that the mesh spacing of 0.025 was suitable by comparing phase shifts evaluated at the same value of R.

Table 2.2 shows the variation of $tan\delta_0^+, tan\delta_0^\pm$ at $k = 0.3_0^{-1}$, as N4 was increased, which corresponds to an increase in R since the other mesh parameters were kept constant. As can be seen, R = 31 is sufficiently large for l = 0,1. Table 2.3 a,b shows the effect on $tan\delta_0^+, tan\delta_1^\pm$ of varying the mesh parameters for a fixed R.

Our choice of mesh parameters was: N4 = 180, N3 = 36, N2 = 20, N1 = 16, H = 0.025, R=31 for l = 0,1 and for l = 2,3,4 we found that a larger value of R was required. For these higher partial waves, we chose N4 = 260, N3 = 60, N2 = 40, N1 = 20, H = 0.025, R= 43.5 and calculated the phase shifts on the ULCC CRAY1S since we wanted NI = 64.

We checked that our choice of mesh was suitable for the whole energy range. Our investigation of the choice of mesh and the verification that the phase shifts and radial wave function were independent of the particular set of mesh parameters (to within 3 figures) was much more extensive then shown in these tables

2.7 Results and discussion.

In table 2.4, the static-exchange phase shifts for the partial waves $l = 0 \rightarrow 5$ for the scattering of slow energy electrons by positronium, below the n = 2 threshold, are shown. We note:

(i) As k tends to zero, the singlet s-wave phase shifts tend to π, but the triplet phase shifts tend to zero.

(ii) With increasing l, but with k constant, the magnitude of the singlet and triplet phase shifts decrease rapidly, by $l = 5$ the phase shifts are negligibly small.

(iii) The singlet and triplet phase shifts are of opposite sign for a given l, there being no direct potential. By $l = 5$, these phase shifts are approximately of equal magnitude.

(iv) The s-wave and p-wave phase shifts give the dominant contribution to the total elastic cross section. For $k \leq 0.10a_0^{-1}$, the dominant contribution is from the s-wave, and for $k \geq 0.15a_0^{-1}$ the dominant contribution is from the p-wave. In Chapter 5 the total and diffusion cross sections are reported and discussed more fully.

Consider point (i). It is interesting that the behaviour of the s-wave phase shifts, within moduli π, resembles so closely the s-wave phase shifts of e^--H scattering (fig. 2.1), yet for the e^--Ps system, the triplet phase shifts tend to zero as k tends to zero, whereas for e^--H they tend to π. For e^--H, we have

$$\Psi^-(\mathbf{r}_1,\mathbf{r}_2) = 2^{-\frac{1}{2}}\left\{\phi_0(\mathbf{r}_1)F^-(\mathbf{r}_2) - \phi_0(\mathbf{r}_2)F^-(\mathbf{r}_1)\right\}$$

which is identically zero when:

$$F^-(\mathbf{r}) = \phi_0(\mathbf{r}). \tag{2.66}$$

This means that a solution to (2.10) is obtained when $u_0^-(r) = r\phi_0(r)$. This function vanishes at $r = 0$ and as $r \to \infty$. Hence if $u_0^-(r)$ is a solution of (2.10) satisfying the boundary conditions (2.9), then

$$u_0^-(r,\lambda) = u_0^-(r) + \lambda r\phi_0(r) \quad (\lambda = constant) \tag{2.67}$$

is also a solution which will have the same phase shift since $r\phi_0(r)$ vanishes asymptotically. Thus, for the triplet e^--H, there exists a bounded solution of (2.10) but does not correspond to a bound-state. This explains why the triplet s-wave phase shift tends to π rather than zero, although according to Levinson's theorem it should tend to zero. For e^--Ps, the static-exchange wave function for the triplet case is:

$$\Psi^-(\mathbf{r}_2,\rho) = 2^{-\frac{1}{2}}\left\{\phi_{Ps}(r_2)F^-(\rho) - \phi_{Ps}(r_1)F^-(\acute{\rho})\right\} \equiv$$

$$\Psi(\mathbf{r}_1,\mathbf{r}_2) = 2^{-\frac{1}{2}}\left\{\phi_{Ps}(r_2)F^-(\mathbf{r}_1 - \frac{1}{2}\mathbf{r}_2) - \phi_{Ps}(r_1)F^-(\mathbf{r}_2 - \frac{1}{2}\mathbf{r}_1)\right\} \tag{2.68}$$

which does not vanish when

$$F^-(\rho) = \phi_{Ps}(\rho), \tag{2.69}$$

hence Levinson's theorem holds for both the singlet and triplet phase shifts of e^--Ps scattering. We verified that the triplet phase shift does indeed go to zero, not π, as k tends to zero by plotting the radial wave function and measuring the phase shift by counting the nodes. Also, we ran the static-exchange program at high energies to check that the phase shift did tend to zero as we go to large energies. The singlet phase shifts tend to π as k tends to zero in accord with the Levinson's theorem since there exists one bound- state of Ps^- which is a singlet state.

Using the static-exchange wave function we predicted the binding energy of Ps^- to be 0.003075 a.u. compared to the best value to date of 0.1200506 a.u. (Bhatia and Drachman, 1983). Although our value for the binding energy is poor, it is suprizing that such a simple wave function is capable of establishing the bound state of Ps^- which is highly correlated system.

We calculated the singlet and triplet scattering lengths of Ps^- extrapolating $tan\delta_0^{\pm}/k$ to zero k and these are shown in table 2. The zero-energy s-wave cross section determined by this method is $521\pi a_0^2$. In Table 2.5, we compare the s-wave phase shifts and scattering lengths calculated to the A.E.1, S.E.1 methods with the static-exchange (S.E.) results. Both the S.E.1 and A.E.1. phase shifts are larger than the S.E. results but the agreement is fairly good (Moduli π) between these three methods. We note, however, that the triplet S.E.1 and A.E.1 s-wave phase shifts tend to π rather than zero. The reason for this can be understood from the simplified static-exchange wave function.

$$\Psi^-_{S.E.1}(\mathbf{r}_1,\mathbf{r}_2) = 2^{-\frac{1}{2}}\left\{\phi_{Ps}(r_2)F^-(\mathbf{r}_1) - \phi_{Ps}(r_1)F^-(\mathbf{r})_2)\right\} \qquad (2.70)$$

which is identically zero when

$$F^-(\mathbf{r}) = \phi_{Ps}(\mathbf{r}). \qquad (2.71)$$

Since the full static-exchange method is superior to the simplified static-exchange method in that the radial wave function has the correct asymptatic form and there is (correctly) no direct potential in the integro-differential equation, I have not tabulated higher order phase shifts determined by the S.E.1., A.E.1 methods.

The static-exchange method, however, does have the disadvantage that it makes no allowance for the polarization (distortion) of the target Ps atom. As

discussed in section 2.3, the effect of polarization on the results of e^--H scattering becomes increasingly important for higher-order l. The effect of polarization was important in the p-wave at very low energies and in the d-wave, over a larger energy range. We would expect a similar behaviour for the e^--Ps system. By including a polarization potential with a suitable cut-off function into the static exchange integro-differential for the e^--H system, the resulting phase shifts agreed reasonably well with the accurate variational results.

Therefore, we added the term of the form:

$$V_{pol} = -\frac{\alpha_{Ps}}{2\rho^4} w(\rho) \tag{2.72}$$

multiplied by $2\mu_{Ps}$- to the right-hand side of the integro-differential equation for the e^--Ps system (2.48) to represent the polarization of positronium, where $w(\rho)$ is a cut-off function such that:

$$w(\rho) \rightarrow 1 \; as \; \rho \rightarrow \infty. \tag{2.73}$$

Following Peach (1980), we took

$$w(\rho) = [1 - \sum_{j=0}^{2} \frac{x}{j!} e^{-x}], \; x = \beta\rho. \tag{2.74}$$

Peach (1980) obtained the parameter β for the Ne-e system by ensuring that the adiabatic-exchange results reproduce as closely as possible the experimental data.

As stated earlier in this section, the dominant contribution to the total elastic cross section for the energy region corresponding to $0 \leq k(a_0^{-1}) < 0.5$ come from the s and p-waves, and for $k \geq 0.15a_0^{-1}$ the main contribution is from the triplet p-wave. In order to calculate accurate total elastic and differential cross sections we determined the s- and p-wave phase shifts very accurately by performing a variational calculation (which is discussed in chapter 3 and 4). We obtained the parameter β by matching the ^{3}P adiabatic exchange phase shifts with the accurate ^{3}P variational results. Using this choice of β, we determined the phase shifts for the singlet and triplet states and for the higher order phase shifts within the adiabatic-exchange approximation. These results are reported in chapter 5.

2.8 Conclusions

In this chapter I have presented the static exchange and adiabatic exchange phase shifts which we calculated for e^--H scattering, below the n = 2 threshold. Satisfactory agreement was obtained with the accurate variational results.

Due to the success of the static-exchange method for e^--H system, we used this method to tackle the e^--Ps problem. Singlet and triplet scattering lengths and the phase shifts for the partial waves $l = 0 \rightarrow 5$ were determined. The static-exchange wave function was able to 'bind' the Ps^- ion although the resulting value for the binding energy was poor. We also investigated the effect of simplifying the static-exchange wave function so that the form resembled closely the static-exchange wave function for the e^--H system where the 'infinite' nucleus approximation was used.

To determine the reliability of the static-exchange results and to obtain accurate total and differential cross sections we discussed the need of obtaining very accurate s and p-wave phase shifts by the variational method and higher order phase shifts by using the adiabatic-exchange approximation. The s-wave and p-wave variational calculations are described in chapters 3 and 4, respectively. In chapter 5, the adiabatic-exchange phase shifts for the various partial waves are presented.

Chapter 3

s-wave variational calculation

3.1 Introduction

In this chapter, s-wave elastic scattering of electrons by positronium (Ps), below the n=2 threshold has been investigated using the Kohn variational method with a flexible trial function. Very accurate singlet and triplet phaseshifts have been determined, with an estimate of their accuracy.

This calculation was performed for three reasons

(1) The e^--Ps system is basically very simple. A full understanding of a three body system, will be of great benefit in atomic scattering theory.

(2) Accurate results can be used to test the reliabilty of various approximate methods which have to be used in more complicated problems. We need to know the suitability of the static- and adiabatic-exchange methods, for the e^--Ps scattering problem (see chapter 2).

(3) For the photodetachment cross section, very good bound-state and p-wave continuuum wavefunctions are required. In the determination of the p-wave function, angular integrations are involved. It is advisable therefore to perform a calculation for the s-wave first.

The Kohn variational method enables accurate phase shifts, which are exact to the 1^{st} order, to be determined. If the trial function is carefully chosen so that it will differ by only a small amount from the actual solution of the Schroedinger equation, then this second order term will be very small.

The basic theory behind the variational method is described in the next section. The Kohn and inverse Kohn variational principles are seen to be obtained from specific cases of the general Kato's identity.

In §3.3, the suitabilty of the variational method for the problem of scattering low energy electrons from positronium is discussed. Our particular choice of the s-wave function is described in §3.4. The calculation performed to determine the

stationary phase shift from the Kohn and inverse Kohn variational principles is explained in §3.5. Details are given of the computer program in §3.6. The s-wave scattering results are presented in section §3.7 together with a discussion.

In §3.8, the ^{1,3}S resonances associated with the n=2 threshold are described. The bound-state calculation to determine the binding energy of Ps^- is discussed in §3.9 and a comparison of results with other authors is made. This chapter is concluded with a summary, the conclusions reached and a discussion of where further work is needed(§3.10).

3.2 Theory

(a) Variational Principles.

For simplicity, in deriving the variational principles, just consider scattering by a single particle. However, these variational principles are of more general nature, and can be applied to more complicated situations where there is n-electrons or to a multi-channel process, see for example the review by Callaway (1978) and the monograph by Nesbet (1980).

The true wave function $\psi_l(\mathbf{r})$ satisfies the Schoedinger equation,

$$(H - E)\psi_l(\mathbf{r}) = 0 \tag{3.1}$$

where H is the Hamiltonian of the system. Defining the operator L,

$$L = \frac{2m}{\hbar^2}(H - E), \tag{3.2}$$

then

$$L\psi_l(\mathbf{r}) = 0,$$

where m is the mass of the particle.

The wavefunction $\psi_l(\mathbf{r})$ satisfies the boundary conditions:

$$\psi_l(r \to 0) \sim r^l \tag{3.3}$$

and

$$\psi_l(\mathbf{r}) \underset{r\to\infty}{\sim} Y_{lm}(\Omega)k^{\frac{1}{2}}\left\{\frac{\cos(kr-\frac{1}{2}l\pi+\theta)}{kr}+\cot(\delta_l-\theta)\frac{\sin(kr-\frac{1}{2}l\pi+\theta)}{kr}\right\} \tag{3.4}$$

where δ_l is the true phaseshift.

Consider a trial function $\psi_l^t(\mathbf{r})$ in which it is required to satisfy boundary conditions of the same form:

$$\psi_l^t(r\to 0) \sim r^l \tag{3.5}$$

and

$$\psi_l^t(\mathbf{r}) \underset{r\to\infty}{\sim} Y_{lm}(\Omega)k^{\frac{1}{2}}\left\{\frac{\cos(kr-\frac{1}{2}l\pi+\theta)}{kr}+\cot(\delta_l^t-\theta)\frac{\sin(kr-\frac{1}{2}l\pi+\theta)}{kr}\right\} \tag{3.6}$$

where δ_l^t is the trial phaseshift, but does not necessarily have to satisfy:

$$L\psi_l^t(\mathbf{r}) = 0.$$

The variational principle relies strongly on the condition that the trial wave function $\psi_l^t(\mathbf{r})$ only differs by a small amount of a small amount $\delta\psi(\mathbf{r})$ from the true wave function,

$$\psi_l^t(\mathbf{r}) = \psi_l(\mathbf{r}) + \delta\psi_l(\mathbf{r}) \tag{3.7}.$$

This condition can generally be met by carefully constructing the wave function from the physical considerations. The function $\delta\psi_l$ has the properties:

$$\delta\psi_l \quad :(r\to 0) \sim r^l, \tag{3.8}$$

and

$$\delta\psi_l(\mathbf{r}) \underset{r\to\infty}{\sim} Y_{lm}k^{\frac{1}{2}}\delta\lambda\frac{\sin(kr-\frac{1}{2}l\pi+\theta)}{kr} \tag{3.9}$$

where $\delta\lambda = \lambda^t - \lambda$,

$$\lambda^t = \cot(\delta_l^t-\theta),\ \lambda = \cot(\delta_l-\theta).$$

Consider the functional $I[\psi_l^t(\mathbf{r})]$ defined by:

$$I[\psi_l^t(\mathbf{r})] = \int \psi_l^t(\mathbf{r})L\psi_l^t(\mathbf{r})\,d\mathbf{r} \tag{3.10}.$$

This is identically zero if $\psi_l^t(\mathbf{r}) \equiv \psi_l(\mathbf{r})$ since $L\psi_l(\mathbf{r}) = 0$.

Now, let δI denote the change in I given by:

$$\delta I = I[\psi_i^t(\underline{r})] - I[\psi_i(\underline{r})]$$

$$= \int \delta\psi_i(\underline{r}) \hat{L} \psi_i(\underline{r}) d\underline{r} + \int \psi_i(\underline{r}) \hat{L} \delta\psi_i(\underline{r}) d\underline{r} \qquad (3.11)$$

$$+ \int \delta\psi_i(\underline{r}) \hat{L} \delta\psi_i(\underline{r}) d\underline{r} \quad .$$

It can be shown using Green's Theoram that

$$\int \psi_i(\underline{r}) \hat{L} \delta\psi_i(\underline{r}) d\underline{r} = \int \delta\psi_i(\underline{r}) \hat{L} \psi_i(\underline{r}) d\underline{r}$$

$$- \delta\lambda \qquad (3.12)$$

which gives

$$\delta I = 2\int \delta\psi_i(\underline{r}) \hat{L} \psi_i(\underline{r}) d\underline{r} - \delta\lambda + \int \delta\psi_i(\underline{r}) \hat{L} \delta\psi_i(\underline{r}) d\underline{r},$$

and since $L\psi_l(\mathbf{r}) = 0$, we obtain

$$\delta(I + \lambda) = \int \delta\psi_l(\mathbf{r}) L \delta\psi_l(\mathbf{r})\, d\mathbf{r}. \qquad (3.13)$$

This expression is known as Kato's identity (Kato,1950). The term on the right hand side of (3.13) is a second order quantity and may be neglected provided $\delta\psi_l(\mathbf{r})$ is small.

Thus,

$$\delta(I + \lambda) = 0. \qquad (3.14)$$

and this is known as Kato's stationary expression. The term $I + \lambda$ is stationary with respect to small variations in the trial function about the exact wavefunction.

By setting $\theta = \frac{\pi}{2}$, the Kohn's variational principle, (Kohn, 1948) can be established,

$$\delta(I - R) = 0 \tag{3.15}$$

where $\delta R = R^t - R$, $R^t = \tan\delta^t$, $R = \tan\bar{\delta}$, $\bar{\delta}$ being the stationary phase shift which is exact to the first order. The trial wavefunction satisfies the asymptotic boundary conditions:

$$\psi_l^t(\mathbf{r}) \underset{r\to\infty}{\sim} Y_{lm} k^{\frac{1}{2}} \left\{ \frac{\sin(kr - \frac{1}{2}l\pi)}{kr} + \tan\delta_l^t \frac{\cos(kr - \frac{1}{2}l\pi)}{kr} \right\} \tag{3.16}.$$

The inverse Kohn (Hulthén's second) variational principle, (Hulthén, 1948) can be obtained by setting $\theta = 0$ in equations (3.6), (3.4).

$$\delta(I + \acute{R}) = 0, \tag{3.17}$$

where $\delta\acute{R} = \acute{R}^t - \acute{R}$, $\acute{R}^t = \cot\acute{\delta}^t$, $\acute{R} = \cot\bar{\delta}$, and the asymptotic boundary condition satisfied by $\psi_l^t(\mathbf{r})$ is:

$$\psi_l^t(\mathbf{r}) \underset{r\to\infty}{\sim} Y_{lm} k^{\frac{1}{2}} \left\{ \frac{\cos(kr - \frac{1}{2}l\pi)}{kr} + \cot\acute{\delta}^t \frac{\sin(kr - \frac{1}{2}l\pi)}{kr} \right\} \tag{3.18}.$$

It is convenient to express the trial wavefunction in terms of a set of linear parameters, $c_i, i = 1, 2, \ldots N'$, $\cot(\delta^t - \theta)$ which are unknown. To determine these quantities, slight variations in these linear parameters are allowed such that the quantity $(I + \lambda)$ is to remain stationary.

The two main variational procedures are due to Kohn (1948) and Hulthén (1944), (Hulthén 1^{st} variational method). To explain these, take $\theta = \frac{\pi}{2}$ for simplicity.

In the Kohn variational method,

$$\delta(I - R) = \sum_{i=1}^{N'} \frac{\partial I}{\partial c_i} \delta c_i + \frac{\partial I}{\partial R} \delta R - \delta R = 0 \tag{3.19}$$

and since the linear parameters chosen to be independent, then

$$\frac{\partial I}{\partial c_i} = 0, \quad i = 1, 2, \ldots N', \quad \frac{\partial I}{\partial R} = 1 \tag{3.20}.$$

The linear parameters $(c_i, i = 1, 2, \ldots N', \tan\delta^t)$ are determined by solving these set of linear simultaneous equations (3.20).

The trial phase shift δ^t is substituted back into equation (3.15) to obtain a phase shift $\bar{\delta}_K$ which is correct to the first order.

$$\bar{R}_K = R_t - I[\psi_l^t(\mathbf{r})] \qquad (3.21),$$

where $\bar{R}_K = \tan\bar{\delta}_K, R_t = tan\delta^t$, since $I[\psi_l(\mathbf{r})]$. $\bar{\delta}^K$ is known as Kohn's stationary phaseshift.

In Hulthén's 1^{st} variational method, the linear parameter $c_i, i = 1, 2, \ldots N$, $\tan\delta^t$ are determined by requiring that

$$I[\psi_l^t(\mathbf{r})] = 0 \qquad (3.22)$$

as well as the condition,

$$\delta(I - R_t) = 0 \qquad (3.23).$$

is satisfied. Since,

$$I[\psi_l^t(\mathbf{r})] = I[\psi_l(\mathbf{r})] = 0,$$

then

$$R^H = R^t.$$

This particular method suffers from the disadvantage that $I[\psi_l^t(\mathbf{r})]$ is quadratic in $\tan\delta^t$, so that two values of $\tan\delta^t$ are obtained and only one of these values is of any use. Because of this difficulty, we used the Kohn and inverse Kohn methods. It is worth performing both the Kohn and inverse Kohn calculations because a singularity could arise from one of the methods at a particular value of k.

(b) Schwartz singularities.

An inherent difficulty of the Kohn (and inverse Kohn) variational method is that a schwartz singularity (Schwartz 1961b) can occur in the phase shift at a particular energy and for a certain number of linear parameters, giving an erroneous result. To understand the cause of this singularity (Bransden, 1983, page 63), write the wavefunction in the form,

$$\psi_l^t(\underline{r}) = u(\underline{r}) + \tan\delta_l^t \, w(\underline{r}) + \sum_{i=1}^{n} c_i \phi_i \,, \qquad (3.24)$$

where $u(0) = w(0) = 0$, and

$$u(\underline{r}) \underset{r\to\infty}{\sim} Y_{lm}(\Omega)\sqrt{k}\,\frac{\sin(kr - \frac{1}{2}l\pi)}{kr},$$

$$w(\underline{r}) \underset{r\to\infty}{\sim} Y_{lm}(\Omega)\sqrt{k}\,\frac{\cos(kr - \frac{1}{2}l\pi)}{kr},$$

and ϕ_i are square integrable functions which vanish at the origin and asymptotically.

Substitute the wavefunction into the functional $I[f_l^t(\mathrm{r})]$ to obtain:

$$I[f_l^t] = A + B R_t + C R_t^2 + \sum_{i=1}^{n} c_i D_i \,, \qquad (3.25)$$
$$+ R_t \sum_{i=1}^{n} c_i E_i + \sum_{i,j}^{n} c_i c_j F_{ij} \,,$$

where

$$A = \langle u \mathcal{L} u \rangle, \quad B = \langle u \mathcal{L} w \rangle + \langle w \mathcal{L} u \rangle,$$
$$C = \langle w \mathcal{L} w \rangle, \quad D_i = 2\langle u \mathcal{L} \phi_i \rangle,$$
$$E_i = 2\langle w \mathcal{L} \phi_i \rangle,$$

and

$$F_{ij} = \langle \phi_i \mathcal{L} \phi_j \rangle, \quad R_t = \tan\delta_l^t \,.$$

Without loss of generality, the square intergrable functions ϕ_i can be constructed

so that,

$$F_{ij} = \langle \phi_i \mathcal{L} \phi_j \rangle = (k^2 - k_i^2)\,\delta_{ij} .$$

The Kohn variational method requires that

$$\frac{\partial I}{\partial C_i} = 0 , \quad i = 1, 2, \cdots N', \quad \frac{\partial I}{\partial R} = 1$$

(see equation on 3.20). Thus,

$$\frac{\partial I}{\partial C_i} = D_i + R_t E_i + 2(k^2 - k_i^2) C_i = 0 \qquad (3.26)$$

$$\frac{\partial I}{\partial R} = B + 2C R_t + \sum_{i=1}^{n} C_i E_i = 1$$

and this set of linear $(N'+1)$ simulteneous equations are solved to obtain the $(N'+1)$ unknowns. The equation for R_t is:

$$R_t = \left(2C - \sum_{i=1}^{n} \frac{E_i^2}{2(k^2 - k_i^2)}\right)^{-1} \left(1 - B + \sum_{i=1}^{n} \frac{D_i E_i}{2(k^2 - k_i^2)}\right) \qquad (3.27)$$

and this does have a finite value in the limit $k^2 \to k_i^2$, the limiting value being $-D_i/E_i$. However, a more detailed investigation shows that the anomalies which occur in the Kohn or inverse Kohn variational methods arises from singular points of the matrix of the full inhomogeneous equation, and not from the matrix with elements $(\phi_i \mathcal{L} \phi_j)$. The full inhomogeneous equation for the Kohn variational method is given by equation (3.58). The occurence of these anomalies has been discussed more fully by Nesbet (1980).

(c) Minimum Principles.

In the bound-state problem, the energy eigen value determined by the variational method will be a minumum and gives an upper bound to the true ground state energy. As more terms are added to the trial function, the results converge monotonically to the exact value. This minimum principle can be extended to excited bound-states provided the trial function is sufficiently flexible. In scattering, Kato's identity gives the exact phase shift,

$$\tan \delta_{ex} = \tan \delta^t - I[\psi_l^t(\mathbf{r})] + I[\delta\psi_l^t(\mathbf{r})] \qquad (3.28).$$

The quantity $I[\delta\psi_l^t(\mathbf{r})]$ is a second order term, and is neglected to give the Kohn variational principle,

$$[\tan \delta] = \tan \delta^t - I[\psi_l^t(\mathbf{r})] \qquad (3.29)$$

The phase shift evaluated, $[\tan \delta]$ is stationary with respect to small variations in the trial function, but is not necessarily a minimum. The error in the phase-shift is given by $I[\delta\psi_l^t(\mathbf{r})]$, which is a quantity which cannot be calculated since the exact wave function is not known. However, if the sign of this quantity $I[\delta\psi_l^t(\mathbf{r})]$ could be determined, then the stationary phase-shift would provide a bound to the exact phase shift.

Unfortunately, in a scattering calculation, is it generally not possible to determine the sign of this error term. It would be necessary to know the number of eigen values of the Hamiltonian H below the value of the energy E which we are working at, to state that $I[\delta\psi_l^t(\mathbf{r})]$ must be positive (Schwartz 1961a). For scattering at a finite energy, it is clear that we cannot make such a statement since there is a continous spectrum.

However, in a few isolated instances, it is possible to provide a bound on the phase shifts, and this has been discussed by Kato (1951) and Callaway (1980). The target wave function has to be exact and the one-body approximation is used. Rosenberg and Spruch (1959, and Rosenberg et al 1960) have provided a bound on the scattering length for zero energy scattering. The sign of $I[\delta\psi_l^t(\mathbf{r})]$ was able to be determined. This minimum principle for zero energy scattering can readily be applied and it can be used in many particle scattering problems provided that

the target wave function is known. Since it is valuable to know the bounds on the scattering length and how reliable the trial wave function is at zero energy, it is worth while to consider how the bound principle is established.

From equation (3.13), we obtain

$$a_{ex} = a_t + I[\psi_0^t(\mathbf{r})] - I[\delta\psi_0^t(\mathbf{r})] \tag{3.30}$$

where the scattering length is defined as,

$$a = -\lim_{k\to 0} \frac{\tan\delta}{k},$$

a_t = trial scattering length, a_{ex} = exact scattering length and, we are considering s-wave zero energy scattering.

The wave function satisfies the boundary conditions.

$$\Psi_0^{ex}(0) \text{ is finite}$$

$$\underline{\Psi}_0^{ex}(\underline{r}) \underset{r\to\infty}{\sim} \frac{1}{(4\pi)^{1/2}} \left\{1 - \frac{a_{ex}}{r}\right\}, \tag{3.31}$$

and

$$\Psi_0^t(0) \text{ is finite}$$

$$\underline{\Psi}_0^{t}(\underline{r}) \underset{r\to\infty}{\sim} \frac{1}{(4\pi)^{1/2}} \left\{1 - \frac{a_t}{r}\right\}$$

Denote $a_t - a_{ex}$ by δa,

$$\delta a = a_t - a_{ex} \tag{3.32}$$

To bound the error in the scattering length, the sign of $I[\delta\psi_0^t(\mathbf{r})]$ needs to be determined. The other terms on the right hand side equation (3.30) are quantities which can be calculated.

For simplicity, assume that the system has no bound states. (The argument can be extended to where the potential supports bound states, as explained in Rosenberg et al 1960, Bransden, 1983, pg. 69).

According to the Raleigh Ritz principle, if the system has no bound-states,

$$\int \phi H \phi \, d\tau \geq 0$$

$$\Rightarrow \int \phi L_0 \phi \, d\tau \geq 0 \tag{3.33}$$

(where $L_0 = \frac{2m}{\hbar^2} H$) for any normalisable function ϕ.

Although the function $\delta\psi_0^t(\mathbf{r})$ is not normalisable, the function

$$\delta\psi_0^t(\mathbf{r}) exp(-\lambda r)$$

is, so that the condition

$$I[\delta\psi_0^t(\underline{r}) e^{-\lambda r}] \geq 0 \tag{3.34}$$

holds, where

$$I[\delta\psi_0^t(\underline{r}) e^{-\lambda r}] = \int \delta\psi_0^t(\underline{r}) e^{-\lambda r} L_0 \delta\psi_0^t(\underline{r}) e^{-\lambda r} d\underline{r} .$$

It can be shown that: $I[\delta\psi_0^t(\underline{r}) e^{-\lambda r}] - I[\delta\psi_0^t(\underline{r})]$

$$= \int_0^\infty \delta f_0(r)(exp(-2\lambda r) - 1)\left(\frac{-d^2}{dr^2}\delta f_0(r) + \frac{2m}{\hbar^2} V(\underline{r}) \delta f_0(r)\right) dr$$

$$- \lambda^2 \int_0^\infty [\delta f_0(r)]^2 exp(-2\lambda r) dr \tag{3.35}$$

$$+ 2\lambda \int_0^\infty exp(-2\lambda r) \delta f_0(r) \frac{d}{dr} \delta f_0(r) dr$$

where we have defined f_0 by

$$\psi_0 = \frac{1}{(4\pi)^{\frac{1}{2}}} \frac{f_0(r)}{r}$$

since we are dealing with s-wave scattering. For simplicity we have taken $V(\mathbf{r}) = V(r)$. As $\lambda \to 0$,

$$\lim_{\lambda \to 0} I[\delta\psi_0^t(\mathbf{r})e^{-\lambda r}] - I[\delta\psi_0^t(\mathbf{r})] = 0, \tag{3.36}$$

and from (3.30, 3.33, 3.36),the condition

$$a_{ex} \leq a_t + I[\psi_0^t(\mathbf{r})] \tag{3.37}$$

is obtained.

Thus it can be seen that the scattering length satisfies the minimum principle, the object is to make the right hand side of equation (3.37) as small as possible.

Although in most instances, the Kohn variational principle for scattering at positive energies does not in principle satisfy the bound principle, it is found in practice (Schwartz, 1961a) that the phase shifts do monotonically converge as more terms are added to the trial function. Also, as more terms are added to the wave function, the agreement between the phase shift calculated by the Kohn and inverse Kohn variational methods improves and the difference between the stationary and trial phase shift lessens. With a suitable choice of the form of the trial functions the convergence in the stationary phase shifts can be quite rapid, so that it is possible to extrapolate to an infinite number of parameters and obtain essentially exact phase shift. One possible way of doing this is described §3.7.

3.3 The suitability of the variational method to describe the scattering of low-energy electrons by positronium.

The problem of scattering of low energy electrons by positronium, below the n=2 threshold should be well treated by a variational approach, since:

(a) the target (Ps) wave function is known exactly,

(b) e^--Ps is basically a very simple system,

(c) we are only considering one channel, that of elastic scattering.

(d) the variational method was successful for the corresponding $e^{\pm}-H$ scattering problems (Schwartz, 1961 a,b, Humberston 1982,4). Resonance structure was revealed in e^--H scattering in the vicinity of the n=2 and n=3 thresholds of hydrogen (Callaway, 1978).

The e^--Ps system closely resembles the e^--H system in that both systems consist of two electrons and a positive charge and that the target atom is degenerate. Ps^- and H^- are weakly bound ions and have only one bound-state. Thus, the form of the trial function for e^--H should presumably be suitable for the e^--Ps system, although extra care needs to be taken in the e^--H scattering problem since the centre of mass does not coincide with a particle.

The trial wave function used for singlet (+) and triplet (-) s-wave scattering takes the form (Schwartz, 1961a):

$$\underline{\Psi} = \psi + \chi, \qquad (3.39)$$

where

$$\psi = (1 \pm P_{12}) \frac{1}{\sqrt{2}} \frac{1}{(4\pi)^{1/2}} \phi_1(\underline{r}_2) \left[\frac{\sin kr_1}{kr_1} + \tan\delta_0^b \frac{\cos kr_1}{kr_1} (1 - e^{-\mu_2 r_1}) \right],$$

$$\chi = \frac{1}{\sqrt{2}} * \frac{1}{\sqrt{\pi}} * \frac{1}{4\sqrt{\pi}} \sum_{l,m,n \geq 0} C_{lmn} e^{-\mu/2(r_1+r_2)} r_{12}^l (r_1^m r_2^n \pm r_1^n r_2^m),$$

$$k_i + l_i + m_i \leq \omega, \quad k_i, l_i, m_i \in [0, 1, 2, \ldots, \omega]$$

and $\phi_H(r_2)$ is the normalized exact ground state wave function of hydrogen. P_{12} is the operator which interchanges the spatial co-ordinates $\mathbf{r}_1, \mathbf{r}_2, \mathbf{r}_i (i = 1, 2)$ being the position vectors of the two electrons with respect to the proton.

The non-linear parameter μ can be used to investigate the quality of the results. The short-range correlation term χ of the wave function $\chi$of the wave function Ψ is that which was used so successfully by Hylleraas to describe the bound- state of 2-electron system.

For the normalization of the wave-function, equation (3.39), the appropriate form for the Kohn variational principle is:

$$\tan \bar{\delta}_K = \tan \delta_0^t - k \int \Psi L \Psi \, d\tau_1 d\tau_2. \tag{3.40}$$

Humberston (1982, 4) has calculated the K matrix elements for the s-wave scattering of positrons by atomic hydrogen in the ore gap. (The ore gap is the energy interval between the Ps-formation threshold and the 1st excitation level of the target atom). This is a two channel problem: elastic scattering and Ps formation. Much of the formulation for the Ps formation channel can readily be adapted to the problem of e^--Ps scattering.

3.4 Choice of trial function for the elastic scattering of s-wave electrons by positronium, below the n=2 threshold.

The trial function Ψ_0^t should be carefully chose, from physical consideration, so that the error in the stationary phase shift ($\langle \delta\psi L \delta\psi \rangle$) will be small, otherwise spurious results could occur. It is important that the wave function is flexible so that it can represent well the various physical processes such as electron correlation, exchange and distortion of the target atom.

The trial wave function must be well behaved over all required space and satisfy the boundary conditions:

$$\psi_0^t(\rho \to 0) \; is \; finite,$$

$$\psi_0^t(\rho) \underset{\rho\to\infty}{\sim} \sqrt{\frac{k}{2}} \frac{1}{(4\pi)^{1/2}} \left\{ \frac{\sin k\rho}{k\rho} + \tan\delta_0^t \frac{\cos k\rho}{k\rho} \right\} \phi_{Ps}(r_2), \qquad (3.41)$$

(see fig.2.5 for the co-ordinate diagram) which is the correct normalization of the asymototic boundary condition for the Kohn variational principle in the form

$$\bar{R}_K = R_t - I[\psi_l^t(\mathbf{r}_2, \rho)], \qquad (3.42)$$

The $\frac{1}{\sqrt{2}}$ terms in (3.41) arises because of exchange and the positronium wave function $\phi_{Ps}(\mathbf{r}_2)$ is normalized so that:

$$\int \phi_{Ps}^*(\mathbf{r}_2)\phi_{Ps}(\mathbf{r}_2)\, d\mathbf{r}_2 = 1. \qquad (3.43)$$

In constructing a suitable trial function for e^--Ps, we made use of the experience gained by other workers who studied the scattering problems of $e^{\pm}$-H (Schwartz, 1961 a,b), e^+-H (Humberston, 1982,4), neutron-deuteron (Humberston, 1964).

Asymptotically, the wave function must be the product of the target wave function and the wave function of the scattered electron, suitably antisymmetrized.

We therefore chose to add a term of this form explicitly into the wave function and to let the other terms in the wave function to vanish asymptotically.

Our trial function, which contains three non-linear parameters (α, γ, μ), is of the form:

$$\Psi_0^{\pm t}(r_1, r_2, r_3) = \frac{1}{\sqrt{2}} \frac{1}{(4\pi)^{1/2}} \left[(1 \pm P_{12}) k^{1/2} \phi_{r_3}(r_2) \left\{ \frac{\sin kp}{kp} + \tan \delta_0^{\pm t} \frac{\cos kp}{kp} (1 - e^{-\mu p})^3 \right\} + \sum_{i=1}^{N'} c_i^{\pm} e^{-(\alpha s + \gamma r_3)} s^{k_i} t^{l_i} r_3^{m_i} \right] \quad (3.44)$$

where $s = r_1 + r_2, t = r_1 - r_2, r_3$ are the Hylleraas co-ordinates, see fig.2.5 for the $(r_1, r_2), (r_2, \rho)$ co-ordinate system.

The condition

$$k_i + l_i + m_i \leq \omega, \quad k_i, l_i, m_i \in [0, 1, 2, \ldots \omega]$$

was satisfied and l_i was taken to be even for the singlet state and odd for the triplet. The number of linear parameters N' in the singlet and in the triplet wave function for a given value of ω is shown in table 2.1. This wave function is correctly normalized to satisfy the boundary condition given by (3.41).

Using abbreviations, the wave function can be written in the form:

$$\Psi_0^{\pm} = S + \tan \delta_0^{\pm t} C + \chi \quad (3.48)$$

where χ is the closed channel component, and given by

$$\chi = \sum c_i^{\pm} \phi_i,$$

$$\phi_i = (2)^{-\frac{1}{2}} (4\pi)^{-\frac{1}{2}} e^{-(\alpha s + \gamma r_3)} s^{k_i} t^{l_i} r_3^{m_i}. \quad (3.49)$$

The open channel component is,

$$(S + \tan \delta_0^{\pm t} C), \quad (3.50)$$

where $S = S_1 \pm S_2$, $C = C_1 \pm C_2$, S_1 and C_1 are the direct terms

$$S_1 = (2)^{-\frac{1}{2}}(4\pi)^{-\frac{1}{2}} k^{\frac{1}{2}} \phi_{Ps}(r_2) \frac{\sin k\rho}{k\rho}$$

$$C_1 = (2)^{-\frac{1}{2}}(4\pi)^{-\frac{1}{2}} k^{\frac{1}{2}} \phi_{Ps}(r_2) \frac{\cos k\rho}{k\rho}(1 - e^{-\mu\rho})^3, \quad \text{and}$$

S_2 and C_2 are the exchange terms.

The term $(1 - e^{\mu\rho})^n$, where $n = 3$, is known as the shielding function and it tends to unity for $\rho \sim \infty$. Its purpose is to remove the singularity in the wave function which would otherwise be present. It is essential that the wave function is well behaved at the origin and that the condition,

$$\Psi_0^{\pm} \sim \rho^{l} (l=0), \quad as\, \rho \to 0,$$

is satisfied. The value of n is determined by ensuring that the wave function and kinetic energy is finite at the origin and the derivatives of these quantities with respect to the distance ρ is smooth, (see Humberston, 1964). This is especially important in the e^--Ps scattering problem because there is no particle at the centre of mass.

The value of μ is chosen so that the shielding function acts for a sensible range of ρ. Obviously the value of μ is dependent on the selected value of n. It is important that the shielding function does not 'kill' the irregular solution at too large a distance and thus prevent the short range correlation terms having an effect. Also, since the wave function is to be well-behaved, the shielding function must not come into action as such small distances to cause the wave function to have a steep slope near the origin ($\rho \to 0$). A careful choice of μ is required.

The short-range terms, the closed channel component of the total wave function are to describe the interaction when the three particles are close together, such as electron correlation, exchange and distortion of the target atom. Since the total wave function must satisfy the boundary conditions, equation (3.45) and (3.46), it is essential that the short-range correlation terms vanish asymptotically.

Suitable forms for the short-range terms are:

$$\chi_{lmn} = \sum_{l,m,n} d^{\pm}_{lmn} e^{-\alpha(r_1+r_2)} e^{-\gamma r_3} (r_1^m r_2^n \pm r_1^n r_2^m) r_3^l, \qquad (3.51)$$

and

$$\chi_{lmn} = \sum_{i=1}^{N'} c_i^{\pm} e^{-\alpha s} e^{-\gamma r_3} s^{k_i} t^{l_i} r_3^{m_i}, \tag{3.52}$$

where the interparticle distances r_1, r_2, r_3 are illustrated in fig. 2.5.

(The two forms, equation (3.51) and (3.52) are identical for the same value of ω.) In most scattering and bound-state calculations, the non-linear parameter (γ) has been set to zero. However, Humberston (1982) found that relatively little extra work is involved in including the term $e^{-\gamma r_3}$. The advantage of this term is that it gives extra flexibility to the wave function and allows for electron correlation through the electron-electron distance r_3. This is especially important for weakly bound systems such as H^- and Ps^-.

These short-range correlation terms were very successful in describing the bound-state of two electron systems. It, therefore, seems reasonable to use these terms in the total scattering wave function to represent the behaviour of the particles at close interparticle distances. Schwartz (1961a,b) used the form given by equation (3.51) in his e^--H scattering wave function and Humberston (1964) used the form given by equation (3.52) in the wave function to describe neutron-deutron scattering.

We chose to use the second form, given by equation (3.52) for the $e^{\pm}$-Ps scattering problem. This form for the short-range correlation term is probably easier to compute since with the other form you have to ensure that you do not include terms in the summation which give zero contribution. The $n = 1, n = 2$ radial wave functions for positronium are proportional to $e^{-0.5r_2}, e^{-0.25r_2}$ respectively. Therefore, a sensible value for the non-linear parameter α would lie between 0.25 and 0.5. Initially we set $\alpha = 0.40$.

The forms for the short-range term (equations 3.51 and 3.52) are convenient since it allows the wave function to be systematically improved by adding more terms in the expansion. As the set of functions,

$$e^{-\alpha s} e^{-\gamma r_3} s^{k_i} t^{l_i} r_3^{m_i},$$

form a complete set, in principle the inclusion of all such terms ($i = 1 \rightarrow \infty$) would yield the exact eigenfunction and phase shift.

3.5 Calculation

In determining the matrix element,

$$(\Psi_0^{\pm} L \Psi_0^{\pm})$$

the following individual matrix elements need to be evaluated:

$$(a)\ (SLS),\ (CLS),\ (SLC),\ (CLC),$$

$$(b)\ (SL\phi_i),\ (CL\phi_i),\ (\phi_i LS),\ (\phi_i LC),$$

$$(c)\ (\phi_i L \phi_j),$$

where the wave function is written in the form,

$$\Psi_0^{\pm} = \left\{ S + \tan\delta_0^t C + \sum_{i=1}^{N'} c_i^{\pm} \phi_i \right\},$$

and

$$S = S_1 \pm S_2, C = C_1 \pm C_2,$$

see equation (3.48).

The components of the wavefunction S_1, C_1, ϕ_i are given by equations (3.49) and (3.50). S_2 and C_2 being the exchange terms. These matrix elements are classified into groups (a), (b), (c).

Group (a) : open-open channel matrix elements.

These are matrix elements of L constructed between open channel components of the wave function. In terms of the direct and exchange part of the wave function, they are given by:

$$(SLS) = 2\Big\{ (S_1 L S_1) \pm (S_2 L S_1) \Big\}$$

$$(CLS) = 2\Big\{ (C_1 L S_1) \pm (C_2 L S_1) \Big\}$$

$$(SLC) = 2\Big\{ (S_1 L C_1) \pm (S_2 L C_1) \Big\},$$

where (S_1LS_1), (C_1LS_1), (S_1LC_1), (C_1LC_1) are formed from direct direct continuum functions, and (S_2LS_1), (C_2LS_1) (S_2LC_1), (C_2LC_1) from exchange-direct functions. It is important to note that the open-open and the direct-direct matrix elements are not hermitian, so that and $(SLC) \neq (CLS)$ and $(S_1LC_1) \neq (C_1LS_1)$. The direct direct matrix elements are of long-range, the integrand falling of as $\frac{1}{\rho^2}$ and not exponetially. Therefore, these matrix elements are evaluated analytically since convergence with the number of integration points using numerical quadrature would be slow.

Now

$$LS_1 = \frac{4}{3}\left(\frac{1}{r_3} - \frac{1}{r_1}\right)S_1, \tag{3.53}$$

so that $(S_1LS_1) = (C_1LS_1) = 0$ by symmetry in r_1 and r_3.

It can easily be shown that

$$(S_1LC_1) = (C_1LS_1) + 0.5 \tag{3.54}$$

by using Green's Theorm and thus

$$(SLC) = (CLS) + 1$$

$$(S_1LC_1) = 0.5 \tag{3.55}$$

and

$$(SLC) = 1.0.$$

Integrating the term (C_1LC_1) was straightforward.

The exchange direct matrix elements are hermitian; when Green's theorem is applied, the surface term vanishes. This can be readily understood, since when $\rho \to \infty$ in the direct term, the exchange term will vanish and conversely as $\rho \to \infty$. These integrations were performed using Gauss-Laguerre quadrature with 40 points.

Group (b): open-closed channel matrix elements.

These matrix elements of L are constructed from open channel functions with closed channel functions. They are hermitian, so that

$$(SL\phi_i) = (\phi_i LS),$$

$$(CL\phi_i) = (\phi_i LC).$$

We found it easier to compute $(\phi_i LS), (\phi_i LC)$ rather than the equivalent terms. The integrations were performed using Gauss-Laguerre quadrature with 40 points.

Group (c): closed-closed channel matrix elements.

These matrix elements of L are constructed from closed channel functions with closed channel functions. The term $L\phi_j$ was evaluated by expresssing the hamiltonian H in the form:

$$H = -\frac{1}{(s^2-t^2)r_3}\left\{(3s^2-t^2-2r_3^2)r_3\frac{\partial^2}{\partial s^2} + 8sr_3\frac{\partial}{\partial r_3}\right.$$

$$+(s^2-3t^2+2r_3^2)r_3\frac{\partial^2}{\partial t^2} - 8r_3 t\frac{\partial}{\partial t}$$

$$+(s^2-t^2)r_3\frac{\partial^2}{\partial r_3^2} + 2(s^2-t^2)\frac{\partial}{\partial r_3} + (r_3^2-t^2)2s\frac{\partial^2}{\partial s\partial r_3}$$

$$\left.+(s^2-r_3^2)2t\frac{\partial^2}{\partial r_3\partial t}\right\} - \frac{2}{(s+t)} - \frac{2}{(s-t)} + \frac{1}{r_3},$$

a.u.

Since $\phi_i L\phi_j$ is a polynomial of r_1, r_2, r_3, the integration can be performed exactly by Gauss-Laguerre quadrature (Froberg, 1979).

Once the components of $(\Psi_0^{\pm} L\Psi_0^{\pm})$ are formed, the linear parameters $(c_i, i = 1, 2, \ldots N)$, including the tangent of the trial phase shift, are evaluated by performing the operations,

$$\frac{\partial I}{\partial c_i} = 0, \quad i = 1, 2, \ldots N,$$

$$\frac{\partial I}{\partial R} = 1, \quad (R = \tan\delta^t) \tag{3.57}$$

which leads to solving the matrix equation,

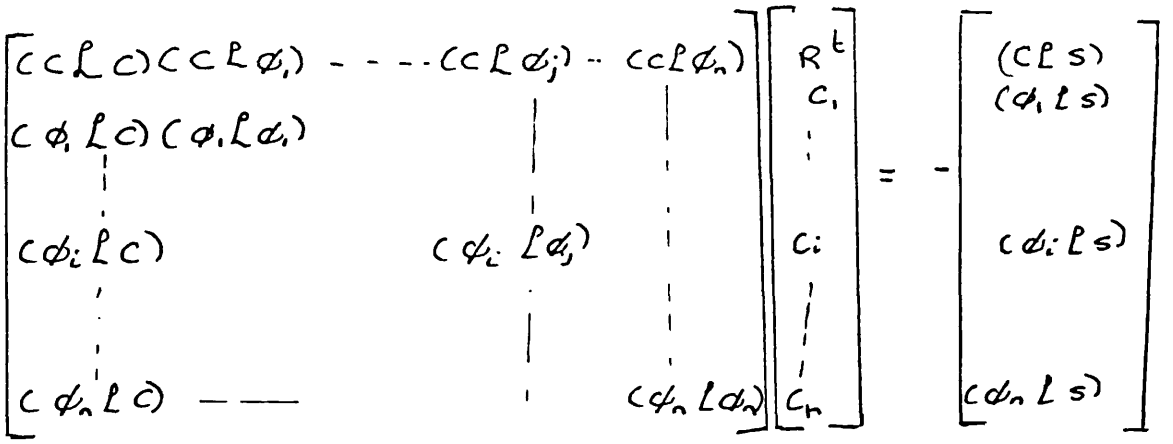

$$AX = -B \qquad (3.58)$$

where matrix A is symmetrical. In obtaining the matrix equation (3.58), the various symmetries of the individual matrix elements were used, such as equations (3.54), (3.55) and the hermitian properties of some of the matrix elements.

After determining the linear parameters and the trial phase shifts, the stationary phase shift, which is exact up to the 1st order term, is calculated from the Kohn variational principle, equation (3.24),

$$R_K = R_t - I[\psi_l^t(\mathbf{r}_2, \rho)],$$

since R_t and I are now known quantities.

Volume element and method of integration.

The volume element over all space is $d\mathbf{r}_1 d\mathbf{r}_2$ in terms of the $(\mathbf{r}_1, \mathbf{r}_2)$ coordinate system and $d\mathbf{r}_2 d\rho$ in terms of the $(\mathbf{r}_2, \rho)$ coordinate system. Since the s-wave function is spherically symmetric, this greatly simplies the necessary integration which has to be performed.

For the direct direct matrix element where the integration was performed analytically, $d\mathbf{r}_2, d\rho$ is the more convenient form of volume element to be used. These integrations are of the form,

$$\int f(r_2, \rho) d\tau$$

and the volume element reduces to

$$d\tau = (4\pi)^2 r_2^2 dr_2 \rho^2 d\rho.$$

For the integration of the other matrix elements, the volume element $d\mathbf{r}_1 d\mathbf{r}_2$ is used. Care has to be taken because of the presence of r_3 and the mixed co-ordinate systems, $(\mathbf{r}_2, \rho)$, $(\mathbf{r}_1, \hat{\rho})$ and $(\mathbf{r}_1, \mathbf{r}_2)$.

All of the matrix elements can be expressed in the form,

$$\int g(r_1, r_2, r_3)\, d\tau.$$

Consider the volume element,

$$d\tau_1 = r_1^2 dr_1 \sin\theta_1 d\theta_1 d\phi_1 r_2^2 dr_2 \sin\theta_2 d\theta_2 \phi_2$$

$$d\tau_1 = 8\pi r_1 r_2 r_3 dr_1 dr_2 dr_3,$$

where the ranges of integration are given by:

$$0 \leq r_1 \leq \infty, 0 \leq r_2 \leq \infty, |r_1 - r_2| \leq r_3 \leq |r_1 + r_2|.$$

Defining new variables x, y, z which are linear functions of r_1, r_2, r_3 the range of integration simplifies. The volume element becomes:

$$d\tau_1 = \frac{8\pi^2}{4} r_1 r_2 r_3 dx dy dz,$$

where

$$x = r_1 + r_2 - r_3,$$

$$y = r_2 + r_3 - r_1,$$

$$z = r_3 + r_1 - r_2,$$

and the range of integrations are,

$$0 \leq x \leq \infty, 0 \leq y \leq \infty, 0 \leq z \leq \infty.$$

Thus, the 6-dimensional integrals are reduced to 3-dimensional integration over the interparticle distances (or simple functions of them).

This integration, for all the matrix elements (except the direct direct matrix element) is performed numerically using the Gauss-Laguerre quadrature.

3.6 Structure of program and computational details.

(i) Flow chart of program

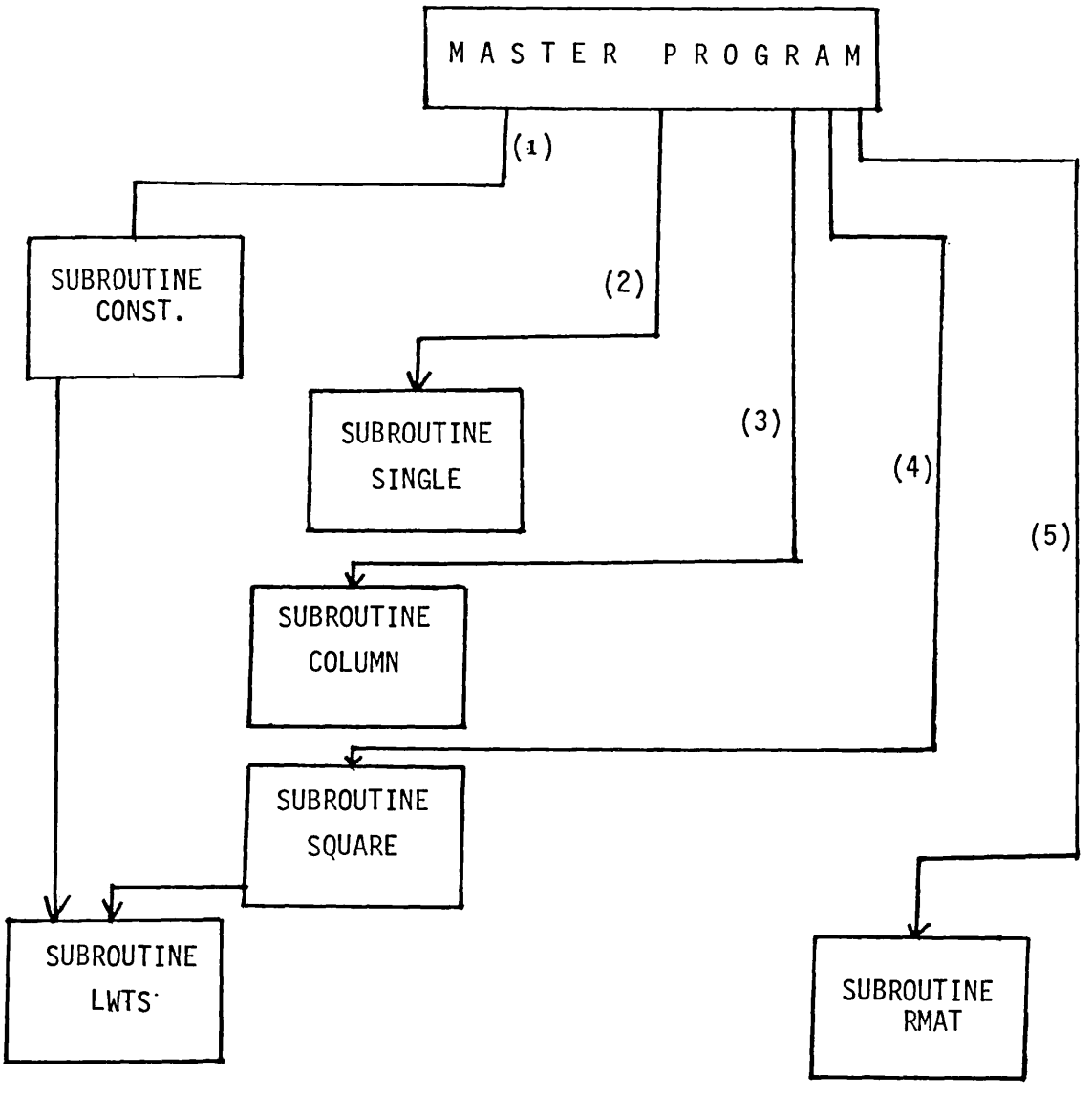

(ii) Layout and function of the sub programs.

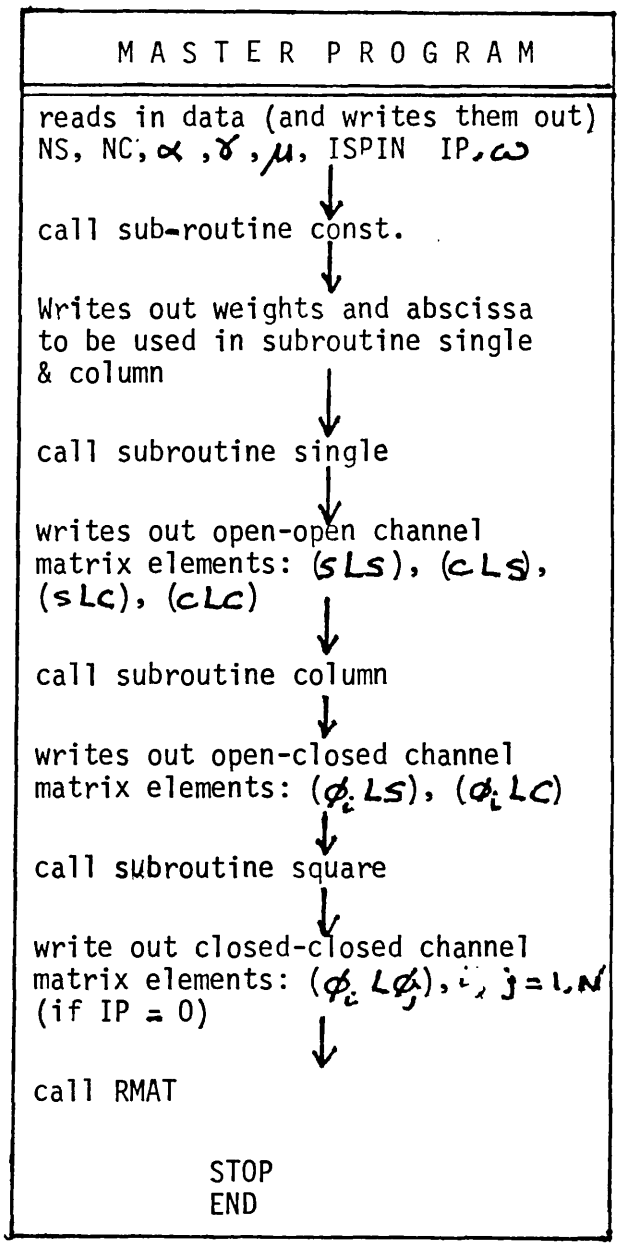

DATA

NS = number of integration points to use in exchange-direct matrix elements, of subroutine single.

NC = number of integration points to use in open-channel matrix elements, of subroutine column.

α, γ, μ, non-linear parameters, see equation (3.43)

ω - see text

IP: used to switch on or off the write statement for $(\phi_i L \phi_j)$

SUBROUTINE CONST.

Calculates various constants which are required in program

↓

Call subroutine LWTS (which calculates weights and abscissa for a given NS, NC)

↓

Generates N (the total number of linear parameters), and the set $\{k_i, l_i, m_i\}$ $i = 1, N$

↓

Select members of this set in which l_i is even for singlet (or odd for triplet).

↓

Determines total number of linear parameters, N', in this selected subset of $\{k_i, l_i, m_i\}$

↓

reads in the number of energies to be considered (NK), and the values of k, the wave number of the electrons in the C.O.M. frame.

SUBROUTINE SINGLE

Evaluates open-open channel matrix elements
$(SLS), (CLS), (SLC), (CLC)$

(a) The direct-direct matrix element
$((S_1LS_1), (C_1LS_1), (S_1LC_1), (C_1LC_1))$ are set to their values.

(b) The integration with respect to the variables x,y,z for the exchange-direct matrix elements $((S_2LS_1), (C_2LS_1), (S_2LC_1), (C_2LC_1))$ is performed using Gauss-Laguerre quadrature with NS intergration points. The weights and abscissa are supplied by LWTS via subroutine const.

SUBROUTINE COLUMN

Evaluates open-closed channel matrix elements,
$(\phi_i LS)$, $(\phi_i LC)$.

The integration with respect to x, y, z is performed using Gauss-Laguerre quadrature with NC number of integration points.

SUBROUTINE SQUARE

Evaluates closed-closed channel matrix elements,
$(\phi_i L\phi_j)$ and $(\phi_i \cdot \phi_j)$.

The integration with respect to x,y,z is performed using Gauss-Laguerre quadrature.
No. of integration points used = $\omega + 2$

SUBROUTINE LWTS
Calculates weights and abscissa for Gauss-Laguerre quadrature for a given number of integration points.

SUBROUTINE RMAT
Constructs matrix A and B (see equation (3.58) from the indididual matrix elements. Solves AX = B to determine the linear parameters $(c_i, i=1,..N)$ and $\tan\delta_0^{\pm t}$ Obtains stationary phase shifts from using: $\tan\bar{\delta}_K = \tan\delta_t - I[\psi_0^t(r_t,\rho)]$, see equation (3.24) Also calculates $\tan\delta_t(IK)$, $\tan\bar{\delta}(IK)$ from using the Inverse Kohn variational method. From the stationary phase shifts, calculates s-wave partial elastic cross section.

(ii) Computational details

The structure of this program was based on that which was used by Humberston (1982, 4) for the e^+-H variational calculation. Details of the e^+-H program can be found in Brown (1986). The calculations were performed on the U.L.C.C. Cray1s.

3.7 s-wave scattering results (for $k \leq 0.5a_0^{-1}$) together with a discussion.

(i) The tangent of the s-wave stationary phase shift, as ω is increased from 2 to 7, is shown in table 3.2, fig. 3.1 for the singlet case and in table 3.3, fig. 3.2 for the triplet. Reasonable convergence is obtained over most of the energy range with the choice of non-linear parameters,

$$\alpha = 0.40, \gamma = 0.05, \mu = 0.5.$$

These non-linear parameters have not been optimized since it was felt that the convergence was sufficiently good and it has been stated by Humberston (1982,4), that it is better to invest the computational effort in increasing the number of linear parameters. However, optimized non-linear parameters would undoubtely improve the convergence. It is noted that the convergence is fairly slow for k in the range $0.10 \leq k \leq 0.25a_0^{-1}$ for the singlet scattering and for k in the range $0.30 \leq k \leq 0.40a_0^{-1}$ for the triplet. At $k = 0.5a_0^{-1}$ the results are somewhat peculiar and this is to be expected since it corresponds to threshold energy. Very close to threshold, the convergence deteriotes. The reason for this being:

(a) the presence of Feshbach resonances (Ho, 1979,84) and

(b) as explained by Schwartz (1961a), the wave function needs to allow for long-range effects near the threshold, and this cannot properly be done with the set of short-range terms. Above the n=2 threshold, the wave function will have a term $e^{i\acute{k}r}$, where $\acute{k} = (k - 0.5)a_0^{-1}$ so that just below threshold, k$'$is a small imaginary number which means that the true wave function will have a long-range tail.

We followed Humberston (1982,4) in extrapolating the phase shifts to infinite ω, using an assumed power law behavior, namely:

$$\tan\delta(\omega) = \tan\delta(\omega = \infty) + \frac{c}{\omega^p}, \tag{3.59}$$

where p and c are estimated empirically and depend on the energy and whether it is singlet or triplet state . For our results, the value of p lies in the range, $1 \leq p \leq 4.5$. The higher the value of p, the more rapid the convergence enabling $\tan\delta$ to be extrapolated to infinite ω with confidence. Convergence is slow if $p = 1$, and $p = 2$

corresponds to 'acceptable' convergence. Fig.3.3 displays the results for $k = 0.40a_0^{-1}$ and for the triplet state, where a linear relationship is obtained for $p = 2$. The singlet and triplet phase shifts calculated with $\omega = 7$ and the extrapolated phase shifts are shown in table 3.4 for the range of wavenumbers $0.05 \leq k(a_0^{-1}) \leq 0.50$.

In fig. 3.4, the extrapolated singlet and triplet phase shifts are plotted as a function of the wave number k. For the triplet phase shifts, π has been added in order to display the triplet results on the same graph as the singlet. In fig. 2.1, the s-wave singlet and triplet s-wave variational results for e^--H, calculated by Schwartz (1961 a,b), are illustrated for k below the n=2 threshold ($k = 0.866a_0^{-1}$). It is remarkable the close similarity between the e^--H and the e^--Ps systems. The Kohn variational method determines the tangent of the phase shift, and not the phase shift directly. We learnt from the static-exchange results, Chapter 2, that the singlet results tend to π as k goes to zero which is in accord with Levinson's theorem since Ps^- has one bound-state which is a singlet state. The same is true for singlet e^--H scattering. However, it should be noted that the triplet phase shift tend to zero for the e^--Ps as k tends to zero, and not to π which is the case for e^--H. The reason for this is discussed in Chapter 2.

(ii) Singlet and triplet scattering lengths.

At very low energies,$k \leq 0.1a_0^{-1}$, the convergence of $\tan\delta$ with respect to ω is slow. Even by $\omega = 10$, the phase shifts have not reached their fully converged values, see figs. 3.5 and 3.6 and table 3.6. This means that the value of the extrapolated phase shift is predicted with a large degree of uncertainity. In fig. 3.7 and 3.8 we show that a linear relationship is established between $\tan\delta$ and $\frac{1}{\omega^p}$ when $p = 1$ for the singlet case at $k = 0.01a_0^{-1}$ (fig. 3.7) and for the triplet case at $k = 0.03a_0^{-1}$ (Fig.3.8). To obtain the scattering lengths, we used the effective range formula (O'Malley et al, 1961)

$$\tan\delta_0 = Ak + Bk^2 + Ck^3 \ln k \qquad (3.60)$$

and fitted this to the phase shift obtained at $k = 0.01, 0.02, 0.03a_0^{-1}$ to obtain the constants A, B, C. The phase shift evaluated at $\omega = 10$ and $\omega = \infty$ were used to determine the scattering length $(-A)$, these results being shown in table 3.5.

The terms $\tan\delta_0$ and Ak are of comparable size. This means that the constants B and C are very sensitive to the actual value of the phase shifts. Thus, although we believe our estimate of the scattering length to be reliable, we can not confidently determine the constants B and C until the phase shifts at these very low energies is improved. In fact, we were unable to predict the values of B and C given by O'Malley for the effective range formula, namely:

$$B = -\frac{\pi}{3}\alpha_d, \quad C = \frac{4}{3}\alpha_d A.$$

In table 3.5, a comparison is made of our singlet scattering length with the value calculated by Bhatia and Drachman (1985) using their Ps^- bound-state wavefunction (Bhatia and Drachman, 1983).

The singlet scattering length satisfies the formula,

$$\frac{1}{a} = \gamma - \frac{1}{2}r_0\gamma^2 \tag{3.61}$$

where $\epsilon_b = \frac{3\gamma^2}{4} a.u.$ is the binding energy in a.u., r_0 is the effective range (a.u.) and is determined from

$$r_0 = \frac{1}{\gamma} - \frac{1}{4\pi C^2}, \tag{3.62}$$

C being a constant evaluated from the normalization of the bound-state wave function.

Our estimation of the scattering length $(-A)$ and the constants B and C could probably be improved by using a least square fit to formulas (3.60). The extrapolated phase shifts with the smallest degree of uncertainity being weighed the most heavily. A technique to perform this operation is described by McDowell (1971).

However, it would be better to perform a zero-energy calculation, such as that by Humberston and Wallace (1972) for e^+-H and by Spruch (1960) and Schwartz (1961a) for $e^\pm$-H, since this would provide a strict bound on the scattering length. The zero-energy wave function should allow for long-range polarization (Schwartz, 1961b). This is discussed in more detail at the end of chapter 4.

3.8 ^{1,3}S resonances.

The Ps^- ion supports a system of doubly excited states which occur just below the various thresholds of the Ps atom. Like for H^-, the dipole potential between the ns-np degenerate states of the parent atom is responsilbe for the occurence of the autoionizing resonances. The dipole polarizability of Ps is large, $36a_0^3$, which is eight times that for hydrogen.

Ho (1979, 1984) has calculated some low-lying doubly excited resonances of Ps^- associated with the n=2 up to n=5 Ps thresholds. He used the complex rotational method (1983b) together with the use of the stabilzation method (Hazi and Taylor, 1970; Fels and Hazi 1972).

The position of the ^{1,3}S resonances, in terms of energy, for Ps^- is scaled by the reduced mass of Ps compared to the corresponding resonaces found in H^-. However, Ho (1984) noted that the singlet resonances have lower energies than the triplet counterparts when they have the same dominant configuration. The reverse is true for H^- and He. This difference can be explained by the fact that the polarization potential, which is atttractive, is much larger for Ps than for H and He^+.

Botero and Greene (1985) have determined the lowest $^1S^e$ resonance of Ps^- using the adiabatic treatment in hyperspherical coordinates. This method provided upper and lower bounds on the energy, although they are not true bounds for doubly excited states.

Using the 'core pair' approximation, Arifov et al (1977) has also calculated the lowest $^1S^e$ resonance associated with the n=2 threshold of Ps.

In all these calculations, the bound-state part of the full wave function has been used to determine the resonance parameters. This is valid provided the interaction of the doubly excited state with the continuum can be neglected. Since these resonances are extremely narrow, this is shown to be the case.

We expected that our s-wave scattering wave function would reveal some resonance structure in e^--Ps scattering. This wavefunction is very flexible, the inter-electronic distance is explicity included by the term $r_3^n e^{-\gamma r_3}$. The lowest $^1S^e$ resonance was detected by running the program with a very fine energy mesh ($\Delta k \sim$

0.0001) and with $\omega = 7$ which corresponds to 70 linear parameters in the singlet wave function. In fig. 3.9, this resonance is shown.

Our method does not easily enable us to classify the configurations of the resonances associated with the various thresholds of Ps. We followed Ho (1979, 1984) by using the configuration obtained from the corresponding H^- system. The lowest $^1S^e$ resonance has the configuration $(2s)^2$. However, it should be realized that a single particle classificaion scheme is not really suitable to describe the doubly excited resonances for a system such as Ps^-. A description of more appropriate classification scheme is discussed by Herrick (1982), Lin (1983) and Botero and Greene (1985).

We calculated the position and width of the $^1S^e$ resonance by using a program written by Dr. L.A. Morgan. In this program, the Breit-Wigner formula is used in the form,

$$\acute{\delta}(E) = \tan^{-1} \frac{\Gamma_{res}}{2(E - E_{res})} + \sum_{i=0}^{2} a_i (E)^i \tag{3.63}$$

where

$$\delta^{res} = \tan^{-1} \frac{\Gamma_{res}}{2(E - E_{res})},$$

E_{res} = position of the resonance (units of energy) and Γ_{res} =width of the resonance (full width at half height).

The summation in equation (3.63) is to represent the slowly varying, non-resonant phase shift, i.e the background phase shift.

An initial guess of the quantities E_{res}, Γ_{res}, a_0, a_1, a_2 needs to be made, and then the program, by using the NAG (mark 11, 1983) routine E04 FDF, calculates the minimum of the function,

$$\acute{\delta}(E) - \delta(E)$$

where $\delta(E)$ is the total phase shift obtained from our scattering calculation. Thus, the resonance parameters a_0, a_1, a_2 are determined by a least square fit.

In table 3.7, a comparison is made of the resonance parameters which we calculated for the lowest $^1S^e$ resonance with the results of other authors. In this table, the energy position is measured from the ground state energy.

Reasonable agreement is obtained in the position and width of the resonance determined from the various methods. As can be seen, the widths of the resonance is extremely narrow, about 40 times smaller than the widths of the corresponding resonance in H^-.

Probably, the most reliable determination of the position of the $(2s)^2\ ^1S^e$ resonance is due to Ho (1979, 84), (see table 3.7) because although he only used 1 non-linear parameter, this was optimized to the n=2 state. He also used 203 terms in the Hylleraas wavefunction.

We could probably improve our determination of the resonance parameters for the $^1S^e$ resonance, as well as increasing our chance of detecting other resonances, by increasing ω and optimizing the two non-linear parameters appropriate to the n=2 threshold.

There are other ways in which our present wave function could be improved in the vicinity of the n=2 threshold, for instance:

(a) adding more flexibilty into the short-range terms by having non-linear parameters associated with the two electrons. A possible short-range term would be of the form

$$(e^{-\alpha r_1}e^{-\beta r_2}r_1^l r_2^m \pm e^{-\beta r_1}e^{-\alpha r_2}r_1^m r_2^l)r_3 e^{-\gamma r_3}, \qquad (3.64)$$

and this would be suitable to use in search of resonances of the configuration 2sns, where $n \neq 2$.

(b) Adding long-range terms suggested by Seiler et al (1971),

$$\frac{\sin k\rho}{\rho^2}, \quad \frac{\cos k\rho}{\rho^2}.$$

However, we feel that it would be better to spend this extra effort by adding the n=2 states of positronium explicity to the wave function.

3.9 Binding energy of Ps^-.

The short-range correlation terms of the full s-wave scattering wave function was used to represent the bound-state. The total ground-state energy was calculated by using the Rayleigh Ritz variational method and the NAG (mark 11, 1983) routine F02 AEF which solves the matrix equation

$$AX = \lambda BX \tag{3.65}$$

where

$$A_{ij} = \langle \phi_i H \phi_j \rangle$$

$$B_{ij} = \langle \phi_i / \phi_j \rangle,$$

X_i the eigenvectors, and λ the eigenvalues, the lowest of these being the ground-state energy. Also, ϕ was normalized so that

$$\langle \phi_i / \phi_j \rangle = 1. \tag{3.66}$$

This calculation was performed for two reasons, namely:

(1) It provided a check on subroutine square, which is the subroutine which evaluates the closed closed channel matrix element. The binding energy has been independently determined by Ho (1983a) and Bhatia and Drachman (1983) among others.

(2) a very good bound-state wave function is required for the photodetachment cross section.

Table 3.8 compares our value for the binding energy with that determined by other workers. Our most accurate value agrees to within 0.004% of the best value to date which is that obtained by Bhatia and Drachman (1983).

For this calculation, we varied the non-linear parameters α and γ using 70 linear parameters in the wave function in order to optimize the binding energy. Our optimum choice for the non-linear parameter is:

$$\alpha = 0.30, \gamma = 0.048 ,$$

and in table 3.8 the variation of the binding energy with ω for this choice of non-linear parameters is shown. Even by $\omega = 8$, the binding energy has not reached its fully converged result.

3.10 Conclusions.

In this chapter, accurate singlet and triplet phase shifts for the scattering of low energy electrons by positronium, below the n=2 thresholds have been presented. Our value for the singlet scattering length is in good agreement with that calculated independently by Bhatia and Drachman (1985). The bound-state part of the full scattering wave function predicts a value for the binding energy of Ps^- which agrees to within 0.004% of the best value to date (Bhatia and Drachman, 1983). This bound-state wave function should be good enough to use in the photodetachment calculation where the cross section is very sensitive to the value of the electron affinity predicted by the wave function.

At very low energies, convergence could be improved by adding long-range energy dependent terms which take into account polarization effects. This would improve our determination of the scattering length. However, it would be worthwhile to do a zero-energy calculation in order to obtain a true bound on the scattering length.

Very close to the n=2 threshold convergence started to deteriote and this was due to the present wave function being insufficiently good to describe the long-range behaviour which arises because of the presence of the threshold. Possible long-range terms to add to the wave function, are of the form (Seiler et al. 1971),

$$\frac{\sin k\rho}{\rho^2}, \quad \frac{\cos k\rho}{\rho^2}.$$

It is worthwhile to improve the wave function in this energy region in the hope of revealing some more of the resonance structure. With the present wave function, the lowest $^1S^e$ resonance was detected and reasonable agreement was obtained with Ho (1979, 84) for the resonance parameters. The resonance was extremely narrow ($\approx 1 meV$). Methods to improve the wave function in the vicinity of the n=2 threshold have been discussed in section 3.8. Probably the most significant improvement to make would be to explicity include the n=2 states of positronium. This would enable the present calculation to be extended up to the n=3 threshold.

Chapter 4

p-wave variational calculation and possible long-range energy dependent terms.

4.1 Introduction.

The elastic scattering of low-energy p-wave electrons by positronium, below the n=2 threshold has been investigated by the Kohn and inverse Kohn variational methods. This calculation was performed since:

(a) An accurate ^1P continuum wavefunction is required in the determination of the photodetachment cross section.

(b) From the S.E.1 and S.E. results (chapter 2), it was seen that the dominant contribution to the total and differential cross section over most of the energy range came from the $^{1,3}P$ phase shifts. Therefore, these phase shifts need to be accurately determined.

Since our primary aim in this investigation of the Ps^- system was to evaluate reliably the photodetachment cross section, we concentrated in the p-wave study in producing an accurate ^1P wave function.

The theory of the Kohn variational method, which was developed in section 3.2 is applicable to the p-wave. Much of the p-wave calculation to determine the phase shift is very similar to the s-wave calculation discussed in section 3.4. Therefore in this chapter, I shall just outline where the p-wave differs from the s-wave. This is done in section 4.2, where a description of the $^{1,3}P$ wavefunction is given.

In section 4.3, the variation of the ^1P phase shift with the non-linear parameters and the convergence of the $^{1,3}P$ phase shifts with the number of linear parameters is examined. Our best results are presented, discussed and compared with those obtained for e^--H scattering (Armstead, 1968).

The convergence of the p-wave phase shifts at very low energies, with respect to the number of linear parameters in the trial function, was found to be slow. In section 4.4, a discussion is given of possible long-range energy dependent terms which could be added to the wave function to improve convergence. Long-range

energy dependent terms would be useful for other partial waves, not just the p-wave. It is especially interesting to consider the effect of long-range terms for zero-energy s-wave scattering, since the scattering length is a bound quantity and thus such a calculation could be used to determine the quality of the long-range terms.

In section 4.5, the behaviour of the ^{1}P phase shifts just below the n=2 threshold is examined. Possible ^{1,3}P resonances are reported together with a brief discussion on how our variational wave function could be improved to describe the n=2 threshold more adequately.

Finally, in section 4.6, conclusions are stated and suggestions are made on where further work is required.

4.2 The ^{1,3}P trial function and the p-wave calculation.

The p-wave function contains one unit of angular momentum, and needs to be symmetric under interchange of the two electrons for the singlet state and antisymmetric for the triplet state. Also, the scattering is symmetric about the y-z plane, where the z-direction is parallel to the direction of the incoming particle, although it does depend on the polar angle θ.

Our p-wave trial function is of the form (Ward et al,1986 a,b,c)

$$\Psi_1^{\pm}(r_1,r_2,r_3) = 2^{-1/2}(1 \pm P_{12})\, k^{1/2}\, \phi_{1s}(r_2)\, Y_{10}(\hat{r}_1)$$
$$[J_1(kr_1) - \tan\delta_1^{\pm t}\, n_1(kr_1)(1-e^{-\mu r_1})^n]$$
$$+ 2^{-1/2}\left[Y_{10}(\hat{r}_1)\, r_1 \pm Y_{10}(\hat{r}_2)\, r_2\right] \sum_{i=1}^{N_1-1} c_i^{\pm} e^{-\gamma^{\pm} r_3 - \alpha^{\pm} s}\, s^{k_i}\, t^{l_i}\, r_3^{m_i}$$
$$+ 2^{-1/2}\left[Y_{10}(\hat{r}_1)\, r_1 \mp Y_{10}(\hat{r}_2)\, r_2\right] \sum_{j=N_1}^{N} d_j^{\pm} e^{-\gamma^{\pm} r_3 - \alpha^{\pm} s}\, s^{k_i}\, t^{l_i}\, r_3^{m_i} \qquad (4.1)$$

where n=5,

$$k_i + l_i + m_i \leq \omega, \quad k_i, l_i, m_i \in [0, 1, 2, \ldots\ \omega]$$

and l_i must be even in the first summation and odd in the second. In this expression, the upper (lower) sign refers to the singlet (triplet) state and the co-ordinates

used are described in section 3.4 and shown in fig.2.5. The total number of linear parameters N is shown in table 3.1 for a given ω, the number of terms of even $l_i(=N_1-1)$ corresponds to the total number of terms in the singlet s-wave function for that value of ω. We optimized the three non-linear parameters contained in this wavefunction, for the singlet state.

The wave function is correctly normalized for the Kohn variational principle written in the form:

$$\bar{R}_K = R_t - I[\psi_l^t(\mathbf{r}_2,\boldsymbol{\rho})] \tag{4.2}$$

(see equations (3.21) and (3.44) and the boundary conditions ,which are

$$\Psi_1^{\pm}(\rho \to 0) \sim \rho^l \tag{4.3}$$

$$\Psi_1^{\pm} \underset{\rho\to\infty}{\sim} 2^{-\frac{1}{2}} k^{\frac{1}{2}} \phi_{Ps}(r_2) Y_{10}(\hat{\rho})[j_1(k\rho) - \tan\delta_{1t}^{\pm} n_1(k\rho)]$$

are satisfied.

We took n=5 in the shielding function to ensure that the wave function and kinetic energy was well behaved at the origin. For the short-range terms, the distance ρ multiplied by the spherical harmonic since it is essential that as $\rho \to 0$ the wave function is single valued. As with the s-wave, the interaction between the two electrons is represented by the term $e^{-\gamma r_3} r_3^{m_i}$.

The wave function can be written in the abbreviated form:

$$\Psi_i^{\pm} = SY + \tan\delta_{1t}^{\pm} CY + \chi \tag{4.4}$$

where

$$SY = S_1Y_1 \pm S_2Y_2, \quad CY = C_1Y_1 \pm C_2Y_2,$$

$$S_1Y_1 = \sqrt{\frac{k}{2}}\phi_{Ps}(r_2)Y_{10}(\hat{\rho})j_1(k\rho),$$

$$S_2Y_2 = \sqrt{\frac{k}{2}}\phi_{Ps}(r_1)Y_{10}(\hat{\rho})j_1(k\rho),$$

$$C_1Y_1 = -\sqrt{\frac{k}{2}}\phi_{Ps}(r_2)Y_{10}(\hat{\rho})n_1(k\rho)(1-e^{-\mu\rho})^5,$$

$$C_2Y_2 = -\sqrt{\frac{k}{2}}\phi_{Ps}(r_1)Y_{10}(\hat{\rho})n_1(k\rho)(1-e^{-\mu\rho})^5,$$

$$\chi = 2^{-1/2}\left[Y_{10}(\hat{\rho})\rho \pm Y_{10}(\hat{\rho}')\rho'\right]\sum_{i=1}^{N1-1} f_i$$

$$+ 2^{-1/2}\left[Y_{10}(\hat{\rho})\rho \mp Y_{10}(\hat{\rho}')\rho'\right]\sum_{i=N1}^{N} f_i ,$$

where $f_i = c_i e^{-\alpha s - \gamma r_3} s^{k_i} t^{l_i} r_3^{m_i}$, l_i even for $i = 1 \rightarrow N1-1$, odd for $i = N1 \rightarrow N$. As with the s-wave case, the individual matrix elements to consider for the determination of $(\Psi_1^{\pm} L \Psi_1^{\pm})$ when the wavefunction is written in the form (4.4), can be classified into three groups, namely:

Group (a): open-open channel matrix elements.

$$(SYLSY) = 2\Big\{(S_1Y_1LS_1Y_1) \pm (S_2Y_2LS_1Y_1)\Big\}$$

$$(SYLCY) = 2\Big\{(S_1Y_1LC_1Y_1) \pm (S_2Y_2LC_1Y_1)\Big\} \qquad (4.5)$$

$$(CYLSY) = 2\Big\{(C_1Y_1LS_1Y_1) \pm (C_2Y_2LS_1Y_1)\Big\}$$

$$(CYLCY) = 2\Big\{(C_1Y_1LC_1Y_1) \pm (C_2Y_2LC_1Y_1)\Big\}$$

open-open direct-direct exchange-direct

Group (b): open-closed channel matrix elements

$$((Y_{10}(\hat{\rho})\rho + Y_{10}(\hat{\rho}')\rho')f_i \; LS_1) = (S_1 L(Y_{10}(\hat{\rho})\rho + Y_{10}(\hat{\rho}')\rho')f_i)$$

$$((Y_{10}(\hat{\rho})\rho - Y_{10}(\hat{\rho}')\rho')f_i \; LS_1) = (S_1 L(Y_{10}(\hat{\rho})\rho - Y_{10}(\hat{\rho}')\rho')f_i)$$

(4.6)

$$((Y_{10}(\hat{\rho})\rho + Y_{10}(\hat{\rho}')\rho')f_i \; LC_1) = (C_1 L(Y_{10}(\hat{\rho})\rho + Y_{10}(\hat{\rho}')\rho')f_i)$$

$$((Y_{10}(\hat{\rho})\rho - Y_{10}(\hat{\rho}')\rho')f_i \; LC_1) = (C_1 L(Y_{10}(\hat{\rho})\rho - Y_{10}(\hat{\rho}')\rho')f_i)$$

(c)closed-closed channel matrix elements

$$((Y_{10}(\hat{\rho})\rho + Y_{10}(\hat{\rho}')\rho')f_i \; L(Y_{10}(\hat{\rho})\rho + Y_{10}(\hat{\rho}')\rho')f_i)$$

$$((Y_{10}(\hat{\rho})\rho + Y_{10}(\hat{\rho}')\rho')f_i \; L(Y_{10}(\hat{\rho})\rho - Y_{10}(\hat{\rho}')\rho')f_i)$$

(4.7)

$$((Y_{10}(\hat{\rho})\rho - Y_{10}(\hat{\rho}')\rho')f_i \; L(Y_{10}(\hat{\rho})\rho + Y_{10}(\hat{\rho}')\rho')f_i)$$

$$((Y_{10}(\hat{\rho})\rho - Y_{10}(\hat{\rho}')\rho')f_i \; L(Y_{10}(\hat{\rho})\rho - Y_{10}(\hat{\rho}')\rho')f_i)$$

The direct direct matrix elements had to be performed analytically because they were of long-range.

Since

$$LS_1 = \frac{4}{3}\left(\frac{1}{r_3} - \frac{1}{r_1}\right),$$

and

$$(C_1 Y_1 LS_1 Y_1) = (S_1 Y_1 LC_1 Y_1) - 0.5$$

we have

$$(S_1 Y_1 LS_1 Y_1) = (C_1 Y_1 LS_1 Y_1) \equiv 0 \tag{4.8}$$

and

$$(S_1 Y_1 LC_1 Y_1) = 0.5.$$

The analytical integration required for $(C_1 Y_1 L C_1 Y_1)$ was straight forward.

In the evaluation of the other matrix elements we made maximum use of the s-wave analysis and program as well as the various symmetries of the p-wave problem. The internal variables of integration used in the s-wave program were r_1, r_2, r_3. We therefore used:

$$d\tau = dr_1 dr_2$$

as the volume element over all space rather than the equivalent form of $d\tau = dr_2 d\rho$. When this form of volume element $d\tau$ is used and integration is performed over the external variables in a manner discussed below, then the remaining integral for the closed-closed channel matrix element will be a polynomial in r_1, r_2, r_3. Hence, this integration with respect to r_1, r_2, r_3 (or x, y, z) for the closed-closed channel matrix elements can be performed exactly by Gauss-Laguerre quadrature.

We note that

$$(Y_{10}(\hat{\rho})\rho + Y_{10}(\hat{\rho}')\rho') = \sqrt{\frac{3}{4\pi}} \frac{1}{2}(r_1 \cos\theta_1 + r_2 \cos\theta_2)$$

(4.9)

and

$$(Y_{10}(\hat{\rho}')\rho' - Y_{10}(\hat{\rho}')\rho') = \sqrt{\frac{3}{4\pi}} \frac{3}{2}(r_1 \cos\theta_1 - r_2 \cos\theta_2)$$

Using the co-ordinate system $(\mathbf{r}_1, \mathbf{r}_2)$, the kinetic-energy operator can be written in

the form:

$$\hat{T} = -\nabla^2_{\underline{r}_1} - \nabla^2_{\underline{r}_2} - \nabla_{\underline{r}_1} \cdot \nabla_{\underline{r}_2} ,$$

so that

$$\hat{T}\left(Y_{10}(\hat{\underline{\rho}})\rho + Y_{10}(\hat{\underline{\rho}}')\rho'\right) f_i$$

$$= \sqrt{\frac{3}{4\pi}} \frac{1}{2} \left\{ (r_1 \cos\theta_1 + r_2 \cos\theta_2) \hat{T} f_i - \cos\theta_1 \, 3 \left.\frac{\partial f_i}{\partial r_1}\right|_{\substack{r_2 \\ r_3}} - \cos\theta_2 \, 3 \left.\frac{\partial f_i}{\partial r_2}\right|_{\substack{r_1 \\ r_3}} \right\},$$

and (4.10)

$$\hat{T}\left(Y_{10}(\hat{\underline{\rho}})\rho - Y_{10}(\hat{\underline{\rho}}')\rho'\right) f_i$$

$$= \sqrt{\frac{3}{4\pi}} \frac{3}{2} \left\{ (r_1 \cos\theta_1 - r_2 \cos\theta_2) \hat{T} f_i - \cos\theta_1 \left(\left.\frac{\partial f_i}{\partial r_1}\right|_{\substack{r_2 \\ r_3}} + \frac{2r_1}{r_3} \left.\frac{\partial f}{\partial r_3}\right|_{\substack{r_1 \\ r_2}} \right) \right.$$

$$\left. + \cos\theta_2 \left(\left.\frac{\partial f}{\partial r_2}\right|_{\substack{r_1 \\ r_3}} + \frac{2r_2}{r_3} \left.\frac{\partial f}{\partial r_3}\right|_{\substack{r_1 \\ r_2}} \right) \right\} \qquad (4.11)$$

where

$$f_i = c_i e^{-\alpha s - \gamma r_3} s^{k_i} t^{l_i} r_3^{m_i}$$

and Tf_i has been coded for the s-wave program.

All of the integrals required for the exchange direct, open closed and closed closed chanel matrix elements are of the type I_1, I_2, I_3 defined by:

$$I_1 = \int \cos^2\theta_1 F(r_1, r_2, r_3)\, d\tau,$$

$$I_2 = \int \cos^2\theta_2 F(r_1, r_2, r_3)\, d\tau, \qquad (4.12)$$

$$I_3 = \int \cos\theta_1 \cos\theta_2 F(r_1, r_2, r_3)\, d\tau$$

where $F(r_1, r_2, r_3)$ is some function of the integral variables r_1, r_2, r_3 and

$$\cos\theta_\rho = \frac{1}{\rho}(r_1 \cos\theta_1 - \frac{1}{2} r_2 \cos\theta_2),$$

$$\cos\theta_{\acute{\rho}} = \frac{1}{\acute{\rho}}(r_2\cos\theta_2 - \frac{1}{2}r_1\cos\theta_1)$$

Consider the volume element,

$$d\tau = d\mathbf{r}_1 d\mathbf{r}_2$$

$$d\tau = r_1^2 dr_1 \sin\theta_1 d\theta_1 d\phi_1 r_2^2 dr_2 \sin\theta_2 d\theta_2 d\phi_2.$$

The integration with respect to these six variables is quite complicated since the integrand is expressed in terms of the mixed co-ordinates $(\mathbf{r}_1, \mathbf{r}_2)$, $(\mathbf{r}_2, \rho)$ as well as the interelectronic distance r_3. To make this integration easier, the integration was performed in a definite order and use was made of the symmetry at the system. Whilst performing the integration over $\mathbf{r}_2$, $\mathbf{r}_1$ is considered to be the z-axis, and the volume element becomes:

$$d\mathbf{r}_1 d\mathbf{r}_2 = 2\pi r_1^2 dr_1 \sin\theta_1 d\theta_1 r_2^2 dr_2 \sin\theta_{12}\theta_{12} d\acute{\phi}_2$$

$$d\mathbf{r}_1 d\mathbf{r}_2 = 2\pi r_1 r_2 r_3 dr_1 dr_2 dr_3 \sin\theta_1 d\theta_1 d\acute{\phi}_2$$

where $\theta_{12} = \cos^{-1}\hat{\mathbf{r}}_1.\hat{\mathbf{r}}_2$ and $\acute{\phi}_2$ is the azimuthal angle of $\mathbf{r}_2$ with respect to $\mathbf{r}_1$. Hence, there are now only two external variables at intergration to consider, $\theta_1, \acute{\phi}_2$, and the integrals I_1, I_2, I_3 reduce to

$$I_1 = \frac{2}{3}(2\pi)^2 \int_0^\infty \int_0^\infty \int_{|r_1-r_2|}^{r_1+r_2} F(r_1, r_2, r_3)\, r_1\, r_2\, r_3\, dr_1\, dr_2\, dr_3$$

$$I_2 = \frac{2}{3}(2\pi)^2 \int_0^\infty \int_0^\infty \int_{|r_1-r_2|}^{r_1+r_2} F(r_1, r_2, r_3)\, r_1\, r_2\, r_3\, dr_1\, dr_2\, dr_3 \qquad (4.13)$$

$$I_3 = \frac{2}{3}(2\pi)^2 \int_0^\infty \int_0^\infty \int_{|r_1-r_2|}^{r_1+r_2} F(r_1, r_2, r_3)\cos\theta_{12}\, r_1\, r_2\, r_3\, dr_1\, dr_2\, dr_3$$

where r_1, r_2, r_3 are internal variables.

As in the s-wave problem, the dummy variables x, y, z defined by :

$$x = r_1 + r_2 + r_3$$

$$y = r_2 + r_3 - r_1$$

$$z = r_3 + r_2 - r_1$$

are introduced so that the limits of integration are simplified,

$$0 \leq x \leq \infty, \quad 0 \leq y \leq \infty, \quad 0 \leq z \leq \infty$$

and

$$dr_1 dr_2 dr_3 = \frac{1}{4} dx dy dz.$$

Integration with respect to these variables is performed using Gauss-Laguerre quadration with 35 integration points for the exchange direct and open closed channel matrix elements and with $(\omega + 4)$ points for the closed closed channel matrix elements.

The structure of the p-wave program is based on that which was used for the s-wave (§3.6). In subroutine const , for a given ω, the value of N and N1 are calculated and the values at k_i, l_i, m_i are determined so that l_i is even for $i = 1 \rightarrow N1 - 1$ and odd for the remaining values of i. In subroutine single, the open open channel matrix elements are evaluated and in subroutine column, the open closed channel matrix elements are evaluated. The closed closed channel matrix elements are calculated in subroutine square. In subroutine RMAT, the matrix equation (3.58) is solved and the stationary phase shift (3.24) evaluated.

4.3 Results and discussion.

(1) Variation of non-linear parameters, α, γ, μ

For our initial choice of non-linear parameters, we used the same set of non-linear parameters which were used in the s-wave trial function, namely: $\alpha = 0.40, \gamma = 0.05$, $(\mu = 0.5)$ (Ward et al. 1986c). However, at very low energies, the phase shifts and their slope (with respect to k) should be positive in accordance with the effective range formula (O'Malley et al, 1961), and this was not the case for the ^{1}P phase shifts. It was, therefore, necessary to optimize the non-linear parameters in the ^{1}P wave function and we did this at $\omega = 5$. Fig. 4.1 to 4.9 and tables 4.1 to 4.6 show the variation of the phase shifts ($\tan \delta_1^+$) with the non-linear parameters, and from these results, we note that the very low energy results, $k \leq 0.1 a_0^{-1}$ are much more dependent on the choice of non-linear parameters, then for the energy interval corresponding to $0.1 < k(a_0^{-1}) < 0.5$.

In fig. 4.1, table 4.1, the variation of the low-energy phase shifts with ω is illustrated. The best value of α lies at small values, which indicates that the short-range terms are trying to represent the long-range behaviour due to the polarization potential. These short-range terms have difficulty in doing this, and this is noticed by the fact that the optimum value in the Kohn results lie at different positions to the optimum value for the inverse Kohn. We chose the value $\alpha = 0.15$ for $k < 0.1 a_0^{-1}$.

In Fig. 4.2, it can be seen that the variation of the phase shifts with α is much flatter for the higher values of k, $(0.1 \leq k(a_0^{-1}) < 0.5)$ and good agreement was obtained between the Kohn and inverse Kohn results. For these values of k, we chose $\alpha = 0.30$.

From table 4.1, it is clear that the optimum value for α is 0.3 for $k = 0.1, 0.2, 0.3 a_0^{-1}$. For $k = 0.4 a_0^{-1}$, the optimum value is $\alpha \geq 0.4$. The slope of the phase shifts with α, for α in the range $0.2 \leq \alpha \leq 0.4$. is positive for $k = 0.4 a_0^{-1}$ but negative for the threshold value of k of $0.5 a_0^{-1}$. A dipole potential is created by the coupling of the 2s-2p degenerate states and this potential at large ρ is proportional to $\frac{1}{\rho^2}$. This means that the true wave function for values of k just below and at

threshold will have a long tail. The short-range terms attempt to represent this long-range behaviour by showing a preference for smaller values of α.

At threshold, $k = 0.5a_0^{-1}$, the first inelastic channel opens. The electron has just enough energy to excite the Ps atom, and since the electron will be left with no kinetic energy, we expect the wave function to be flat. Thus, it seems reasonable at $k = 0.5a_0^{-1}$ to have a low value of α or even a negative value. However, our present wave function does not include explicity the $n = 2$ states of Ps, and thus we should confine ourselves to scattering below threshold. (The inverse Kohn value at $\alpha = 0.2$ for $k = 0.5$ could be a Schwartz singularity).

In figs. 4.3, 4.4, 4.5, 4.6 and tables 4.2, 4.3, the variation of the phase shifts with γ is displayed, using $\alpha = 0.15$ for $k < 0.1a_0^{-1}$ and $\alpha = 0.30$ for the range $0.1 \leq k(a_0^{-1}) < 0.5$. The variation of the very low energy ($k < 0.05a_0^{-1}$) phase shift with γ is shown in fig. 4.3. It is apparent that the short-range terms are inadequate to describe the entire physical situation at these very low energies, i.e. long-range polarization effects as well as short-term correlation. The 'optimum' value of γ is hard to select, the optimum value is different for the Kohn and inverse Kohn results and is very energy dependent. We chose the value of $\gamma = 0.01$ for $k < 0.05a_0^{-1}$, but perhaps a negative value of γ would be more suitable. By $k = 0.05a_0^{-1}$, the variation with γ is more steady and an 'optimum' value of γ can be chosen (figs. 4.4, 4.5, 4.6). For the range $0.05 \leq k(a_0^{-1}) < 0.1$, we chose $\gamma = 0.03$ and for $0.1 \leq k(a_0^{-1}) < 0.5$ the value of $\gamma = 0.06$. It is reasonable that the value of γ is larger for the higher energies because the long-range polarization effects become less important. The variation of the phase shift with γ for $k > 0.1a_0^{-1}$ is very smooth and good agreement is achieved between the Kohn and inverse Kohn results.

The optimum value of μ which is the non-linear parameter appearing in the shielding function increases as k increased (see fig.4.7, 4.8, 4.9 tables 4.4, 4.5, 4.6.) For $k < 0.1a_0^{-1}$, the optimum value is probably less than 0.3, although it is difficult to determine and for $k > 0.1a_0^{-1}$ the value of 0.3 seems suitable. This dependancy of μ on k is reasonable since the shielding function takes longer to reach unity (in terms of distance) for a small value of μ and will have more effect on the wave function if k is large since a large value of k corresponds to a short wavelength and thus more oscillations in the wave function for a given distance. It is undesirable

for the shielding function to 'kill' the wave function over too large a distance and thus destroy any effect that the short-range terms may have. (Remember that the asymptotic region is determined by the value of $k\rho$, not just ρ.) Therefore, if k is large, a large value of μ, $\mu > 0.1$ is required. We chose $\mu = 0.3$ for the entire energy range, i.e. for $k \leq 0.5a_0^{-1}$.

The optimum choice at the three non-linear parameters for the ^{1}P wave function was:

$$\alpha = 0.15, \quad \gamma = 0.01, \quad \mu = 0.3 \quad k < 0.05a_0^{-1}$$

$$\alpha = 0.15, \quad \gamma = 0.03, \quad \mu = 0.3 \quad 0.05 \leq k(a_0^{-1}) < 0.1,$$

$$\alpha = 0.3 \ , \quad \gamma = 0.06, \quad \mu = 0.3, \quad 0.1 \leq k(a_0^{-1}) < 0.5.$$

with these choice of parameters, the ^{1}P phase shifts were positive at very low energies as required.

Although the optimum value for the triplet is not necessarily the same as for the singlet state, we used the same set of non-linear parameters for convenience. This set of non-linear parameters gave better results for the triplet than the previous set ($\alpha = 0.40, \gamma = 0.05, \mu = 0.5$) and the convergence with respect to ω was sufficiently good.

(ii) Convergence of the ^{1,3}P phase shifts with respect to ω.

The convergence of the p-wave phase shifts is shown in figs 4.10 to 4.16 and tables 4.7 to 4.12. At very low energies, $k < 0.1a_0^{-1}$ (figs. 4.10, 4.11, 4.13, 4.14), the rate of convergence with ω is slow. This is to be expected since the long range polarization effects are more important for very low energies, and the short-range terms which vanish exponetially for large ρ, have difficulty in representing the long range behaviour.

From figs. 4.10, 4.13, we see that at $k = 0.02, 0.03, 0.04a_0^{-1}$ the rate of convergence in the ^{1,3}P phase shifts is very slow and there is some disagreement between the Kohn and inverse Kohn results over the whole range of ω considered ($2 \leq \omega \leq 9$). Even by $\omega = 9$, the results have not fully converged, and the agreement between Kohn and inverse Kohn results is less than 2%.

However, as k is increased, the rate of convergence in the ^{1,3}P phase shifts improves and there is much better agreement between Kohn and inverse Kohn results. This agreement is to within 0.06% for the range $0.06 \leq k(a_0^{-1}) \leq 0.10$ and to within 0.02% for the range $0.1 < k < 0.5$ when $\omega = 9$. For the triplet, there were anomolies in some of the Kohn results. This anomaly appears at only one value of ω and moved to lower energies as ω is increased (fig. 4.14). Very close to the threshold, the rate of convergence deteriotes somewhat, and this is due to the presence of the incoming threshold. This region was examined in more detail and has been discussed in section 4.5, where we report some possible ^{1,3}P resonances.

In table 4.13, 4.14 we give our best results for the $^{1,3}P$ phase shifts evaluated at $\omega = 9$. The Kohn and inverse Kohn results agree to the number of figures quoted and better. From the convergence graphs and tables, we estimated the fully converged result ($\delta_1^{\pm}(\omega = \infty)$). The behaviour of the phase shift ($\delta_1^{\pm}(\omega = 9)$) as a function of k is illustrated in fig. 4.17, 4.18, 4.19 for the singlet, and in fig. 4.20, 4.21 for the triplet. At very low energies, where the dominant potential is that from polarization, both singlet and triplet results are positive, in accord with the form of the effective range formula (O'Malley, 1961).

$$\tan \delta_1 = \frac{\pi}{15}\alpha k^2 + A_1 k^3 + O(k^4). \tag{4.14}$$

By $k = 0.03a_0^{-1}$, the singlet phase shift has reached its maximum and at $k = 0.047a_0^{-1}$ they became negative. The phase shifts continue to decrease as k increases, until very close to the n=2 threshold where there is a sudden rise in the phase shifts at $k = 0.484a_0^{-1}$. In §4.4, we attempt to explain this behaviour. However, the triplet phase shifts are positive over the entire energy range of k considered, the maximum being at $k = 0.25a_0^{-1}$.

The variational results calculated by Armstead (1968) for e^--H scattering, below the n=2 threshold are shown in figs. 2.2 a,b. The shape of the singlet phase shift curve closely resembles that for e^--Ps. As k increases from zero, the phase shift become positive, reaching the maximum at $k \approx 0.3a_0^{-1}$ and then steadily decreases, going through zero at $k = 0.49a_0^{-1}$. At $k = 0.7a_0^{-1}$, the phase shift rapidly increase and go positive, the n=2 threshold is at $k = 0.866a_0^{-1}$. However, the singlet phase shift are between one and two orders of magnitude smaller then the e^--Ps phase shifts. The triplet phase shifts for e^--H scattering steadily increase from zero as k increases but does not show a maximum. Very close to the n=2 threshold, a ^{3}P resonance is seen. The triplet phase shifts for e^--H and e^--Ps scattering are the same order of magnitude.

In table 4.15, the ^{1}P phase shifts for the e^--Ps scattering evaluated at $\omega = 9$ using n=3,4,5,6,7 in the shielding function are shown. The phase shifts are stable to a change of n=4 to n=7 for k in the range $0.15 \leq k(a_0^{-1}) \leq 0.40$, and thus the value of n=5 seems to be suitable. At $k = 0.10a_0^{-1}$, a larger value of n might be more appropriate, although as noticed by the convergence and the agreement between Kohn and inverse Kohn results, the phase shifts for $k = 0.10a_0^{-1}$ seem somewhat strange, indicating a possible Schwartz singularity in the vicinity of this energy.

Table 4.16 shows the variation of the phase shifts with NS, the number of integration points used in the determination of exchange-direct and open-closed channel matrix elements. For k in the range $0.15 \leq k(a_0^{-1}) \leq 0.35$, the phase shifts have reached their fully converged results to within four significant figures by NS = 25, and for $k = 0.05, 0.10, 0.40, 0.45a_0^{-1}$ to within three figures for this value of NS. Close to the n=2 threshold, $k \geq 0.46a_0^{-1}$, the rate of covergence is slower, agreement being obtained to at least three figures for NS = 35 and 40, but only to two figures in increasing NS from 25 to 40. This energy region needs further investigation.

4.4 Behaviour of the p-wave phase shifts at very low energies ($k \leq 0.1a_0^{-1}$), and possible long-range energy dependent terms for the s- and p-waves.

We saw in the last section, from the results of the variation of the phase shifts with the non-linear parameters and the rate of convergence with ω, that for very low values of k, $k < 0.1a_0^{-1}$, the short-range terms are inadequate to describe long-range effects caused by the polarization potential which is proportional to $\frac{1}{\rho^4}$ for large ρ. Long-range terms, which effectively generate the long-range polarization potential, need to be added to the wave function for zero and low energies. These terms are important in the region where the short- range terms of a given ω are negligibly small and the asymptotic region has not been reached. Positronium has a large polarizability $36a_0^3$, which is eight times that of hydrogen.

Although these long range terms can take any form since we are using a variational approach, presumably better results and more rapid convergence will be obtained if these terms represent the physical situations and then $\delta\psi$ (see chapter 3) will be small. Also, since we already have three non-linear parameters in our scattering wave function, we do not want to introduce any non-linear parameters in the long-range term. The Kohn variational method solves a set of $(N+1)$ linear simultaneous equations to determine the $(N+1)$ unknowns which are linear in the wave function. However, the non-linear parameters are obtained by optimization, and this procedure as well as being time consuming in terms of computer time, suffer from the disadvantage that there is no guarantee that the apparent optimum values are in fact the true optimum.

Suitable long range terms have been reported in the literature for zero energy s-wave scattering. Spruch et al (1960) have shown that at zero-energy and for a target of polarizibility α_d, the asymptotic wave function for the free particle is

$$\left(1 - \frac{a}{r} - \frac{\alpha_d}{2r^2}\right) \tag{4.15}$$

where a is the scattering length and $\frac{\alpha}{r^4}$ is the asymptotic polarization potential.

Schwartz (1961) for zero energy s-wave electron scattering by hydrogen, used

the wave function

$$\phi = (1 \pm P_{12}) 2 e^{-r_2} \left[1 - \frac{a}{r_1} f_1 \frac{-2.25}{r_1^2} f_2 - \frac{\cos\theta_2 (r_2 + r_2^2/2)}{r_1^2} f_3 \right] / 4\pi\sqrt{2} \qquad (4.16)$$

where the f's are functions used to shield the singularities as $r \rightarrow 0$. The second term in the wave function is the long range term obtained by Spruch et al (1960). However, it had little effect in improving the convergence of the scattering length.

The third term was derived by Temkin and Lamkin (1961) who used the polarized orbital approximation. In this approximation, allowance is made for both exchange and polarization in the total scattering wave function. The wave function is written as the product of the distorted target wave function and the wave function for the scattering electron and is properly (anti)-symmetrized. First order perturbation theory is used to calculate the distorted target wave function, the perturbation being that due to the free static electron and this is known as the adiabatic approximation. Temkin and Lamkin (1961) only retained the $l = 1$ component of this first order wave functions, since this is the dominant contribution. This is known as the dipole approximation. They also introduced a step function so that when the scattered electron is closer to the nucleus than the target, this first order wave function vanishes. The polarized orbital method is explained more fully by Temkin (1959), Temkin and Lamkin (1961), Drachman (1972) and Bransden (1983, pg. 212-220). Schwartz noticed that the inclusion of this adiabatic term in his zero-energy scattering variational wave function greatly improves convergence. In fact, for the zero energy e^+-H system, Houston and Drachman (1971) only included this dipole adiabatic term in their variational wave function and neglected the monopole polarization term of Spruch.

Humbertston and Wallace (1972) used a very flexible variational wave function for the zero energy e^+-H scattering and they investigated the effect of the

various correlation terms. Their wave function is of the form:

$$\Psi_t = \frac{1}{(4\pi)}\left\{\left(1 - \frac{a_t(1-e^{-\delta r_1})}{r_1} + \frac{b_1(1-e^{-\delta r_1})^2}{r_1^2}\right.\right.$$

$$\left.\left. + b_2(r_2 + r_2^2/2)\cos\theta\,\frac{(1-e^{-\delta r_1})^3}{r_1^2}\right) 2e^{-r_2}\right.$$

$$+ \exp\left\{-(\alpha_1 r_1 + \beta_1 r_2 + \gamma_1 r_3)\right\} \sum_i c_i\, r_1^{l_i} r_2^{m_i} r_3^{n_i}$$

$$+ \exp\left\{-(\alpha_2 r_1 + \beta_2 r_2 + \gamma_2 r_3)\right\} \sum_i d_i\, r_1^{l_i} r_2^{m_i} r_3^{n_i}$$

$$= f - a_t g + b_1 \chi + b_2 \chi_2 + \sum_i c_i \phi_i + \sum d_i \xi_i ,$$

(4.17)

where ϕ_i and ξ_i are short-range terms which have been discussed earlier in the chapter and $\cos\theta = \hat{\mathbf{r}}_1.\hat{\mathbf{r}}_2$. The linear parameters of the long range terms, b_1, b_2, ..., were determined by the variational method, although $b_1 = -2.25$ and $b_1 = 1.0$ from the adiabatic approximation. (A fuller description of the various terms of this wave function together with a co-ordinate diagram is provided in their paper.) They found like Schwartz that the dipole adiabatic polarization term greatly improved convergence but the other long range term has much less effect. Humberston (1973) using a very similar form of wave function, with success for zero energy positron helium scattering.

Based on the e^+-H wave function of Humberston and Wallace, a possible

wave function to use for zero energy s-wave e^--Ps scattering is of the form:

$$\Psi_0^{\pm}(r_1,r_2,r_3) = \frac{1}{\sqrt{2}}(1 \pm P_{12}) \frac{1}{(4\pi)^{1/2}} \Big[\phi_{Ps}(r_2) \Big\{ 1 - \frac{a_t}{\rho}(1-e^{-\gamma\rho})^n + \frac{b_1}{\rho^2}(1-e^{-\gamma\rho})^{n+1} + (b_2 r_2 + b_3 r_2^2)\cos\alpha (1-e^{-\gamma\rho})^{n+2} \Big\} + \sum_i c_i e^{-\alpha s} e^{-\gamma r_3} s^{k_i} t^{l_i} r_3^{m_i} \Big] \qquad (4.18)$$

where $\cos\alpha = \hat{\mathbf{r}}_2 \cdot \boldsymbol{\rho}$, and $n = 3$. An extra linear parameter b_3 has been introduced since there is no reason to confine $b_3 = \frac{1}{2}b_2$ which is obtained from the adiabatic approximation. This flexibility was also used by Humberston for the e^+-He system. The scattering length is defined as

$$a^{\pm} = -\lim_{k\to 0} \frac{\tan\delta_0^{\pm}}{k} \qquad (4.19)$$

and the normalization of the wave function is correct for the Kohn variational principle written in the form

$$\bar{a} = a_t + \langle \Psi_t L \Psi_t \rangle. \qquad (4.20)$$

It is useful to perform the zero energy s-wave calculations since this will enable a bound on the scattering length to be obtained. Also, since we intend to include energy dependent long range terms into the s-(and p-) wave function, it will enable us to check the reliability of the wave function at zero energy by comparing with the scattering length results of zero energy calculation, where we know the form of a suitable s-wave function.

For scattering at small positive energies, I do not know of any published work on possible energy dependent long range terms, suitable for low energies, which

(a) generate the polarization potential ($\sim 1/\rho^4$) and can be added to a variational wave function of any order of angular momentum.

(b) reduce to the zero energy s-wave form, for example that given by Schwartz (1961), equation (4.16).

Callaway (1978) reviewed the various terms which have been added to the wave function for $e^-(e^+)$-atom scattering in which the target atom is degenerate, to improve convergence just before the n = 2 threshold. The long range behaviour of the correct wave function is the vicinity of the n = 2 threshold, is due to the dipole interaction between the 2s-2p degenerate (or nearly) degenerate target atom. This potential falls of asymptotically as $\frac{1}{r^2}$. Seiler et al (1971) considered e^+-H scattering and added terms of the form

$$(1 - e^{\beta r})^{l+2} \frac{\sin kr}{r^2} \qquad (4.22)$$

$$(1 - e^{\beta r})^{l+2} \frac{\cos kr}{r^2}$$

to the wave function for energies above the n = 2 threshold. This greatly improved the accuracy and convergence of the results in this energy region. As $k \to 0$, the form of first long-range term of (4.16) is obtained (i.e. $\frac{1}{r_1^2}$) but not the second term ($\cos\theta_{12}\frac{(r_2+r_2^2/2)}{r_1^2}$) which was the most important of these two terms in improving convergence at zero energy scattering.

We require some energy dependent long range terms to add to our e^-Ps wave function which would satisfy the following conditions:

(a) contain only linear parameters and are simple in form,

(b) can be used for partial waves of any order l,

(c) represent adequately the polarization of the target, the polarization potential falls asymptotically as $\frac{1}{\rho^4}$

(d) reduce to the zero energy wave function, given by equation (4.18) as k goes to zero, since this form of wave function was suitable for e^+-H, and

(e) which are able to describe the long range effects due to the dipole potential which is created by the 2s-2p degenerate states and fall off asymptotically as $\frac{1}{\rho^3}$. This would enable convergence near the n = 2 threshold to be improved.

Positronium has a large polarizability, $36a_0^3$, which means that suitable long range terms are needed in the wave function in order to improve convergence at very

low energies and close to the n = 2 threshold. Long range terms which meet these requirements would presumably be suitable for other systems where polarization effects are important.

Since the polarized orbital wave functions have been successful for systems such as e^--H, e^--He, and e^--Alkali atom scattering at positive energies, and that the adiabatic term was useful to include in a variational wave function for zero energy $e^{\pm}$-H scattering., we decided to investigate whether the polarized orbital approach could be used to construct suitable long range terms which could be used in the $e^{\pm}$-Ps variational wave function.

The polarized orbital wave function for e^--Ps is written in the form:

$$\Psi_i^{\pm}(\mathbf{r}_2,\rho) = [1 \pm P_{12}][\phi_{Ps}(\mathbf{r}_2) + \phi_{pol}(\mathbf{r}_2,\rho)]F^{\pm}(\rho) \tag{4.23}$$

where $F^{\pm}(\rho)$ is the free electron wave function. Following through the analysis of Temkin and Lamkin (1961) which is explained in detail by Bransden (1983, pg. 212-220), it can be shown that a possible trial function for s-wave scattering is of the form:

$$\underline{\Psi}_0^{\pm} = \sqrt{\frac{k}{2}}\,(1 \pm P_{12})\,\frac{\phi_{Ps}(r_2)}{(4\pi)^{1/2}}\left[\left\{\frac{\sin k\rho}{k\rho} + \tan\delta_0^{\pm}\,\frac{\cos k\rho}{k\rho}\,(1-e^{-\mu\rho})^3\right\}\right.$$

$$+ b_1\,\frac{\sin k\rho}{\rho^2}(1-e^{-\mu\rho})^4 + c_1\,\frac{\cos k\rho}{\rho^2}\,(1-e^{-\mu\rho})^4 \qquad (4.24)$$

$$\left. + b_2\,(r_2 + b_3 r_2^2)\cos\alpha\,\frac{\sin k\rho}{k\rho^3}\,(1-e^{-\mu\rho})^5\right]$$

$$+ \frac{1}{\sqrt{2}}\,\frac{1}{(4\pi)^{1/2}}\sum_i d_i\, e^{-\alpha^{\pm} s}\, e^{-\gamma^{\pm} r_3}\, s^{k_i} t^{l_i} r_3^{m_i},$$

where we have also included long-range terms suggested by Seiler et al. (1971):

$$\frac{\sin k\rho}{\rho^2}, \quad \frac{\cos k\rho}{\rho^2}.$$

in the hope of also improving convergence near the n=2 threshold. In the wave function, equation(4.24), we have left b_1, b_2, b_3, c_1 as linear parameters to be variational determined. At zero-energy, this wave function reduces to that given by Spruch et al. (1960) and by Humberston and Wallace (1972), suitably modified for e^--Ps. These long-range terms are treated in the same way as the short-range terms, and it can be readily seen how such a wave function can be generalized to the p- and d-waves.

4.5 Behaviour of the ^{1,3}P phase shifts close to the n=2 threshold.

Ho (1979, 84) stated that he would expect Feshbach resonances to be present in e^--Ps scattering. These type of resonances which are associated with the threshold of the target atom are present in the corresponding e^--H system. Positronium, like hydrogen, is degenerate, but the polarizability of positronium is eight times that of hydrogen. Recently, (possible) ^{1,3}P resonances for the e^--Ps system have been theortically predicted (Botero and Greene (1986) and Ward et al. (1986b)).

(i) ^{3}P phase shifts.

The deterioration of the convergence in the ^{3}P phase shifts, with respect to ω, suggested the possibilty of finding resonances using our variational wave function. We set $\alpha = 0.25$ which corresponds to the value in the exponential of the n=2 radial wave function. The other non-linear parameter γ was suitably optimized, we chose $\gamma = 0.00$. By scaling down the position of the ^{3}P resonances found in e^--H scattering by the reduced mass of positronium, we had some indication of the energy region of where to search for these resonances. We used a very narrow energy mesh ($\Delta k = 0.000$) and the lowest resonance was detectable for $\omega \geq 5$. Using $\omega = 9$ and the resonance fit formula described in the last chapter, we predicted the position and width of this resonance (table 4.17, fig.4.21). We verified this resonance by the stabilization method, (Hazi and Taylor, 1970) in which the hamiltonian is diagonalized using the bound-state part of the full scattering wave function and a stable eigenvalue is looked for as ω is increased. An eigenvalue of value E = 0.35329

Ryd was stable as ω was increased from 3 to 7 (fig. 4.22). Unfortunately, we could not increase ω to 9 since there was some rounding off errors, causing the matrix with elements $\langle \phi_i / \phi_j \rangle$ not being positive definite for $\omega \geq 8$.

At a slightly higher energy, there appeared to be another resonance (fig. 4.21) but the value of $\omega = 9$ had to be used in the full scattering wave function to detect this resonance. It was therfore not possible for us to confirm this resonance by the stabilization technique. In table 4.17, we give the position and width of this apparent resonance. Both these ^{3}P resonances agree well with the position of the corresponding resonances found in H^-, scaled by $\mu_{Ps}(= \frac{1}{2}a.u)$. To investigate this region in more detail it is necessary to include explicity the n=2 states of positronium.

(ii) ^{1}P phase shifts.

Using the non-linear parameters optimized for the energy range corresponding to $0.1 \leq k(a_0^{-1}) < 0.5$, the phase shifts decrease with increasing k for $k < 0.484a_0^{-1}$ (fig. 4.18). At $k = 0.484a_0^{-1}$, there is a sudden rise in the phase shifts up to the n=2 threshold (fig. 4.19).

This feature 'looks' very similar to the behaviour of the ^{1}P phase shifts of e^- - Alkali scattering calculated by Moores (1976). Threshold behaviour has been described in a paper by Wigner (1948). For potentials which are of short-range, Ross and Shaw (1961) have shown that the reactance matrix may be written in the form:

$$R^L = k^{l+\frac{1}{2}}(M)^{-1}k^{l+\frac{1}{2}}$$

where $k^{l+\frac{1}{2}}$ represents a diagonal matrix with elements

$$(k^{l+\frac{1}{2}})_{m_i} = \delta_{m_i} k_i^{l_i+\frac{1}{2}}.$$

The matrix M is slowly varying as a function of energy. It is analytic about the threshold, and may be expanded as a power series in E about threshold at $E = E_0$

$$M(E) = M(E_0) + \frac{1}{2}R_0(E - E_0)$$

where R_0 is the effective range matrix. This multi-channel effective range formula reduces to the usual single channel effective range formula when $M = k^{2l+1}\cot\delta_l$

for short-range potentials. It is important to note that the flux must be conserved across a threshold. For the p-wave, the elastic cross section decreases immediately above threshold and the inelastic cross section starts to rise (see equations (4) and (5) given by Moores (1976)). The elastic cross section will have an infinite derivative at threshold, for this partial wave, in the form of a cusp or a step. For Li and Na, a cusp is obtained in the ^{1}P elastic cross section and this effect is enhanced by the presence of a resonance in the ^{1}P phase shifts. This feature will be noticed in the photodetachment cross section since the final state is ^{1}P.

A fundamental difference exists betweeen the e^- -Alkali and the e^--Ps system in that the Ps atom is degenerate. The potential terms arising from the coupling between the degenerate s and p states are proportional to $\frac{1}{\rho^2}$ for large ρ (see Bransden (1983), chapters 5 and 7, Callaway (1978)). This is a long-range intearaction, and the normal effective range formula, either for multi-channel or single channel scattering, breaks down for long-range potentials (Spruch et al ,1960). Therefore, we cannot use the same argument to explain the behaviour of the ^{1}P phase shifts and the elastic cross section for the e^--Ps system as was used for the e^-- Alkali system. Rather, because of the coupling between the 2s-2p degenerate states, we would expect an infinite series of Feshbach resonances converging onto the n=2 thresholds as is the case for e^- -H (Bransden (1983), pg 328). This would result in the phase shifts rising sharply to infinity as the n=2 threshold is approached (Greene, 1986).

However, since we have not explicity included the n=2 states of positronium in our wave function, we cannot expect to obtain a good description of the resonant structure associated with the n=2 threshold from our calculation. The convergence of the phase shifts with respect to ω in the vicinity of the n=2 threshold is poor (table 4.18). Also, somewhat surprisingly, the rate of convergence with respect to the number of integration points (NS) for the exchange direct and open closed channel matrix element is slow (table 4.16). (However, since we are working below the n=2 threshold our results should still provide a bound on the true phase shifts).

As is seen from fig. 4.18, the ^{1}P phase shifts determined in our calculation do show a sharp rise close to the threshold and it seems that our wave function is attempting to describe the correct behaviour. The n=2 states are partly included implicity via the short-range terms.

We therefore decided to investigate this region more carefully. By setting $\alpha = 0.25$, optimizing the non-linear parameter γ and running the program with a very fine energy mesh ($\Delta k = 0.00001$), we were able to locate the lowest ^{1}P resonance. Unfortunately, since this resonance was only detectable with $\omega \geq 9$, we were unable to verify it by using the stabilization technique. Also, we noticed that the position of this resonance and the agreement between Kohn and inverse Kohn results were very sensitive to the choice of γ. We chose $\gamma = -0.02$ since the apparent resonance was very narrow we only quote a value for its position (table. 4.17). Botero and Greene (1986) by using the adiabatic treatment in hyperspherical coordinates were able to predict a weak series of narrow Feshbach resonances lying just below the n=2 threshold and a shape resonance just above. Our value for the position of the lowest ^{1}P resonance agrees reasonably well with their result and with the corresponding resonance in H^- scaled down by $\mu_{Ps}(= \frac{1}{2} a.u.)$

In the last section, we stated that terms of the form

$$\frac{\sin k\rho}{\rho^2}, \quad \frac{\cos k\rho}{\rho^2}$$

(Seiler et al ,1971) would hopefully improve convergence of the phase shift close to the n=2 threshold, which is desirable. By intoducing another non-linear parameter in the short-range terms, so that r_1 and r_2 could have different non-linear parameters associated with them, we might increase our chance of detecting resonances.

However, the real improvement would be made by intoducing the n=2 states of positronium explicity in the wave function. With our present wave function, all that we can confidently say is that there appears to be some ^{1}P resonance structure associated with the n=2 threshold and some possible ^{3}P resonances.

4.6 Conclusions.

We have presented very accurate ^{1,3}P phase shifts determined by the Kohn and inverse Kohn variational methods for the scattering of low-energy electrons by positronium below the n = 2 threshold. Some possible ^{1,3}P resonances have been detected.

The present calculalation could be improved by

(a) taking into account the polarization of the target at very low energies, for instance by including long-range terms of the form discussed in section 4.4, and

(b) by explicity including the n =2 states of positronium.

This would enable the calculation to be extended up to the n = 3 threshold as well as hopefully revealing some more resonance structure.

Chapter 5

The elastic scattering of slow electrons by positronium: A comparison of the results evaluated by various methods and the total and differential cross sections for the scattering process.

5.1 Introduction.

In the e^--H system, the effect of polarization of the target was significant for partial waves $l \geq 2$ (see chapter 2).The adiabatic exchange method (Drachman and Temkin,1972) produced results which agree reasonably well with the accurate phase shifts determined by variational method for the partial waves $l = 0, 1, 2$. Since the polarizibility of positronium is eight times that of hydrogen namely 36 a_0^3, it is important to make some allowance for the distortion of positronium in the e^--Ps system. This we did by using the adiabatic exchange (A.E) approximation which is discussed in section 5.2.

A comparision is made of the $^{1,3}S$, $^{1,3}P$ phase shifts and scattering lengths determined by the approximate methods (static exchange (S.E), adiabatic exchange) with the very accurate variational results, in section 5.3. (The static exchange method has been described in chapter 2, the variational method in chapters 3 and 4).In section 5.3, the A.E results are compared with the S.E results for the higher partial waves. The behaviour of the e^--Ps results is compared with those obtained for e^--H.

Total elastic, momentum-transfer, ortho-para conversion and elastic differential cross sections are presented in section 5.4 for scattering below the n=2 threshold of positronium. For the evaluation of these cross sections, the accurate s and p-wave variational phase shifts are used together with the A.E phase shifts for the higher partial waves until convergence with the Born polarization term is obtained. These cross sections have also been determined by using the S.E phase shifts for $l \geq 2$ up to a value of l where the phase shifts are negligibly small. In section 5.5. the conclusions of this chapter are given.

5.2. Adiabatic-exchange method applied to the e^--Ps system.

Asymptotically, the polarization potential is of the form:

$$V_{pol}(\rho) \sim -\frac{\alpha_{Ps}}{\rho^4} \tag{5.1}$$

where α_{Ps} is the polarizability of positronium, $36a_0^3$. This term (5.1), with a suitable cut-off function, is added to the static exchange integro-differential equation (2.48) to give:

$$\left(\frac{d^2}{d\rho^2} + k^2 - \frac{l(l+1)}{\rho^2}\right) u_l^{\pm}(k,\rho) = \mu_{Ps^-} V_{pol}(\rho) w(\rho) u_l^{\pm}(k,\rho) + \int_0^{\infty} k_l^{\pm}(\rho,\hat{\rho}) u_l^{\pm}(k,\hat{\rho})\, d\hat{\rho} \tag{5.2}$$

where $w(\rho)$ is the cut-off term which is used to prevent a singularity at the origin and is such that $w(\rho) \to 1$ as $\rho \to \infty$. It is to be noted that the polarization term has to be multiplied by the reduced mass of the Ps^- system, namely $\mu_{Ps^-} = \frac{2}{3} a.u.$

We followed Peach(1980) in our choice of cut-off function:

$$w(\rho) = \left[1 - \sum_{j=0}^{2} \frac{x^j}{j!} e^{-x}\right]^2$$

where $x = \beta\rho$. The parameter β was determined by matching the adiabatic exchange triplet p-wave phase shifts with the very accurate variational results at $k = 0.3a_0^{-1}$. We chose β in this manner because we noted from the S.E., S.E.1 and A.E.1 (chapter 2) phase shifts, that the dominant contribution to the total and differential cross section for scattering below the n=2 threshold, came from the triplet p-wave. Using this value of $\beta(\beta = 0.803354)$ we solved equation (5.2) to obtain the partial waves and phase shifts for $l \to l_{max}$, l_{max} is the value of l where the adiabatic exchange phase shifts have converged to a sufficient accuracy with the Born-polarization term:

$$\tan \delta_l(k^2) = \frac{\mu_{Ps}\alpha_{Ps}\pi k^2}{(2l-1)(2l+1)(2l+3)}. \tag{5.4}$$

For higher partial waves, phase shifts evaluated from the Born-polarization term are used in the calculation of the various cross sections. The adiabatic exchange results are presented in the next section where they are compared with the static exchange and variational results.

5.3. Comparison of the results determined by various methods.

(1) s-wave.

In fig. 5.1 and table 5.1, the singlet and triplet s-wave phase shifts determined by: (a) the static-exchange S.E. (b) the adiabatic exchange and (c) the variational method are shown. For display, π has been added to the triplet results, although in fact the triplet phase shifts tend to zero as k tends to zero for reasons explained in chapter 2. As in the e^--H problem, (fig.2.1) the triplet phase shifts from the S.E. method are in close agreement with, but below, the variational result and the singlet phase shift from the S.E. method are considerably below. The static-exchange approximation is a better approximation in the triplet case where the wave function is anti-symmetrical. In table 5.3, the singlet and triplet scattering lengths and the zero-energy cross section calculated by the two methods are shown. The binding energy of Ps^- determined by the S.E. wave function is 0.003075 a.u., determined by the short-range correlation part of the full Kohn variational wave function with $\omega = 8$ is 0.1200462 a.u. compared to the most accurate value to date (Bhatia and Drachman, 1983) of $0.1200506 a.u.$. Obviously the Kohn variational wave function is much superior to the static exchange wave function and describes reasonably well electron correlation.

Since different cut-off functions were used for the e^--Ps and e^--H systems in the adiabatic exchange approximation, it is unwise to compare the agreement between the A.E. and variational results between the two systems. For e^--Ps, in the singlet case, the adiabatic exchange method with $\beta = 0.8003354$ provides phase shifts, which although are still lower than the variational results, are a better estimate to the accurate variational results than the S.E. phase shifts. This value of β was obtained by matching the adiabatic exchange phase shifts with the triplet p-wave variational results. With $\beta = 0.8003354$, the tangent of the phase shift ($\tan \delta_0^-$) agreed well with the static exchange and variational results. However, the adiabatic exchange phase shift went to π as k tends to zero, rather than to zero. With a lower value of β, $\beta = 0.2961558$, excellent agreement was obtained between the adiabatic exchange and variational results as can be seen from fig 5.1 and table 5.1. The adiabatic-exchange phase shifts correctly tends to zero as k tends to zero.

(2) p-wave.

In table 5.1 figs. 5.2 and 5.3, singlet and triplet p-wave phase shifts for the elastic scattering of slow electrons by positronium, below the n = 2 theshold, are shown. These phase shifts have been evaluated by: (a) the static exchange (S.E.). (b) the adiabatic exchange A.E. and (c) the Kohn variational methods.

Consider the singlet p-wave which is shown in fig 5.2. Very good agreement is obtained between the static exchange and variational phase shifts over the entire energy range considered, $0 \leq E(eV) < 5.102eV$. In the e^--H case (figs.2.2 a,b), the agreement between the phase shifts obtained by these two methods is nowhere near as good. However, the variational phase shifts have the same general behaviour in the two systems: positive at very low energies, becoming negative and decreasing at a larger energy, and a sharp rise near the n = 2 threshold. Also, the general behaviour of the static exchange results in the two systems is very similar: decreasing rapidly with increasing energy and are negative. For the e^--Ps system, the adiabatic exchange results, obtained using $\beta = 0.8003354$ are a reasonable estimate to the 'true' phase shifts, although they are larger than the accurate variational results over the whole energy range. For this partial wave, ^{1}P, the static exchange is in better agreement with the variational results than the A.E. phase shift.

In fig. 5.3, the triplet p-wave results for the e^--Ps system are illustrated. Although the static exchange results have the same basic shape as the variational results, the maximum being at the same position in energy ($k \approx 0.275$), they are somewhat lower, showing the need to allow for the distortion of the target atom. In fact, by including a polarization potential in the way described in §5.2, varying β excellent agreement between the adiabatic exchange and variational results can be established. The adiabatic exchange phase shifts, in which $\beta = 0.8003354$ was used, is shown in the figure.

It is convenent to represent the error in the S.E. and A.E. phase shifts, $\delta_l^{\pm}(S.E.)$ and $\delta_l^{\pm}(A.E.)$, relative to the accurate variational values by the ratios (for method 'X')

$$R_l^{\pm}(X) = \left(1 - \frac{\delta_l^{\pm}(X)}{\delta_l^{\pm}(V)}\right) \tag{5.5}$$

which is known as the Quality Factor. These ratios are compared in Table 5.4 for

X = S.E. and X = A.E. The A.E. results are in general superior to the S.E. results except for the ^1P, suggesting that for this partial wave another value of β may be more appropriate.

(3) d-wave.

From the discussion of the e^--H system in chapter 2 and from the triplet p-wave results for e^--Ps (fig. 5.3) it is clear that some allowance must be made for the polarization of positronium for partial wave $l \geq 2$. At present, there are no d-wave results determined from the Kohn variational method available.

In fig. 5.4, the singlet and triplet d-wave results which have been evaluated by the static exchange and adiabatic exchange methods are illustrated. These results are tabulated in table 5.1 where they are compared with the phase shifts evaluated by the Born polarization term. In the A.E treatment, exchange and polarization is considered. In the S.E treatment no allowance is made for polarization, only exchange is considered. The Born-polarization (B.P) term is obtained by solving the integro-differential equation:

$$\left(\frac{d^2}{d\rho^2} + k^2 - \frac{l(l+1)}{\rho^2}\right) u_l^{\pm}(k,\rho) = -\mu_{Ps^-} \frac{\alpha_{Ps^-}}{\rho^4} u_l^{\pm}(k,\rho)$$

(O'Malley et al. 1961), i.e. the only potential considered is that due to polarization.

The behaviour of the d-wave phase shift as a function of k is displayed in fig. 5.4. The singlet phase shifts in both the A.E. and S.E. approximations are positive for all $k \leq 0.5a_0^{-1}$. However, in the triplet case, the phase shifts are positive only for $k \leq 0.15a_0^{-1}$ in the A.E treatment and are negative for all k in the S.E treatment. For both singlet and triplet phase shifts, the A.E. results are larger than the S.E. results.

It is interesting to compare the d-wave for e^--Ps with that obtained for e^--H, see chapter 2, fig 2.3. In the e^--H system, the S.E singlet and triplet phase shifts are extremely small for $k < 0.25a_0^{-1}$. At larger values of k, the singlet and triplet phase shift diverge rapidly from each other, the singlet phase shifts become negative and the triplet are positive. This is the reverse of the behaviour for e^--Ps, where the singlet phase shifts are positive and the triplet phase shift are negative

for $k \geq 0.15a_0^{-1}$. In e^--H, the A.E singlet and triplet phase shifts are positive for all $k > 0$.

This difference in the two systems is somewhat surprizing considering that the behaviour of the ^{1,3}S, 1,3P phase shifts in e^--Ps closely resemble that obtained in e^--H. However, after carefully checking the analysis and programs for the S.E treatment of e^--Ps, I believe the results to be correct. It must be remembered, that the direct potential which exists for the e^--H system is absent in e^--Ps, and this could explain the differences in the d-wave results in the two systems. In fact, the behaviour of the ^{1,3}D phase shifts for the scattering of low energy of the positronium by hydrogen atoms, where there is no direct potential, is very similar to that obtained for e^--Ps. It is also interesting to note that the ^{3}S phase shift for o-Ps -H scattering, as for e^--Ps, tends to zero as k tends to zero.

(4) l = 3 and higher partial waves.

The static exchange, adiabatic exchange and Born-polarization phase shifts for the partial waves l = 3 are shown in table 5.1. It is seen, that the static exchange phase shifts are very small, especially at low energies. The accuracy of these phase shifts is only to the first two figures.

As l increases, the magnitude of the static exchange phase shifts for a given k, decreases until exchange effects are so small that the adiabatic exchange results have converged to the phase shifts given by the Born polarization term. We chose $l_{max} = 2$ for $k = 0.05a_0^{-1}$, 3 for $k = 0.10$ and $0.15a_0^{-1}$, 4 for $k = 0.20a_0^{-1}$ and 5 for $k \geq 0.25a_0^{-1}$, where $(l_{max} + 1)$ is the value of l, where to sufficient accuracy we can use the Born polarization term in the evaluation of the cross section. In table 5.2, the $l = 5$ phase shifts for $k = 0.25, 0.30, 0.35a_0^{-1}$ are shown in the adiabatic exchange and Born polarization approximations. However, for this value of l, the A.E. phase shifts are not very accurately determined but they do give the order of magnitude of the results.

5.4 Total and differential cross sections.

We have calculated accurate total elastic (σ_{el},) momentum transfer (σ_D), ortho-para conversion (σ_c) cross sections and (less accurately) elastic differential ($I_{el}(\theta, k^2)$) cross section for the elastic scattering of slow electrons by positronium, below the n = 2 threshold. The formulas for those cross sections are given below:

$$\sigma_{el}(k^2) = \frac{4}{k^2}\sum_{l=0}^{\infty}(2l+1)\sin^2\delta_l(k^2) \quad \pi a_0^2, \tag{5.5}$$

$$\sigma_D(k^2) = \frac{4}{k^2}\sum_{l=0}^{\infty}(l+1)\sin^2(\delta_l - \delta_{l+1}) \quad \pi a_0^2 \quad , \tag{5.6}$$

$$\sigma_c(k^2) = \frac{1}{4k^2}\sum_{l=0}^{\infty}(2l+1)\sin^2(\delta_l^+ - \delta_l^-) \quad \pi a_0^2, \tag{5.7}$$

$$I_{el}(\theta, k^2) = \left|\sum_{l=0}^{\infty}\frac{1}{2ik}(2l+1)(e^{2i\delta_l}-1)P_l(\cos\theta)\right|^2 \quad a_0^2 Sr^{-1},$$

and for the forward direction (Dasgupta and Bhatia, 1984), we used

$$I_{el}(0,k^2) = I_{el}(0,k^2)\Big|_{l<l_0} + \left[\frac{\pi\,\mu(Ps^-)\,\alpha(Ps)\,l_0}{4l_0^2-1}\right]^2\sum_{l=0}^{l_0-1}(2l+1)\sin 2\delta_l$$

$$+ \left[\frac{\pi\,\mu(Ps^-)\,\alpha(Ps)\,l_0 k}{4l_0^2-1}\right]^2 \tag{5.8}$$

where $l_0 = l_{max} + 1$.

Since in an unpolarized beam of electrons there will be three times as many electrons in the triplet state (-) as in the singlet state (+), the total and differential cross sections for scattering of an unpolarized beam is:

$$\sigma_{el} = \frac{1}{4}(\sigma_{el}^+ + 3\sigma_{el}^-) \quad \pi a_0^2 \tag{5.9},$$

$$\sigma_D = \frac{1}{4}(\sigma_D^+ + 3\sigma_D^-) \quad \pi a_0^2 \ , \tag{5.10}$$

$$I_{el}(\theta, k^2) = \frac{1}{4}(I_{el}^{+}(\theta, k^2) + 3I_{el}^{-}(\theta, k^2)). \tag{5.11}$$

To obtain the zero energy limit of these cross sections, we used the variational singlet (a_0^+) and triplet (a_0^-) scattering lengths, so that:

$$\sigma_{el}(0) = [(a_0^+)^2 + 3(a_0^-)^2] = \sigma_D(0), \tag{5.12}$$

$$I_{el}(\theta, k^2) = \frac{1}{4}[(a_0^+)^2 + 3(a_0^-)^2]. \tag{5.13}$$

It is also worth while to calculate the effective scattering total cross section $R(\theta_0)$ since the detector will in practise subtend a finite angle θ. This cross section is defined by:

$$R(\theta_0) = \frac{2\pi}{\sigma_{el}} \int_{\theta_0}^{\pi} I_{el}(\theta, k^2) \sin\theta \, d\theta \tag{5.14}$$

where θ_0 is the acceptance angle (Bhatia et al, 1977).

In fig. 5.5 and table 5.5, the total elastic, momentum transfer and ortho-para conversion cross sections are given where the $l = 0, 1$ variational phase shifts, $l = 2 \rightarrow l_{max}$ A.E phase shifts, and higher order phase shifts evaluated by the Born-polarization term were used.

The zero energy total elastic and momentum transfer cross section is $208\pi a_0^2$. The dominant contribution to σ_{el} comes from the triplet p-wave. In fact, the s and p-waves account for more than 96% of the total cross sections for $k \leq 0.3a_0^{-1}$ and for the range $0.3 < k(a_0^{-1}) \leq 0.45$ at least 35%. For $k < 0.1875a_0^{-1}$, $\sigma_D > \sigma_{el}$ and for larger values of k, $\sigma_D < \sigma_{el}$. The momentum transfer cross section is a measure of the average forward momentum of the projectile lost in the collision. When scattering is isotropic $\sigma_D = \sigma_{el}$, but if the scattering is concentrated in the backward direction $\sigma_D > \sigma_{el}$ while if it is concentrated in the forward direction $\sigma_D < \sigma_{el}$.

The ortho-para conversion cross section σ_c is much smaller than σ_{el} or σ_D. In table 5.5, the ratio of $\frac{\sigma_c}{\sigma_{el}}$ is given, the minimum of this quantity being at $k = 0.10a_0^{-1}$. σ_c has it maximum value at $81\pi a_0^2$ at $k = 0.175a_0^{-1}$. (This cross section σ_c has been previously calculated by Baltenko and Segal (1983), but they used the Born-approximation and inappropriate set of co-ordinates).

The effective scattering total cross section ($R(\theta_0)$) is illustrated in fig. 5.6 as a function of k for the angles $\theta_0 = 5°, 10°, 15°, 20°$. For each angle, as k is increased from zero, $R(\theta_0)$ rises to a maximum at about $k = 0.10a_0^{-1}$, and then steadily decreases with further increase in k. This rate of decrease in k is much steeper the larger the acceptance angle θ_0.

In table 5.6 and in fig. 5.7 for $k = 0.1, 0.2, 0.3a_0^{-1}$ the elastic differential cross section $I_{el}(\theta, k^2)$ is displayed. The minima which occurs in $I_{el}(\theta, k^2)$ shifts towards a larger angle as k is increased, and becomes lower in value as can be seen in table 5.7. For $k = 0.10a_0^{-1}$, the maximum occurs at 50° and for $k = 0.30a_0^{-1}$, the maximum at 110^0. This is consistent with the discussion given on the momentum-transfer cross section, where it was stated that for $k < 0.1875a_0^{-1}$, the scattering was concentrated in the backward direction and for larger values of k, it is concentrated in the forward direction.

Finally, in fig 5.8, the elastic differential cross section in the forward direction as a function of k is shown where we have used equation (5.8). which is appropriate for our range of k. The zero energy limit of $I_{el}(0, k^2)$ is $52\pi a_0^2$, and as k increases, $I_{el}(0, k^2)$ decreases down to a minimum of $32\pi a_0^2$ at $k = 0.0875a_0^{-1}$. For larger values of k, $I_{el}(0, k^2)$ steeply rises and there exists a large polarization peak for $k \geq 0.2a_0^{-1}$. The singlet s-wave phase shift is the dominant contribution to $I_{el}(0, k^2)$ for very low values of k ($k < 0.1a_0^{-1}$) where exchange effects are important. However, by $k = 0.1a_0^{-1}$, the triplet p-waves gives the dominant contribution to this cross section for the remaining energy range considered ($k < 0.5a_0^{-1}$). Together, the s and p-waves account for over 90% of $I_{el}(0, k^2)$ for $k \leq 0.25a_0^{-1}$, and for over 58% for k in the range $0.25 < k \leq 0.45a_0^{-1}$.

We have re-calculated σ_{el}, σ_D, σ_c, $I_{el}(\theta, k^2)$, using the $l = 0, 1$ variational phase shifts and $l = 2, l_{max}$ S.E. phase shifts, and these cross sections shall be denoted by $\sigma_{el}^{S.E}$, $\sigma_c^{S.E}$, $I_{el}^{S.E}$. It was found that $\sigma_{el}^{S.E}$ only differs from σ_{el} by less than 1% for k in the range $0 < k(a_0^{-1}) \leq 0.45$. For this range of k, the difference between $\sigma_D^{S.E}$ and σ_D was less than 5% and, $\sigma_c^{S.E}$ and σ_c to less than 2%. The singlet static exchange cross section was smaller than the A.E. cross sections, using $l = 0, 1$ variational phase shifts in both calculations. However, the reverse situation was true for the triplet case. A larger difference existed between $I_{el}^{S.E}(0, k^2)$ and

$I_{el}(0, k^2)$, as expected. The difference being less than 22% for $k \leq 0.3a_0^{-1}$ and as much as 46% for the range $0.3 < k(a_0^{-1}) \leq 0.45$.

5.5 Conclusions.

In this chapter, adiabatic-exchange phase shifts have been reported for the elastic scattering of slow electrons by positronium, below the n = 2 threshold. Satisfactory agreement was obtained with the accurate s and p variational phase shifts.

Total elastic, momentum transfer, ortho-para and effective scattering total cross sections have been presented as well as the elastic differential cross sections. A series of minima were located in the elastic differential cross section.The position of these minima shifted towards a larger angle as k was increased. We hope that these results will be useful in the future when the experiments are performed. The feasibility of measuring these cross sections is discussed in the concluding chapter of this thesis.

Chapter 6

The photodetachment cross section of the positronium negative ion

6.1 Introduction.

There are several important reasons for studying the photodetachment of the positronium negative ion, namely:

(1) A monoenergetic beam of Ps, of controllable energy, could be achieved by producing Ps^-, accelerating it to a desired energy and then photodetaching the electron. This was suggested by Mills (1981a).

(2) Some doubly excited resonances of Ps^- have been theoretically determined (Ho, 1979, 84; Botero and Greene, 1986 and Ward et al. 1986a, b). The experimental verification of these resonances by the conventional method of electron-atom scattering would be very difficult because the widths of the resonances are narrower than the energy resolution of the electron beam. A photodetachment experiment would hopefully reveal $^1P^0$ resonances (Feshbach and shape) which are associated with the various thresholds of Ps.

This chapter begins with a section (§6.2) on the theory used to derive the expressions for the photodetachment cross section and its evaluation. A discussion (§6.3) is given on the photodetachment of H^-, which has been extensively studied.

It is worthwhile to examine the theoretical treatment of the photodetachment of H^- before commencing the calculation for Ps^-. This is because the two ions are very similar, for instance

(a) both systems are weakly bound and have only one bound-state,

(b) they consist of two electrons and a particle of charge +e.

From the H^- calculations we can learn which type of wave functions will produce the most reliable results, the conditions these wave functions should satisfy, and then apply this information to the Ps^- problem.

The various calculations performed for the photodetachment of Ps^- are described in §6.4, the results are given in §6.5 and a discussion provided in §6.6. The conclusions presented in §6.7.

6.2 THEORY

The time dependent perturbation theory is used to derive expressions for the photodetachment cross section. To determine this cross section, both bound and continuum wave functions of the negative ion are required.

We have restricted our calculation, of the photodetachment cross section of Ps^- (Ward et al,1986 a,b), to low energy photons, so that the residual Ps atom will be left in its ground state. The photons are of wavelength λ greater than $2.283\ 10^3 \mathring{A}$ which is equivalent to electron energies less than 5.102 ev ($k = 0.5a_0^{-1}$). For these wavelengths,(wavelengths much larger than the size of Ps^-), the dipole approximation (see Appendix A2) is valid.

In a theoretical description of the photodetachment process, the negative ion is considered to be interacting with an oscillating dipole electric field. In classical theory, the radiative characteristics of an oscilating dipole can be expressed in terms of its length, its moment, or its acceleration. This lead Chandrasekhar (1945) to express the photodetachment cross section in terms of a length, velocity and acceleration matrix element using quantum theory. In the next section, I have discussed the relative merits of the different forms.

To derive the photodetachment cross section of Ps^-, we have to work in the centre of mass frame. With other systems, for example H^-, He, the centre of mass and the lab-frame coincide because of the 'infinitely' heavy nucleus. In the appendix A2, the photodetachment cross section is derived in the centre of mass frame, both in the length and velocity formulation. The length form of the photodetachment cross section is given by:

$$\sigma_\lambda(L) = 6.8115 \times 10^{-20} k(k^2 + \gamma^2)|\mu_z^L|^2\ cm^2 \tag{6.1}$$

where $\epsilon_b = \frac{\gamma^2}{2\mu_2}$ a.u., k,μ_z are expressed in atomic units and the length matrix element is

$$\mu_z^L = \langle \Psi_f | (\vec{r}_2 + \mu_2 \vec{\rho})_{z-cpt} | \Psi_i \rangle\ a.u \tag{6.2}$$

with μ_2 being the reduced mass of the bound electron with respect to the residual atom. For the coordinates $\vec{r}_1, \vec{r}_2, \vec{\rho}$, see coordinate diagram (fig. 2.5). We chose a

coordinate system such that the z-direction is arranged to be in the direction of the ejected electron.

The velocity form of the photodetachment cross section is given by:

$$\sigma_\lambda(V) = 2.7246 \times 10^{-19} \mu_2^2 \frac{k}{(k^2+\gamma^2)} |\mu_z^V|^2 \ cm^2 \tag{6.3}$$

where

$$\mu_z^V = \langle \Psi_f | (\frac{\nabla_{\vec{r}_2}}{\mu_1} + \nabla_{\vec{\rho}})_{z-cpt} | \Psi_i \rangle \ a.u. \tag{6.4}$$

and μ_1 is the reduced mass of the bound electron with respect to the positive charge. For H^-, $\mu_2 \approx \mu_1 \approx 1 \ a.u$, thus

$$\sigma_\lambda(L) = 6.8115 \times 10^{-20} k(k^2+\gamma^2) |\mu_z^L|^2 \ cm^2 \tag{6.5}$$

where

$$\mu_z^L = \langle \Psi_f | (z_1 + z_2) | \Psi_i \rangle \ a.u. \tag{6.6}$$

and

$$\sigma_\lambda(V) = 2.7246 \times 10^{-19} \frac{k}{(k^2+\gamma^2)} |\mu_z^V|^2 \ cm^2 \tag{6.7}$$

where

$$\mu_z^V = \langle \Psi_f \left| \left(\frac{\partial}{\partial z_1} + \frac{\partial}{\partial z_2} \right) \right| \Psi_i \rangle \ a.u. \tag{6.8}$$

which are the expressions given by Chandrasekhar(1945). For Ps^-, $\mu_2 = \frac{2}{3}, \mu_1 = \frac{1}{2} \ a.u$,thus

$$\sigma_\lambda(L) = 6.8115 \times 10^{-20} k(k^2+\gamma^2) |\mu_z^L|^2 \ cm^2 \tag{6.9}$$

where

$$\mu_z^L = \langle \Psi_f | (z_2 + \frac{2}{3}\rho_z) | \Psi_i \rangle \ a.u. \tag{6.10}$$

and

$$\sigma_\lambda(V) = 1.2109 \times 10^{-19} \frac{k}{(k^2+\gamma^2)} |\mu_z^V|^2 \ cm^2 \tag{6.11}$$

where

$$\mu_z^V = \langle \Psi_f \left| \left(2\frac{\partial}{\partial z_2} + \frac{\partial}{\partial \rho_z} \right) \right| \Psi_i \rangle \ a.u \tag{6.12}$$

which are the expressions given by Bhatia and Drachman (1985 a).

As the bound-state of Ps^- is a singlet s-state, only the ^1P component of the continuum wave function will give a non-vanishing contribution to the matrix element.

Very good bound-state wave functions of Ps^- exist, see discussion in chapter 3. The wave function for the final state is equivalent to the wave function which describes the p-wave elastic scattering of slow electrons by positronium, below the n=2 threshold (see chapter 4).

6.3 Discussion on the photodetachment of H^-.

Since Wildts (1939) discovery that H^- ions are the dominant source of opacity in the visible and infra-red radiation regions in the atmospheres of stars of cooler late spectral type, there has been extensive work to determine its photodetachment cross section.

At the start of this present work, October 1983, there had been no published theoretical or experimental work on the photodetachment of Ps^- . The Ps^- ion closely resembles the H^- ion, both consist of two electrons and a particle of positive charge +e. For this reason, it is worthwhile to investigate the calculations which have been performed for H^- to extract information such as:

(a) the sensitivity of the cross section on the accuracy of the bound-state and continuum wave function,

(b) the type of wave functions which will lead to the most reliable results,

(c) a criterion for establishing the reliability of a particular calculation, which would provide guidance on how to tackle the Ps^- problem.

There are several detailed review articles on the photodetachment of H^-, written for example by Bates (1978), Branscomb (1962), Burke (1976) and Risley (1975). The development on the theoretical considerations of the photodetachment of H^- can be divided into four overlapping steps:

(1) The impovement in the bound-state wavefuction by adding more terms in the Hylleraas expansion,

(2) Using the velocity form of the cross section (Chandrasekhar ,1945)

(3) Improvements made to the continuum wavefuction,

(4) Using a bound-state wave function which has the correct asymptotic form, for instance by adding a tail-like function to the Hylleraas expansion (Rotenberg and Stein, 1969).(See §6.4 for this form of tail function).

Below, I have just outlined some of the work which might be applicable in study of Ps^-, since a detailed coverage is provided by the review articles.

The pioneering paper on the photodetachment cross section of H^- was by Massey and Bates (1940) who used the Hylleraas-Bethe 3-parameter wave function for the bound-state, and a plane wave for the ejected electron. They used the length form of the photodetachment cross section. The wave functions are given by:

$$\Psi_B(\vec{r}_1,\vec{r}_2) = Ne^{-\alpha(r_1+r_2)}\left\{1+\gamma(r_1-r_2)^2+\beta r_{12}\right\} \tag{6.13}$$

and

$$\Psi_f(\vec{r}_1,\vec{r}_2) = (2\pi)^{-\frac{1}{2}}\left\{e^{-r_1}e^{ikz_2}+e^{-r_2}e^{ikz_1}\right\} \tag{6.14}$$

In 1942, Williamson stated that the reliability of the bound-state wave function to be used in the photodetachment cross section, should be judged on how well it predicts the electron affinity, rather than the total energy. The 3-parameter Hylleraas-Bethe wave function was inadequate to describe the photodetachment process, and therefore, Williamson (1942) performed a calculation in which he used a 6-parmeter Hylleraas expansion and the plane wave approximation. The wave function predicts a value for the electron affinity which agrees to within 5% of the value subsequently found by Pekeris(1962) who used a 444-parameter wave function.

A very significant paper was written by Chandreskhar and Krogdahl(1943), who tried to establish some criterion for estimating the reliabity of the cross section calculated with a given bound-state and continuum wave function. They investigated which regions of configuration space gave the dominant contribution to the length form of the matrix element for different wavelengths. The bound-state wave function needed to be accurate out to least 5 bohr, and this was more important for longer wavelengths. However, in determining the bound-state wave function from the Rayleigh-Ritz variational principle, the dominant contribution to the energy

integral comes from distances close to the centre of the ion. The wave function will be poorly determined at large distances. The photodetachment cross section is therefore sensitive to the value of the electron affinity and convergence is slow as more terms in the bound-state wave function are added.

The reliability of the bound-state wave function at distances which contribute domiantly to the cross section and the reliability of the cross section can be established from how well the sum-rules are satisfied. The two relevant sum-rules are:

$$\frac{mc}{\pi e^2}\int_{\nu_0}^{\infty}\sigma_\nu\, d\nu \leq N \tag{6.15}$$

and

$$\frac{mc}{\pi\hbar a_0}\int_{\nu_0}^{\infty}\nu^{-1}\sigma_\nu\, d\nu \leq \frac{2}{3a_0^2}\int \Psi_B^{*}\left(\sum_{i=1}^{N}\underline{r}_i\right)^2\Psi_B\, d\tau_1 \ldots d\tau_N \tag{6.16}$$

where N = number of electrons (Branscomb ,1962). The equality sign applies when σ_ν is the total photodetachment cross section. Generally, the contribution to the integral from the excited states of the atom are neglected and then the inequality sign applies. A good discussion of the application of the sum-rules to the photodetachment cross section are found in papers by Chandrasekhar and Krogahl (1943), Dalgarno and Lynn (1957), Dalgarno and Kingston (1959) and in the review article by Branscomb (1962).

Chandrasekhar (1945) obtained expressions for the photodetachment cross section in terms of the length, velocity and acceleration matrix elements, which give identical results if exact wave functions are used or if the wave functions are exact solutions of some model Hamiltonian. The matrix elements emphasize different regions of configuration space, and thus they are not of equal merit if approximate wave functions are used. The acceleration form is dependent on the wave function being accurate at distances very close to the centre of the ion, the length form at distances relatively far. The velocity form is dependent on distances intermediate

between the above two extremes. Which form of the cross section is to be preferred, depends on the choice of the initial and final state wave functions. However, the acceleration form generally will give the poorest results, and the velocity form is to be favoured if the bound-state wave function has to be determined by the Rayleigh-Ritz principle. Much more rapid convergence of the cross section with respect to the number of terms in the Hylleraas expansion was obtained when the velocity form of the cross section was used rather than the length form.

Geltman (1962), calculated the photodetachment cross section using the length, velocity and acceleration forms of the matrix element. He made systematic improvements to both the bound-state and continuum wave function and thus was able to predict the reliabilty of his results. He used the 20-parameter Hylleraas (Hart and Herzberg, 1957) and the 70-parameter Schwartz (unpublished) wave functions for the bound-state. For the continuum wave function, he used a plane wave and a p-wave function which was detemined by the Hulthén-Kohn variational method and allowed for (a) radial correlation, (b) radial and angular correlation. The full correlated p-wave function contained 6 linear and 3 non-linear parameters.

Other calculations have been performed in which the 70 parameter Schwartz wave function was used for the bound-state but with different continuum wave functions. Bell and Kingston (1967) used a polarized-orbital wave function, Doughty et al. (1966) used a Hartree-Fock expansion which included the 1s,2s,2p,3s,3p and 3d hydrogenic functions.

The next important stage in the development of the photodetachment calculation was to add a tail function to the Hylleraas expansion (Rotenberg and Stein, 1969) to obtain a bound-state wave function of the correct asymptotic form. This made a remarkable difference to the convergence of the length form of the cross section with respect to the addition of terms in the Hylleraas expansion. Ajmera and Chung (1975) used 5, 15, and 33 parameters in the Rotenberg and Stein wave function. The continuum wave function used was derived by the simplified Kohn-Feshbach variational method. The agreement between the length and velocity forms of the cross section were better for this calculation than for any previous calculation. Resonable agreement was obtained with the experimental data (Smith and Burch, 1959).

It was later recognized that for consistency, the bound-state and continuum wave function used in the cross section calculation should be derived by the same technique. The various methods used were:

(a) the multichannel J-matrix technique to obtain pseudostate close coupling expressions (Broad and Reinhardt ,1976)

(b) the perturbation variation method (Stewart, 1978)

(c) the close coupling pseudostate expansion with the addition of the Hylleraas-type correlation terms (Wishart, 1979).

Wishart claims that his results are accurate to within 1% for incident photon wavelengths in the range $16300\mathring{A} \rightarrow 1250\mathring{A}$.

Some of the photodetachment cross section results are displayed in figs.6.1, 6.2, 6.3, 6.4.

In fig. 6.1, a comparison is made of the length formulation of the photodetachment cross section in which different bound-state wave functions are used, namely:

(a) the 2-parameter Chandrasekhar wave function, (see Bransden and Joachain, 1983 pg. 275)

(b) the 3-parameter Hylleraas-Bethe wave function, (Massey and Bates, 1940)

(c) the 70-parameter Schwartz wave function (Geltman, 1962) but the same continuum wave function that of a plane wave to represent the outgoing electron.

The 2-parameter bound-state wave function is completely inadequate to describe the photodetachment process. As the number of parameters in the bound-state wave function is increased from 3 to 70, the peak in the cross section shifts towards the red, and the cross section is much larger in magnitude. The photodetachment cross section calculated by using the 3-parameter wave function is not sufficiently accurate at long wavelengths for $\lambda > 4000\mathring{A}$. Yet the electron affinity predicted by this wave function differs by only 9% from the value predicted by the 70-parameter wave function. It is concluded that the cross section is very sensitive to the accuracy of the bound-state wave function.

Geltmans (1962) length formulation results are illustrated in fig. 6.2 in which he used Schwartz 70 parameter bound state wave function together with a plane wave for the final state and a 6 linear parameter p-wave continuum wave function which allowed for radial and angular correlation.

It is noted that:

(1) the plane-wave representation is a reasonably good approximation, especially at the longer wavelengths,

(2) the plane-wave approximation calculation overestimates the size of the cross section over most of the energy range.

For comparison, Ajmera and Chung (1975) results are shown in this figure.

The length and velocity photodetachment cross section results in which the 70-parameter Schwartz bound-state and the full correlated 6-linear parameter p-wave continuum function, Geltman(1962), are given in fig. 6.3. For short wavelengths, $\lambda < 6000\mathring{A}$, there is good agreement between these two forms of cross section. The peak in the velocity form of the cross section is further to the red than for the length form, and the peak height is slightly lower. For $\lambda > 10,000\mathring{A}$ there is some discrepancy between the length and velocity results.

Ohmura and Ohmura (1960) calculated the photodetachment cross section of H^- using the 'loosely' bound approximation (Bethe and Peierls,1935, Bethe and Longmire, 1950). In this approximation, the asymptotic form of a very good bound-state wave function is used, together with a plane wave to represent the ejected electron. The full bound-state wave function is that given by Pekeris (1958) and it contains 202 adjustable parameters. Their results are compared with the cross section calculated by Ajmera and Chung (1975),fig.6.4. As shown, the 'loosely' bound approximation is a very good approximation for long wavelengths, $\lambda > 10,000\mathring{A}$.

6.4 Calculations of the photodetachment cross section of Ps^-

$$Ps^- + h\nu \rightarrow Ps(1s) + e^-$$

We calculated the photodetachment cross section for the positronium negative ion, below the n=2 threshold of positronium, using both the length and velocity formulation. Several different type of bound-state and continuum wave functions have been used. In our most accurate calculation, we used our best bound-state and p-wave continuum variational wave functions which have been described in Chapters 3 and 4. For the bound-state and continuum p-wave wave functions, the maximum number of linear parameters we used was 95 and 220 respectively. The number of linear parameters in the wave functions could easily be varied.

In the Appendix A3, the expression for the photodetachment cross section, in terms of both the length and velocity formulations, is given for these variational type bound-state and continuum wave functions. The length form of the photodetachment cross section being:

$$\sigma_\lambda(L) = 6.8115 \times 10^{-20} k(k^2 + \gamma^2)|\mu_z^L|^2 \ cm^2 \tag{6.17}$$

where

$$\mu_z^L = \frac{2}{3}\hat{\mathbf{k}}.\langle \Psi_f(\mathbf{r}_1 + \mathbf{r}_2)\Psi_i\rangle, \ \epsilon = \frac{3\gamma^2}{4},$$

and in the velocity form:

$$\sigma_\lambda(V) = 1.2109 \times 10^{-19} \frac{k}{(k^2 + \gamma^2)}|\mu_z^V|_c^2 m^2 \tag{6.18}$$

where

$$\mu_z^V = 2\hat{\mathbf{k}}.\langle \Psi_f(\nabla_{\mathbf{r}_1} + \nabla_{\mathbf{r}_2})\Psi_i\rangle.$$

In equations (6.17), (6.18), the bound-state wave function is of the form:

$$\Psi_i = \frac{1}{\sqrt{2}}\frac{1}{\sqrt{(4\pi)}}\sum_{j=1}^{N} g_j, \tag{6.19}$$

where

$$g_j = d_j e^{-\alpha r_3} e^{\beta s} s^{k_j} t^{l_j} r_3^{m_j},$$

$$k_j + l_j + m_j \leq \omega_b, k_j, l_j, m_j \in]0, 1, 2, \ldots \omega_b],$$

where l_j is even for all j,

$$s = r_1 + r_2, t = r_1 - r_2$$

and Ψ_i satisfies

$$\int |\Psi_i|^2 \, d\tau = 1.$$

(A description of Ψ_i is given in chapter 3 and Appendix A3). The p-wave continuum wave function which we used, and is described in chapter 4 and Appendix A3, is of the form:

$$\underline{\Psi}_f^+ = \left(\frac{12\pi}{k}\right)^{1/2} \Bigg[(1+P_{12}) \sqrt{\frac{k}{2}} \; \phi_{Ps}(r_2) Y_{10}(\hat{f}) \Big\{ j_1(kp) - \tan\delta_1^+ n_1(kp) \Big[1 - \exp(-\mu p) \Big]^5 \Big\} + \frac{1}{\sqrt{2}} \Big(Y_{10}(\hat{p}) p + Y_{10}(\hat{p}') p' \Big) \sum_{\substack{i=1 \\ \text{even } l_i}}^{N1-1} c_i e^{-ar_3} e^{-bs} s^{k_i} t^{l_i} r_3^{m_i}$$

$$+ \frac{1}{\sqrt{2}} \Big(Y_{10}(\hat{p}) p - Y_{10}(\hat{p}') p' \Big) \sum_{\substack{i=N1 \\ \text{odd } l_i}}^{N} c_i e^{-ar_3} e^{-bs} s^{k_i} t^{l_i} r_3^{m_i} \Bigg] \qquad (6.20)$$

where l_i is even for $i = 1 \rightarrow N1 - 1$, odd for $i = N1 \rightarrow N$. It is to be noted that the p-wave scattering function has been multiplied by $\sqrt{\frac{12\pi}{k}}$ so that the normalization condition

$$\langle \Psi_f / \Psi_f \rangle = (2\pi)^3 \delta(\mathbf{k}' - \mathbf{k})$$

is satisfied. (More details is given in Appendices A2, A3).

By setting $\tan\delta_1^+ = 0$ and $c_i = 0$ $(i = 1, \ldots N)$ in (6.20) in the p-wave function we obtained the photodetachment cross section in the plane-wave approximation, Ψ_f being the p-wave component of :

$$\Psi_f = \frac{1}{\sqrt{2}} (\phi_{Ps}(r_2) e^{i\mathbf{k}\cdot\boldsymbol{\rho}} + \phi_{Ps}(r_1) e^{i\mathbf{k}\cdot\boldsymbol{\rho}'}) \qquad (6.21)$$

but with a very accurate bound-state wave function.

The photodetachment cross section has also been calculated in the length formulation using the plane wave approximation (Ward et al, 1986a,b,c) together with very simple bound-state wave function given by Ferrante and Zarcaro and Lano (1970). The expression for the length form of the matrix element in which Ferrantes 2-parameter wave function is used for the bound-state,

$$\Psi_B = N(e^{-\alpha r_1 - \beta r_2} + e^{-\beta r_1 - \alpha r_2}) \tag{6.22}$$

with

$$N = 3.9318 \times 10^{-3}, \alpha = 0.519584, \beta = 0.141599$$

is given by:

$$\mu_z^L(2) = \frac{256\pi^2 i N}{3\sqrt{\pi}} \Big\{ F'(\alpha, k, (\beta+\tfrac{1}{2}), -k/2)$$

$$+F'(\beta, k, (\alpha+\tfrac{1}{2}), -k/2) + F'((\alpha+\tfrac{1}{2}), -k/2, \beta, k)$$

$$+F'((\beta+\tfrac{1}{2}), -k/2, \alpha, k)\Big\} \tag{6.23}$$

where

$$F'(\gamma, A, \delta, B) = \frac{A\gamma\delta}{(\gamma^2+A^2)^3(\delta^2+B^2)^2} \tag{6.24}$$

When the 3-parameter wave function (Ferrante, 1970) is used for the bound-state,

$$\Psi_B = N(e^{-\alpha r_1 - \beta r_2} + e^{-\beta r_1 - \alpha r_2}) r_3 e^{-\gamma r_3} \tag{6.25}$$

$$N = 1.9056 \times 10^{-3}, \alpha = 0.518928, \beta = 0.141372,$$

the matrix element is given by:

$$\mu_z^L(3) = \frac{\pi^2 N i}{k\sqrt{\pi}} \int_0^\infty\int_0^\infty\int_0^\infty (e^{-\alpha r_1 - \beta r_2} + e^{-\beta r_1 - \alpha r_2}) e^{-r_2/2} e^{-\gamma r_3} \frac{r_1 r_2 r_3^2}{\rho}$$

$$(r_2\cos\alpha + \tfrac{2}{3}\rho)\left(\cos k\rho - \frac{\sin k\rho}{k\rho}\right) dx\,dy\,dz \tag{6.26}$$

where $\alpha = \cos^{-1}\hat{r}.\hat{\rho}$. The integration techniques discussed in the Appendix A3 have been used to derive $\mu_z^L(3)$. The remaining integration is performed by using

Gauss-Laguerre quadrature. The 2-parameter wave function predicts a value for the electron affinity of 0.00665144 a.u. and the 3-parameter wave function predicts a value of 0.00 939454a.u..

Bhatia and Drachman (1985 a,b) have calculated the photodetachment cross section by using the plane-wave approximation together with two different types of bound-state wave functions.

In their first calculation (which I shall denote by calculation A) they used the 'loosely' bound approximation in which they took the asymptotic form of a 220-parameter wave function (Bhatia and Drachman, 1983). A similar calculation has been performed by Ohmura and Ohmura (1960) for H^-, and has proved to be successful especially at long wavelengths.

The full 220-parameter wave function is given by:

$$\Psi_i(r_1,r_2,r_3)=\sum_{l,m,n} C(l,m,n)\left[r_1^l r_2^m e^{-(\gamma r_1+\delta r_2)}+r_2^l r_1^m e^{-(\gamma r_2+\delta r_1)}\right]r_3^m \qquad (6.27)$$

where γ, δ are 'optimized' non-linear parameters. This wave function predicts a value for the electron of 0.012005057 a.u., which is the best value to date.

The asymptotic form of the wave function is

$$\Psi_i = \frac{Ce^{-\gamma\rho_j}}{\rho_j}\phi_{1s}(r_j)\begin{cases} j=1, \rho_j=\rho-r_j=r_2 \\ j=2, \rho_j=\rho-r_j=r_1 \end{cases} \qquad (6.28)$$

(Bhatia and Drachman ,1985a) where $\epsilon_b = \frac{3\gamma^2}{4} a.u.$

The photodetachment cross section is obtained in an analytical form

$$\sigma_\lambda(L,V) = 1.32\times 10^{-18}\frac{k^3}{(k^2+\gamma^2)^3} cm^2. \qquad (6.29)$$

Note, that in this approximation in which the model hamiltonian has been used, the length and velocity forms of the cross section are identical.

Bhatia and Drachman (1985b) have also calculated the photodetachment cross section at very low energies, $k^2 < 0.002$ Ryd, by using the full 120 term-Hylleraas wave function (Bhatia and Drachman, 1983) together with a plane wave for the final state. This calculation I shall refer to as calculation B.

The sum-rule S_{-1} is written as

$$S_{-1} = \frac{1}{2\pi^2 \alpha a_0^2} \int_0^{\lambda_0} \frac{\nabla_\lambda}{\lambda} d\lambda = \frac{8}{27} \langle \Psi_B | (r_1 + r_2)^2 | \Psi_B \rangle$$

$$= \frac{8}{27} [4\langle r_1^2 \rangle - \langle r_{12}^2 \rangle] \qquad (6.30)$$

for the photodetachment of Ps^- (Bhatia and Drachman, 1985a), where λ_0 is the threshold wavelength for the process.

Since in our variational calculations, we have only considered below the n=2 threshold, the left-hand side of equation (6.30) is re-written as:

$$S_{-1} = \frac{1}{2\pi^2 \alpha a_0^2} \left\{ \int_0^{\lambda(n=2)} \frac{\nabla_\lambda}{\lambda} d\lambda + \int_{\lambda(n=2)}^{\lambda_0} \frac{\nabla_\lambda}{\lambda} d\lambda \right\} \qquad (6.31)$$

$$= S_{-1}^{(1)} + S_{-1}^{(2)}$$

and the contribution to the sum-rule $S_{-1}^{(1)}$ for wavelengths in the range $0 < \lambda < \lambda(n = 2)$ is calculated using (6.29).

The expectation values $\langle r_1^2 \rangle$, $\langle r_{12}^2 \rangle$ have been calculated by Kolos et al (1960) which gives an independent check on the right hand side of equation (6.30). They used 50 terms in a wave function of the form

$$\psi = const\, exp(-\alpha_{12} r_{12} - \alpha_{23} r_{23} - \alpha_{31} r_{31}) P(r_{12} r_{13} r_{23}) \qquad (6.32)$$

where P is a polynomial and $\alpha_{12}, \alpha_{23}, \alpha_{31}$ are 'optimized' non-linear parameters.

6.5 Results.

(1) Sensitivity of the photodetachment cross section on the bound-state wave function

Our most accurate p-wave continuum wave function was used, which contained three 'optimized' non-linear and 220 linear parameters. The number of linear parameters in the variational bound-state wave function was varied, but the same set of optimized non-linear parameters were used for each value of ω_b. The values of ω_b used were 1,3,5,7,8 which correspond to 3,13,34,70,94 linear parameters respectively. The variation of the cross section on the number of linear parameters in the bound-state wave function is shown in table 6.1 ,fig. 6.5. for the length formulation and table 6.2, fig. 6.6 for the velocity formulation. Tables 6.1 and 6.2 give the value of the electron affinity predicted from each bound-state wave function.

In fig. 6.7, 6.8, 6.9, 6.10, 6.11, the length and velocity results of the cross section are shown for each value of ω_b ($\omega_b = 1, 3, 5, 7, 8$). The most accurate results obtained are shown in table 6.3, fig. 6.11 in which 95 linear, 2 non-linear parameters have been used in the variational bound-state wave function, and 220 linear, 3 non-linear parameters have been used in the p-wave continuum wave function. The bound-state wave function predicts a value for the electron affinity of 0.012004615 a.u. compared to the most accurate value of 0.012005057 a.u. by Bhatia and Drachman (1983). (These photodetachment results are an improvement on that reported by Ward et al (1986a) since a better bound-state wave function has been used, in which ω_b was increased to 8 and the non-linear parameters were optimized.)

The trial Kohn phase shift have been used in the p-wave function rather than the stationary Kohn phase shifts. Table 6.4 compares the cross section, in both the length and velocity forms, at a few wavelengths, for which the trial and stationary phase shifts have been used.

(2) Sensitivity of the photodetachment cross section on the continuum wave function.

The 95 linear parameter bound-state wave function was used and the number of linear parameters in the p-wave continuum wave function was varied. The

variation in the cross section with respect to the value of ω_c used in the p-wave continuum wave function is shown in table 6.5 for the length formulation and table 6.6 for the velocity formulation.

Note, the cross section calculated with $\omega_c = 3$ are unreliable for the region $21.0 < \lambda(10^3 \mathring{A}) < 25$ since the trial phase shift differ in sign and magnitude from the Kohn results, and a schwartz singularity could be present.

A comparison is made in table 6.7 of the length and velocity results when a plane wave has been taken for the final wave function with the accurate results calculated with the 220-linear parameter p-wave. In both cases, the 95-linear parameter bound-state wave function has been used. In fig. 6.12, the length and velocity cross section calculated using the plane wave approximation are illustrated.

(3) Length formulation of the cross section calculated using the simple bound- state wave functions.

In table 6.8 and fig. 6.13, the photodetachment cross section is shown in the length form, where

(a) 2-parameter Ferrante wave function,

(b) 3-parameter Ferrante wave function,

(c) 95 linear parameter variational wave function, have been used for the initial state and the plane wave approximation has been used for the final state.

These results are compared with the accurate calculation in which the 220 linear parameter p-wave and the 95 linear parameter bound-state wave functions were used.

(4) Comparison with Bhatia and Drachman (1985a,b) results.

Fig. 6.14 shows the comparison of Bhatia and Drachmans (1985a) results, calculation A with our length formulation results in which we used the 95 linear parameter variational bound-state wave function together with:

(a) a plane wave to represent the ejected electron,

(b) the full 220 linear parameter p-wave for the continuum wave function.

In Table 6.9, a comparison is made between the results of calculation B with our results in which we used the 95 linear parameter bound-state wave function together with two different types of continuum function: a plane wave and a 220-linear parameter p-wave.

In table 6.10, we show how well the sum-rule S_{-1} is satisfied for the photodetachment cross section in which the variational bound-state and continuum wave functions were used. The sum-rule S_{-1} is satisfied to within 0.9% when the length form has been used, and to within 2% for when the velocity form was used. In this table, a comparison is made with Bhatia and Drachman's (1985 a) results in which they used the 'loosely' bound approximation (Calculation A) and with the value calculated for the right-hand side of equation (6.30) by using the expectation values $\langle r_1^2 \rangle$, $\langle r_{12}^2 \rangle$ determined by Kolos et al (1960).

6.6 Discussion.

In discussing the results, it must be remembered that the length and velocity forms of the cross section become more dependent on the wave functions being accurate at large distances as the wavelength of the photon is increased. The velocity form of the cross section weighs more heavily the wave function at closer distances to the centre of the ion than the length form. Our accurate bound-state and continuum wave functions have been determined by the variational method and this leads to internal consistency in the evaluation of the matrix elements. Generally, the velocity form of the cross section is to be preferred if the bound-state wave function has been determined by the Rayleigh-Ritz variational principle, but this depends also on the choice of the continuum function.

From fig. 6.5 and 6.6, it can be seen that both the length and velocity forms of the cross section are very sensitive to the accuracy of the bound-state wave function. The convergence of the cross section with respect to the number of linear parameters in the bound-state wave function is much more rapid for the velocity form of the cross section than for the length form. The velocity results have almost fully converged by $\omega_b = 7$. The bound-state wave functions corresponding to $\omega_b = 1, 3, 5$ are inadequate to describe the photodetachment process especially

at long wavelengths when the length form of the cross section is used. This is evident from figs. 6.7, 6.8, 6.9. As the bound-state wave function is improved, the agreement between the length and velocity forms of the cross section becomes better. By $\omega_b = 7$ (fig. 6.10), reasonable agreement has been obtained, being to within 4.5% for $\lambda \lesssim 25 \times 10^3 \mathring{A}$, and to within 20% in the range $25 < \lambda(10^3 \mathring{A}) \leq 32.5$. By $\omega_b = 8$ (fig. 6.11, table 6.3), the agreement between the length and velocity forms becomes very good, although there is a slight discrepancy at the longer wavelengths. The agreement is to within 1.6% for $\lambda \leq 27.5 \times 10^3 \mathring{A}$, and for the range $27.5 < \lambda(10^3 \mathring{A}) \leq 32.5$ to within 7.3%.

The maximum in the cross section occurs at $\lambda = 20 \times 10^3 \mathring{A}$ and this value is $66.04 \times 10^{-18} cm^2$ for the length form, and $65.06 \times 10^{-18} cm^2$ for the velocity form.

The sharp peak near the n=2 threshold corresponds to the rapid rise in the ^1P phase shifts which has been discussed in chapter 4. The n=2 states of positronium need to be included in the p-wave continuum function to investigate this region. Greene and Botero (1986) have given a description of the resonances associated with the n=2 threshold.

As can be seen from table 6.4, there is a slight difference in the cross section results if the stationary Kohn phase shifts are used instead of the trial phase shifts. This slight discrepancy could be reduced by improving the p-wave function by possibly increasing the number of linear parameters and in adding long-range energy dependent terms into the function.

The length and velocity cross section results (table 6.5, 6.6) only change by a very small amount by increasing the number of linear parameters in the p-wave function from 56 to 220. For $\omega_c = 3$, some pecularity occurs in the results for wavelengths in the range $21.5 \leq \lambda(10^3 \mathring{A}) \leq 23.0$, due to the presence of possibly a schwartz singularity in the ^1P phase shifts.

The velocity cross section is larger than the length results over the whole energy range considered when the 95 linear parameter bound-state wave function and the plane wave approximation is used (Table 6.7, fig. 6.12). The same pattern has been noticed for H^- (Geltman,1962). The plane-wave treatment is a better approximation at large distances from the centre of the ion, and thus is more ap-

plicable for the long wavelengths. It is for such wavelengths that there is best agreement between length and velocity results. The plane wave approximation is more appropriate for the length formulation of the matrix element than the velocity formulation since the length form weighs more heavily the large distances from the centre of the ion. This can be seen from the results displayed in Table 6.7.

The 2 and 3 parameter wave function (Ferrante and Geracitano, 1970), which predicts electron affinity values of 0.00665144 and 0.00939454 a.u respectivly, are totally inadequate to describe the photodetachment process (Table 6.8, fig. 6.13). In fig. 6.14, a comparison is made between the results of calculation A and our length formulation results, in which we used a 95-linear parameter bound-state wave function together with

(a) a plane wave,

(b) a 220-linear parameter p-wave to represent the final state.

For short wavelengths, there is a significant disagreement in the three sets of results. The maximum in Bhatia and Drachman's cross section (calculation A) occurs at a lower wavelength than for either of our results. However, at longer wavelengths, reasonable agreement is obtained between the various results.

For very low energies, long wavelengths, there is very good agreement between the results of calculation B and our results in which we used a 95 linear parameter bound-state wave function together with a plane wave, and a 220 linear parameter p-wave for the final state (Table 6.9). At these long wavelengths, the plane wave approximation is valid.

6.7 Conclusions.

The photodetachment cross section has been calculated using a 95 linear parameter bound state wave function, which predicts an electron affinity of 0.012004615 a.u., and a 220 linear parameter p-wave for the continuum wave function for the energy range below the n=2 threshold of Ps ($0 \rightarrow 0.1875 a.u$). There is very good agreement between the length and velocity forms of the cross section over the energy range considered. (The agreement is to within 1.6% for $\lambda \leq 27.5 \times 10^3 \mathring{A}$ and to within 15% for the longer wave lengths.) The sum-rule was satisfied to within 2%. These two points give an indication of the reliability of our results.

Reasonable agreement has been obtained with Bhatia and Drachman's (1985a) calculation in which they used the 'loosely' bound approximation. The bound-state and continuum variational wave functions were systematically improved and this provided an indication of the accuracy of the final result and where there was need for further improvements.

The slight discrepancy between the length and velocity results at long wavelengths could probably be reduced by:

(1) Adding a tail-like function to the Hylleraas type bound-state wave function (Rotenberg and Stein, 1969, Ajmera and Chung, 1975), and

(2) by the inclusion of long-range energy dependent polarization terms to the p-wave function, see chapter 4.

Near the n=2 threshold, convergence in the ^1P phase shifts could be improved by adding terms of the form

$$\frac{\sin k\rho}{\rho^2}, \frac{\cos k\rho}{\rho^2}$$

in the p-wave function (Seiler et al, 1971). However, at these very short-wavelengths, the cross section is more dependent on the wave functions being accurate at small and intermediate distances than at large distances from the centre of the ion. Thus, the inclusion of long-range terms into the p-wave function will probably have little effect at these wavelengths.

It would be of interest to extend the calculation beyond the n=2 threshold. The n=2 states of positronium would have to be explicity included in the p-wave

function to extend the calculation up to the n=3 threshold. Inclusion of the n=2 levels of Ps would hopefully reveal some of the resonance structure associated with the n=2 threshold as predicted by Botero and Greene (1986).

Experimental verification of the theoretically determined photodetachment cross section is awaited with interest.

Chapter 7

Conclusions

An investigation has been performed to determine the phase shifts and the various cross-sections for the elastic scattering of slow electrons (or positrons) by positronium, below the n=2 threshold. Accurate $^{1,3}S$, $^{1,3}P$ phase shifts were determined by the Kohn and inverse Kohn variational methods. Phase shifts, up to l=5, were evaluated by using the static-exchange (S.E.) and adiabatic-exchange (A.E.) treatment. Very good agreement was obtained between the static-exchange ^3S, ^1P phase shifts with the variational results. When the parameter β appearing in the cut-off function of the adiabatic-term, in the integro-differential equation was matched to the ^3P variational phase shift, the agreement between the adiabatic-exchange and the variational phase shifts was very good for the partial waves $^{1,3}P$,^1S.

The behaviour of the $^{1,3}S$, $^{1,3}P$ phase shift for the e^--Ps system, and the agreement between the S.E. and variational results, is very similar to that obtained for the corresponding e^--H system. However, for e^--Ps, the triplet s-wave goes to zero as k tends to zero, but for e^--H, it tends to π The pattern of the $^{1,3}D$ static-exchange and adiabatic-exchange phase shifts for the two systems are different. At values of k between zero and that corresponding to the n=2 threshold, the triplet (singlet) S.E. phase shift is negative (positive), the reverse is true for e^--H. This difference is probably due to the fact that the direct potential is absent in e^-Ps. The behaviour of the d-wave phase shifts for ortho-positronium scattering by atomic hydrogen, where the direct potential is also absent, is similar to that obtained for e^--Ps.

Accurate singlet and triplet scattering lengths were determined for e^-Ps by using the s-wave variational trial function at low energies, and extrapolating $tan\delta_0^{\pm}\ /k$ to zero k. The binding energy was evaluated by diagonalizing the hamiltonian with the short-range correlation terms of the full s-wave function. $^1S^e$, $^{1,3}P$ resonances, close to the n=2 threshold, were found using our variational wave functions. Agreement with results of other authors for the binding energy, singlet scattering length and the ^1S, ^1P resonance parameters was extremely good.

The total elastic, momentum transfer, ortho-para conversion, elastic differ-

ential cross-sections were calculated for e^--Ps scattering using the s-wave and p-wave variational phase shifts, higher order phase shifts evaluated by the adiabatic-exchange method and then from the Born-polarization term. In chapter 5, a comprehensive discussion is given of the shape of these cross-sections, their features and the position of the maxima and minima.

Results for the photodetachment cross-section of Ps^-, evaluated in both length and velocity forms are presented. The bound-state wave function contained 2 non-linear and 95 linear parameters. We believe these results to be reliable since the agreement between the length and velocity forms was to better than 1.6% for most of the energy range below the n=2 threshold, and the sum-rule S_{-1} was satisfied to within 2%. Close to the n=2 threshold, a very sharp rise in the cross-section was noted.

The behaviour of the scattering properties of e^--Ps, the photodetachment cross-section of Ps^-, and its sensitivity to the accuracy of the bound-state and continuum wave functions are very similar to that obtained for the e^--H (H^-) system. This is quite remarkable since the Ps^- system consists of three particles moving about their centre of mass in some complicated manner, whereas in H^-, two electrons undergo correlated motion about the "infinitely" heavy nucleus. The Ps^- system is less attractive than H^-, and this can be seen from the fact that the binding energy of Ps^- is about half that for H^-.

With the better, more intense positron beams available, it should be possible to perform an experiment to measure elastic and inelastic cross-sections for e^--Ps scattering. From our calculation it is seen that the total elastic cross-section (σ_{el}) is large, for instance at zero energy $\sigma_{el} = 208\pi a_0^2$ and by $k = 0.45 a_o^{-1}$, $\sigma_{el} = 44\pi a_0^2$. Charlton and Jacobsen (1986) are contemplating performing such an experiment which, although it will be crude at first due to the limitations of the positron (electron) beams available, will hopefully reveal the general features of the scattering cross-sections. They suggest firing an intense pulsed positron beam from a LINAC, onto a surface to form positronium. An intense pulsed electron beam is used for the scattering part of the experiment. It is essential that the pulse time width is much less than the vacuum lifetime of o-Ps which is $(0.7242 \pm 0.0008) \times 10^7\ s^{-1}$ (Stroscio, 1975)

Although such experiments will be worthwhile to perform since (e^--Ps) is such a fundamental system, it will be in the distant future before it is feasible to detect detailed structure, such as the resonances associated with the positronium threshold, or to measure elastic differential cross-sections. These experiments will have to wait for e^+ beams of greater intensity and e^+, e^- beams of a very narrow energy resolution. At present, the energy resolution of the electron beams ($\approx 20meV$) is larger than the widths of autoionizing e^--Ps resonances ($\approx 1meV$). However, the $^1P^0$ resonance structure might be revealed via a photodetachment experiment (Ho,1984). Sufficiently strong positron sources are now available to measure the photodetachment cross-section (Mill,1981a) of Ps^-, and this experiment is awaited with great interest.

The (e^--Ps) system is very valuable to study both theoretically and experimentally since it is such a simple system and can be used to test many-electron calculation schemes. It is also a purely leptonic system so it can be used in tests of quantum electrodynamics. Therefore, such a system deserves further investigation. Theoretically, the next important step would be to explicitly include the n = 2 state of positronium in the $^{1,3}S$, $^{1,3}P$ variational wave functions. This would hopefully reveal further resonance structure associated with the n=2 threshold and the behaviour of the ^1P phase shift close to the n=2 threshold might be better understood. It would also enable the photodetachment cross-section to be extended up to the n=3 threshold.

To improve convergence of the ^1P phase shift with respect to the number of parameters and thus their accuracy, at very low energies, long-range terms of the type discussed in chapter 4 could be added to the variational wave function. A zero-energy calculation for the s-wave, which includes long-range terms in the scattering wave function, should be performed to determine singlet and triplet scattering lengths which are bounded. Convergence in the $^{1,3}S$,$^{1,3}P$ phase shifts close to the n=2 threshold could be improved by the inclusion of long-range terms (given by Seiler et al 1971) in the variational wave function. These terms have been discussed in chapter 4.

The accuracy of the elastic differential cross-section would be improved by using d-wave phase shifts determined by a very accurate variational calculation. It

would be worthwhile also to extend the static-exchange calculation to a close coupling calculation where the n=2 states and possibly the n=3 states of positronium are explicity included in the wave function.

Appendix A1

Test of numerical method for solving Integro-differential equation.

The integro-differential equation for the radial wave function obtained in the static exchange approximation for the e^--Ps system, is

$$\left(\frac{d^2}{d\rho^2} + k^2 - \frac{l(l+1)}{\rho^2}\right) u_l^{\pm}(k,\rho) = \int_0^{\infty} k_l^{\pm}(\rho,\rho')\, u_l^{\pm}(k,\rho')\, d\rho' \qquad (A1)$$

see equations (2.48), (2.49) of chapter 2.

To test the numerical method of solving this equation and the accuracy of the numerical solution, we used a test kernel which gives rise to an analytical solution of A1. It was desirable to have a test kernel and analytical solution which resembles closely the form of the true kernel and the actual solution. For simplicity we took $l = 0$ and chose a kernel of the form:

$$K_0^t(\rho,\rho') = (A\rho\rho' - B)\, e^{-\beta(\rho+\rho')}$$

in which the solution of A1 with this kernel is of sinusoidal form. This solution is denoted by: $f_0^t(\rho)$.

To obtain the exact expression for this solution, we used the Laplace transform technique.

Operating on A1 by the Laplace transform:

$$L\left\{\frac{d^2 f_0^t}{d\rho^2} + k^2 f_0^t\right\} = L\left\{\int_0^{\infty} K_0^t(\rho,\rho') f_0^t(\rho')\, d\rho'\right\} \qquad (A2)$$

where

$$L\{f_0^t(\rho)\} = \bar{f}_0^t(p) = \int_0^{\infty} e^{-p\rho} f_0^t(\rho)\, d\rho,$$

to obtain the Laplace transform of $f_0^t(\rho)$,

$$\bar{f}_0^t(p) = \frac{E}{(p^2+k^2)(p+\beta)^2} - \frac{F}{(p+\beta)(p^2+k^2)} + \frac{f_0^t(H)}{H}\,\frac{1}{(p^2+k^2)} \qquad (A3)$$

since $f_0^t(0) = 0$ and $f_0^{t\prime}(0) \approx \frac{f_0^t(h)}{h}$, provided h is small.

In equation A3, E and F are defined by:

$$E = AC = \int_0^\infty A\rho' e^{-\beta\rho'} f_0^t(\rho')\, d\rho', \qquad (A4)$$

$$F = BD = \int_0^\infty B\, e^{-\beta\rho'} f_0^t(\rho')\, d\rho'. \qquad (A5)$$

The solution $f_0^t(\rho)$, in terms of the constants E and F is obtained by applying the inverse Laplace transform of equation A3,

$$f_0^t(\rho) = \frac{E}{(\beta^2+k^2)}\left\{\frac{1}{(\beta^2+k^2)}\left\{-2\beta\cos k\rho + \left(\frac{\beta^2}{k}-k\right)\sin k\rho\right.\right.$$

$$\left.\left. + 2\beta e^{-\beta\rho} + \rho e^{-\beta\rho}\right\} - \frac{F}{(\beta^2+k^2)}\left\{e^{-\beta\rho}\cos k\rho + \frac{\beta}{k}\sin k\rho\right\}\right.$$

$$+ \frac{f_0^t(H)}{H}\,\frac{\sin k\rho}{k} \qquad (A6)$$

in which

$$C = C1(k, \beta, A, B)\,\frac{f_0^t(H)}{H}, \qquad (A7)$$

$$D = D1(k, \beta, A, B)\,\frac{f_0^t(H)}{H} \qquad (A8)$$

where C1, D1 are simple functions of $\beta, k,$, A,B, which are known.

Substituting A7, A8 into A6 setting $\rho = H$, and dividing throughout by $f_0^t(H)$, it

can be shown:

$$g(\beta,k,H) = \frac{C7}{(\beta^2+k^2)}\left\{\frac{1}{(\beta^2+k^2)}\left(-2\beta\cosh kH + \left(\frac{\beta^2}{k^2}-k\right)\sinh kH + 2\beta e^{-\beta H}\right) + H e^{-\beta H}\right\} - \frac{D7}{(\beta^2+k^2)}\left(e^{-\beta H} - \cosh kH + \frac{\beta}{k}\sinh kH\right) + \frac{\sinh kH}{k} - H = 0 \qquad (A9)$$

The value of β, for a given k, which satisfies A9, is used in equation A6. Setting $f_0^t(H) = 1$, without loss of generality, and using the corresponding value of β for a given k, the solution $f_0^t(\rho)$ as a function of ρ is calculated from A6.

With the choice H= 0.01, A=10, B=0.01, the agreement between the analytical and numerical solution was to better than 6 figures for $k = 0.1$ ($\beta = 5.903$), to mainly 6 figures for $k = 1$ ($\beta = 2.119$), $k = 2$ ($\beta = 0.931690$) and to mainly 5 figures for $k = 3$ ($\beta = 0.664366$). This agreement between the numerical and analytical solution, especially at low k, is entirely satisfactory.

Appendix A2

Derivation of the formula for the photodetachment cross section

Consider a two-electron system; two electrons and a nucleus of positive charge +e.

The coordinate diagram for this system in the laboratory frame is illustrated in fig. A2.1, and the relative coordinates are shown in fig. 2.5.

The full time-dependent Schroedinger equation for the two-electron system in a electromagnetic field is:

$$i\hbar \frac{\partial}{\partial t}\Psi(\underline{r}_1', \underline{r}_2', \underline{r}_3', t) = \left[\frac{1}{2m_e}(-i\hbar\nabla_1 + e\underline{A})^2 + \frac{1}{2m_e}(-i\hbar\nabla_2 + e\underline{A})^2 + \frac{1}{2M}(-i\hbar\nabla_3 - e\underline{A})^2 - \frac{Ze^2}{(4\pi\varepsilon_0)r_1} - \frac{Ze^2}{(4\pi\varepsilon_0)r_2} + \frac{Ze^2}{(4\pi\varepsilon_0)r_3}\right]\Psi(\underline{r}_1', \underline{r}_2', \underline{r}_3', t) \quad (A1)$$

where m_e = mass of an electron, M is the mass of the third particle of charge $+e$, and

$$\nabla_1 = \nabla_{f_1},\ \nabla_2 = \nabla_{f_2},\ \nabla_3 = \nabla_{f_3}$$

(see Eyring et al., 1946, chp.8 and Bransden and Joachain, 1983, chp.4)

Expanding the brackets to obtain:

$$i\hbar \frac{\partial}{\partial t}\Psi(\underline{r}_1', \underline{r}_2', \underline{r}_3', t) = \left[-\frac{\hbar^2}{2m_e}\nabla_1^2 - \frac{\hbar^2}{2m_e}\nabla_2^2 - \frac{\hbar^2}{2M}\nabla_3^2 - \frac{ie\hbar\underline{A}\cdot\nabla_1}{m_e} - \frac{ie\hbar\underline{A}\cdot\nabla_2}{m_e} + \frac{ie\hbar\underline{A}\cdot\nabla_3}{M} + \frac{e^2|\underline{A}|^2}{2m_e} + \frac{e^2|\underline{A}|^2}{2m_e} + \frac{e^2|\underline{A}|^2}{2M} - \frac{Ze^2}{(4\pi\varepsilon_0)r_1} - \frac{Ze^2}{(4\pi\varepsilon_0)r_2} + \frac{Ze^2}{(4\pi\varepsilon_0)r_3}\right]\Psi(\underline{r}_1', \underline{r}_2', \underline{r}_3', t) \quad (A2)$$

In the case of a weak field, $|\mathbf{A}|^2$ can be neglected since it is small compared to the linear term. Transforming from the coordinates $(\acute{r}_1, \acute{r}_2\acute{r}_3)$ to $(\mathbf{r}_2, \boldsymbol{\rho}, \mathbf{R})$, where $\mathbf{r}_2, \boldsymbol{\rho}$

are the relative coordinates and **R** is the position vector of the centre of mass from a fixed orgin, to obtain

$$i\hbar \frac{\partial}{\partial t}\bar{\Psi}(\underline{r}_2,\underline{\rho},\underline{R},t)=\left[-\frac{\hbar^2}{2\mu_1}\nabla^2_{\underline{r}_2}-\frac{\hbar^2}{2\mu_2}\nabla^2_{\underline{\rho}}-ie\hbar\underline{A}.\left(\frac{\nabla_{\underline{r}_2}}{\mu_1}+\frac{\nabla_{\underline{\rho}}}{m_e}\right)\right.$$

$$\left.-\frac{Ze^2}{(4\pi\varepsilon_0)r_1}-\frac{Ze^2}{(4\pi\varepsilon_0)r_2}+\frac{Ze^2}{(4\pi\varepsilon_0)r_3}-\frac{\hbar^2}{2(M+2m_e)}\nabla^2_{\underline{R}}-\frac{ie\hbar\underline{A}.\nabla_{\underline{R}}}{(M+2m_e)}\right]\bar{\Psi}(\underline{r}_2,\underline{\rho},\underline{R},t) \qquad (A3)$$

where μ_1 is the reduced mass of the bound electron w.r.t the psitive charge and μ_2 is the reduced mass of the free electron w.r.t the residual atom. For Ps^-, $\mu_1 = \frac{1}{2}m_e$, $\mu_2 = \frac{2}{3}m_e$, $M = m_e$ and for H^-, $\mu_1 \approx \mu_2 \approx m_e$, $M \to \infty$. Using the separation of variable technique, the total wave function is expressed as the product of the target wave function and the wave function describing the centre of mass motion,

$$\bar{\Psi}(\underline{r}_2,\underline{\rho},\underline{R},t) = \psi(\underline{r}_2,\underline{\rho},t)\,\phi(\underline{R},t)\ ,$$

So that equation A3 becomes:

$$\frac{i\hbar}{\phi(\underline{R},t)}\frac{\partial}{\partial t}\phi(\underline{R},t)-\frac{1}{\phi(\underline{R},t)}\left[\frac{-\hbar^2}{2(M+2m_e)}\nabla^2_{\underline{R}}-\frac{ie\hbar\underline{A}.\nabla_{\underline{R}}}{(M+2m_e)}\right]\phi(\underline{R},t)$$

$$=\frac{-i\hbar}{\psi(\underline{r}_2,\underline{\rho},t)}\frac{\partial}{\partial t}\psi(\underline{r}_2,\underline{\rho},t)+\frac{1}{\psi(\underline{r}_2,\underline{\rho},t)}\left[\frac{-\hbar^2}{2\mu_1}\nabla^2_{\underline{r}_2}-\frac{\hbar^2}{2\mu_2}\nabla^2_{\underline{\rho}}\right.$$

$$\left.-\frac{Ze^2}{(4\pi\varepsilon_0)r_1}-\frac{Ze^2}{(4\pi\varepsilon_0)r_2}+\frac{Ze^2}{(4\pi\varepsilon_0)r_3}-ie\hbar\underline{A}.\left(\frac{\nabla_{\underline{r}_2}}{\mu_1}+\frac{\nabla_{\underline{\rho}}}{m_e}\right)\right]$$

$$\psi(\underline{r}_2,\underline{\rho},t)$$

$$=C \qquad (A4)$$

where C is independent of the spacial variables $\mathbf{r}_2, \boldsymbol{\rho}, \mathbf{R}$.

It is assumed that A is independent of position, i.e. the wavelength of the radiation is large compared with the size of the atom (ion) (Feynman, 1961). The equation of motion for the centre of mass is obtained from A4,

$$i\hbar \frac{\partial}{\partial t}\phi(\underline{R},t) = \left[\frac{-\hbar^2}{2(M+2m_e)}\nabla_{\underline{R}}^2 - \frac{ie\hbar}{(M+2m_e)}\underline{A}\cdot\nabla_{\underline{R}}\right]\phi(\underline{R},t) \qquad (A5)$$

$$+ C\phi(\underline{R},t)$$

To show that C=0, the substition given by Daniele and Ferrante, (1982) is used:

$$\phi(\underline{R},t) = \chi(\underline{R})\, e^{-iE_{cm}t/\hbar}\, e^{-\beta(t)}$$

where $E_{cm} = \frac{\hbar^2 K_{cm}^2}{2(M+2m_e)}$ and $\beta(t) = i\int_0^t \frac{e}{(M+2m_e)} K_{cm}\cdot A(\tau)\, d\tau$, to obtain

$$\left[E_{cm} + \frac{e\hbar}{(M+2m_e)}\underline{K}_{cm}\cdot\underline{A}(t)\right]\chi(\underline{R})e^{-iE_{cm}t/\hbar}\, e^{-\beta(t)}$$

$$= \left[\frac{-\hbar^2}{2(M+2m_e)}\nabla_{\underline{R}}^2 - \frac{ie\hbar}{(M+2m_e)}\underline{A}\cdot\nabla_{\underline{R}}\right]\chi(\underline{R})e^{-iE_{cm}t/\hbar}\, e^{-\beta(t)}$$

$$+ C\chi(\underline{R})e^{-iE_{cm}t/\hbar}\, e^{-\beta(t)} \qquad (A6)$$

Now, $k_{cm} = -i\nabla_R$, and in the coulomb gauge

$$\nabla\cdot(\underline{A}\,\underline{\psi}) = \underline{A}\cdot(\nabla\underline{\psi}) + (\nabla\cdot\underline{A})\underline{\psi} = \underline{A}\cdot(\nabla\underline{\psi}),$$

Hence, $$\frac{-\hbar^2}{2(M+2m_e)}\nabla_{\underline{R}}^2\chi(\underline{R}) = (E_{cm} - C)\chi(\underline{R}),$$

which is a plane wave equation, C=0 and the solution being:

$$\chi(\mathbf{R}) = e^{i\mathbf{K}.\mathbf{R}}.$$

Thus, with C=0 and in the approximation that $|\mathbf{A}|^2$ can be treated as a constant

over the size of the ion, the Schroedinger equation for the relative motion is:

$$i\hbar \frac{\partial}{\partial t}\psi(\underline{r}_2,\underline{\rho},t) = \left[-\frac{\hbar^2}{2\mu_1}\nabla^2_{\underline{r}_2} - \frac{\hbar^2}{2\mu_2}\nabla^2_{\underline{\rho}} - \frac{Ze^2}{(4\pi\varepsilon_0)r_1} - \frac{Ze^2}{(4\pi\varepsilon_0)r_2}\right.$$

$$\left. + \frac{Ze^2}{(4\pi\varepsilon_0)r_3} - ie\hbar\underline{A}\cdot\left(\frac{\nabla_{\underline{r}_2}}{\mu_1} + \frac{\nabla_{\underline{\rho}}}{m_e}\right)\right]\psi(\underline{r}_2,\underline{\rho},t) \qquad (A7)$$

This is written as:

$$\frac{\partial}{\partial t}\psi(\underline{r}_2,\underline{\rho},t) = [H_0 + H_1]\,\psi(\underline{r}_2,\underline{\rho},t). \qquad (A8)$$

where H_0 is unperturbed Hamiltonian

$$H_0 = -\frac{\hbar^2}{2\mu_1}\nabla^2_{\underline{r}_2} - \frac{\hbar^2}{2\mu_2}\nabla^2_{\underline{\rho}} - \frac{Ze^2}{(4\pi\varepsilon_0)r_1} - \frac{Ze^2}{(4\pi\varepsilon_0)r_2} + \frac{Ze^2}{(4\pi\varepsilon_0)r_3} \qquad (A9)$$

and the perturbed Hamiltonian H_1 is given by:

$$H_1 = -ie\hbar\,\underline{A}\cdot\left(\frac{\nabla_{\underline{r}_2}}{\mu_1} + \frac{\nabla_{\underline{\rho}}}{m_e}\right). \qquad (A10)$$

and is solved by using the time dependent perturbation theory. The wave function $\psi(\mathrm{r}_2,\rho,t)$ is expanded in terms of the unperturbed eigenfunctions ψ_k which are solutions of

$$H_0\psi_k = E_k\psi_k$$

so that

$$\psi(\underline{r}_2,\underline{\rho},t) = \sum_k c_k(t)\,\psi_k(\underline{r}_2,\underline{\rho})\,e^{-iE_kt/\hbar} \qquad (A11)$$

where the coefficients $c_k(t)$ satisfy

$$\dot{c}_b(t) = (i\hbar)^{-1}\sum_k H'_{bk}(t)\,c_k(t)e^{i\omega_{bk}t} \qquad (A12)$$

where

$$H'_{bk} = \left\langle \psi_b(\underline{r}_2,\underline{\rho})\middle| -ie\hbar\underline{A}\cdot\left(\frac{\nabla_{\underline{r}_2}}{\mu_1} + \frac{\nabla_{\underline{\rho}}}{m_e}\right)\middle|\psi_k(\underline{r}_2,\underline{\rho})\right\rangle \qquad (A13)$$

and $\omega_{bk} = \frac{(E_b - E_k)}{\hbar}$.

The system is assumed to be in a well defined stationary state of energy E_a described by the wave function ψ_a, and the pulse of radiation is switched on at time t=0, thus $c_b(t \leq 0) = \delta_{ka}$, and 1^{st} order perturbation theory gives:

$$c_b^{(1)}(t) = -\frac{e}{}\int_0^t \langle \psi_b(\underline{r}_i, \underline{r}_f) | \underline{A} \cdot \left(\frac{\nabla_{\underline{r}_i}}{\mu_i} + \frac{\nabla_{\underline{r}_f}}{m_e} \right) | \psi_a(\underline{r}_i, \underline{r}_f) \rangle e^{i\omega_{ba}t'} dt' \qquad (A14)$$

The vector potential is written as:

$$\underline{A}(\underline{r}, t) = \int_{\Delta\omega} A_0(\omega)\, \hat{\varepsilon} \left[\exp[i(\underline{k}_\gamma \cdot \underline{r} - \omega t + \delta_\omega)] + c.c. \right] d\omega$$

which gives:

$$c_b^{(1)}(t) = -\frac{e}{}\int_{\Delta\omega} d\omega A_0(\omega) \left[e^{i\delta_\omega} \langle \psi_b | e^{i\underline{k}_\gamma \cdot \underline{r}}\, \hat{\varepsilon} \cdot \left(\frac{\nabla_{\underline{r}_i}}{\mu_i} + \frac{\nabla_{\underline{r}_f}}{m_e} \right) | \psi_a \rangle \int_0^t dt\, e^{i(\omega_{ba} - \omega)t'} \right.$$

$$\left. + e^{-i\delta_\omega} \langle \psi_b | e^{i\underline{k}_\gamma \cdot \underline{r}}\, \hat{\varepsilon} \cdot \left(\frac{\nabla_{\underline{r}_i}}{\mu_i} + \frac{\nabla_{\underline{r}_f}}{m_e} \right) | \psi_a \rangle \int_0^t dt' e^{i(\omega_{ba} + \omega)t'} \right]$$

The first term corresponds to absorption and the second term to emission. Thus, for absorption, the probability for the system to be in state b at time t is:

$$|c_b^{(1)}(t)|^2 = 2\int_{\Delta\omega} d\omega \left[\frac{eA_0(\omega)}{m} \right]^2 |M_{ba}(\omega)|^2 F(t, \omega - \omega_{ba}) \qquad (A15)$$

where

$$M_{ba}(\omega) = m_e \langle \psi_b | e^{i\underline{k}_\gamma \cdot \underline{r}}\, \hat{\varepsilon} \cdot \left(\frac{\nabla_{\underline{r}_i}}{\mu_i} + \frac{\nabla_{\underline{r}_f}}{m_e} \right) \psi_a \rangle$$

and

$$F(t, \omega - \omega_{ba}) = \frac{1 - \cos(\omega - \omega_{ba})t}{(\omega - \omega_{ba})^2} .$$

Since $F(t, \omega - \omega_{ba})$ is strongly peaked and $A_0(\omega)$, $|M_{ba}(\omega)|^2$ are slowly varying

functions of ω, equation A15 becomes:

$$|C_b^{(1)}(t)|^2 = 2\pi\left[\frac{eA_0(\omega_{ba})}{m_e}\right]^2 |M_{ba}(\omega_{ba})|^2 t$$

The absorption cross-section is given by:

$$\sigma_{ba} = \frac{\hbar\omega_{ba}}{I(\omega_{ba})} \frac{d}{dt} |C_b^{(1)}(t)|^2$$

where the Intensity $I(\omega_{ba}) = 2\epsilon_0\omega_{ba}^2 c A_0^2(\omega_{ba})$. Thus,

$$\sigma_{ba} = \frac{4\pi^2\alpha\hbar^2}{m_e^2\omega_{ba}} |M_{ba}(\omega_{ba})|^2 \qquad (A16)$$

where

$$M_{ba}(\omega_{ba}) = m_e\langle\psi_b| e^{i\underline{k_\gamma}\cdot\underline{r}} \hat{\varepsilon}\cdot\left(\frac{\nabla_{r_2}}{\mu_1} + \frac{\nabla_{r_1}}{m_e}\right)|\psi_a\rangle . \qquad (A17)$$

It is assumed that we are dealing with weak fields and that the vector potential **A** can be treated as a constant over the size of the atom (ion).
For wave lengths large compared with the size of the atom (ion), i.e. for $|k_\gamma.r| << 1$,

$$exp(i\mathbf{k}.\mathbf{r}) \approx 1.$$

(Hilbert, 1978) Taking $exp(i\mathbf{k}.\mathbf{r}) = 1$ in equation A17 is known as the dipole approximation, and thus (A18)

$$M_{ba}(\omega_{ba}) = m_e\langle\psi_b| \hat{\varepsilon}\cdot\left(\frac{\nabla_{r_2}}{\mu_1} + \frac{\nabla_{r_1}}{m_e}\right)|\psi_a\rangle .$$

In photodetachment, the electron is emitted in a certain direction (θ, ϕ) and its energy is not quantized. Therefore, to obtain the photodetachment cross section, the absorption cross section is multiplied by the density of final states $(\tilde{\rho}_b(\omega))$ and integrated over all particular angles, (Bhatia, 1985),

$$\sigma = \frac{4\pi^2\alpha\hbar^2}{m^2\omega} \int_\Omega |M_{ba}(\omega)|^2 \tilde{\rho}_b(\omega) d\Omega \qquad (A19)$$

where $\tilde{\rho}_b(\omega)\, d\Omega = \frac{\mu_{r_2} - k}{\hbar}\, d\Omega$.

The velocity matrix element $M_{ba}(\omega)$ can be expressed in terms of a length form by using Heisenberg's equation of motion for the dynamical variables $\mathbf{r}_2, \rho$.

$$M_{ba}^{V} = m_e \langle \psi_b | \hat{\varepsilon} \cdot \left(\frac{\nabla_{r_2}}{\mu_1} + \frac{\nabla_\rho}{m_e} \right) | \psi_a \rangle$$

$$= \frac{i m_e}{\hbar} \hat{\varepsilon} \cdot \langle \psi_b | \left(\frac{\vec{P}_{r_2}}{\mu_1} + \frac{\vec{P}_\rho}{m_e} \right) | \psi_a \rangle$$

$$= \frac{i m_e}{\hbar} \hat{\varepsilon} \cdot \langle \psi_b | \dot{\underline{r}}_2 + \frac{\mu_2 \dot{\rho}}{m_e} | \psi_a \rangle \qquad (A20)$$

$$= -\frac{m_e \omega}{\hbar} \hat{\varepsilon} \cdot \langle \psi_b | \underline{r}_2 + \frac{\mu_2}{m_e} \rho | \psi_a \rangle .$$

Changing the normalization of the final state wave function from

$$\psi_b \underset{\rho \to \infty}{\sim} (2\pi)^{-3/2} e^{i \underline{k} \cdot \rho} \quad \text{to} \quad \psi_f \sim e^{i \underline{k} \cdot \rho}$$

such that $\langle \psi_f | \psi_f \rangle = \delta(\mathbf{k}' - \mathbf{k})$, σ needs to be multiplied by $(2\pi)^3$. Hence, the resulting cross-section is:

$$\sigma_\lambda = \frac{\mu_2 k \alpha \omega}{2\pi \hbar} \int | \hat{\varepsilon} \cdot \langle \psi_f | (\underline{r}_2 + \frac{\mu_2}{m_e} \rho) | \psi_i \rangle |^2 d\Omega$$

where ψ_i represents the initial state.

$\therefore$

$$\sigma_\lambda(L) = \frac{2}{3} \frac{\mu_2 k \alpha \omega}{\hbar} |\mu^L|^2$$

where $$\mu^L = \hat{\underline{k}} \cdot \langle \psi_f | (\underline{r}_2 + \frac{\mu_2}{m_e} \rho) | \psi_i \rangle .$$

From energy conservation,

$$\omega = \frac{k^2}{2\mu_2} + \frac{\gamma^2}{2\mu_2} \quad \text{a.u.}$$

where $\frac{\gamma^2}{2\mu_2}$ is the electron affinity of the negative ion and ω is the angular frequency in atomic units.

Hence, the photodetachment cross section in the length formulation is given by:

$$\sigma_\lambda(L) = 6.8115 \times 10^{-20} k(k^2+\gamma^2)|\mu^L|^2 \text{ cm}^2, \quad (A21)$$

where k, γ are expressed in atomic units, and the dipole length matrix element is:

$$\mu^L = \hat{k} \cdot \langle \psi_f | (\underline{r}_2 + \mu_2 \underline{\rho}) | \psi_i \rangle \text{ a.u.} \quad (A22)$$

From A20

$$\langle \psi_f | (\underline{r}_2 + \mu_2 \underline{\rho}) | \psi_i \rangle = -\frac{1}{\omega} \langle \psi_f | \frac{\nabla_{\underline{r}_2}}{\mu_1} + \nabla_{\underline{\rho}} | \psi_i \rangle \text{ a.u.}$$

and thus the photodetachment cross-section in the velocity formulation is given by:

$$\sigma_\lambda(V) = 2.7246 \times 10^{-19} \mu_2^2 \frac{k}{(k^2+\gamma^2)} |\mu^V|^2 \text{ cm}^2 \quad (A23)$$

where

$$\mu^V = \hat{k} \cdot \langle \psi_f | \left(\frac{\nabla_{\underline{r}_2}}{\mu_1} + \nabla_{\underline{\rho}} \right) | \psi_i \rangle \text{ a.u.} \quad (A24)$$

The initial state wave function is normalized to $\int |\psi_i|^2 d\tau = 1$ (A25)
and the continuum wavefunction is normalized so that:

$$\langle \psi_f / \psi_f \rangle = (2\pi)^3 \delta(\mathbf{k}' - \mathbf{k}). \quad (A26).$$

Appendix A3

Photodetachment cross-section of Ps^- using variational bound-state and p-wave continuum wave functions.

The bound-state wave function is given by:

$$\Psi_i = \frac{1}{\sqrt{2}} \frac{1}{(4\pi)^{1/2}} \sum_{j=1}^{N'} g_j , \qquad (A1)$$

where

$$g_j = d_j e^{-\alpha r_3} e^{-\beta s} s^{k_j} t^{l_j} r_3^{m_j},$$

$$k_j + l_j + m_j \leq \omega_b,\ k_j, l_j, m_j \in [0, 1, 2, \ldots \omega_b],$$

l_j is even for all j, $s = r_1 + r_2$, $t = r_1 + r_2$ and Ψ_i satisfies

$$\int |\Psi_i|^2 \, d\tau = 1.$$

The p-wave continuum wave function is given by:

$$\Psi_f^+ = \left(\frac{12\pi}{k}\right)^{1/2} \Big[(S\Upsilon + \bar{S}\bar{\Upsilon}) + \tan\delta_1^+ (C\Upsilon + \bar{C}\bar{\Upsilon}) + \frac{1}{\sqrt{2}} (Y_{10}(\hat{\rho})\rho + Y_{10}(\hat{\rho}')\rho') \sum_{i=1}^{N1-1} f_i \qquad (A2)$$

$$+ \frac{1}{\sqrt{2}} (Y_{10}(\hat{\rho})\rho - Y_{10}(\hat{\rho}')\rho') \sum_{i=N1}^{N'} f_i \Big]$$

where l_i is even for $i = 1 \rightarrow N1 - 1$, odd for $i = N1 \rightarrow N$,

$$k_i + l_i + m_i \leq \omega_c,\ k_i, l_i, m_i \in [0, 1, 2, \ldots \omega_c],$$

and

$$SY = \sqrt{\frac{k}{2}}\ \phi_{p_3}(r_2)\ Y_{10}(\hat{\rho})\ J_1(k\rho),$$

$$\bar{S}\bar{Y} = \sqrt{\frac{k}{2}}\ \phi_{p_3}(r_1)\ Y_{10}(\hat{\rho}')\ J_1(k\rho'), \qquad (A3)$$

$$CY = -\sqrt{\frac{k}{2}}\ \phi_{p_3}(r_2)\ Y_{10}(\hat{\rho})\, n_1(k\rho)\left[1-\exp(-\mu\rho)\right]^5,$$

$$\bar{C}\bar{Y} = -\sqrt{\frac{k}{2}}\ \phi_{p_3}(r_1)\ Y_{10}(\hat{\rho}')\, n_1(k\rho')\left[1-\exp(-\mu\rho')\right]^5,$$

and

$$f_i = c_e^{-ar_3} e^{-bs} s^{k_i} t^{l_i} r_3^{m_i}.$$

Note, the p-wave scattering function has been multiplied by $\sqrt{\frac{12\pi}{k}}$ so that the normalization condition

$$\langle \Psi_f / \Psi_f \rangle = (2\pi)^3 \delta(\mathbf{k}' - \mathbf{k})$$

is satisfied.

(i) Length formulation.

$$\sigma_L = 6.8115 \times 10^{-20}\, k(k^2+\gamma^2)\, |M_z^L|^2\, cm^2 \qquad (A4)$$

where

$$M_z^L = \langle \bar{\Psi}_f | (r_2 + \tfrac{2}{3}\rho)_{3-cpt} | \bar{\Psi}_i \rangle$$

$$= \tfrac{2}{3} \langle \bar{\Psi}_f (r_1 \cos\theta_1 + r_2 \cos\theta_2) \bar{\Psi}_i \rangle \qquad (A5)$$

in which the coordinate system is chosen so that the z-axis is parallel to the direction of the emitted electron. The matrix element written explicity in terms of the

variational bound state and continuum wave functions is:

$$M_z^L = \left(\frac{12\pi}{k}\right)^{1/2} \frac{2}{3} \frac{1}{\sqrt{2}} \frac{1}{(4\pi)^{1/2}} \sum_{j=1}^{N'} \Big\{ 2 \langle S Y(r_1\cos\theta_1 + r_2\cos\theta_2) g_j \rangle$$

$$+ 2\tan\delta_1^+ \langle C Y(r_1\cos\theta_1 + r_2\cos\theta_2)\, g_j \rangle$$

$$+ \frac{1}{\sqrt{2}} \sum_{i=1}^{N1-1} \langle C Y_{10}(\hat{\rho})\rho + Y_{10}(\hat{\rho}')\rho')(r_1\cos\theta_1 + r_2\cos\theta_2) f_i\, g_j \rangle$$

$$+ \frac{1}{\sqrt{2}} \sum_{i=N1}^{N} \langle (Y_{10}(\hat{\rho})\rho - Y_{10}(\hat{\rho}')\rho')(r_1\cos\theta_1 + r_2\cos\theta_2) f_i\, g_j \rangle \Big\},$$

(A6)

where $Y_{10}(\hat{\rho}) = \sqrt{\frac{3}{4\pi}}\cos\theta_\rho = \sqrt{\frac{3}{4\pi}} \frac{1}{\rho}(r_1\cos\theta_1 - \frac{1}{2} r_2\cos\theta_2)$,

$$C Y_{10}(\hat{\rho})\rho + Y_{10}(\hat{\rho}')\rho') = \sqrt{\frac{3}{4\pi}} \frac{1}{2}(r_1\cos\theta_1 + r_2\cos\theta_2)$$

$$C Y_{10}(\hat{\rho})\rho - Y_{10}(\hat{\rho}')\rho') = \sqrt{\frac{3}{4\pi}} \frac{3}{2}(r_1\cos\theta_1 - r_2\cos\theta_2).$$

(A7)

Note: The matrix elements required for σ_L are of the same form as the open closed and closed closed channel matrix elements of the p-wave calculation. Therefore, these integrations were performed in the same way as that used for the p-wave matrix elements, and this procedure is described in chapter 4.

After performing the integration over the external variables, the length matrix ele-

ment becomes:

$$\mu_z^L = \left(\frac{12\pi}{k}\right)^{1/2} \frac{1}{24} \sqrt{\frac{\pi}{6}} \sum_{j=1}^{N'} \left\{ \sqrt{k} \int_0^\infty\int_0^\infty\int_0^\infty \frac{e^{-\frac{1}{2}r_2}}{\rho} \left\{ \frac{\sin k\rho}{(k\rho)^2} - \frac{\cos k\rho}{k\rho} \right\} g_j \right.$$

$$\times (5r_1^2 - r_2^2 - r_3^2)\, r_1 r_2 r_3 \, dx\,dy\,dz$$

$$+ \tan\delta_1^+ \sqrt{k} \int_0^\infty\int_0^\infty\int_0^\infty \frac{e^{-\frac{1}{2}r_2}}{\rho} \left\{ \frac{\cos k\rho}{(k\rho)^2} + \frac{\sin k\rho}{k\rho} \right\} [1 - \exp(-\mu\rho)]^5 g_j$$

$$\times (5r_1^2 - r_2^2 - r_3^2)$$

$$r_1 r_2 r_3 \, dx\,dy\,dz$$

$$+ 8\sqrt{2\pi} \sum_{i=1}^{N1-1} \int_0^\infty\int_0^\infty\int_0^\infty r' f_i g_j \, r_1 r_2 r_3 \, dx\,dy\,dz$$

$$\left. + 12\sqrt{\frac{\pi}{2}} \sum_{N1}^{N} \int_0^\infty\int_0^\infty\int_0^\infty (r_1^2 - r_2^2) f_i g_j \, r_1 r_2 r_3 \, dx\,dy\,dz \right\}$$

(A 8)

where

$$r' = \frac{1}{4}\left\{ 2(r_1^2 + r_2^2) - r_3^2 \right\},$$

$$\rho^2 = \frac{1}{4}\left\{ 2(r_1^2 + r_3^2) - r_2^2 \right\},$$

and where x, y, z are defined by

$$x = r_1 + r_2 - r_3$$

$$y = r_2 + r_3 - r_1$$

$$z = r_3 + r_1 - r_2$$

(ii) Velocity formulation

$$\nabla_V = 1.2109 \times 10^{-19} \frac{k}{(k^2 + \gamma^2)} |\mu^V|^2 \, cm^2 \qquad (A9)$$

where $\mu^V = \langle \bar{\Psi}_f | (2\nabla_{\underline{r}_2} + \nabla_f) | \Psi_i \rangle$ a.u

$$= 2 \langle \Psi_f | (\nabla_{\underline{r}_1} + \nabla_{\underline{r}_2}) | \Psi_i \rangle . \qquad (A10)$$

After performing the integration over the external variables in the manner discussed

in chapter 4, the velocity matrix element becomes:

$$M_2^V = \left(\frac{12\pi}{k}\right)^{1/2} \frac{1}{2}\sqrt{\frac{\pi}{6}} \sum_{j=1}^{N'} \left[\sqrt{k} \int_0^\infty\int_0^\infty\int_0^\infty \frac{e^{-\frac{1}{2}r_2}}{\rho} \left\{\frac{\sin k\rho}{(k\rho)^2} - \frac{\cos k\rho}{k\rho}\right\}\right.$$

$$\left\{\left(r_1 - \tfrac{1}{2}r_2\right)\left(1+\cos\theta_{12}\right)\left(-\beta + k; s^{-1}\right) + \left(r_1 + \tfrac{1}{2}r_2\right)\left(1-\cos\theta_{12}\right)L; t^{-1}\right\}$$

$$g_j; r_1 r_2 r_3 dx dy dz\Big\}$$

$$+ \tan\delta_1^+ \sqrt{k} \int_0^\infty\int_0^\infty\int_0^\infty \frac{e^{-\frac{1}{2}r_2}}{\rho} \left\{\frac{\cos k\rho}{(k\rho)^2} + \frac{\sin k\rho}{k\rho}\right\} \left[1 - \exp(-\mu\rho)\right]^S \qquad (A11).$$

$$\left\{\left(r_1 - \tfrac{1}{2}r_2\right)\left(1+\cos\theta_{12}\right)\left(-\beta + k; s^{-1}\right) + \left(r_1 + \tfrac{1}{2}r_2\right)\left(1-\cos\theta_{12}\right)L; t^{-1}\right\}$$

$$g_j; r_1 r_2 r_3 dx dy dz\Big\}$$

$$+ \frac{\pi}{2} \sum_{i=1}^{N1-1} \int_0^\infty\int_0^\infty\int_0^\infty \left\{\left(-\beta s + k; + L_j\right) + \cos\theta_{12}\left(-\beta s + k; -L_j\right)\right\} f_i\, g_j; r_1 r_2 r_3 dx dy dz\Big\}$$

$$f_i\, g_j; r_1 r_2 r_3 dx dy dz\Big\}\Big]$$

$$+ \frac{3\pi}{2} \sum_{N1}^{N} \int_0^\infty\int_0^\infty\int_0^\infty \left(-\beta t + k; s^{-1}t + L; st^{-1}\right) + \cos\theta_{12}\left(-\beta t + k; s^{-1}t - L; st^{-1}\right)\Big\}$$

$$f_i\, g_j; r_1 r_2 r_3 dx dy dz\Big\}$$

The integrations over the internal variables, x, y, z, were performed numerically using Gauss-Laguerre Quadrature.

References

Arifov,P.U., and Malyan,V.M. and Paisiev,A.A, abstracts of papers, X ICPEAC (Commissariat a l'Energie Atomique, Paris, 1977), pg.824

Armstead, R.L, 1968, Phys.Rev. 171 92

Ajmera,M.P. and Chung,K.T.,1975, Phys. Rev. A 12 475

Baltenko,A.S. and Segal,I.D., 1983, Sov.Phys. -Tech.Phys. 28 508

Bates,D.R.,1978, Phys.Rep. (Phys. Lett. C) 35

Beling,C.D., Simpson,R.I., Charlton,M, Jacobsen,F.M. Griffith,T.C., 1986 "International workshop on slow Positron beam techniques for Solid state and surface studies." University of East Anglia, Norwich, U.K., July, 7-10^{th} 1986, Programme and Abstracts.

Bell,K.L. and Kingston,A.E., 1967, Proc. Phys. Soc. 90 895

Berko,S. Canter,K.F., Mills,A.P.Jr., Lynn,K.G., Roellig,L.O. and Weber,M., 1986, 7^{th} International Conference on Positron Annihilation. (Eds. R.M. Singru and P.C. Jain). World Scientific, Singapore.

Bethe,H.A. and Peierls,R., 1935, Proc. R. Soc. London, Ser. A 148 146

Bethe,H.A. and Longmire,C., 1950, Phys. Rev. 77 647

Bethe,H.A. and Salpeter,E.E., 1957, "Quantum Mechanics of one- and two electron atoms". Springer Verlag, Berlin Gottingen Heidelberg

Bhatia, A.K. 1985, Private communication

Bhatia,A.K., Drachman,R.J. and Temkin,A, 1977 Phys.Rev. A16 1719

Bhatia,A.K. and Drachman,R.J., 1983, Phys. Rev. A 28 2523

Bhatia,A.K. and Drachman,R.J., 1985a, Phys. Rev. A 32 3745

Bhatia,A.K. and Drachman,R.J., 1985b, Private communication.

Bhatia,A.K.and Drachman,R.K., 1986, contributed paper in "Positron (Electron)-Gas Scattering." (Eds. W.E. Kauppila, T.S. Stein, J.M.Wadehra), World Scientific, Singapore.

Botero,J. and Greene,C.H., 1985, Phys.Rev. A32 1249

Botero,J. and Greene,C.H., 1986, Phys. Rev. Lett. 56 1366

Branscomb,L.M., 1962, "Atomic and Molecular Processes." (Ed.D.R.Bates) pg. 100, Academic Press, New York and London.

Branscomb,L.M., 1969,"Physics of one and two Electron Atoms." (Eds H. Kleinpoppen and H.Bopp) pg. 669, North-Holland Publishing Company, Amsterdam.

Bransden,B.H., 1969, Case Stud.At. Collision. Phys. 1 171

Bransden, B.H. 1983, "Atomic Collision Theory" 2^{nd} Edition, Benjamin/Cummings publishing company, inc. London, Amsterdam

Bransden,B.H. and Joachain,C.J., 1983, "Physics of atoms and molecules" Longman, New York and London.

Broad,J.T. and Reinhardt,W.P., 1976, Phys. Rev. A 14 2159

Brown,B.L., 1986, "Positron (Electron)- Gas Scattering", Proceedings of the Third International Workshop, Wayne State University, Detroit, Michigan, July 16-18, 1985. (Eds. W.E. Kauppila, T.S. Stein and J.M. Wadehra, World Scientific, Singapore.

Brown,C.J. and Humberston,J.W. 1984, J.Phys. B. 17 L423

Brown,C.J., 1986, Ph.D. Thesis, University of London.

Buckingham,R.A., and Massey,H.S.W., 1941 Proc.Roy.Soc. A 179 123

Burke,P.G., 1976, "Atomic processes and their application." (Eds P.G.Burke and B.L.Moiseiwitah.) pg 199 North-Holland Publishing Company, Amsterdam, and Oxford.

Burke,P.G., and Roberston,H.H., 1957, Proc.Phys.Soc.A 70 779

Burke, P.G. and Schey, H.M., 1962, Phys.Rev. 126 147

Burke,P.G and Eissner,W. 1983 *In* "Atoms in Astrophysics", Chapter 1, (Eds. P.G. Burke, W.B. Eissner, D.G. Hummer and I.C. Percival)

Burns, M.L., Harding,A.K., Ramaty,R., 1983, "Positron-Electron Pairs in Astrophysics", (Goddard Space Flight Center, 1983, AIP Conference Proceedings.(Series Editor: H.C. Wolfe, No.101, American Institute of Physcis, (New York)

Byron,F.W.,Jr., Joachain,C.J. and Potvilege,R.M., 1982, J.Phys.B 15, 3915

Callaway,J., 1978, Phys.Rep. (Phys. Lett. C) 45 89

Canter,K.F., 1984, "Positron Scattering in Gases". (Eds. J.W. Humberston, M.R.C. McDowell). Plenum Press, New York and London.

Canter,K.F., Coleman,P.G., Griffith,T.C., and Heyland,G.R., 1972 J.Phys.B 5 L167

Chandrasekhar,S. and Kragdahl,M.K. 1943, Ap.J. 98 205

Chandrasekhar,S. 1945, Ap.J. 102 223

Charlton, M., 1985, Rep.Prog.Phys., 1985, 48, 737

Charlton,M. and Jacobsen,F.M, 1986, Invited talk at symposium on the "Production of low-energy Accelerators and Applications" Giessen, September 1986.

Coleman,D.G., Griffith,T.C., and Heyland,G.R., 1973, Proc.R.Soc., A 331 561

Costello,D.G., Groce,D.E., Herring,D.F., and McGowan,J.W., 1972, Phys.Rev. B5, 1433

Costello,D.G., Groce,D.E. Herring,D.F., and McGowan,J.W., 1972, Can.J.Phys.50 23

Dalgarno,A. and Lynn,N. 1957 Proc.Phys.Soc. 70A 802

Dalgerno,A and Kingston,A.E. 1959, Proc.Phys.Soc.73 455

Daniele,R. and Ferrante,G. 1982, J.Phys. B 15 2741

Dasgupta,A. and Bhatia,A.K., 1984, Phys.Rev. A30 1241

Doughty,N.A. Fraser,P.A. and McEachran,R.P. 1966, Mon.Not.R.astr.Soc.132 255

Drachman, R.J., 1972, "Proc.Int.conf.Phys. Electron At. Collisions, 7^{th}", 1971, Invited Talks and Progress Reports, pg.277

Drachman, R.J. 1982a, Can.J.Phys.60 494

Drachman,R.J., 1982b, "Positron annihilation", Proceedings of the sixth International Conference on Positron Annihilation, University of Texas, Arlington, April 3-7, 1982, North-Holland Publishing Company, Amsterdam, New York, Oxford.

Drachman,R.J. 1984 Private communication

Drachman,R.J., and Temkin, A., 1972 *In* "Case studies in Atomic Collision Physics." (Eds. E.W. McDaniel an M.R.C. McDowell) North Holland, Amsterdam, vol.2. pg.394.

Eyring,H, Walter,J and Kimball,G.E. 1945, "Quantum Chemistry" New York, John Wiley and Sons, Inc. Chapman and Hall, Ltd. London.

Fels,M.F. and Mittleman,M.H., 1967, Phys.Rev. 163 129

Fels,M.F., and Hazi,A.U., 1972, Phys.Rev. A5 1236

Ferrante, G. 1968, Phys.Rev. 170 76

Ferrante,G. and Geracitano,R. 1970, Lettere al Nucvo Cimento serie I, 3 45

Feynman,R.P. 1961, "Quantum Electro-dynamics" W.A. Benjamin, Inc., Publishers New York.

Fox,L. and Goodwin,E.T, 1949, Proc.Camb.phil.Soc. 45 373

Fraser,P.A., 1968, Adv. At.Mol.Phys. 4 63

Froberg, C., 1979, "Introduction to Numerical Analysis" 2^{nd} Edition, Addison-Wesley Publishing Company, London.

Gailitis, M, 1965, Sov.Phys.-JETP. 20 107

Geltman,S. 1962. Ap.J. 136 935

Ghosh,A.S., Sil,N.C. and Mandal,P., 1982, Phys.Rep. (Phys. Lett. C) 87 313

Gidley,D.W., Frieze, W.E., Mayer,R. and Lynn,K.G. 1986, contributed paper in "Positron (Electron)- Gas Scattering." (Eds. W.E. Kauppila, T.S. Stein, J.M.Wadehra) World Scientific, Singapore.

Greene, C.H., 1986, Private communication.

Griffith,T.C. and Heyland,G.R., 1978, Phys.Rep., (Phys. Lett. C) 170

Gullikson,E.M., 1986 "International workshop on slow Positron beam techniques for solid state and surface studies", University of East Anglia, Norwich, U.K. July 7-10^{th}, 1986, Programme and Abstracts.

Haas,F.A. and Roberston,H.H., 1959, Proc.Phys.Soc. A 73 160

Hara,S and Fraser,P.A. 1975 J.Phys.B 8 L472

Hart,J.F. and Herzberg,G. 1957 Phys.Rev. 106 79

Hazi, A.U. and Taylor, H.S., 1970, Phys.Rev. A1 1109

Herrick,D.R., 1982, Adv.Chem.Phys. 52 1

Hilbert,A. 1978, chp.1 Atomic Structure Theory, "Progress in Atomic Spectoscopy, Part A". (Eds. W.Harle and H.Kleinpeppen). Plenum Press, New York and London.

Ho,Y.K., 1979 Phys.Rev. A19 2347

Ho,Y.K., 1983a J.Phys.B 16 1503

Ho,Y.K., 1983b Phys.Rep. (Phys.Lett. C) 99 1

Ho,Y.K., 1984, Phys.Rev. 102A 348

Ho,Y.K., 1985 Phys.Rev. A32 2501

Houston S.K. and Drachman, R.J., 1971, Phys.Rev. A 3 1335

Hulthen, L. 1944, Kgl. Fysiogr. Sallsk. Lund Forhandl., 14 no. 18

Hulthen, L. 1948, Arkiv.f.Mat.Astron.Fysik, 35A no.25 1

Humberston, J.W. 1964 Ph.D. Thesis, University of London.

Humberston, J.W., 1973, J.Phys.B6 L305

Humberston,J.W., 1979, Adv.At.Mol.Phys. 15 101

Humberston,J.W. 1982. Can. J.Phys. 60 591

Humberston,J.W., 1984, J.Phys. B17 2353

Humberston,J.W., 1986, Adv.At. Mol.Phys., 22 1 (Eds. D.R.Bates and B. Bederson), Academic Press, N.Y.

Humberston,J.W. and Wallace,J.B.G., 1972, J.Phys.B 5 1138

Kato, T. 1950 Phys.Rev. 80 475

Kohn, W., 1948, Phys.Rev., 74 1763

Kato, T., 1951 , Progr.Theor.Phys., 6 394

Kolos,W. Roothaan,C.C.J. and Sack,R.A., 1960, Rev.Mod.Phys 32, 178

Larrichia,G. Davies,S.A., Charlton,M and Griffith,T.C. 1986, "International Workshop on Slow Positron beam techniques for solid state and surfaces studies", University of East Anglia, Norwich, U.K. July 7-10th, 1986, Programme and Abstracts.

Leventhal,M. and Brown,B.L., 1986, "Positron (Electron)- Gas Scattering", Proceedings of the Third International Workshop, Wayne State University, Detroit, Michigan, July, 16-18 1985.(Eds. W.E. Kauppila, T.S. Stein, J.M. Wadehra, World Scientific, Singapore.

Leventhal,M, MaCallum,C.J., 1986, 7th International Conference on Positron Annihilation. (Eds. R.M. Singru and P.C. Jain) World Scientific, Singapore.

Leventhal, M, MacCallum, Huters, A.F., Stang, P.d., 1986 Ap.j.

Lin,C.D., 1983, Phys.Rev.Lett. 51 1348

Lynn, K.G., Mills, A.P.,Jr., Roelling, L.O. and Weber,M., 1986, "Electronic and Atomic Collisions", Invited papers, X1V ICPEAC, Palo Alto, 1985, (Eds. D.C.Lorents, W.E.Meyerhof, J.R. Peterson) North Holland, Amsterdam, Oxford, New York, Tokyo.

Marriott,R. 1958, Proc.Phys.Soc. 72 121 (Private communication to R. Marriott by I.C. Percival)

Massey,H.S.W., 1971, Conf.At.Phys., $2^n d$ 1970, pg.307

Massey,H.S.W.,1976, Physics Today, March, 1976, 42

Massey,H.S.W.,1982, Can.J.Phys. 60 461

Massey,H.S.W. and Bates,D.R. 1940 Ap.J.91 202

McEachran,R.P., and Stauffer,A.D., 1986,"Positron (Electron)-Gas Scattering", Proceedings of the Third International Workshop, Wayne State University, Detroit, Michigan, July 16-18, 1985. (Eds. W.E.Kauppila, T.S.Stein and J.M. Wadehra, World Scientific, Singapore.

McDowell,M.R.C., 1971, Atomic Physics 2, "Proceedings of the Second International Conference on Atomic Physics", July, 21-24, 1970, Oxford, (Conference chairman: G.K.Woodgate, ed. P.G.H. Sandars). Plenum Press, London and New York.

McDowell,M.R.C., Morgan,L.A., Myerscough,V.P., 1973 J.Phys.B 6 1435

McDowell,M.R.C., Morgan,L.A. and Myserscough,V.P., 1974, Comput.Phys.Commun. 7 38

McKinley,J.M., 1986, "Positron (Electron)- Gas Scattering", Proceedings of the Third International Workshop, Wayne State University, Detroit, Michigan, July 16-18, 1985. (Eds. W.E. Kauppila, T.S. Stein, J.M. Wadehra). World Scientific, Singapore.

Mills,A.P.Jr., 1980, Appl.Phys., 23 189

Mills,A.P.Jr., 1981a. Phys.Rev.Lett. 46 717

Mills,A.P.,Jr., 1981b, Phys.Rev. A24 3242

Mills,A.P.,Jr., 1983b, Phys.Rev.Lett. 50 671

Mills,A.P.Jr., 1983b, "Positron Solid-state Physics", Proceedings of the International School of Physics, "ENRICO FERMI" North-Holland Publishing Company, Amsterdam, New York, Oxford.

Mills,A.P. and Crane,W.S., 1985, Phys.Rev. A31, 593

Moores, D.L., 1976, "Electron and Photon Interactions with Atoms." (Eds. H. Kleinpoppen and M.R.C. McDowell,) pg. 109, Plenum Press, New York and London.

Morse,P.M. and Feshbach,H. 1953. "Methods of Theorectical Physics" McGraw-Hill Book Company, Inc. New York, Toronto, London.

NAG Fortran Library Manual, Mark 11

Nesbet, R.K. 1980, "Variational Methods in Electron- Atom Scattering Theory," Physics of Atoms and Molecules", Series Editors: P.G. Burke and H. Kleinpoppen, Plenum Press, New York and London

Nieminen,R.M., 1984, "Positron Scattering in Gases", (Eds. J.W. Humberston, M.R.C. McDowell) Plenum Press, New York and Londn

Ohmura,T. and Ohmura,H, 1960, Phys.Rev. 118 154

O'Malley, T.F. Spruch, L and Rosenberg, L, 1961, J.Math.Phys. 2 491

Peach G, 1980 Comment.At.Mol.Phys. 11 101 Pekeris,C.L. 1958, Phys.Rev. 112 1649

Pekeris,C.L. 1962, Phys.Rev. 126 1470

Register,D., and Poe, R.T. 1975, Phys.Lett. 51A 431

Risley,J.S. 1975 "Atomic Physics IV, Proceedings of the Fourth International Conference in Atomic Physics, Heidelberg 1974" (Eds. G.ZuPutlitz, E.W.Weber and A.Winnacker). Plenum Press, New York.

Roberston,H.H., 1956, Proc.Camb.Phil.Soc., 52, 538

Rosenberg, L., Spruch, L. 1959, Phys.Rev. 116 1034

Rosenberg, L., Spruch, L. and O'Malley, T.F., 1960, Phys.Rev. 119 164

Ross, M.H. and Shaw, G.L., 1961, Ann.Phys.(N.Y.) 13 147

Rotenberg,M. and Stein,J. 1969 Phys.Rev. 182 1

Schwartz, C. 1961a, Phys.Rev. 124 1468

Schwartz, C., 1961b, Ann.Phys. (New York) 16 36

Seiler, G.J., Oberoi, R.S, Callaway, J., 1971 Phys.Rev A3 2006

Sivaram,C. and Krisham,V. 1982, Astron Space Sci.85 31

Smith, S.J. and Burch,D.S. 1959, Phys.Rev. 116 1125

Spruch, L, O'Malley, T.F., and Rosenberg, L., 1960, Phys.Rev.Lett. 5 375

Spruch, L. and Rosenberg, L., 1960, Phys.Rev. 117 143

Stein,T.S., Gomez,R.d., Hsieh, Y.-F., Kauppila,W.E., Kwan,C.Y., and Wan,Y.J., 1985, Phys.Rev.Lett. 55 488

Stewart,A.L. 1978 J.Phys. B11 3851

Stroscio,M 1975 Phys.Rep. (Phys. Lett. C) 22 215

Temkin, A. 1957 Phys.Rev. 107 1004

Temkin, A and Lamkin, J.C. 1961 Phys.Rev. 121 788

Ward,S.J. and McDowell,M.R.C., 1984 unpublished paper

Ward,S.J., Humberston J.W. and McDowell,M.R.C., 1985, J.Phys.B18 L525

Ward,S.J., Humberston,J.W. and McDowell,M.R.C., 1986a, Europhysics Lett,1 167.

Ward,S.J., and Humberston,J.W. and McDowell,M.R.C., 1986b, to be published in J.Phys.B.

Ward, S.J., Humberston, J.W and McDowell, M.R.C., 1986c, contributed paper in "Positron (Electron)-Gas Scattering." (Eds. W.E. Kauppila, T.S. Stein, J.M. Wadehra), World Scientific, Singapore.

Wheeler, J.A., 1946, Ann.N.Y.Acad.Sci. 48 219

Wigner, E.P. 1948, Phys.Rev. 73 1002

Wildt,R. 1939, Ap.J 89 295

Williamson,R.E. 1942 Ap.J. 96 438

Wishart,A.W. 1979 J.Phys.B 12 3511-3519.

Tables

Table 2.1

Variation of $\tan\delta_o^+$, $\tan\delta_1^+$, $\tan\delta_1^-$ at $k = 0.30\ a_o^{-1}$ with NI (mesh points used for $\tan\delta_o^+$, N4 = 180, N3 = 60, N2 = 40, N1 = 20, R = 55, H = 0.05, for $\tan\delta_1^{\pm}$, N4 = 160, N3 = 60, N2 = 40, N1 = 20, R = 47, H = 0.05).

NI	8	16	32	48	64
$\tan\delta_o^+$	0.6923	0.6646	0.6615		0.6613
$\tan\delta_1^+$		-0.5501	-0.5448	-0.5439	-0.5436
$\tan\delta_1^-$		0.6754	0.6658	0.6643	0.6639

Table 2.2

Variation of $\tan\delta_o^+$, $\tan\delta_1^+$, $\tan\delta_1^-$ at $k = 0.3\ a_o^{-1}$ with R : Varying N4 but keeping other mesh parameters fixed (N3 = 60, N2 = 40, N1 = 20, H = 0.05).

(a) NI = 32

R N4	15 80	23 100	31 120	39 140	47 160	55 180	63 200	83 250
$\tan\delta_o^+$	0.6588	0.6629	0.6615	0.6615	0.6615	0.6615	0.6615	0.6615
$\tan\delta_1^+$	-0.5365		-0.5448	-0.5448	-0.5448	-0.5448		-0.5448
$\tan\delta_1^-$	0.6968		0.6658	0.6658	0.6658	0.6658		0.6658

(b) NI = 64

R	47	55
N4	160	180
$\tan\delta_o^+$	0.6613	0.6613

Table 2.3

With R fixed, investigating the effect of varying the other mesh parameters (N3, N2, N1, H) on

(a) $\tan\delta_0^+$ at $k = 0.3\ a_0^{-1}$ (R = 31, NI = 64, N4 = 180, 120, 90)
(b) $\tan\delta_1^+$ at $k = 0.3\ a_0^{-1}$ (R = 24.8, NI = 32, N4 = 240, 120, 60)

(a)

Mesh	1	2	3	4	5	6	7
H	0.031	0.062	0.025	0.05	0.031	0.05	0.025
N4	180	90	180	90	180	120	180
N3	84	42	36	18	70	60	32
N2	40	20	20	10	60	40	26
N1	24	12	16	8	40	20	20
$\tan\delta_0^+$	0.6620	0.6603	0.6612	0.6626	0.6617	0.6613	0.6610
δ_0^+	0.5848	0.5836	0.5842	0.5852	0.5846	0.5843	0.5841

(b)

Mesh	1	2	3
H	0.020	0.040	0.080
N4	240	120	60
N3	120	60	30
N2	80	40	20
N1	40	20	10
$\tan\delta_1^+$	-0.5445	-0.5451	-0.5451
$\tan\delta_1^-$	0.6656	0.6666	0.6674

Table 2.4

L = 0-5 phaseshifts for e^-–Ps scattering, below the n = 2 threshold, determined by the full static-exchange method.

Singlet

$k(a_o^{-1})$	δ_o^+	δ_1^+	δ_2^+	δ_3^+	δ_4^+	δ_5^+
0*	20.5±2					
0.05	2.230	-0.009	0.000097			
0.10	1.654	-0.058	0.0026	-0.00007		
0.15	1.272	-0.149	0.0152	-0.0009	0.00004	
0.20	0.987	-0.264	0.0454	-0.0042	0.0004	
0.25	0.764	-0.384	0.0919	-0.0119	0.0016	-0.0002
0.30	0.584	-0.498	0.144	-0.0247	0.0044	-0.0007
0.35	0.439	-0.598	0.188	-0.0413	0.0092	-0.0018
0.40	0.320	-0.682	0.217	-0.0595	0.0155	-0.0037
0.45	0.223	-0.750	0.231	-0.0772	0.0227	-0.0061

Triplet

$k(a_o^{-1})$	δ_o^-	δ_1^-	δ_2^-	δ_3^-	δ_4^-	δ_5^-
0*	5.8±0.2					
0.05	-0.291	0.014	-0.00009			
0.10	-0.570	0.107	-0.0024	0.00007		
0.15	-0.829	0.294	-0.0134	0.0009	-0.00004	
0.20	-1.064	0.476	-0.0386	0.0043	-0.0004	
0.25	-1.273	0.569	-0.0770	0.0124	-0.0016	0.0002
0.30	-1.457	0.586	-0.123	0.0260	-0.0044	0.0007
0.35	-1.619	0.561	-0.170	0.0435	-0.009	0.0019
0.40	-1.761	0.519	-0.212	0.0618	-0.0152	0.0037
0.45	-1.887	0.472	-0.248	0.0782	-0.0224	0.0062

* scattering lengths in a.u.

Table 2.5

s-wave phase shifts for e^--Ps scattering, below the n = 2 threshold using the A.E.1, S.E.1 and S.E. methods, see text.

	SINGLET			TRIPLET		
k	A.E.1.	S.E.1.	S.E.	A.E.1.	S.E.1.	S.E.
0*		13.9±0.2	20.5±0.2		4.04±0.10	5.8±0.2
0.05	2.601	2.389	2.230	2.977	2.939	-0.291
0.10	2.145	1.983	1.654	2.795	2.740	-0.570
0.15	1.791	1.631	1.272	2.612	2.547	-0.829
0.20	1.515	1.366	0.987	2.434	2.365	-1.064
0.25	1.298	1.158	0.764	2.268	2.195	-1.273
0.30	1.122	0.988	0.584	2.112	2.035	-1.457
0.40	0.873	0.741	0.320	1.842	1.759	-1.761

* scattering lengths in a.u.

Table 3.1

The number of linear parameters in the s- and p-wave variational trial functions.

$l = 0$

Singlet	Triplet	ω
3	1	1
7	3	2
13	7	3
22	13	4
34	22	5
50	34	6
70	50	7
95	70	8
125	95	9
161	125	10

$l = 1$

Singlet	Triplet	ω
4	4	1
10	10	2
20	20	3
35	35	4
56	56	5
84	84	6
120	120	7
165	165	8
220	220	9

Table 3.2

$\tan\delta_o^+$ evaluated by the Kohn (K) and Inverse Kohn (IK) variational methods.

Number of linear parameters		7	13	22	34	50	70	
$k(a_o^{-1})$		2	3	4	5	6	7	$\omega(\infty)$
0.05	K	-0.7199	-0.7100	-0.7000	-0.6910	-0.6842	-0.6806	-0.676(± 5)
	IK	-0.7211	-0.7107	-0.7003	-0.6910	-0.6839	-0.6804	
0.10	K	-2.143	-2.067	-2.017	-1.976	-1.949	-1.939	-1.930(± 5)
	IK	-2.139	-2.066	-2.014	-1.966	-1.955	-1.940	
0.15	K	-18.61	-13.73	-12.19	-11.14	-10.76	-10.58	-10.3(± 2)
	IK	-18.08	-11.53	-12.56	-11.25	-10.76	-10.55	
0.20	K	4.172	4.668	4.700	4.949	5.020	5.066	5.13(± 7)
	IK	3.115	4.556	4.772	4.952	4.988	5.056	
0.25	K	2.060	2.127	2.200	2.239	2.248	2.261	2.27(± 1)
	IK	1.973	2.159	2.201	2.233	2.252	2.261	
0.30	K	1.522	1.449	1.473	1.487	1.499	1.503	1.505(± 5)
	IK	1.348	1.449	1.468	1.489	1.501	1.502	
0.35	K	0.9718	1.100	1.089	1.130	1.139	1.140	1.144(± 2)
	IK	1.030	1.096	1.117	1.130	1.137	1.140	
0.40	K	0.8138	0.8931	0.9076	0.9165	0.9228	0.9254	0.928(± 3)
	IK	0.8368	0.8853	0.9086	0.9159	0.9232	0.9253	
0.45	K	0.6897	0.6750	0.7704	0.7722	0.7816	0.7831	0.787(± 1)
	IK	0.6765	0.7464	0.7702	0.7746	0.7815	0.7838	
0.50	K	0.5976	0.6557	0.7022	0.6656	0.6737	0.6794	0.71(± 1)
	IK	0.5972	0.6586	0.6930	0.6657	0.6734	0.6799	

The brackets indicate the estimated accuracy in the last figure.

Table 3.3

$\tan\delta_0^-$ evaluated by the Kohn (K) and Inverse Kohn (IK) variational methods.

Number of linear parameters		3	8	13	22	34	50	
ω		2	3	4	5	6	7	$\omega(\infty)$
$k(a_0^{-1})$								
0.05	K	-0.3031	-0.2882	-0.2806	-0.2747	-0.2729	-0.2702	-0.26(±2)
	IK	-0.3031	-0.2884	-0.2811	-0.2754	-0.2724	-0.2701	
0.10	K	-0.6364	-0.6194	-0.6056	-0.5986	-0.5964	-0.5954	-0.594(±1)
	IK	-0.6498	-0.6180	-0.6046	-0.5981	-0.5965	-0.5954	
0.15	K	-1.115	-1.055	-1.035	-1.031	-1.028	-1.027	-1.023(±3)
	IK	-1.105	-1.039	-1.037	-1.031	-1.028	-1.027	
0.20	K	-1.848	-1.740	-1.708	-1.700	-1.692	-1.688	-1.685(±4)
	IK	-1.470	-1.744	-1.707	-1.699	-1.693	-1.689	
0.25	K	-3.358	-3.144	-3.042	-3.014	-2.998	-2.989	-2.981(±8)
	IK	-3.589	-3.141	-3.038	-3.021	-2.997	-2.989	
0.30	K	-7.213	-8.231	-7.596	-7.473	-7.343	-7.269	-7.2(±1)
	IK	-11.14	-8.162	-7.649	-7.438	-7.282	-7.282	
0.35	K	10.94	23.36	27.04	33.31	36.14	37.09	41(±2)
	IK	13.68	18.88	29.67	33.34	35.15	37.11	
0.40	K	4.419	5.441	5.579	5.703	5.757	5.814	5.90(±8)
	IK	4.553	5.098	5.579	5.692	5.766	5.808	
0.45	K	2.787	1.894	3.192	3.222	3.256	3.263	3.30(±1)
	IK	2.787	3.014	3.132	3.229	3.256	3.272	
0.50	K	2.069	2.096	2.279	2.291	2.305	2.314	2.34(±2)
	IK	2.043	2.171	2.248	2.291	2.304	2.315	

The brackets indicate the estimated accuracy in the last figure.

Table 3.4

K - matrix and phaseshifts for the s-wave elastic scattering of electrons by positronium obtained by the variational method.

	SINGLET			TRIPLET		
$k(a_o^{-1})$	$\tan\delta_c^+$ $(\omega=7)^a$	$\tan\delta_o^+$ $(\omega=\infty)^b$	δ_o^+ $(\omega=\infty)^c$	$\tan\delta_o^-$ $(\omega=7)^a$	$\tan\delta_o^-$ $(\omega=\infty)^b$	δ_o^- $(\omega=\infty)^c$
0.05	-0.681	-0.676(±5)	2.547(±4)	-0.27	-0.26(±2)	-0.25(±1)
0.10	-1.939	-1.930(±5)	2.049(±1)	-0.595	-0.594(±1)	-0.5361(±8)
0.15	-10.58	-10.3 (±2)	1.668(±2)	-1.027	-1.023(±3)	-0.797(±2)
0.20	5.07	5.13(±7)	1.378(±2)	-1.688	-1.685(±4)	-1.035(±1)
0.25	2.26	2.27(±1)	1.156(±2)	-2.989	-2.981(±8)	-1.247(±1)
0.30	1.503	1.505(±5)	0.984(±2)	-7.27	-7.2(±1)	-1.432(±2)
0.35	1.140	1.144(±2)	0.852(±1)	37.1	41(±2)	-1.596(±1)
0.40	0.925	0.928(±3)	0.748(±2)	5.81	5.90(±8)	-1.739(±2)
0.45	0.783	0.787(±1)	0.667(±1)	3.26	3.30(±1)	-1.865(±1)
0.50	0.679	0.71 (±1)	0.617(±7)	2.314	2.34(±2)	-1.975(±3)

a K matrix calculated by the Kohn variational method at $\omega = 7$

b Fully converged results, K matrix extrapolated to $\omega = \infty$

c Phaseshifts corresponding to the extrapolated K matrix

The brackets indicate the estimated accuracy in the last figure.

Table 3.5

Scattering lengths and very low energy s-wave phaseshifts for (e^-, Ps) scattering.

Singlet

k	$\tan\delta_o^+$ (ω=10)	$\tan\delta_o^+$ (ω=∞)
0^*	12.3	12.0 ±3
0.01	-0.123	-0.121 ±0.003
0.02	-0.249	-0.244 ±0.005
0.03	-0.381	-0.372 ±0.008

a^+ (BD) = 12.233 ±0.006

Triplet

k	$\tan\delta_o^-$ (ω=10)	$\tan\delta_o^-$ (ω=∞)
0^*	5.0	4.6 ±0.4
0.01	-0.051	-0.047 ±0.003
0.02	-0.102	-0.96 ±0.005
0.03	-0.155	-0.147 ±0.006

0^* scattering lengths, units a_o

a^+ (BD) : Bhatia and Drachman's (1985) singlet scattering length obtained from using their bound - state Ps^- wave function.

Table 3.6

Convergence of very low energy s-wave phaseshifts.

Singlets

$k(a_o^{-1})$	0.01		0.02		0.03	
	K	IK	K	IK	K	IK
ω						
2	-0.1306	-0.1308	-0.2642	-0.2646	-0.4042	-0.4049
3	-0.1292	-0.1293	-0.2614	-0.2616	-0.3996	-0.4000
4	-0.1277	-0.1277	-0.2582	-0.2583	-0.3946	-0.3947
5	-0.1262	-0.1263	-0.2552	-0.2553	-0.3900	-0.3900
6	-0.1251	-0.1251	-0.2528	-0.2528	-0.3862	-0.3862
7	-0.1244	-0.1244	-0.2516	-0.2516	-0.3843	-0.3843
8	-0.1240	-0.1240	-0.2506	-0.2506	-0.3828	-0.3828
9	-0.1236	-0.1236	-0.2499	-0.2499	-0.3817	-0.3818
10	-0.1233	-0.1233	-0.2493	-0.2493	-0.3816	-0.3810
$(\omega=\infty)$	-0.121(±3)		-0.244(±5)		-0.372(±8)	
$\tan(\omega=\infty)/k$	12.1		12.2		12.4	

Triplets

$k(a_o^{-1})$	0.01		0.02		0.03	
	K	IK	K	IK	K	IK
ω						
2	-0.05935	-0.05935	-0.1190	-0.1190	-0.1793	-0.1793
3	-0.05645	-0.05647	-0.1132	-0.1132	-0.1705	-0.1706
4	-0.05492	-0.05494	-0.1101	-0.1102	-0.1660	-0.1661
5	-0.05357	-0.05359	-0.1075	-0.1076	-0.1622	-0.1623
6	-0.05273	-0.05274	-0.1059	-0.1059	-0.1599	-0.1600
7	-0.05197	-0.05198	-0.1045	-0.1045	-0.1580	-0.1581
8	-0.05141	-0.05142	-0.1035	-0.1035	-0.1567	-0.1568
9	-0.05094	-0.05094	-0.1026	-0.1026	-0.1557	-0.1557
10	-0.05056	-0.05056	-0.1020	-0.1020	-0.1549	-0.1550
$(\omega=\infty)$	-0.047(±3)		-0.096(±5)		-0.1474(±6)	
$\tan(\omega=\infty)/k$	4.7		4.8		4.9	

where

K = $\tan\delta_o^{\pm}$, determined by the Kohn variational method.

IK = $\tan\delta_o^{\pm}$, determined by the Inverse Kohn variational method.

The brackets indicated the estimated accuracy in the last figure.

Table 3.7

The $(2s)^2\ ^1S^e$ resonance in (e^-, Ps)
(R_∞ = 13.60580ev)

	Position(ev)	Width(ev)
Arifov et al (1977)	4.735	
Ho (1984)	4.734	1.2
Botero and Greene(1985)	4.7253 4.6815	
Ward et al (1985)	4.768	1.6

Table 3.8

Binding energy of Ps^- in a.u.

(a) Using different bound-state wavefunctions.

	Bound-state wavefunction	ε_b(a.u.)
Greene and Botero 1985	Hyperspherical wavefunction	0.0146 0.0097
Ward et al,1986b	95 linear parameters,.2 optimized non-linear parameters (α=0.30, γ=0.048) variational wavefunction.	0.01200462
Ho 1983	125 linear parameters, 1 optimized non-linear parameter (α=0.3560) variational wavefunction	0.01200490
Bhatia and Drachman 1983	220 linear parameters, 2 optimized non-linear parameters (γ=0.604, δ=0.313) variational wavefunction	0.01200506

(b) Variation of binding energy with ε_b, using our bound-state wavefunction (see text).

ω_b	No. of linear parameters	ε_b(a.u.)
1	3	0.00941249
2	7	0.01063598
3	13	0.01098254
4	22	0.01194015
5	34	0.01195684
6	50	0.01200052
7	70	0.01200270
8	95	0.01200462

Table 4.1

Variation of $\tan\delta_1^+$ ($\omega = 5$) with non-linear parameter α, for $\gamma = 0.05$, $\mu = 0.5$, $\omega = 5$, $n = 5$ NS = NC = 35

$\alpha \rightarrow$		0.4	0.3	0.25	0.20	0.15	0.13	0.1
$k(a_o^{-1})$	Method							
0.02	K	-0.2370 E-03	-0.7260 E-04	0.3246 E-04	0.1554 E-03	0.2791 E-03	0.3172 E-03	0.3272 E-03
	IK	-0.2472 E-03	-0.7761 E-04	0.3026 E-04	0.1500 E-03	0.2439 E-03	0.2489 E-03	0.1989 E-03
0.04	K	-0.2077 E-02	-0.1115 E-02	-0.5927 E-03	-0.8753 E-04	0.2584 E-03	0.2909 E-03	0.6601 E-04
	IK	-0.2133 E-02	-0.1135 E-02	-0.5957 E-03	-0.9187 E-04	0.2057 E-03	0.1798 E-03	+0.1150 E-03
0.05	K	-0.4259 E-02	-0.2789 E-02	-0.2093 E-02	-0.1518 E-02	-0.1259 E-02	-0.1313 E-02	-0.1788 E-02
	IK	-0.4353 E-02	-0.2814 E-02	-0.2093 E-02	-0.1518 E-02	-0.1274 E-02	-0.1358 E-02	-0.1847 E-02
0.10	K	-0.4019 E-01	-0.3873 E-01	-0.3898 E-01	-0.3933 E-01	-0.3635 E-01	-0.3957 E-01	-0.4195 E-01
	IK	-0.3988 E-01	-0.3872 E-01	-0.3896 E-01	-0.3929 E-01	-0.3981 E-01	-0.4051 E-01	-0.4384 E-01
0.20	K	-0.2415	-0.2408	-0.2414	-0.2437			
	IK	-0.2412	-0.2404	-0.2414	-0.2439			
0.30	K	-0.5011	-0.5011	-0.5031	-0.5068			
	IK	-0.5013	-0.4949	-0.5031	-0.5070			
0.40	K	-0.7396	-0.7408	-0.7436	-0.7480			
	IK	-0.7399	-0.7403	-0.7444	-0.7491			
0.50	K	-0.8374	-0.8203	-0.8076	-0.7986			
	IK	-0.8364	-0.8214	-0.8057	-0.8170			

where, K = $\tan\delta_1^+$ evaluated by the Kohn variational method, IK = $\tan\delta_1^+$ evaluated by the Inverse Kohn variational method.

Table 4.2

Variation of $\tan\delta_1^+$ ($\omega = 5$) with non-linear parameter γ, for $\alpha = 0.3$, $\mu = 0.5$, $\omega = 5$, n=5, NS=NC=35

γ		0.5	0.1	0.07	0.06	0.05	0.04	0.03	0.01	0.005	0
$k(a_o^{-1})$	Method										
0.1	K	-0.4987 E-01	-0.3897 E-01	-0.3875 E-01	-0.3873 E-01	-0.3873 E-01	-0.3875 E-01	-0.3878 E-01	-0.3891 E-01	-0.3894 E-01	-0.3898 E-01
	IK	-0.4997 E-01	-0.3895 E-01	-0.3875 E-01	-0.3872 E-01	-0.3872 E-01	-0.3875 E-01	-0.3878 E-01	-0.3890 E-01	-0.3893 E-01	-0.3897 E-01
0.2	K	-0.2448	-0.2409	-0.2408	-0.2407	-0.2408	-0.2408	-0.2408	-0.2411	-0.2411	-0.2412
	IK	-0.2447	-0.2408	-0.2407	-0.2407	-0.2404	-0.2410	-0.2409	-0.2411	-0.2412	-0.2413
0.3	K	-0.5032	-0.5013	-0.5011	-0.5010	-0.5011	-0.5012	-0.5015	-0.5025	-0.5028	-0.5031
	IK	-0.5032	-0.5010	-0.5005	-0.5000	-0.4949	-0.5020	-0.5017	-0.5025	-0.5028	-0.5031
0.4	K	-0.7424	-0.7389	-0.7397	-0.7402	-0.7408	-0.7414	-0.7420	-0.7433	-0.7436	-0.7439
	IK	-0.7415	-0.7389	-0.7396	-0.7399	-0.7403	-0.7405	-0.7402	-0.7476	-0.7462	-0.7459
0.5	K	-0.8559	-0.8268	-0.8232	-0.8219	-0.8203	-0.8169	-0.8181	-0.8150	-0.8144	-0.8137
	IK	-0.8559	-0.8285	-0.8243	-0.8229	-0.8214	-0.8198	-0.8181	-0.8144	-0.8132	-0.8120

where, K = $\tan\delta_1^+$ evaluated by the Kohn variational method,

IK = $\tan\delta_1^+$ evaluated by the Inverse Kohn variational method.

Table 4.3

Variation of $\tan\delta_1^+$ ($\omega = 5$) with non-linear parameter γ, for $\alpha = 0.15$, $\mu = 0.5$, $\omega = 5$, $n = 5$, NS=NC=35

$\gamma \rightarrow$		0.1	0.05	0.04	0.03	0.02	0.01	0	-0.025	-0.050	-0.075	-0.10
$k(a_o^{-1})$	Method											
0.02	K	0.1206 E-03	0.2791 E-03		0.3522 E-03		0.4326 E-03	0.4754 E-03	0.5861 E-03	0.6814 E-03	0.6911 E-03	0.4881 E-03
	IK	0.1164 E-03	0.2439 E-03		0.2849 E-03		0.3132 E-03	0.3208 E-03	0.3169 E-03	0.2817 E-03	0.2235 E-03	0.1440 E-03
0.03	K					0.7486 E-03	0.8141 E-03		0.9796 E-03			
	IK					0.5880 E-03	0.6053 E-03		0.5608 E-03			
0.04	K	-0.2305 E-03	0.2584 E-03	0.3357 E-03	0.4034 E-03	0.4595 E-03	0.5009 E-03	0.5236 E-03	0.4716 E-03	0.2338 E-03		
	IK	-0.2325 E-03	0.2057 E-03	0.2586 E-03	0.2956 E-03	0.3142 E-03	0.3122 E-03	0.2877 E-03	0.1296 E-03	-0.1366 E-03		
0.05	K	-0.1684 E-02	-0.1259 E-02	-0.1216 E-02	-0.1190 E-02	-0.1183 E-02	-0.1198 E-02	-0.1242 E-02		-0.1988 E-02		
	IK	-0.1685 E-02	-0.1274 E-02	-0.1244 E-02	-0.1235 E-02	-0.1249 E-02	-0.1289 E-02	-0.1358 E-02		-0.2111 E-02		
0.08	K	-0.1731 E-01	-0.1750 E-01	-0.1756 E-01	-0.1765 E-01			-0.1829 E-01		-0.2077 E-01		
	IK	-0.1760 E-01	-0.1771 E-01	-0.1774 E-01	-0.1781 E-01			-0.1839 E-01		-0.2136 E-01		

Where K = $\tan\delta_1^+$ evaluated by the Kohn variational method,

IK = $\tan\delta_1^+$ evaluated by the Inverse Kohn variational method.

Table 4.4

Variation of $\tan\delta_1^+$ ($\omega = 5$) with non-linear parameter μ, for $\alpha = 0.30$, $\gamma = 0.06$, $\omega = 5$, $n = 5$, NS=NC=35

$\mu \rightarrow$		0.6	0.5	0.4	0.3	0.2	0.1	0.05
$k(a_o^{-1})$	Method							
0.1	K	-0.3941 E-01	-0.3873 E-01	-0.3858 E-01	-0.3857 E-01	-0.3858 E-01	-0.3855 E-01	-0.3886 E-01
	IK	-0.3928 E-01	-0.3872 E-01	-0.3854 E-01	-0.3853 E-01	-0.3854 E-01	-0.3855 E-01	-0.3821 E-01
	A	-0.3935 E-01	-0.3873 E-01	-0.3856 E-01	-0.3855 E-01	-0.3856 E-01	-0.3855 E-01	-0.3853 E-01
0.2	K	-0.2430	-0.2407	-0.2400	-0.2398	-0.2398	-0.2417	-0.2056
	IK	-0.2429	-0.2407	-0.2399	-0.2397	-0.2396	-0.2322	-0.1520
	A	-0.2430	-0.2407	-0.2400	-0.2398	-0.2397	-0.2369	-0.1788
0.3	K	-0.5032	-0.5010	-0.5008	-0.5005	-0.5010	-0.4105	-0.2461
	IK	-0.5020	-0.5001	-0.5000	-0.4998	-0.5008	-0.3683	-0.1959
	A	-0.5026	-0.5005	-0.5004	-0.5002	-0.5009	-0.3894	-0.2210
0.4	K	-0.7426	-0.7402	-0.7395	-0.7387	-0.7577	-0.6383	-0.3893
	IK	-0.7426	-0.7399	-0.7388	-0.7387	-0.7427	-0.6129	-0.5302
	A	-0.7426	-0.7401	-0.7391	-0.7387	-0.7502	-0.6256	-0.4598
0.5	K	-0.8228	-0.8219	-0.8176	-0.8122	-0.8546	-1.1940	-1.2724
	IK	-0.8232	-0.8229	-0.8246	-0.8223	-0.8604	-1.3366	-0.9244
	A	-0.8230	-0.8224	-0.8211	-0.8173	-0.8575	-1.2653	-1.0984

Where K = $\tan\delta_1^+$ evaluated by the Kohn variational method, IK = $\tan\delta_1^+$ evaluated by the Inverse Kohn variational method, and A is the average of the Kohn and Inverse Kohn.

Table 4.5

Variation of $\tan\delta_1^+$ ($\omega = 5$) with non-linear parameter μ, for $\alpha = 0.15$, $\gamma = 0.03$, $\omega = 5$, $n = 5$, NS=NC=35

μ		0.6	0.5	0.4	0.3
$k(a_o^{-1})$	Method				
0.05	K	-0.1244 E-02	-0.1190 E-02	-0.1131 E-02	-0.1066 E-02
	IK	-0.1252 E-02	-0.1235 E-02	-0.1235 E-02	-0.1253 E-02
	A	-0.1248 E-02	-0.1213 E-02	-0.1183 E-02	-0.1159 E-02
0.08	K	-0.1788 E-01	-0.1765 E-01	-0.1738 E-01	-0.1695 E-01
	IK	-0.1873 E-01	-0.1781 E-01	-0.1738 E-01	-0.1732 E-01
	A	-0.1831 E-01	-0.1773 E-01	-0.1738 E-01	-0.1714 E-01

Where K = $\tan\delta_1^+$ evaluated by the Kohn variational method, IK = $\tan\delta_1^+$ evaluated by the Inverse Khon variational method and A is the average and the Kohn and Inverse Kohn.

Table 4.6

Variation of $\tan\delta_l^+$ ($\omega = 5$) with non-linear parameter μ, for $\alpha = 0.15$, $\gamma = 0.01$, $\omega = 5$, $n = 5$, NS=NC=35

μ		0.6	0.5	0.4	0.3
$k(a_o^{-1})$	Method				
0.02	K	0.4256 E-03	0.4326 E-03	0.4402 E-03	0.4474 E-03
	IK	0.2910 E-03	0.3132 E-03	0.3335 E-03	0.3582 E-03
0.04	K	0.4485 E-03	0.5009 E-03	0.5546 E-03	0.6007 E-03
	IK	0.3096 E-03	0.3122 E-03	0.3182 E-03	0.3300 E-03

where K = $\tan\delta_l^+$ evaluated by the Kohn variational method,
IK = $\tan\delta_l^+$ evaluated by the Inverse Kohn variational method.

Table 4.7

Convergence of $\tan\delta_1^+$ with for very low values of wave number k. Choice of non-linear parameters, $\alpha = 0.15$, $\gamma = 0.01$, $\mu = 0.3$ (n = 5, NS=NC=35)

ω		2	3	4	5	6	7	8	9
$k(a_o^{-1})$	Method								
0.01	K	-0.1917 E-04	+0.4898 E-05	0.4931 E-04	0.7518 E-04	0.1109 E-03	0.1369 E-03	0.1659 E-03	0.1906 E-03
	IK	-0.2298 E-04	-0.4045 E-05	0.3618 E-04	0.6025 E-04	0.1008 E-03	0.1275 E-03	0.1617 E-03	0.1865 E-03
0.02	K	-0.1746 E-03	-0.3820 E-05	0.2950 E-03	0.4474 E-03	0.6425 E-03	0.7592 E-03	0.8740 E-03	0.9503 E-03
	IK	-0.2019 E-03	-0.6523 E-04	0.2091 E-03	0.3582 E-03	0.5868 E-03	0.7146 E-03	0.8559 E-03	0.9356 E-03
0.03	K	-0.6945 E-03	-0.2167 E-03	0.5448 E-03	0.8591 E-03	0.1209 E-02	0.1355 E-02	0.1468 E-02	0.1512 E-02
	IK	-0.7719 E-03	-0.3797 E-03	0.3325 E-03	0.6658 E-03	0.1099 E-02	0.1283 E-02	0.1440 E-02	0.1494 E-02
0.04	K	-0.1935 E-02	-0.1040 E-02	0.2008 E-03	0.6007 E-03	0.9534 E-03	0.1051 E-02	0.1103 E-02	0.1130 E-02
	IK	-0.2081 E-02	-0.1324 E-02	-0.1431 E-03	0.3300 E-03	0.8059 E-03	0.9727 E-03	0.1067 E-02	0.1104 E-02

where K = $\tan\delta_1^+$ evaluated by the Kohn variational method and

IK = $\tan\delta_1^+$ evaluated by the Inverse Kohn variational method.

Table 4.8

Convergence of $\tan\delta_1^+$ with ω for k in the range $0.05 \leq k(a_o^{-1}) < 0.1$, choice of non-linear parameters, $\alpha = 0.15$, $\gamma = 0.03$, $\mu = 0.3$ (n = 5, NS=NC=35)

ω		2	3	4	5	6	7	8	9	$\omega = \infty$ *
$K(a_o^{-1})$	(Method)									
0.05	K	-0.4446 E-02	-0.3219 E-02	-0.1523 E-02	-0.1066 E-02	-0.7391 E-03	-0.6528 E-03	-0.6782 E-03	-0.6166 E-03	-0.0004 (±2)
	IK	-0.4617 E-02	-0.3515 E-02	-0.1811 E-02	-0.1253 E-02	-0.8216 E-03	-0.7037 E-03	-0.6480 E-03	-0.6150 E-03	
0.06	K	-0.8369 E-02	-0.6686 E-02	-0.4819 E-02	-0.4364 E-02	-0.4129 E-02	-0.4385 E-02	-0.4040 E-02	-0.3993 E-02	
	IK	-0.8605 E-02	-0.7060 E-02	-0.5171 E-02	-0.4572 E-02	-0.4247 E-02	-0.4104 E-02	-0.4038 E-02	-0.3993 E-02	
0.07	K	-0.1419 E-01	-0.1202 E-01	-0.1019 E-01	-0.9644 E-02	-0.9190 E-02	-0.9437 E-02	-0.9360 E-02	-0.9325 E-02	
	IK	-0.1449 E-01	-0.1246 E-01	-0.1060 E-01	-0.9893 E-02	-0.9615 E-02	-0.9426 E-02	-0.9361 E-02	-0.9328 E-02	
0.08	K	-0.2218 E-01	-0.1941 E-01	-0.1771 E-01	-0.1695 E-01	-0.1718 E-01	-0.1685 E-01	-0.1678 E-01	-0.1676 E-01	
	IK	-0.2254 E-01	-0.1992 E-01	-0.1821 E-01	-0.1732 E-01	-0.1704 E-01	-0.1685 E-01	-0.1679 E-01	-0.1675 E-01	
0.09	K	-0.3244 E-01	-0.2895 E-01	-0.2733 E-01	-0.2577 E-01	-0.2663 E-01	-0.2641 E-01	-0.2635 E-01	-0.2631 E-01	
	IK	-0.3287 E-01	-0.2955 E-01	-0.2797 E-01	-0.2691 E-01	-0.2346 E-01	-0.2643 E-01	-0.2635 E-01	-0.2630 E-01	

K = $\tan\delta_1^+$ evaluated by the Kohn variational method,
IK = $\tan\delta_1^+$ evaluated by the Inverse Kohn variational method.

* Graphical estimates at the phaseshifts for $\omega = \infty$
The brackets indicate the estimated accuracy in the last figure.

Table 4.9

Convergence of $\tan\delta_l^+$ with ω for k in the range, $0.10 \leq k(a_o^{-1}) < 0.5$
Choice of non-linear parameters, $\alpha = 0.3$, $\gamma = 0.06$, $\mu = 0.3$ (N=5,NS=NC=35)

ω		3	4	5	6	7	8	9	$\omega = \infty^*$
$k(a_o^{-1})$	(Method)								
0.10	K	-0.3508 E-01	-0.3969 E-01	-0.3857 E-01	-0.3837 E-01	-0.3831 E-01	-0.3822 E-01	-0.3750 E-01	-0.0381 (±2)
	IK	-0.4165 E-01	-0.3949 E-01	-0.3853 E-01	-0.3835 E-01	-0.3832 E-01	-0.3824 E-01	-0.3813 E-01	
0.20	K	-0.2415	-0.2407	-0.2398	-0.2395	-0.2395	-0.2392	-0.2392	-0.2391 (±1)
	IK	-0.2417	-0.2404	-0.2397	-0.2395	-0.2394	-0.2392	-0.2392	
0.30	K	-0.5042	-0.5010	-0.5005	-0.4999	-0.4998	-0.4995	-0.4994	-0.4990 (±3)
	IK	-0.5091	-0.5013	-0.4998	-0.4999	-0.4997	-0.4995	-0.4993	
0.40	K	-0.7769	-0.7409	-0.7387	-0.7374	-0.7370	-0.7367	-0.7365	-0.7357 (±7)
	IK	-0.7521	-0.7444	-0.7387	-0.7380	-0.7367	-0.7367	-0.7363	
0.49	K	-0.8939	-0.9281		-0.8480	-0.7953		-0.8454	
	IK	-0.9165	-0.8529		-0.8480	-0.8475		-0.8454	

where $K = \tan\delta_l^+$ evaluated by the Kohn variational method.
$IK = \tan\delta_l^+$ evaluated by the Inverse Kohn variational method.

Table 4.10

Convergence of $\tan\delta_1$ with ω for very low values of wave number k.
Choice of non-linear parameters, $\alpha = 0.15$, $\gamma = 0.01$, $\mu = 0.3$ (n = 5, NS=NC=35)

ω		2	3	4	5	6	7	8	9
$k(a_o^{-1})$	(Method)								
0.01	K	0.1993 E-03	0.2580 E-03	0.2882 E-03	0.3316 E-03	0.3597 E-03	0.3917 E-03	0.4185 E-03	0.4442 E-03
	IK	0.1793 E-03	0.2295 E-03	0.2593 E-03	0.3092 E-03	0.3391 E-03	0.3782 E-03	0.4047 E-03	0.4347 E-03
0.02	K	0.1576 E-02	0.2007 E-02	0.2215 E-02	0.2489 E-02	0.2640 E-02	0.2793 E-02	0.2897 E-02	0.2979 E-02
	IK	0.1427 E-02	0.1801 E-02	0.2015 E-02	0.2341 E-02	0.2515 E-02	0.2714 E-02	0.2824 E-02	0.2931 E-02
0.03	K	0.5226 E-02	0.6499 E-02	0.7059 E-02	0.7693 E-02	0.7968 E-02	0.8188 E-02	0.8295 E-02	0.8351 E-02
	IK	0.4777 E-02	0.5903 E-02	0.6522 E-02	0.7317 E-02	0.7685 E-02	0.8011 E-02	0.8143 E-02	0.8243 E-02
0.04	K	0.1212 E-01	0.1465 E-01	0.1570 E-01	0.1664 E-01	0.1697 E-01	0.1716 E-01	0.1726 E-01	0.1739 E-01
	IK	0.1120 E-01	0.1350 E-01	0.1473 E-01	0.1599 E-01	0.1653 E-01	0.1686 E-01	0.1700 E-01	0.1709 E-01

where K = $\tan\delta_1$ evaluated by the Kohn variational method and
IK = $\tan\delta_1$ evaluated by Inverse Kohn variational method.

Table 4.11

Convergence of $\tan\delta_1^-$ with ω for k in the range $0.05 \leqslant k(a_o^{-1}) < 0.1$.
Choice of non-linear parameters $\alpha = 0.15$, $\gamma = 0.03$, $\mu = 0.3$ (n = 5, NS=NC=35)

ω		2	3	4	5	6	7	8	9	$= \infty$ *
$k(a_o^{-1})$	(Method)									
0.05	K	0.2318 E-01	0.2746 E-01	0.2898 E-01	0.3011 E-01	0.3049 E-01	0.3075 E-01	0.2165 E-01	0.3056 E-01	0.0310 (± 2)
	IK	0.2202 E-01	0.2621 E-01	0.2805 E-01	0.2952 E-01	0.3004 E-01	0.3032 E-01	0.3047 E-01	0.3059 E-01	
0.06	K	+0.3927 E-01	0.4538 E-01	0.4765 E-01	0.4892 E-01	0.4951 E-01	0.4699 E-01	0.4927 E-01	0.4953 E-01	
	IK	0.3762 E-01	0.4369 E-01	0.4645 E-01	0.4810 E-01	0.4878 E-01	0.4910 E-01	0.4933 E-01	0.4950 E-01	
0.07	K	0.6104 E-01	0.6904 E-01	0.7239 E-01	0.7395 E-01	0.7628 E-01	0.7405 E-01	0.7451 E-01	0.7480 E-01	
	IK	0.5893 E-01	0.6694 E-01	0.7093 E-01	0.7281 E-01	0.7375 E-01	0.7417 E-01	0.7446 E-01	0.7466 E-01	
0.08	K	0.8899 E-01	0.9896 E-01	0.1039	0.1063	0.1050	0.1063	0.1067	0.1067	
	IK	0.8650 E-01	0.9654 E-01	0.1021	0.1044	0.1057	0.1062	0.1065	0.1068	
0.09	K	0.1234	0.1356	0.1426	0.1522	0.1449	0.1459	0.1457	0.1465	
	IK	0.1206	0.1329	0.1405	0.1435	0.1450	0.1457	0.1461	0.1465	

where K = $\tan\delta_1^-$ evaluated by the Kohn variational method,
IK = $\tan\delta_1^-$ evaluated by the Inverse Kohn variational method.

Table 4.12

Convergence of $\tan\delta_1^-$ with ω for k in the range $0.10 \leq k(a_o^{-1}) < 0.5$
Choice of non-linear parameters, $\alpha = 0.3$, $\gamma = 0.06$, $\mu = 0.3$ (n = 5, NS=NC=35)

ω		3	4	5	6	7	8	9	$\omega = \infty$ *
$k(a_o^{-1})$	(Method)								
0.10	K	0.1933	0.1931	0.1938	0.1940	0.1941	0.1942	0.1952	0.1947 (±3)
	IK	0.1898	0.1933	0.1938	0.1940	0.1941	0.1942	0.1944	
0.20	K	0.8483	0.8494	0.8519	0.8528	0.8529	0.8533	0.8534	0.8537 (±3)
	IK	0.8471	0.8499	0.8520	0.8527	0.8530	0.8533	0.8534	
0.30	K	0.9734	0.9988	0.9810	0.9832	0.9841	0.9845	0.9846	0.9848 (±2)
	IK	0.9730	0.9774	0.9812	0.9828	0.9841	0.9843	0.9846	
0.40	K	0.7570	0.8133	0.8119	0.8179	0.8186	0.8195	0.8199	0.8205 (±5)
	IK	0.8079	0.8116	0.8141	0.8168	0.8186	0.8194	0.8199	
0.49	K	0.8268	0.6013	0.6649	0.6634	0.7138	0.6747	0.6747	
	IK	0.8262	0.6171	0.6598	0.6668	0.6719	0.6741	0.6748	

where K = $\tan\delta_1$- evaluated by the Kohn variational method,
IK = $\tan\delta_1$- evaluated by the Inverse Kohn variational method.

Table4.13

K-matrix ($\tan\delta_1^+$) and phaseshifts for the p-wave singlet elastic scattering of electrons by positronium obtained by the variational method

$k(a_o^{-1})$	$\tan\delta_1^+$ (ω=9)	δ_1^+ (ω=9)	δ_1^+ ($\omega=\infty$)*
0.01	0.0002	0.0002	
0.02	0.0009	0.0009	
0.03	0.0015	0.0015	
0.04	0.0011	0.0011	
0.05	-0.0006	-0.0006	-0.0004(±2)
0.06	-0.0040	-0.0040	
0.07	-0.0093	-0.0093	
0.08	-0.0168	-0.0168	
0.09	-0.026	-0.026	
0.10	-0.038	-0.038	-0.0381(±1)
0.15	-0.124	-0.123	
0.20	-0.239	-0.235	-0.2347(±1)
0.25	-0.368	-0.353	
0.30	-0.499	-0.463	-0.4629(±3)
0.35	-0.625	-0.559	
0.40	-0.736	-0.635	-0.6343(±5)
0.45	-0.821	-0.687	
0.49	-0.845	-0.702	
0.50	-0.782	-0.664	

* Graphical estimates at the phaseshifts for $\omega = \infty$
The brackets indicate the estimated accuracy in the last figure.

Table 4.14

K-matrix ($\tan\delta_1^-$) and phaseshifts for the p-wave triplet elastic scattering of electrons by positronium obtained by the variational method.

$k(a_o^{-1})$	$\tan\delta_1^-(\omega=9)$	$\delta_1^+(\omega=9)$	$\delta_1^-(\omega=\infty)^*$
0.01	0.0004	0.0004	
0.02	0.003	0.003	
0.03	0.008	0.008	
0.04	0.017	0.017	
0.05	0.031	0.031	0.0310(±4)
0.06	0.050	0.050	
0.07	0.075	0.075	
0.08	0.107	0.106	
0.09	0.147	0.145	
0.10	0.194	0.192	0.1923(±3)
0.15	0.525	0.484	
0.20	0.853	0.707	0.7066(±2)
0.25	0.998	0.784	
0.30	0.985	0.778	0.7777(±1)
0.35	0.907	0.737	
0.40	0.820	0.687	0.6868(±3)
0.45	0.746	0.641	
0.49	0.675	0.594	
0.50		6.47	

* Graphical estimates of the phaseshifts for $\omega = \infty$
The brackets indicate the estimated accuracy in the last figure.

Table 4.15

Variation of $\tan\delta_l^+$ with the value of n which appears in the shielding function (NS=NC=35)

n →	(Method)	3	4	5	6	7
$k(a_o^{-1})\downarrow$						
0.10	K	-0.03725	-0.03769	-0.03750	-0.03737	-0.03733
	IK	-0.03813	-0.03814	-0.03813	-0.03813	-0.03813
	Δ	-0.3	-0.2	-0.2	-0.3	-0.3
0.15	K	-0.1235	-0.1235	-0.1235	-0.1235	-0.1235
	IK	-0.1236	-0.1235	-0.1235	-0.1235	-0.1235
	Δ	-0.007	-0.008	-0.008	-0.008	
0.20	K	-0.2392	-0.2392	-0.2392	-0.2392	-0.2392
	IK	-0.2392	-0.2392	-0.2392	-0.2392	-0.2392
	Δ	-0.002	-0.001	-0.001	-0.001	-0.001
0.25	K	-0.3681	-0.3681	-0.3681	-0.3681	-0.3680
	IK	-0.3682	-0.3681	-0.3681	-0.3681	-0.3681
	Δ	-0.003	0.002	0.003	0.003	0.003
0.30	K	-0.4994	-0.4994	-0.4994	-0.4994	-0.4994
	IK	-0.4994	-0.4993	-0.4993	-0.4993	-0.4993
	Δ	0.007	0.008	0.008	0.008	0.008
0.04	K	-0.7364	-0.7365	-0.7365	-0.7365	-0.7365
	IK	-0.7362	-0.7363	-0.7363	-0.7363	-0.7363
	Δ	0.009	0.007	0.008	0.008	0.008

where

K = $\tan\delta_l^+$ evaluated by the Kohn variational method

IK = $\tan\delta_l^+$ evaluated by the Inverse Kohn variational method.

Δ = Difference between tangent of trial phaseshift and stationary phaseshift.

Table 4.16

Variation of $\tan\delta_1^+$ with the number of integration points (NS=NC) used in the Gauss-Laguerre Quadrature to evaluate the direct-direct and the open-closed channel matrix elements.

NS →	(Method)	20	25	30	35	40
$k(a_o^{-1})$ ↓						
0.05	K	-0.9828E-03	-0.9833E-03	-0.9833E-03	-0.9831E-03	-0.9830E-03
	IK	-0.9548E-03	-0.9549E-03	-0.9549E-03	-0.9549E-03	-0.9549E-03
0.10	K	-0.3742E-01	-0.3750E-01	-0.3751E-01	-0.3750E-03	-0.3749E-01
	IK	-0.3813E-01	-0.3813E-01	-0.3813E-01	-0.3813E-01	-0.3813E-01
0.15	K	-0.1235	-0.1235	-0.1235	-0.1235	-0.1235
	IK	-0.1235	-0.1235	-0.1235	-0.1235	-0.1235
0.20	K	-0.2392	-0.2392	-0.2392	-0.2392	-0.2392
	IK	-0.2392	-0.2392	-0.2392	-0.2392	-0.2392
0.25	K	-0.3680	-0.3681	-0.3681	-0.3681	-0.3681
	IK	-0.3681	-0.3681	-0.3681	-0.3681	-0.3681
0 30	K	-0.4993	-0.4994	-0.4994	-0.4994	-0.4994
	IK	-0.4993	-0.4993	-0.4993	-0.4993	-0.4993
0.35	K	-0.6246	-0.6250	-0.6250	-0.6250	-0.6250
	IK	-0.6246	-0.6250	-0.6250	-0.6250	-0.6250
0.40	K	-0.7372	-0.7367	-0.7365	-0.7365	-0.7365
	IK	-0.7370	-0.7365	-0.7363	-0.7363	-0.7363
0.45	K	-0.8159	-0.8197	-0.8204	-0.8205	-0.8205
	IK	-0.8160	-0.8197	-0.8204	-0.8206	-0.8206
0.46	K	-0.8219	-0.8302	-0.8317	-0.8320	-0.8321
	IK	-0.8221	-0.8302	-0.8318	-0.8321	-0.8322
0.47	K	-0.8259	-0.8382	-0.8407	-0.8411	-0.8411
	IK	-0.8250	-0.8382	-0.8407	-0.8411	-0.8411
0.48	K	-0.8257	-0.8432	-0.8462	-0.8465	-0.8465
	IK	-0.8249	-0.8432	-0.8462	-0.8465	-0.8465
0.485	K	-0.8244	-0.8441	-0.8471	-0.8472	-0.8471
	IK	-0.8235	-0.8440	-0.8471	-0.8471	-0.8471
0.490	K	-0.8214	-0.8429	-0.8456	-0.8454	-0.8452
	IK	-0.8207	-0.8428	-0.8456	-0.8454	-0.8452

where

K = $\tan\delta_1^+$ evaluated by the Kohn variational method.

IK = $\tan\delta_1^+$ evaluated by the Inverse Kohn variational method.

Table 4.17

$^{1,3}P$ resonances in (e^--Ps) scattering (see text), energies measured in Ryd, and measured from the g.s.

Calculation	$^1P(1)$		$^3P(1)$		^3P (2)	
	E_R	Γ	E_R	$\Gamma(\times 10^{-4})$	E_R	$\Gamma(\times 10^{-4})$
Ward et al (1986b)	0.3744		0.35334	2.6	0.37492	0.75
Greene and Botero (1986)	0.37483					

Table 4.18

Convergence of $\tan\delta_1^+$ near n = 2 threshold, ($k = 0.50\ a_o^{-1}$)

Choice of non-linear parameters, $\alpha = 0.30$, $\gamma = 0.06$, $\mu = 0.3$ (n = 5, NS = NC = 35)

ω		3	4	5	6	7	8	9
$k(a_o^{-1})$	(Method)							
0.482	K	-0.8949	-0.9476	-0.8474	-0.8496	-0.8439	-0.8473	-0.8470
	IK	-0.9375	-0.8560	-0.8535	-0.8495	-0.8490	-0.8498	-0.8470
	Δ	-0.1	-0.6	-0.08	-0.06	+0.2	+0.02	0.003
0.483	K	-0.8951	-0.9444	-0.8474	-0.8498	-0.8434	-0.8474	-0.8471
	IK	-0.9341	-0.8560	-0.8536	-0.8497	-0.8491	-0.8497	-0.8471
	Δ	-0.1	-0.6	-0.08	-0.006	0.2	0.02	0.004
0.484	K	-0.8952	-0.9415	-0.8472	-0.8498	-0.8426	-0.8475	-0.8472
	IK	-0.9311	-0.8558	-0.8537	-0.8498	-0.8492	-0.8496	-0.8472
	Δ	-0.1	-0.6	0.8	-0.005	0.2	0.02	0.004
0.485	K	-0.8952	-0.9389	-0.8470	-0.8498	-0.8414	-0.8475	-0.8472
	IK	-0.9283	-0.8556	-0.8537	-0.8498	-0.8492	-0.8495	-0.8471
	Δ	-0.1	-0.6	0.08	-0.005	0.3	0.02	0.005
0.486	K	-0.8952	-0.9365	-0.8467	-0.8497	-0.8396	-0.8474	-0.8470
	IK	-0.9257	-0.8553	-0.8536	-0.8497	-0.8491	-0.8493	-0.8470
	Δ	-0.1	-0.5	0.09	-0.004	0.3	0.02	0.005
0.487	K	-0.8950	-0.9343	-0.8463	-0.8495	-0.8369	-0.8471	-0.8468
	IK	-0.9233	-0.8548	-0.8535	-0.8494	-0.8489	-0.8490	-0.8468
	Δ	-0.1	-0.5	0.09	-0.004	0.4	0.02	0.005
0.490	K	-0.8939	-0.9281	-0.8442	-0.8480	-0.7953	-0.8457	-0.8454
	IK	-0.9165	-0.8529	-0.8522	-0.8480	-0.8475	-0.8473	-0.8454
	Δ	-0.1	-0.5	0.1	-0.001	2	0.03	0.006

Table 5.1

Phaseshifts for (e^--Ps) scattering in several models.

(a) $l = 0$, $s = 0$

$k(a_o^{-1})$	Variational V ($\omega = \infty$)	Static-exchange S.E.	Adiabatic-exchange A.E. $\beta = 0.8003354$
0.05	2.547(±4)	2.230	2.449
0.10	2.049(±1)	1.654	1.905
0.15	1.668(±2)	1.272	1.502
0.20	1.378(±2)	0.987	1.196
0.25	1.156(±2)	0.764	0.957
0.30	0.984(±2)	0.584	0.770
0.35	0.852(±1)	0.439	0.613
0.40	0.748(±2)	0.320	0.488
0.45	0.667(±1)	0.223	0.386

$l = 0$, $s = 1$

$K(a_o^{-1})$	Variational V ($\omega = \infty$)	Static-exchange S.E.	Adiabatic-exchange A.E. $\beta = 0.2961558$
0.05	-0.25(±1)	-0.291	-0.269
0.10	-0.5361(±8)	-0.570	-0.541
0.15	-0.797(±2)	-0.829	-0.802
0.20	-1.025(±1)	-1.064	-1.039
0.25	-1.247(±1)	-1.273	-1.249
0.30	-1.432(±2)	-1.457	-1.434
0.35	-1.596(±1)	-1.619	-1.597
0.40	-1.739(±2)	-1.761	-1.740
0.45	-1.865(±1)	-1.887	-1.866

The brackets indicate the estimated accuracy in the last figure.

Table 5.1/continued

(b) $l = 1, s = 0$

$k(a_o^{-1})$	Variational V ($\omega = 9$)	Variational V * ($\omega \to \infty$)	Static-exchange S.E.	Adiabatic-exchange $\beta = 0.8003354$
0.05	-0.0006	-0.0004(±2)	-0.009	-0.003
0.10	-0.038	-0.0381(±1)	-0.058	-0.0315
0.15	-0.123		-0.149	-0.104
0.20	-0.235	-0.2347(±1)	-0.264	-0.202
0.25	-0.353		-0.384	-0.305
0.30	-0.463	-0.4629(±3)	-0.498	-0.400
0.35	-0.559		-0.598	-0.480
0.40	-0.635	-0.6343(±5)	-0.682	-0.542
0.45	-0.687		-0.750	-0.585

$l = 1, s = 1$

$k(a_o^{-1})$	Variational V ($\omega = 9$)	Variational V * ($\omega \to \infty$)	Static-exchange S.E.	Adiabatic-exchange A.E. $\beta = 0.8003054$
0.05	0.031	0.0310(±4)	0.014	0.026
0.10	0.192	0.1923(±3)	0.107	0.183
0.15	0.484		0.294	0.466
0.20	0.707	0.7066(±2)	0.476	0.692
0.25	0.784		0.569	0.778
0.30	0.778	0.7777(±1)	0.586	0.778
0.35	0.737		0.561	0.739
0.40	0.687	0.6868(±3)	0.519	0.688
0.45	0.641		0.472	0.634

* Graphical estimates of the phaseshifts for $\omega = \infty$
The brackets indicate the estimated accuracy in the last figure.

Table 5.1/continued

$l = 2,\ s = 0$

$k(a_o^{-1})$	Static-exchange S.E.	Adiabatic-exchange A.E. $\beta = 0.8003354$	Born-Polarisation B.P.
0.05	0.0001	0.0007	0.0018
0.10	0.0026	0.0093	0.0072
0.15	0.0152	0.0320	0.016
0.20	0.0454	0.0769	0.029
0.25	0.0919	0.141	0.045
0.30	0.144	0.210	0.065
0.35	0.188	0.269	0.088
0.40	0.217	0.308	0.114
0.45	0.231	0.329	0.144

$l = 2,\ s = 1$

$k(a_o^{-1})$	Static-exchange S.E.	Adiabatic-exchange A.E. $\beta = 0.8003354$	Born-Polarisation B.P.
0.05	-0.00009	0.0005	0.0018
0.10	-0.0024	0.0040	0.0072
0.15	-0.0134	0.0012	0.016
0.20	-0.0386	-0.0142	0.029
0.25	-0.0770	-0.0420	0.045
0.30	-0.123	-0.0764	0.065
0.35	-0.170	-0.111	0.088
0.40	-0.212	-0.141	0.114
0.45	-0.248	-0.162	0.144

Table 5.1/continued

(c) $l = 3, \quad s = 0$

$k(a_o^{-1})$	Static-exchange S.E.	Adiabatic-exchange A.E. $\beta = 0.8003354$	Born-Polarisation B.P.
0.05			0.0006
0.10	-0.00007	0.0013	0.0024
0.15	-0.0009	0.0042	0.0054
0.20	-0.0042	0.0050	0.0096
0.25	-0.0119	0.0024	0.015
0.30	-0.0247	-0.0046	0.022
0.35	-0.0413	-0.0148	0.029
0.40	-0.0595	-0.0260	0.038
0.45	-0.0772	-0.0362	0.048

$l = 3, \quad s = 1$

$k(a_o^{-1})$	Static-exchange S.E.	Adiabatic-exchange A.E. $\beta = 0.8003354$	Born-Polarisation B.P.
0.05			0.0006
0.10	0.00007	0.0015	0.0024
0.15	0.0009	0.0060	0.0054
0.20	0.0043	0.0137	0.0096
0.25	0.0124	0.0276	0.015
0.30	0.0260	0.0480	0.022
0.35	0.0435	0.0731	0.029
0.40	0.0618	0.0994	0.038
0.45	0.0782	0.123	0.048

Table 5.2

$l = 5, \quad s = 0,1$

$k(a_o^{-1})$	Born-Polarisation B.P.	Adiabatic-exchange A.E. $\beta = 0.8003354$	
		SINGLET	TRIPLET
0.25	0.004	0.003	0.003
0.30	0.005	0.004	0.006
0.35	0.007	0.005	0.009

Table 5.3

Singlet and triplet scattering lengths and the zero-energy partial cross-section for l = 0 calculated by the SE and the Kohn variational method.

Method employed	Singlet scattering length (a_o)	Triplet scattering length (a_o)	Zero-energy s-wave cross-section πa_o^2
Kohn variational ($\omega \to \infty$)	12.0±0.3	4.6±0.4	208
S E	20.5±0.2	5.8±0.2	521

Table 5.4

Relative differences between the variational phase shifts and the static-exchange and adiabatic-exchange results for $^{1,3}S$, $^{1,3}P$ e^--Ps scattering.

s-wave

$k(a_o^{-1})$	SINGLET		TRIPLET	
	R^+(S.E.)	R^+(A.E.)	R^-(S.E.)	R^-(A.E.) β=0.29161558
0.05	0.13	0.04	-0.16	-0.08
0.10	0.19	0.07	-0.06	-0.009
0.15	0.24	0.10	-0.04	-0.006
0.20	0.28	0.13	-0.03	-0.004
0.25	0.34	0.17	-0.02	-0.002
0.30	0.41	0.22	-0.02	-0.001
0.35	0.48	0.28	-0.01	-0.0006
0.40	0.57	0.35	-0.01	-0.0006
0.45	0.67	0.42	-0.01	-0.0005

p-wave

$k(a_o^{-1})$	SINGLET		TRIPLET	
	R^+(S.E.)	R^+(A.E.)	R^-(S.E.)	R^-(A.E.)
0.05	-14	-4	0.55	0.16
0.10	-0.53	0.17	0.44	0.05
0.15	-0.21	0.16	0.39	0.04
0.20	-0.12	0.14	0.33	0.02
0.25	-0.09	0.14	0.27	0.008
0.30	-0.08	0.14	0.25	0
0.35	-0.07	0.14	0.24	0.003
0.40	-0.07	0.15	0.25	0.002
0.45	-0.09	0.15	0.26	0.01

Table 5.5

Total cross-sections :
Total elastic cross-section (σ_{el})
Momentum transfer cross-section (σ_D)
Ortho-para conversion cross-section (σ_c)

Units a_o^2 (see text)

$k(a_o^{-1})$	σ_{el}	σ_D	σ_c	σ_c/σ_{el}
0	208	208	13.7	0.066
0.05	202	220	11.7	0.058
0.10	190	230	10.9	0.057
0.15	201	225	15.3	0.076
0.20	180	169	15.3	0.085
0.25	136	115	12.4	0.091
0.30	100	82	9.9	0.098
0.35	75	62	8.0	0.108
0.40	57	49	6.6	0.118
0.45	44	39	5.5	0.126

Table 5.6

Elastic differential cross-section $I_{el}(\theta,k^2)\ a_o^2\ Sr^{-1}$. Calculated using l = 0,1 phase shifts determined by the variational method, higher partial phase shifts determined by the adiabatic-exchange method until convergence was obtained with the Born-polarisation phase shifts.

$k(a_o^{-1})$

θ(degs)	0.10	0.15	0.20	0.30	0.40	0.45
0	33	84	113	84	59	51
5	33	81	110	80	53	45
10	33	79	106	75	47	39
15	33	75	101	71	43	34
20	32	71	96	66	39	30
30	31	63	84	57	31	23
50	30	44	57	38	20	14
60	31	36	44	29	15	11
80	36	27	24	14	8	6
90	40	28	19	9	5	4
100	46	33	18	5	3	3
110	53	41	22	4	2	2
120	61	52	31	7	2	2
130	69	66	43	14	5	4
150	82	94	74	40	26	21
180	92	116	100	70	59	54

Table 5.7

Minima in the elastic differential cross-sections.

$I_{el}(\theta,k^2)$ a_o^2 Sr^{-1}

k	0.01	0.15	0.20	0.25	0.30	0.35	0.40	0.45
θ' degs	50	80	100	100	110	110	110	120
$I_{min}(\theta',k^2)$ $a_o^2 Sr^{-1}$	30	27	18	9.4	4.4	2.4	1.9	1.6

θ' is the angle in degrees which gives a minimum in $I_{el}(\theta,k^2)$ for a certain value of k^2.

Table 6-1

Sensitivity of the photodetachment cross-section of Ps^- on the bound-state wavefunction. Length formulation.

Varying number of linear parameters in the bound-state wavefunction.

Optimized non-linear parameters :

$$\alpha_b = 0.30, \quad \gamma_b = 0.048$$

Accurate p-wave continuum wavefunction, optimized non-linear parameters.

$$0 < k < 0.05\ a_o^{-1}, \quad \alpha_c = 0.15, \quad \gamma_c = 0.01, \quad \mu_c = 0.3$$
$$0.05 \leq k < 0.1\ a_o^{-1}, \quad \alpha_c = 0.15, \quad \gamma_c = 0.03, \quad \mu_c = 0.3$$
$$0.1 \leq k < 0.5\ a_o^{-1}, \quad \alpha_c = 0.30, \quad \gamma_c = 0.06, \quad \mu_c = 0.3$$

$\omega_c = 9$, 220 linear parameters

$\sigma_\lambda(L)(10^{-18}\ cm^2)$

$\omega_b \rightarrow$	3	5	7	8
N_b	13	34	70	95
ε_b (a.u.)	0.0109825351	0.0119568421	0.0120026975	0.0120046146
γ_b	0.12100983	0.12626344	0.012650533	0.12651543
$\lambda(10^3 Å)$				
2.3	48.41	40.35	39.94	40.09
2.4	30.54	28.53	28.05	28.15
2.5	28.85	26.67	26.22	26.33
2.7	28.18	25.51	25.51	25.27
3.0	28.70	25.20	25.05	25.15
3.5	30.50	25.55	25.84	25.83
4.0	32.60	26.28	27.00	26.85
4.5	34.76	27.29	28.32	28.03
5.0	36.85	28.53	29.67	29.32
7.5	44.72	37.71	36.50	36.90
10.0	47.35	49.12	44.20	45.03
12.0	46.32	57.15	51.13	51.20
14 0	43.44	62.66	57.93	56.79
15.0	41.53	64.25	60.95	59.25
16.0	39.41	65.03	63.56	61.44
17.0	37.16	65.01	65.62	63.27
18.0	34.82	64.24	67.07	64.69

Table 6·1 /continued

σ_λ(L)(10^{-18} cm^2)

$\omega_b \rightarrow$	3	5	7	8
N_b	13	34	70	95
ε_b (a.u.)	0.0109825351	0.0119568421	0.0120026975	0.0120046146
γ	0.12100983	0.12626344	0.012650533	0.12651543
$\lambda(10^3 Å)$				
19	32.43	62.78	67.83	65.63
20	30.04	60.70	67.87	66.04
20.5	28.85	59.45	67.61	66.04
21.0	27.67	58.08	67.16	65.88
21.5	26.51	56.58	66.54	65.57
22.0	25.35	54.99	65.73	65.10
22.5	24.21	53.29	64.74	64.47
23	23.09	51.51	63.57	63.68
25	18.83	43.74	57.37	58.97
27.5	14.03	33.19	46.60	49.68
30.0	9.94	22.74	33.86	37.50
32.5	6.48	13.20	20.60	23.70
35.0	3.74	5.46	8.69	10.36
37.5	1.71	0.46	0.54	0.65
37.94346	1.41	0.06	0.00	0.00

Table 6·2

Sensitivity of the photodetachment cross-section of Ps^- on the bound-state wavefunction. Velocity formulation.

Varying number of linear parameters in the bound-state wavefunction.

Optimized non-linear parameters: $\alpha_b = 0.30$, $\gamma_b = 0.048$

Accurate p-wave continuum wavefunction, optimized non-linear parameters.

$0 < k < 0.05 a_o^{-1}$, $\alpha_c = 0.15$, $\gamma_c = 0.01$, $\mu_c = 0.3$

$0.05 \leq k < 0.1 a_o^{-1}$, $\alpha_c = 0.15$, $\gamma_c = 0.03$, $\mu_c = 0.3$

$0.1 \leq k < 0.5 a_o^{-1}$, $\alpha_c = 0.30$, $\gamma_c = 0.06$, $\mu_c = 0.3$

$\omega_c = 9$, 220 linear parameters.

$\sigma_\lambda(V)(10^{-18}\ cm^2)$

$\omega_b \rightarrow$	3	5	7	8
N_b	13	34	70	95
ε_b(a.u.)	0.0109825351	0.0119568421	0.0120026975	0.0120046146
γ_b	0.12100983	0.12626344	0.012650533	0.12651543
$\lambda(10^3 Å)$				
2.3	46.77	40.18	40.10	40.12
2.4	29.45	28.45	28.18	28.16
2.5	27.64	26.65	26.34	26.33
2.7	26.63	25.60	25.24	25.25
3.0	26.62	25.48	25.08	25.11
3.5	27.60	26.13	25.72	25.77
4.0	29.08	27.09	26.76	26.80
4.5	30.88	28.20	28.01	28.01
5.0	32.89	29.39	29.35	29.33
7.5	44.84	36.50	37.07	36.92
10.0	57.38	45.09	45.01	45.15
12.0	66.18	52.30	51.06	51.40
14.0	73.07	59.03	56.53	56.86
15.0	75.65	61.98	58.94	59.18
16.0	77.62	64.53	61.06	61.16
17.0	78.95	66.63	62.84	62.77
18.0	79.66	68.19	64.23	63.98

Table 6·2/continued

σ_λ(V)(10^{-18} cm^2)

$\omega_b \rightarrow$ N_b ϵ_b(a.u.) γ	3 13 0.0109825351 0.12100983	5 34 0.0119568421 0.12626344	7 70 0.0120026975 0.012650533	8 95 0.0120046146 0.12651543
$\lambda(10^3$Å)				
19	79.75	69.19	65.17	64.76
20	79.23	69.57	65.63	65.06
20.5	78.75	69.52	65.67	65.03
21.0	78.12	69.31	65.56	64.87
21.5	77.36	68.94	65.32	64.58
22.0	76.47	68.40	64.94	64.16
22.5	75.44	67.70	64.41	63.60
23.0	74.29	66.83	63.72	62.90
25.0	68.52	61.79	59.54	58.75
27.5	59.06	52.17	51.00	50.44
30.0	47.92	39.70	39.34	39.10
32.5	35.55	25.55	25.53	25.55
35.0	23.18	11.66	11.51	11.61
37.5	11.83	1.07	0.76	0.76
37.94346	9.98	0.14	0.00	0.00

Table 6·3

Photodetachment of Ps^-

Accurate bound-state wavefunction. Optimized non-linear parameters, $\alpha_b = 0.30$, $\gamma_b = 0.048$
$\omega_b = 8$, 95 linear parameters.
$\varepsilon_b = 0.0120046146$ a.u.
Accurate p-wave continuum wavefunction, optimized non-linear parameters.

$0 < k < 0.05\ a_o^{-1}$, $\alpha_c = 0.15$, $\gamma_c = 0.01$, $\mu_c = 0.3$
$0.05 \leqslant k < 0.1\ a_o^{-1}$, $\alpha_c = 0.15$, $\gamma_c = 0.03$, $\mu_c = 0.3$
$0.1 \leqslant k < 0.5\ a_o^{-1}$, $\alpha_c = 0.30$, $\gamma_c = 0.06$, $\mu_c = 0.3$

$\omega_c = 9$, 220 linear parameters.

$\lambda(10^3$ Å)	$k(a_o^{-1})$	$\sigma_\lambda(L)(10^{-18}$ cm$^2)$	$\sigma_\lambda(V)(10^{-18}$ cm$^2)$
2.283224	0.5000	63.56	63.59
2.3	0.4981	40.09	40.12
2.4	0.4869	28.15	28.16
2.5	0.4764	26.33	26.33
2.7	0.4571	25.27	25.25
3.0	0.4318	25.15	25.11
4.0	0.3686	25.85	26.80
4.5	0.3449	28.03	28.01
5.0	0.3248	29.32	29.33
7.5	0.2549	36.90	36.92
10.0	0.2115	45.03	45.15
12.0	0.1860	51.20	51.40
14.0	0.1655	56.79	56.86
15.0	0.1565	59.25	59.18
16.0	0.1482	61.44	61.16
17.0	0.1404	63.27	62.77
18.0	0.1332	64.69	63.98
19.0	0.1263	65.63	64.76
20.0	0.1198	66.04	65.06
20.5	0.1167	66.04	65.03
21.0	0.1137	65.88	64.87
21.5	0.1107	65.57	64.58
22.0	0.1077	65.10	64.16
22.5	0.1048	64.47	63.60
23	0.1020	63.68	62.90
25	0.09104	58.97	58.75
27.5	0.07797	49.68	50.44
30.0	0.06511	37.50	39.10
32.5	0.05178	23.70	25.55
35.0	0.03670	10.36	11.61
37.5	0.01378	0.65	0.76
37.94346	0.00077	0.00	0.00

Table 6·4

Photodetachment cross-section of Ps^- using :

(a) the trial Kohn phaseshift,
(b) the stationary Kohn phaseshift, in the p-wave continuum variational wavefunction.

Continuum wavefunction : ω_c = 9, 220 linear parameters,
3 optimized non-linear parameters.

Bound-state wavefunction : ω_b = 8, 95 linear parameters,
2 optimized non-linear parameters.
(α_b = 0.30, γ_b = 0.048)

$\lambda(10^3 Å)$	$\sigma_\lambda(L)(10^{-18}cm^2)$	$\sigma_\lambda(V)(10^{-18}cm^2)$	$\sigma_\lambda(L)(10^{-18}cm^2)$	$\sigma_\lambda(V)(10^{-18}cm^2)$
2.283224	63.56	63.59	63.70	63.66
2.3	40.09	40.12	40.20	40.17
2.4	28.15	28.16	28.21	28.19
2.7	25.27	25.25	25.55	25.36
5.0	29.32	29.33	29.44	29.33
10.0	45.03	45.15	44.86	45.81
15.0	59.25	59.18	56.65	47.44
20.0	66.04	65.06	65.86	64.50
22.5	64.47	63.60	63.05	59.60

Table 6·5

Sensitivity of the photodetachment cross-section of Ps^- on the p-wave continuum wavefunction. Length formulation.

Varying number of linear parameters in p-wave continumm wavefunction.

Bound-state wavefunction :
optimized non-linear parameters, $\alpha_b = 0.30$, $\gamma_b = 0.048$
$\omega_b = 8$, 95 linear parameters.

Accurate p-wave continuum wavefunction :
optimized non-linear parameters
$0 < k < 0.05\ a_o^{-1}$, $\alpha_c = 0.15$, $\gamma_c = 0.01$, $\mu_c = 03$
$0.05 \lesssim k < 0.1\ a_o^{-1}$, $\alpha_c = 0.15$, $\gamma_c = 0.03$, $\mu_c = 0.3$
$0.1 \lesssim k < 0.5\ a_o^{-1}$, $\alpha_c = 0.30$, $\gamma_c = 0.06$, $\mu_c = 0.3$

$\sigma_\lambda(L)(10^{-18}cm^3)$

ω_c / N_c	3 / 20	5 / 56	7 / 120	9 / 220
$\lambda(10^3$ Å)				
2.3	36.28	35.51	39.67	40.09
2.4	31.32	27.78	27.52	28.15
2.5	29.52	26.19	26.24	26.33
2.7	28.23	25.28	25.28	25.27
3.0	28.04	25.21	25.17	25.15
3.5	30.60	25.89	25.85	25.83
4.0	24.30	27.07	26.85	26.85
4.5	27.65	28.09	28.05	28.03
5.0	29.28	29.36	29.34	29.32
7.5	37.29	36.25	36.90	36.90
10.0	44.65	45.07	45.02	45.03
12.0	51.04	51.29	51.21	51.20
14.0	56.60	57.04	56.79	56.79
15.0	59.03	59.01	59.27	59.25
16.0	61.15	61.41	61.46	61.44
17.0	62.89	63.27	63.30	63.27
18.0	64.19	64.69	64.72	64.69
19.0	64.97	65.63	65.68	65.63
20.0	65.12	66.03	66.05	66.04
20.5	64.93	66.01	66.04	66.04
21.0	64.51	65.85	65.88	65.88
21.5	63.80	65.54	65.57	65.57
22.0	62.61	65.06	65.09	65.10

Table 6·5/continued

$\sigma_\lambda(L)(10^{-18}cm^2)$

ω / N_c^c	3 / 20	5 / 56	7 / 120	9 / 220
$\lambda(10^3Å)$				
22.5	60.17	64.43	64.46	64.47
23.0	43.56	63.64	63.67	63.68
25.0	59.62	65.94	58.96	58.97
27.5	50.00	50.06	49.61	49.68
30.0	37.59	37.83	37.20	37.50
32.5	23.71	23.83	23.91	23.70
35.0	10.32	10.36	10.36	10.36
37.5	0.65	0.66	0.65	0.65
37.94346	0.00	0.00	0.00	0.00

Table 6·6

Sensitivity of the photodetachment cross-section of Ps- on the p-wave continuum wavefunction. Velocity formulation.

Varying number of linear parameters in p-wave continuum wavefunction.

Bound-state wave function :
optimized non-linear parameters, $\alpha_b = 0.30$, $\gamma_b = 0.048$
$\omega_b = 8$, 95 linear parameters.
Accurate p-wave continuum wavefunction :
optimized non-linear parameters :

$0 < k < 0.05\ a_o^{-1}$, $\alpha_c = 0.15$, $\gamma_c = 0.01$, $\mu_c = 0.3$
$0.05 < k < 0.1\ a_o^{-1}$, $\alpha_c = 0.15$, $\gamma_c = 0.03$, $\mu_c = 0.3$
$0.1 < k < 0.5\ a_o^{-1}$, $\alpha_c = 0.30$, $\gamma_c = 0.06$, $\mu_c = 0.3$

$\sigma_\lambda(V)(10^{-18}\text{cm}^2)$

ω_c / N_c	3 / 20	5 / 56	7 / 120	9 / 220
$\lambda(10^3\text{Å})$				
2.3	35.97	35.72	39.75	40.12
2.4	31.03	27.92	27.44	28.16
2.5	29.22	26.28	26.22	26.33
2.7	27.87	25.31	25.25	25.25
3.0	27.49	25.19	25.12	25.11
3.5	28.69	25.85	25.79	25.77
4.0	26.25	26.46	26.82	26.80
4.5	28.27	28.06	28.03	28.01
5.0	29.60	29.38	29.35	29.33
7.5	36.88	36.92	36.93	36.92
10.0	45.19	45.17	45.15	45.15
12.0	51.41	51.42	51.41	51.40
14.0	56.94	56.87	56.86	56.86
15.0	59.31	59.20	59.18	59.18
16.0	61.34	61.16	61.17	61.16
17.0	63.01	62.77	62.79	62.77
18.0	64.25	63.97	64.00	63.98
19.0	65.05	64.74	64.77	64.76
20.0	65.35	65.05	65.08	65.06
20.5	65.31	65.02	65.04	65.03
21.0	65.13	64.86	64.88	64.87
21.5	64.79	64.57	64.58	64.58
22.0	64.29	64.15	64.15	64.16

Table 6.6 /continued

σ_λ(V)(10^{-18} cm^2)

ω_c / N_c	3 / 20	5 / 56	7 / 120	9 / 220
$\lambda(10^3$Å)				
22.5	63.52	63.60	63.59	63.60
23.0	60.93	62.91	62.89	62.90
25.0	59.49	62.89	58.74	58.75
27.5	51.06	51.05	50.38	50.44
30.0	39.55	39.36	38.85	39.10
32.5	25.86	25.70	25.73	25.55
35.0	11.74	11.65	11.61	11.61
37.5	0.78	0.77	0.77	0.76
37.94346	0.00	0.00	0.00	0.00

Table 6·7

To compare the photodetachment cross-section of Ps^- using different continuum wavefunctions but the same bound-state wavefunction

Bound-state wavefunction

95 linear parameters, $\omega_b = 8$

optimized linear parameters, $\alpha_b = 0.30$, $\gamma_b = 0.048$

$\epsilon_b = 0.0120046146$ a.u., $\gamma = 0.12651543$

Continuum wavefunction

(a) An accurate p-wave variational wavefunction.
220 linear parameters, $\omega_c = 9$, and three non-linear parameters, which have been optimized.

(b) Plane wave for ejected electron,

	(a)		(b)	
$\lambda(10^3 Å)$	$\sigma_\lambda(L)(10^{-18}cm^2)$	$\sigma_\lambda(V)(10^{-18}cm^2)$	$\sigma_\lambda(L)(10^{-18}cm^2)$	$\sigma_\lambda(V)(10^{-18}cm^2)$
2.283224	63.56	63.59	0.84	5.16
2.3	40.09	40.12	0.87	5.26
2.4	28.15	28.16	1.06	5.84
2.5	26.33	26.33	1.27	6.45
2.7	25.27	25.25	1.76	7.74
3.0	25.15	25.11	2.63	9.82
3.5	25.83	25.77	4.44	13.62
4.0	26.85	26.80	6.61	17.72
4.5	28.03	28.01	9.06	22.03
5.0	29.32	29.33	11.74	26.46
7.5	36.90	36.92	26.97	48.70
10.0	45.03	45.15	42.38	68.59
12.0	51.20	51.40	53.21	81.48
14.0	56.79	56.86	62.23	91.17
15.0	59.25	59.18	65.98	94.75
16.0	61.44	61.16	69.15	97.47
17.0	63.27	62.77	71.71	99.34
18.0	64.69	63.98	73.60	100.36
19.0	65.63	64.76	74.78	100.53
20.0	66.04	65.06	75.21	99.87
20.5	66.04	65.03	75.14	99.23
21.0	65.88	64.87	74.87	98.38
21.5	65.57	64.58	74.41	97.33
22.0	65.10	64.16	73.76	96.09

Table 6.7/continued

	(a)		(b)	
$\lambda(10^{3}\text{Å})$	$\sigma_\lambda(L)(10^{-18}cm^2)$	$\sigma_\lambda(V)(10^{-18}cm^2)$	$\sigma_\lambda(L)(10^{-18}cm^2)$	$\sigma_\lambda(V)(10^{-18}cm^2)$
22.5	64.47	63.60	72.91	94.65
23	63.68	62.90	71.86	93.01
25	58.97	58.75	65.86	84.63
27.5	49.68	50.44	54.70	70.40
30.0	37.50	39.10	40.62	52.91
32.5	23.70	25.55	25.29	33.63
35.0	10.36	11.61	10.85	14.83
37.5	0.65	0.76	0.68	0.96
37.94346	0.00	0.00	0.00	0.00

Table 6·8

Photodetachment cross-section of Ps^- using the length formulation

Plane wave treatment of ejected electron with simple bound-state wavefunctions :

(a) Two-parameter (Ferrante,1970) bound-state wavefunction,
(b) Three-parameter (Ferrante, 1970) bound-state wavefunction.

Compared to the calculations using:

(c) a 95-linear parameter bound-state wavefunction and a plane wave for ejected electron,
(d) a 95-linear parameter variational wavefunction and an accurate 220 linear parameter p-wave variational wavefunction for the continuum state.

$\sigma_\lambda(L)$ (10^{-18} cm^2)

$\lambda(10^3)$	(a)	(b)	(c)	(d)
2.3	0.74	0.61	0.87	40.09
2.4	0.83	0.78	1.06	28.15
2.5	0.93	0.97	1.27	26.33
2.6	1.03	1.19		
2.8	1.26	1.69		
3.0	1.50	2.30	2.63	25.15
3.2	1.76	3.00		
3.4	2.05	3.81		
3.5		4.25	4.44	25.83
3.6	2.35	4.71		
3.8	2.68	5.71		
4.0	3.03	6.79	6.61	26.85
5.0	5.06	13.35	11.74	29.32
7.5	12.74	33.02	26.97	36.90
10.0	23.71	48.79	42.38	45.03
12.5	37.03	56.83		
15.0	51.40	58.11	65.98	59.25
17.5	65.57	54.87		
20.0	78.49	49.10	75.21	66.04
22.5	89.42	42.23	72.91	64.47
25.0	97.89	35.16	65.86	58.97
27.5	103.65	28.42	54.70	49.68
30.0	106.68	22.31	40.62	37.50
32.5	107.07	16.94	25.29	23.70
35.0	105.05	12.34	10.85	10.36
37.5	100.88	8.52	0.68	0.65

Table 6·9

Photodetachment cross-section of Ps at very low energies

Various calculations :

(a) Bhatia and Drachman, Private Communication, 1983. They used an accurate 120 term Hylleraas function (Bhatia et al, 1983) and a plane wave for the ejected electron.

(b) An accurate bound-state variational wavefunction (95 linear parameters and 2 non-linear parameters), and a plane wave for the ejected electron.

(c) An accurate bound-state variational wavefunction (95 linear parameters and 2 non-linear parameters), and an accurate p-wave variational wavefunction (220 linear parameters and 3 non-linear parameters) for the continuum wavefunction.

k^2 (Ryd)	σ_λ(L) $10^{-18}cm^2$	σ_λ(V) $10^{-18}cm^2$	σ_λ(L) $10^{-18}cm^2$	σ_λ(V) $10^{-18}cm^2$	σ_λ(L) $10^{-18}cm^2$	σ_λ(V) $10^{-18}cm^2$
0.0002	0.7943	1.0332	0.7310	1.0328	0.7044	0.8243
0.0004	2.1750	2.8201	2.0092	2.8207	1.9329	2.2434
0.0006	3.8691	5.0016	3.5873	5.0053	3.445	3.9667
0.0008	5.7689	7.4367	5.3680	7.4461	5.1469	5.8801
0.0010	7.8091	10.0410	7.2918	10.0586	6.9804	7.9155
0.002	18.8744	24.0359	17.9117	24.1254	14.3026	16.2202

Table 6.10

SUM-RULE s_{-1} (see text equations 6.30, 6.31)

	(1) S_{-1}	(2) S_{-1}	S_{-1}(L.H.S)	S_{-1}(R.H.S)
Ward et al. 1986b L	1.5	28.0	29.5	29.75
Ward et al. 1986b V	1.5	27.7	29.2	29.75
Bhatia and Drachman (1985a, 86)			31.7	29.775
Kolos et al (1960)				29.94

L = length formulation of cross-section,
V = velocity formulation of cross-section.

Figures

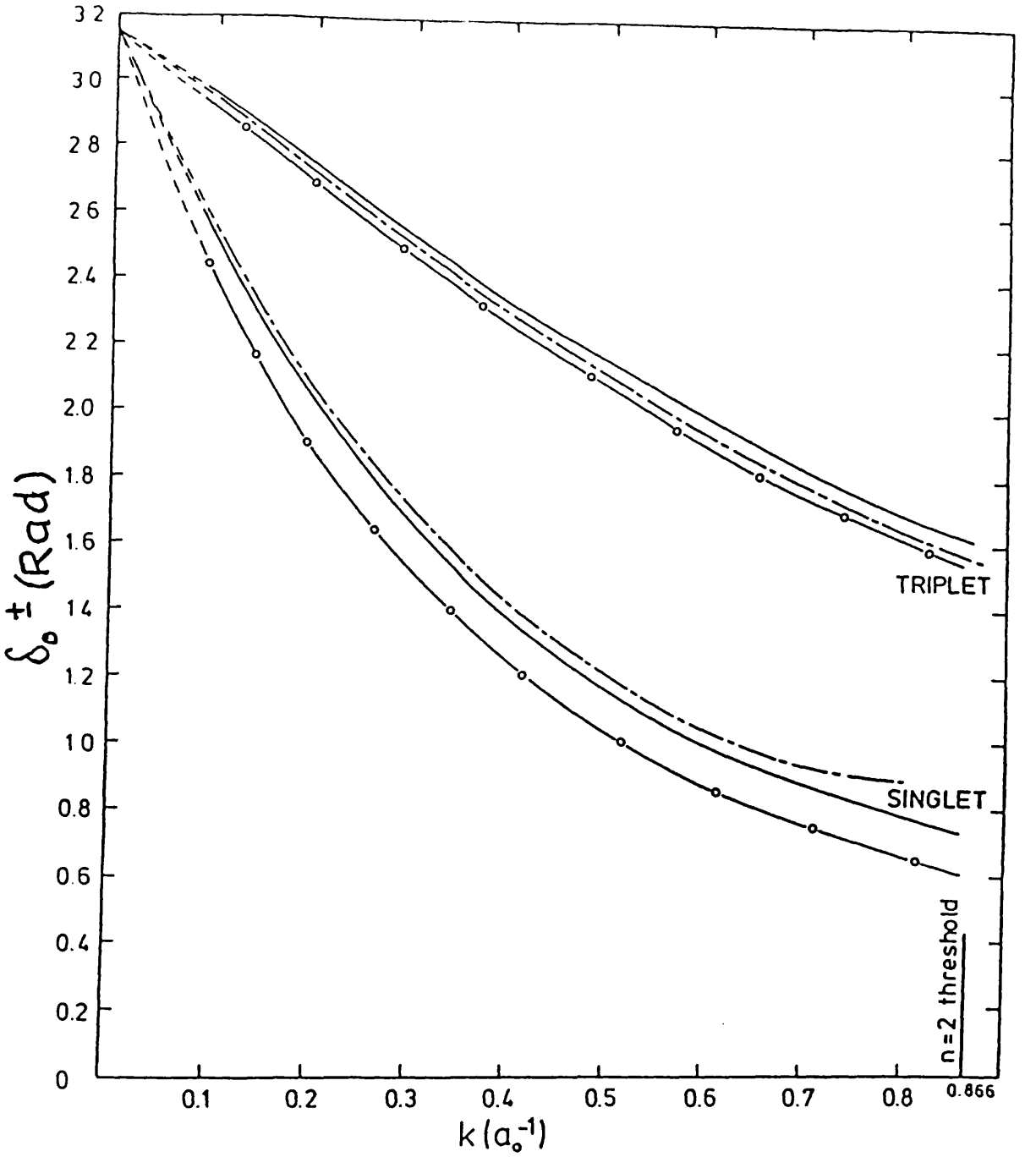

Fig. 2.1

s-wave electron scattering by hydrogen, below the n = 2 threshold ($k = 0.866 a_0^{-1}$) evaluated in various models (see text)

- - - — - Variational (Schwartz, 1961)

—o—o— Static-exchange

——— Adiabatic-exchange

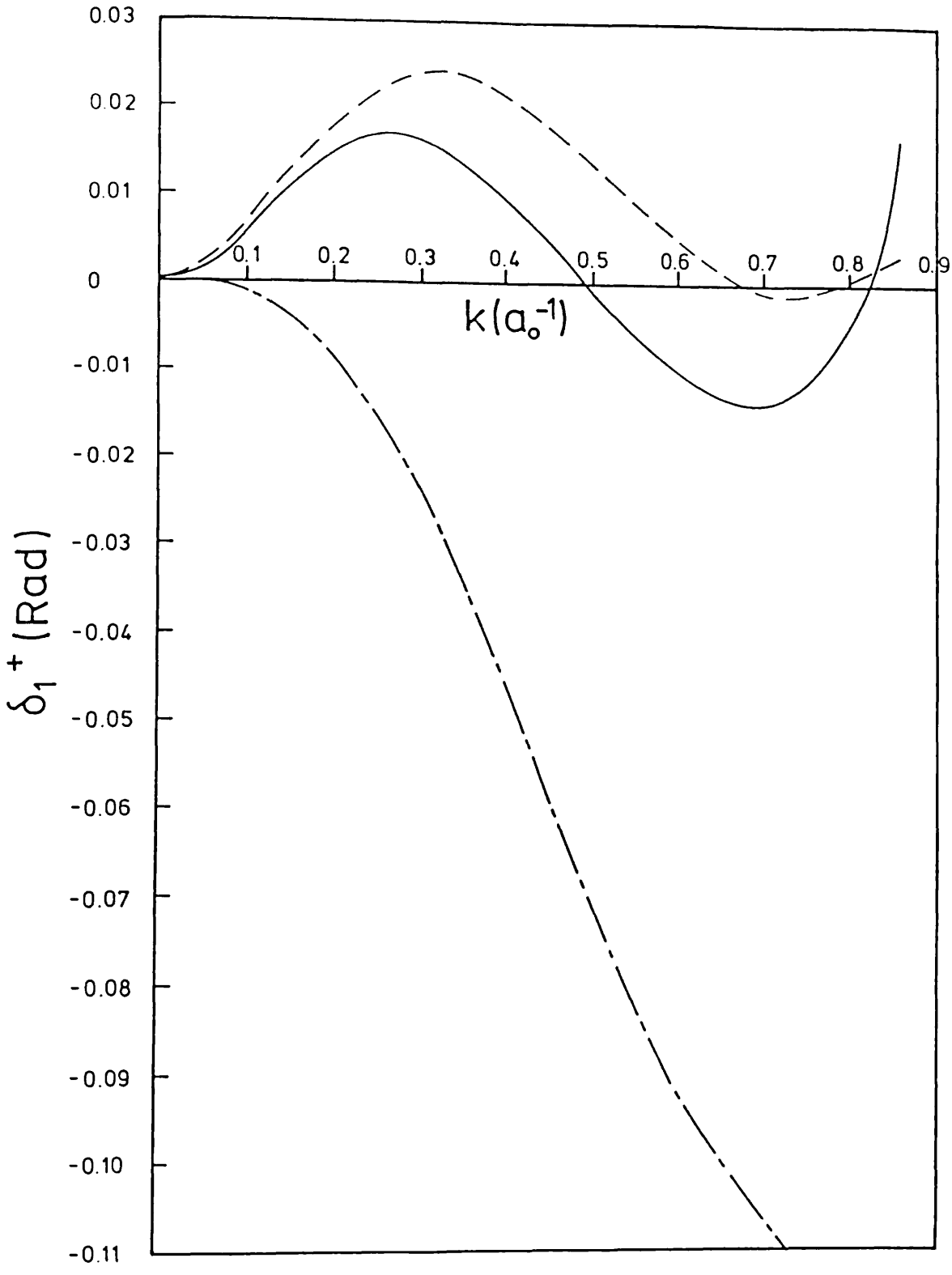

Fig. 2.2a

δ_1^+ phase shifts, in radians, for electron scattering by hydrogen below the n = 2 threshold, evaluated in various models (see text)

———— Variational (Armstead, 1968)

— - — - — Static-exchange

— — — — Adiabatic-exchange

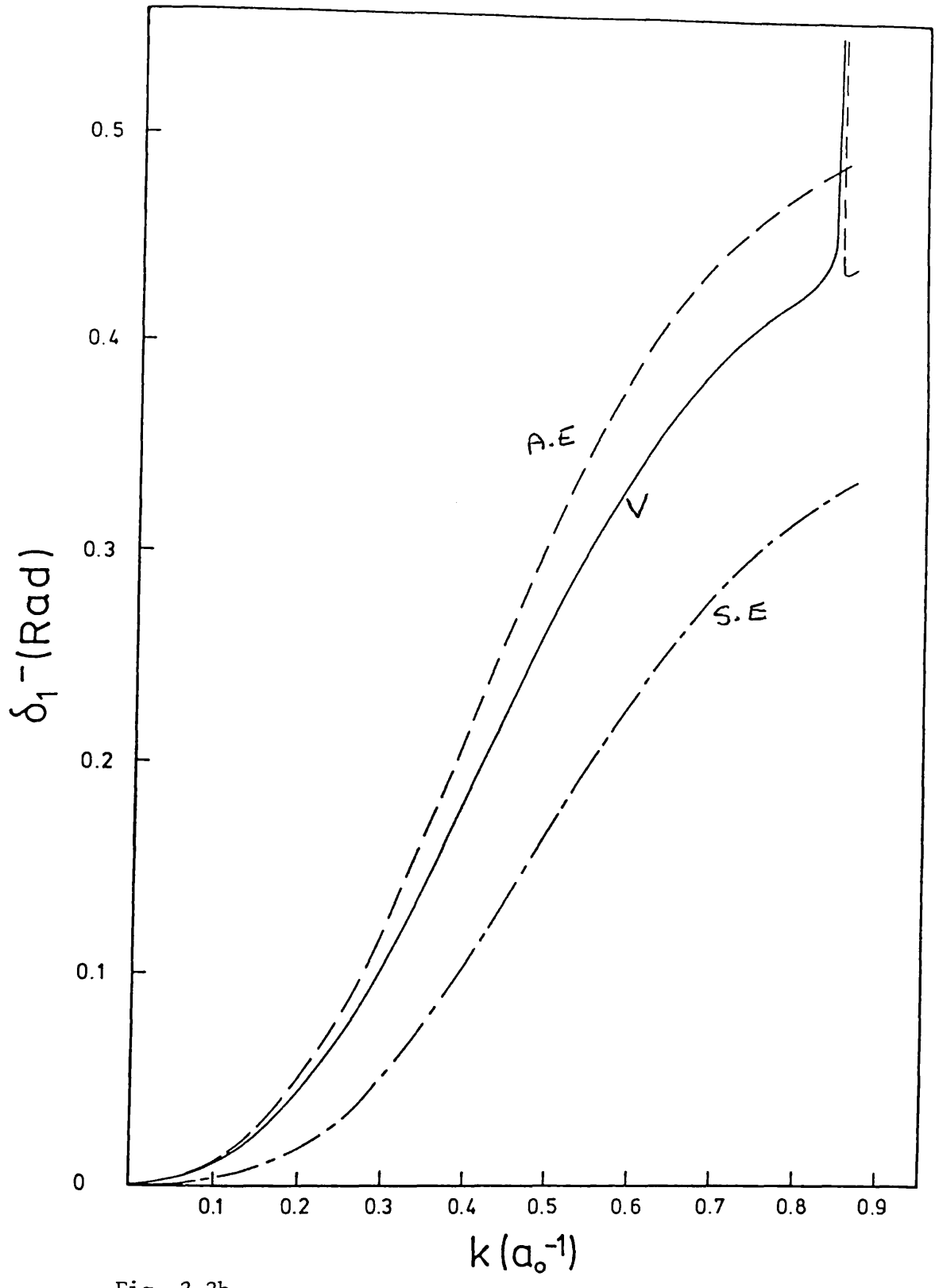

Fig. 2.2b

δ_1^- phase shifts, in radians, for electron scattering by hydrogen below the n = 2 threshold, evaluated in various models (see text)

———— Variational (Armstead, 1968)

— - — - — Static-exchange

— — — - Adiabatic-exchange

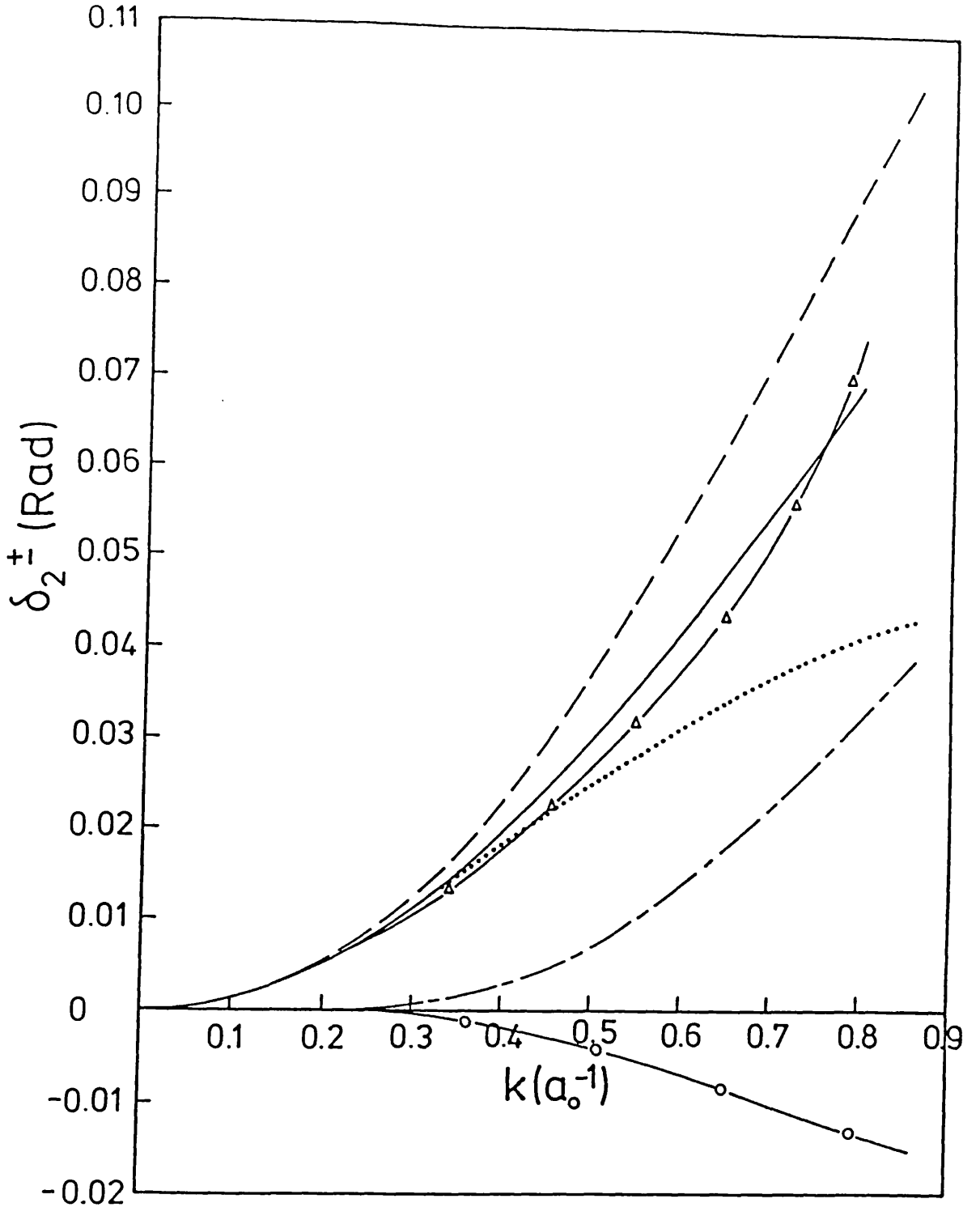

Fig. 2.3

δ_2^{+} phase shifts, in radians for electron scattering by hydrogen below the n = 2 threshold, evaluated in various models.

——————— Variational triplet (Register and Poe, 1975)

— — — Adiabatic-exchange triplet

—·—·—·— Static-exchange triplet

—Δ—Δ Variational singlet (Register and Poe, 1975)

• • • • • • Adiabatic-exchange singlet

—o—o Static-exchange singlet

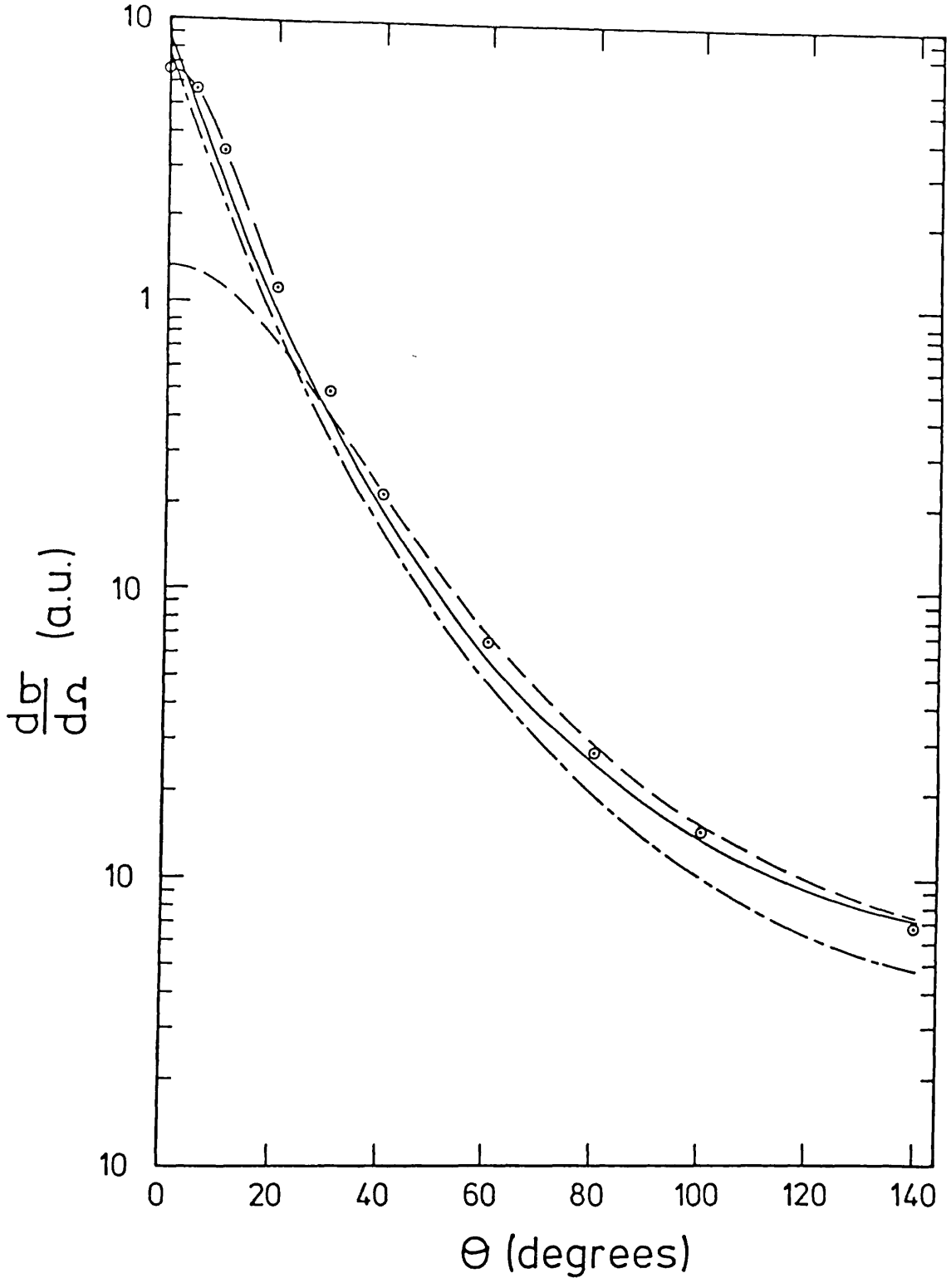

Fig. 2.4

Elastic differential scattering by electron-hydrogen scattering at 100 eV evaluated in various models

— - — - — U.E.B.S. result (Bryon et al, 1982)

——————— E.B.S. result

— — — — Static-exchange result

—⊙—⊙— Adiabatic-exchange result

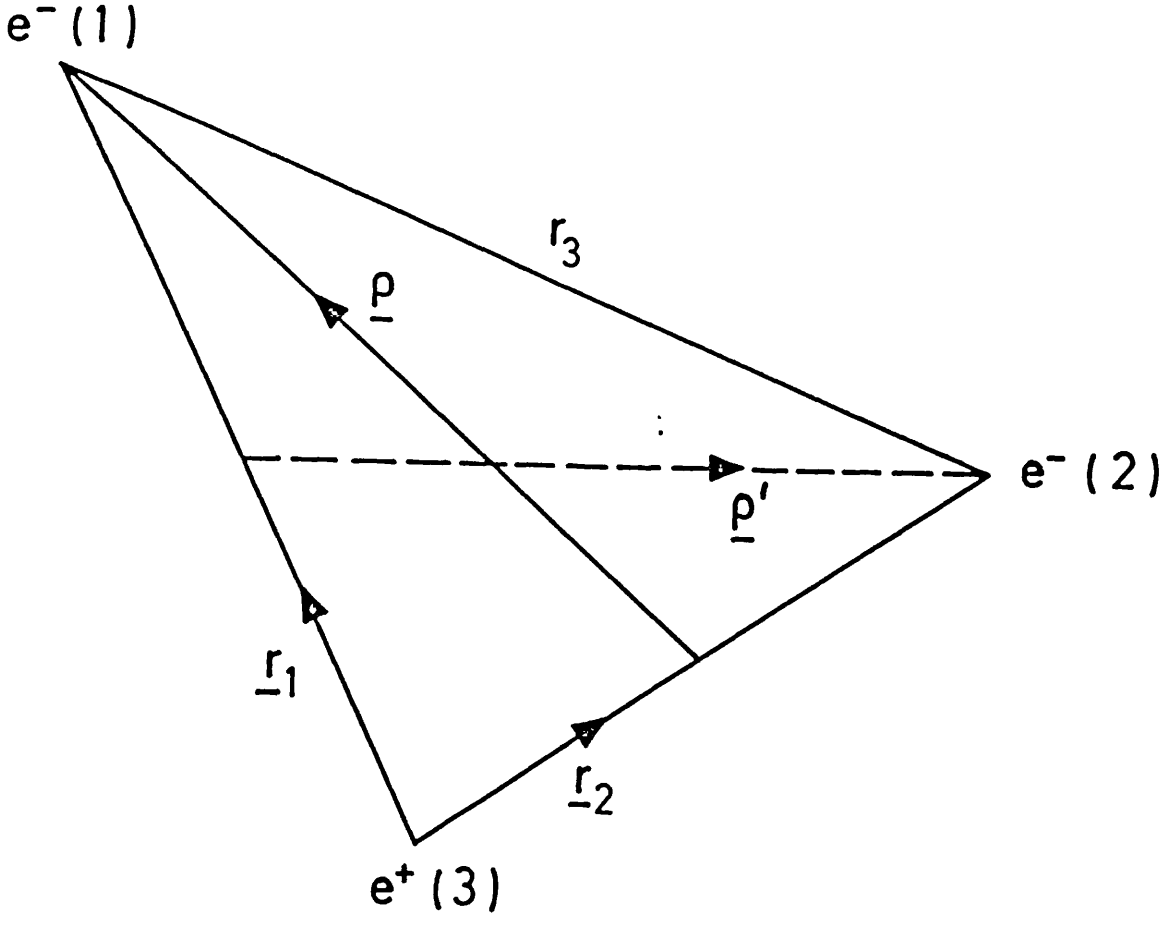

Fig. 2.5

Illustration of the two different coordinate systems used (r_1, r_2 and r_2, ρ) in the e^--Ps problem

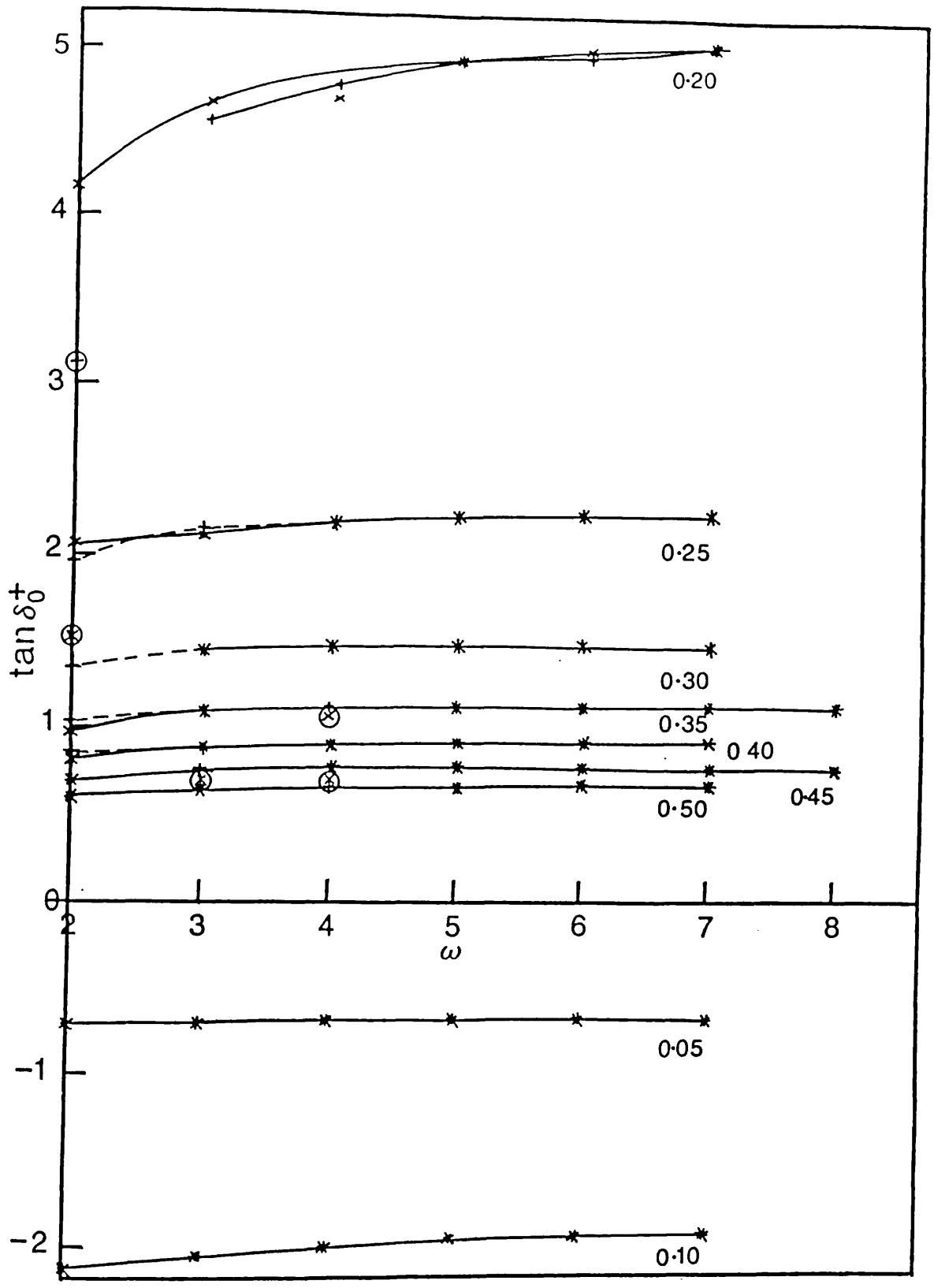

Fig. 3.1

Variation of $\tan\delta_o^+$ with ω in the range $0.05 \leq k\,(a_o^{-1}) \leq 0.50$

x Kohn results

\+ Inverse Kohn results

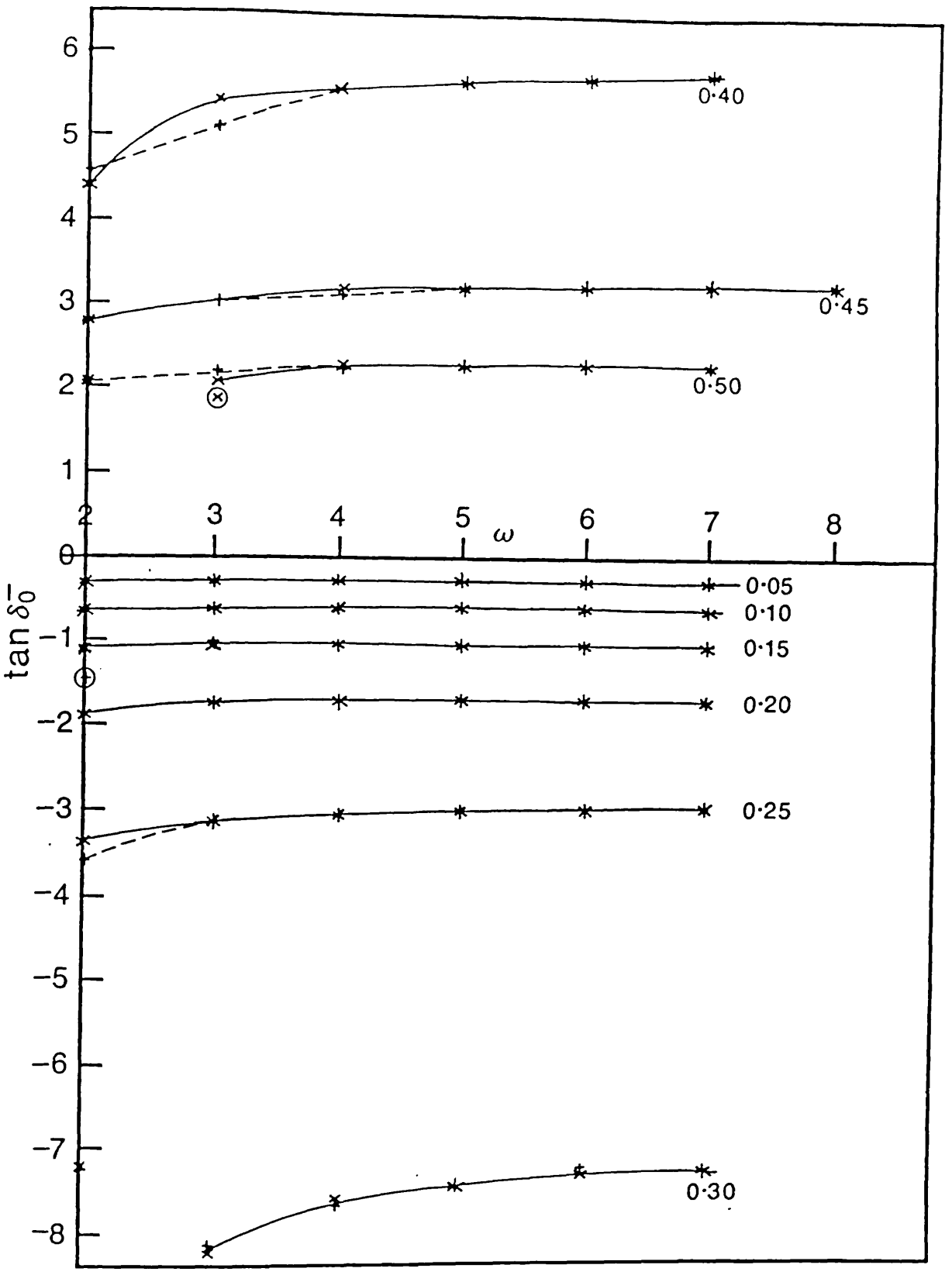

Fig. 3.2

Variation of $\tan\delta_o^+$ with ω in the range $0.05 \leq k(a_o^{-1}) \leq 0.50$

x Kohn results

\- Inverse Kohn results

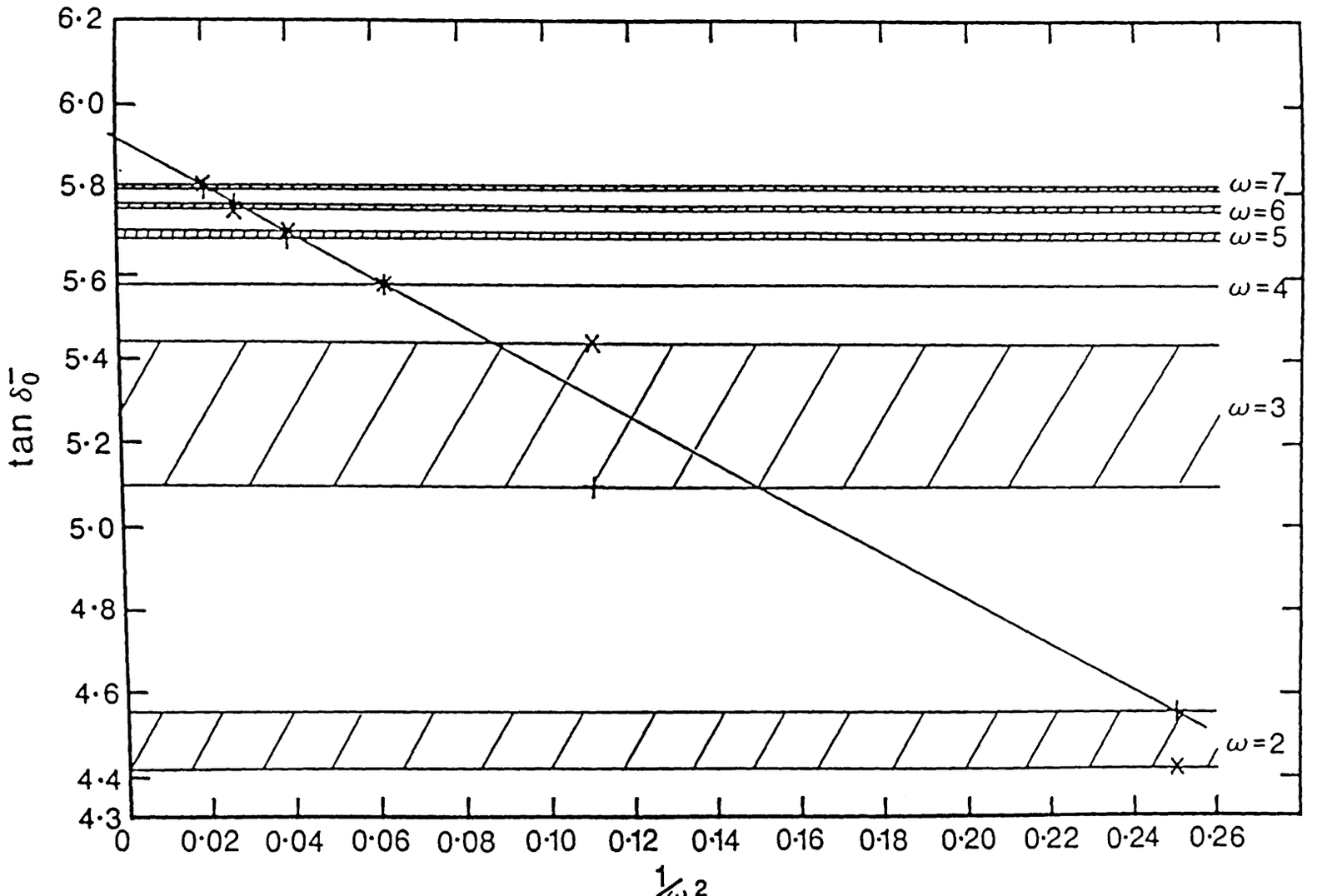

Fig. 3.3 Convergence of $\tan\delta_0^-$ with ω for $k = 0.40\ a_0^{-1}$ according to equation (3.59)

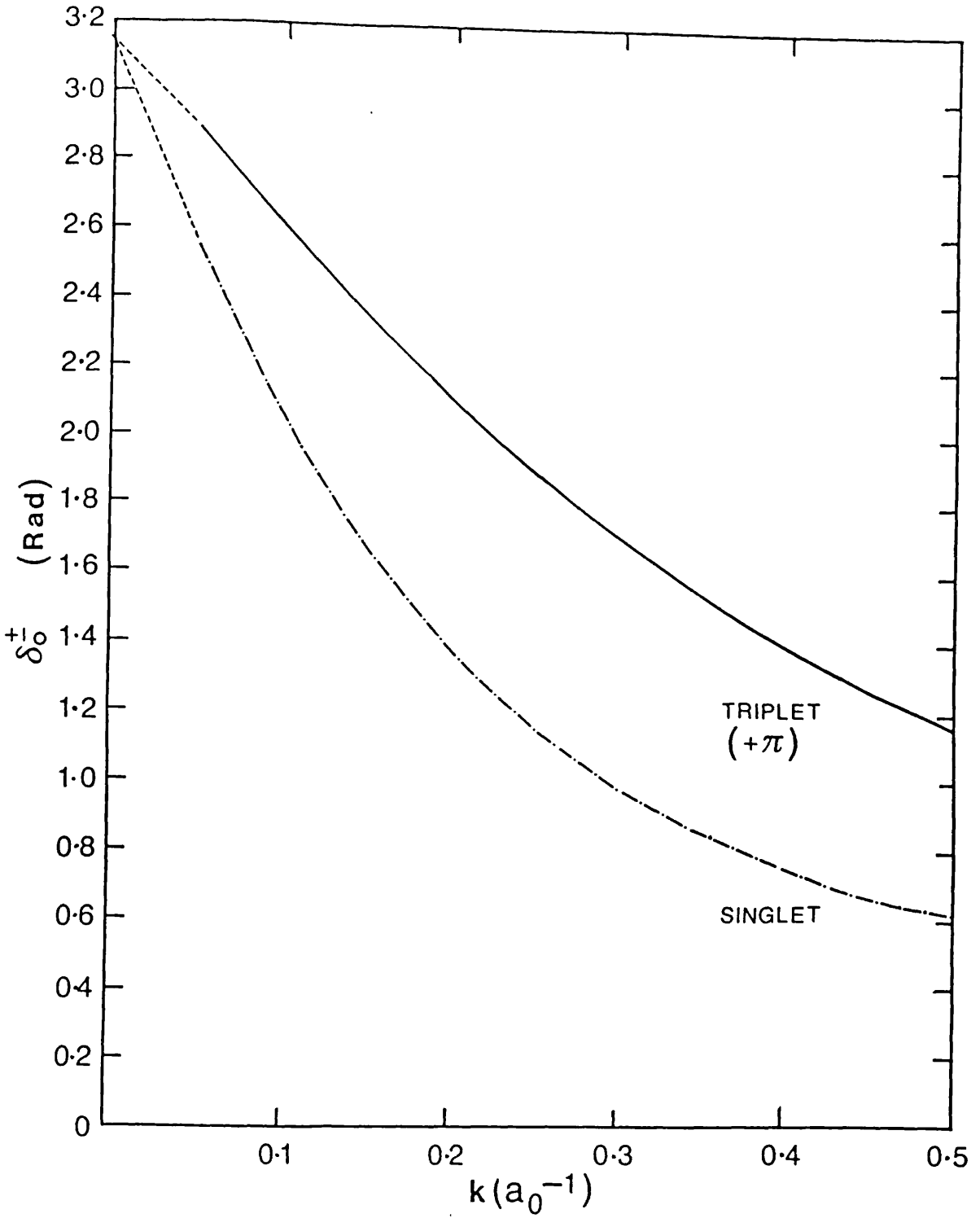

Fig. 3.4

Singlet and triplet s-wave phase shifts extrapolated to infinite ω (δ_0^{+}(Rad)) as a function of the wave number k for e^--Ps scattering below the n = 2 Ps threshold (note: π has been added to the triplet results in order to draw singlet and triplet phase shifts on the same graph, see text).

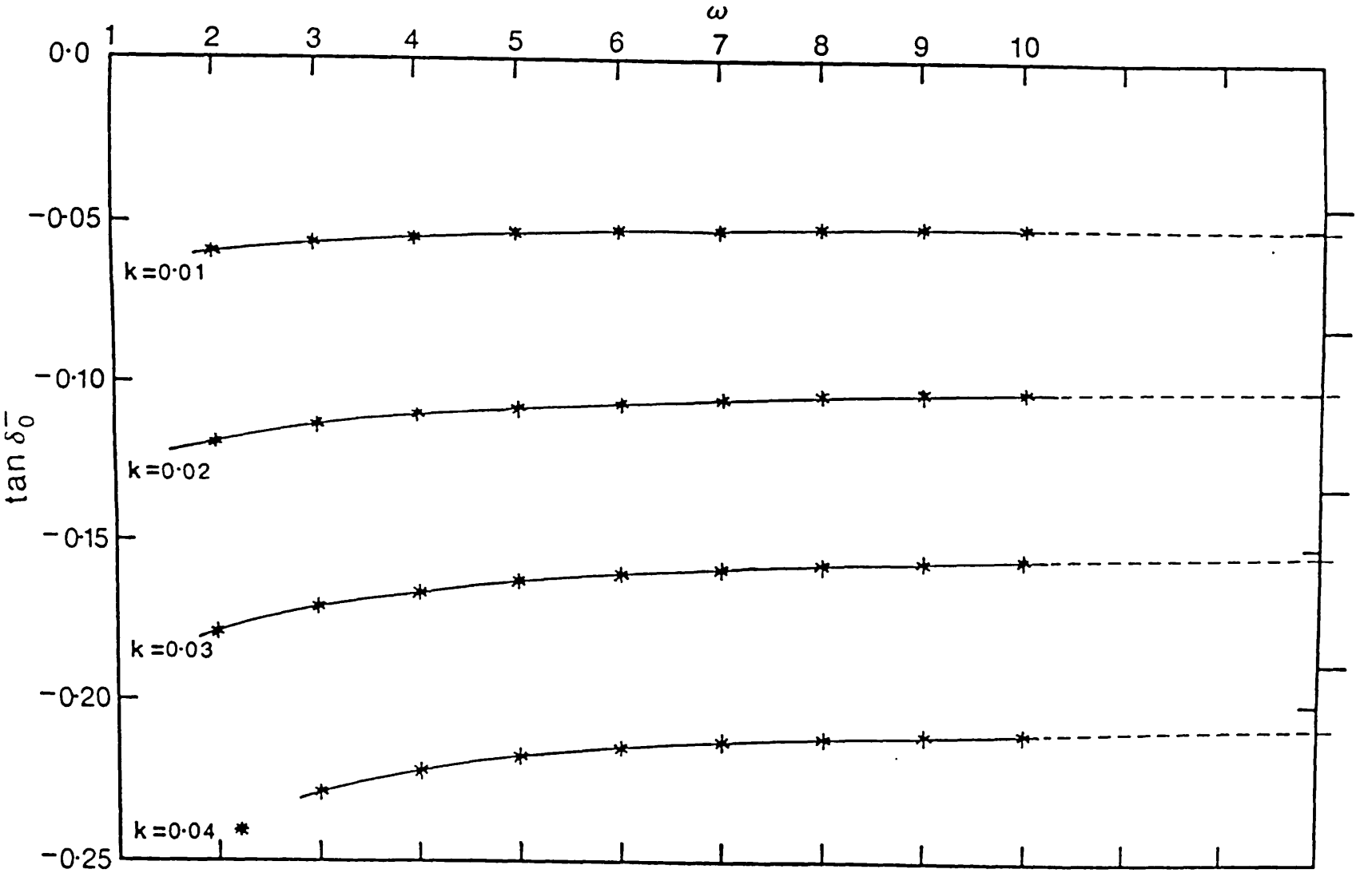

Fig. 3.5 Variation of $\tan\delta_o^-$ with ω for very low values of wave number k, $(0.01 \leq k\ (a_o^{-1}) \leq 0.04)$. x Kohn results, + Inverse Kohn results.

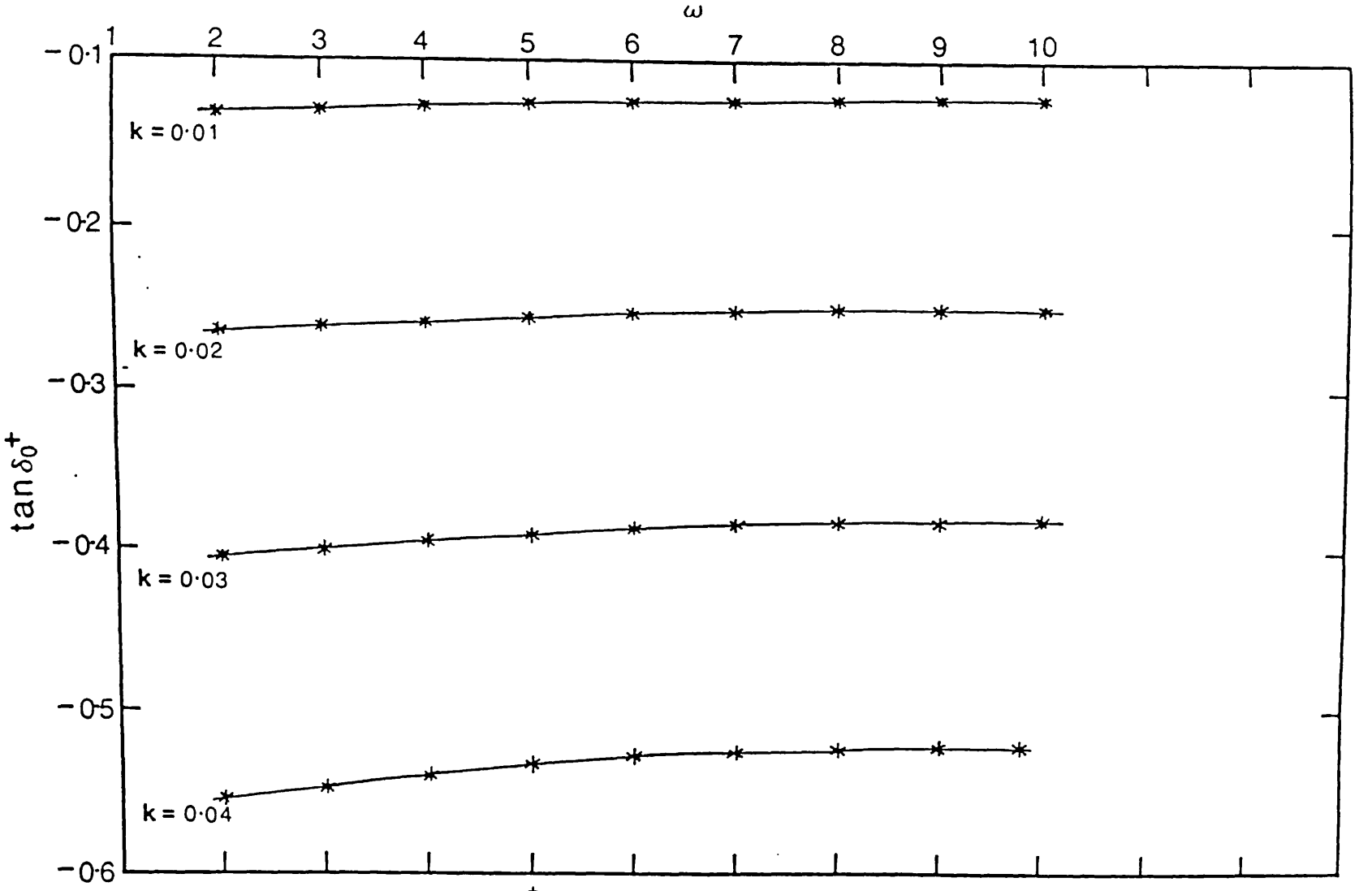

Fig. 3.6 Variation of $\tan\delta_o^+$ with ω for very low values of wave number k, $(0.01 \leq k(a_o^{-1}) \leq 0.04)$. x Kohn results + Inverse Kohn results

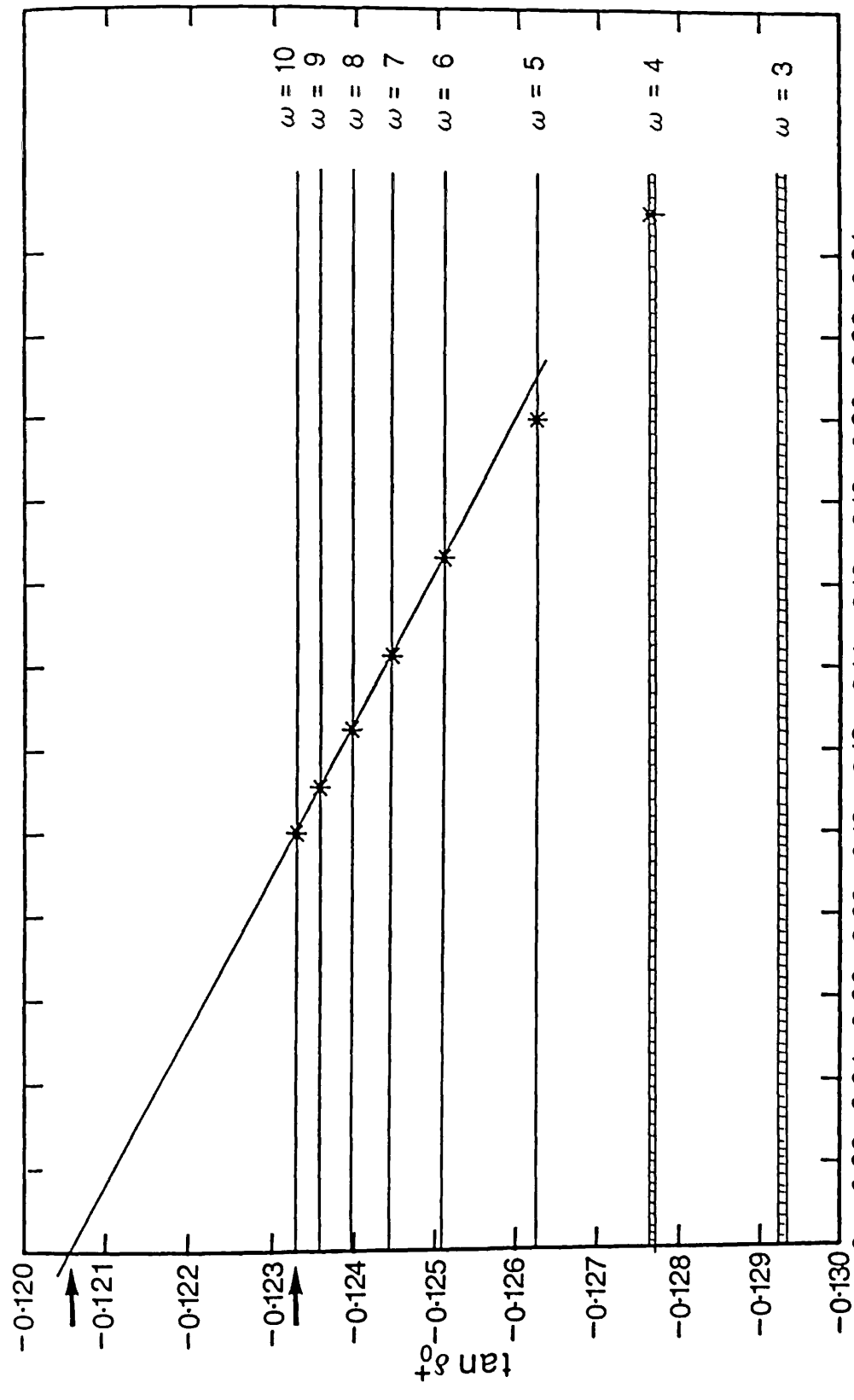

Fig. 3.7 Convergence of $\tan\delta_o^+$ with ω for $k = 0.01\ a_o^{-1}$ according to equation (3.59).

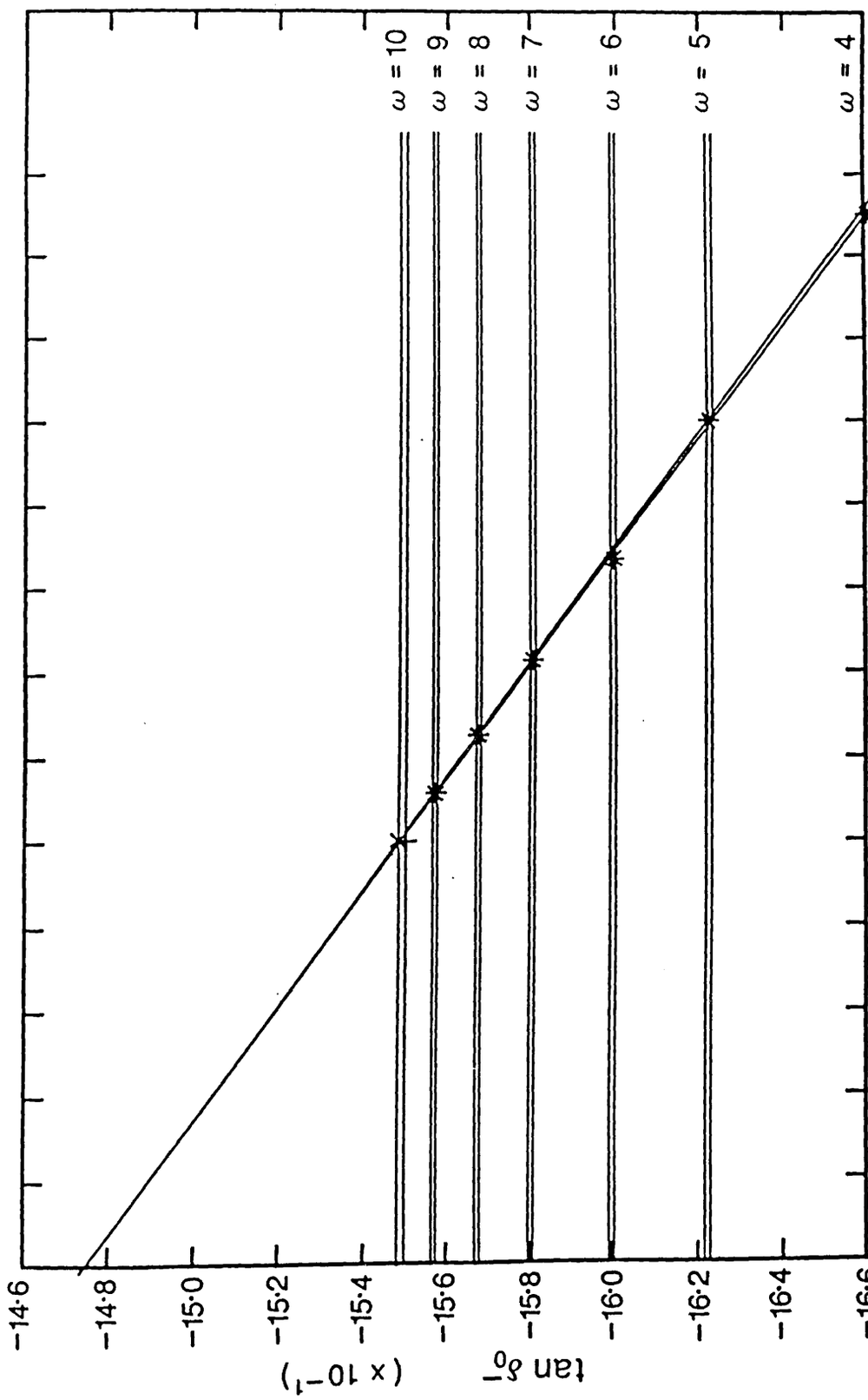

Fig. 3.8 Convergence of $\tan\delta_o^-$ with ω at $k = 0.03\ a_o^{-1}$ according to equation (3.59).

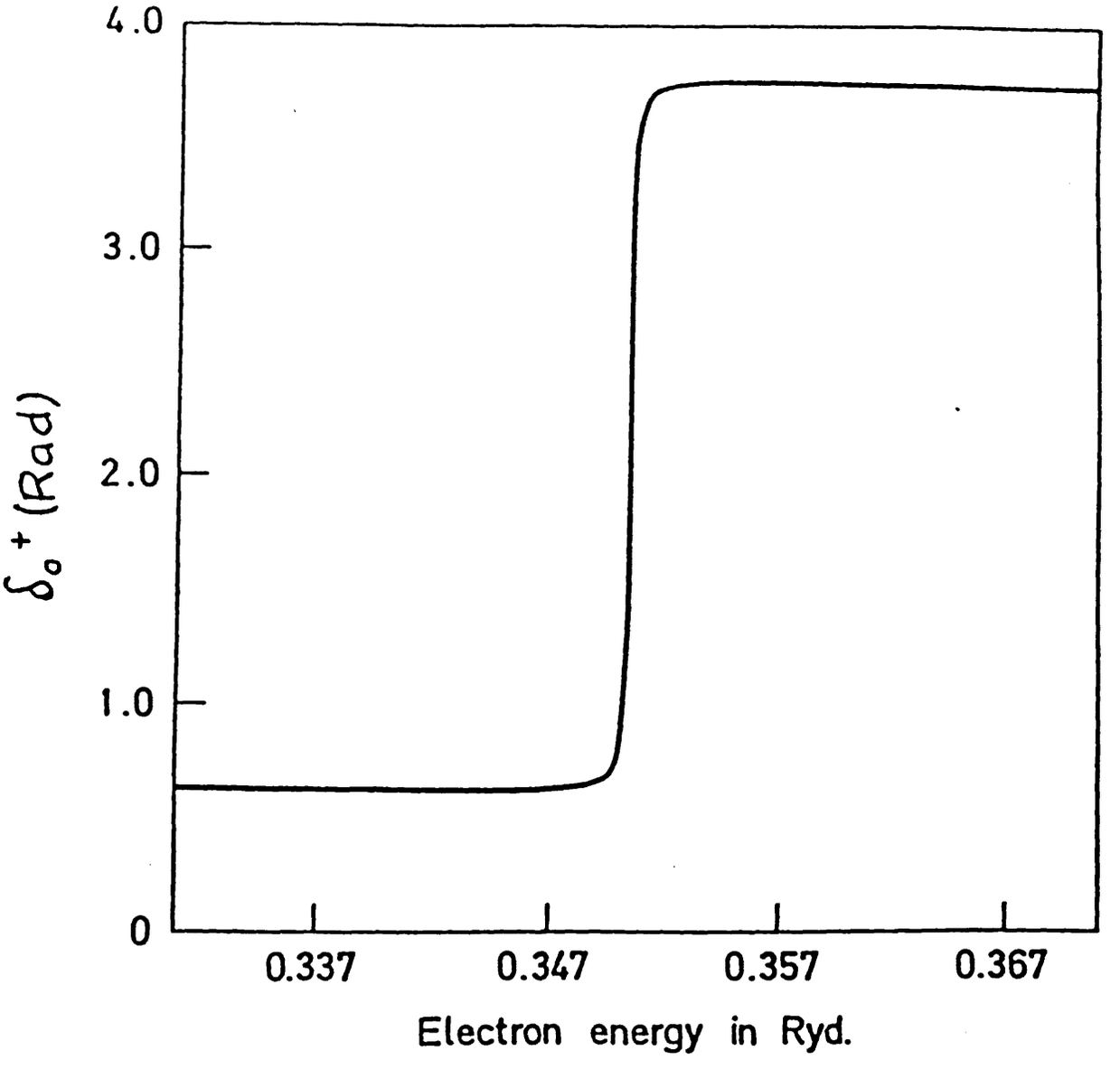

Fig. 3.9 The $^1S^e$ resonance determined by using 3 non-linear parameters in our s-wave scattering function.

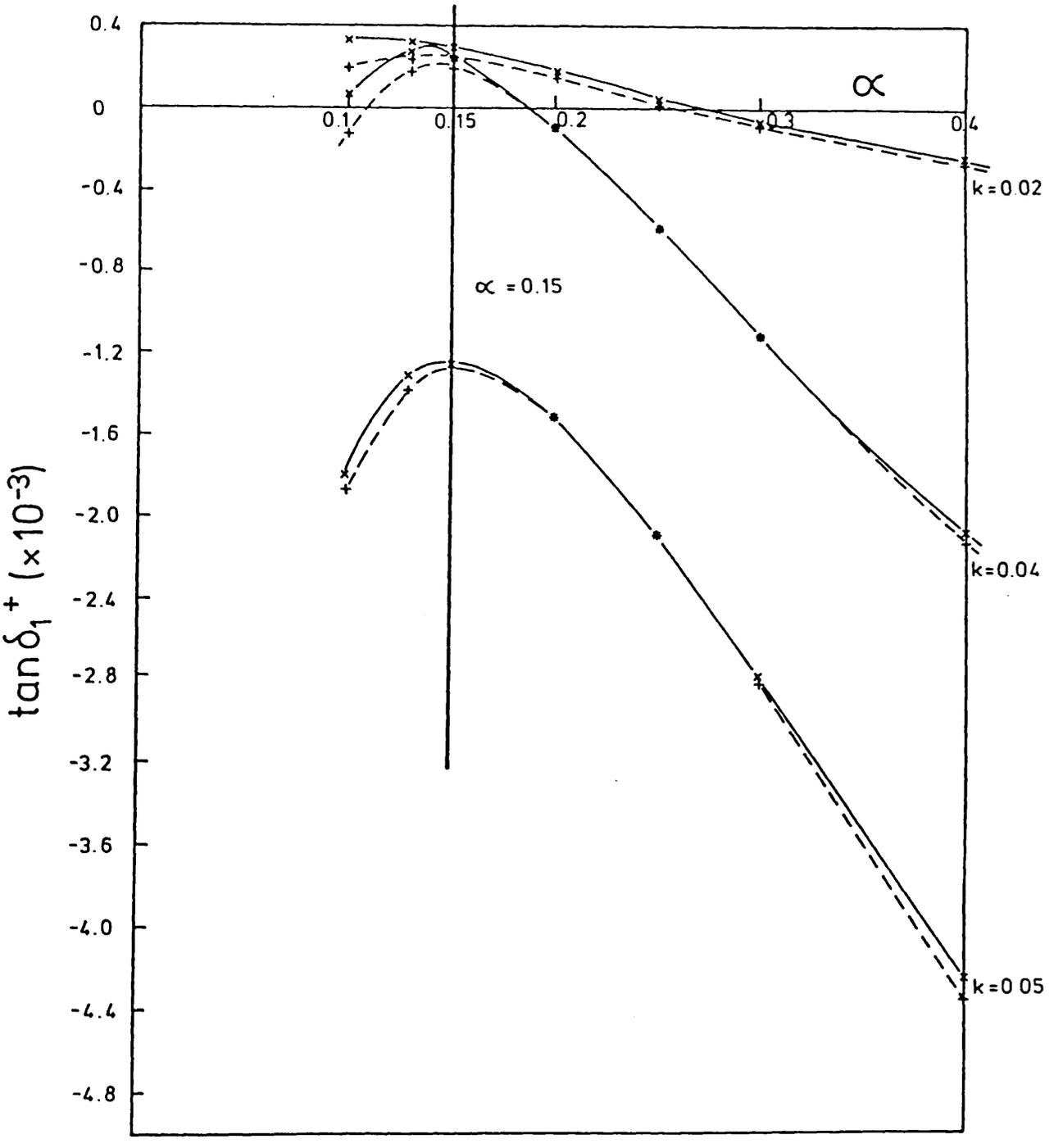

Fig. 4.1 Variation of $\tan\delta_1^+$ with non-linear parameter α but fixed $\gamma(= 0.05)$ and $\mu(=0.40)$ at k = 0.02, 0.04, 0.05 a_o^{-1}.

——————— Kohn results (x)

— — — — — Inverse Kohn results (+)

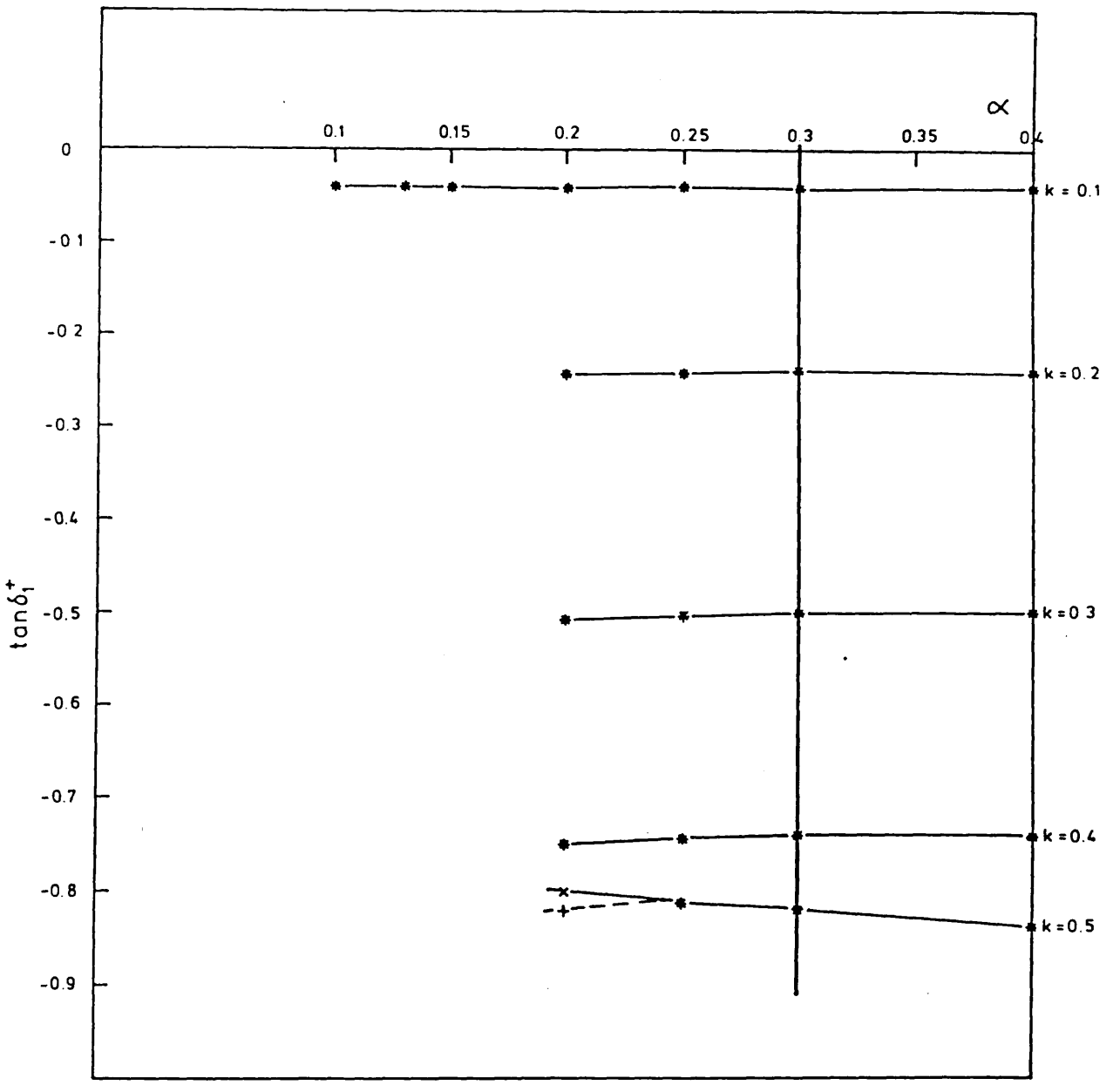

Fig. 4.2 Variation of $\tan \delta_1^+$ with non-linear parameter , but fixed γ(=0.05) and μ(=0.40) for the range $0.1<k(a_o^{-1})<0.5$

———— Kohn results (x)

— — — — Inverse Kohn results (+)

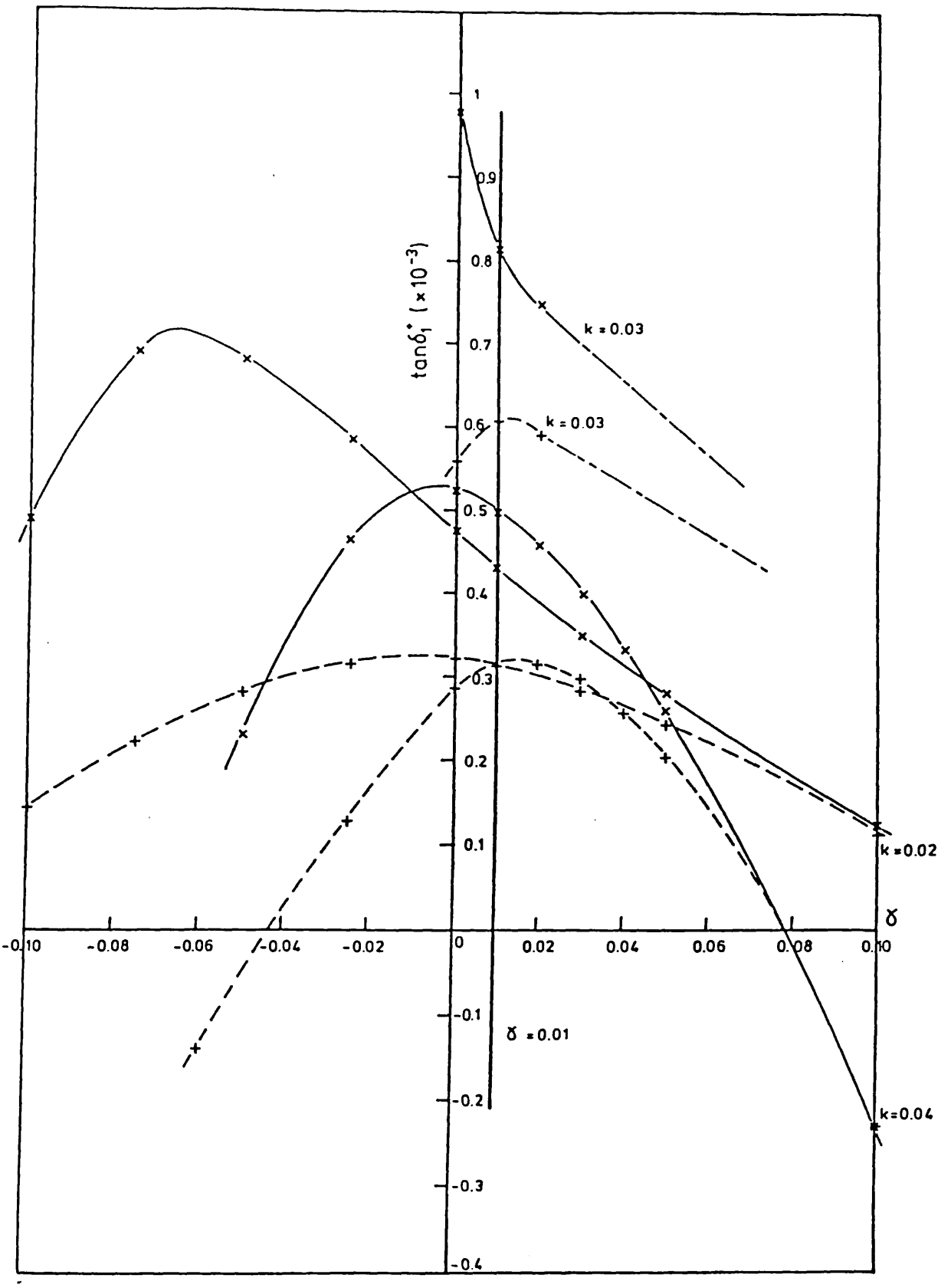

Fig. 4.3 Variation of $\tan\delta_1^+$ with non-linear parameter γ, but fixed α(=0.15) and μ(=0.40) at k = 0.02, 0.03, 0.04 a_o^{-1}.

———— Kohn results (x)

— — — — Inverse Kohn results (+)

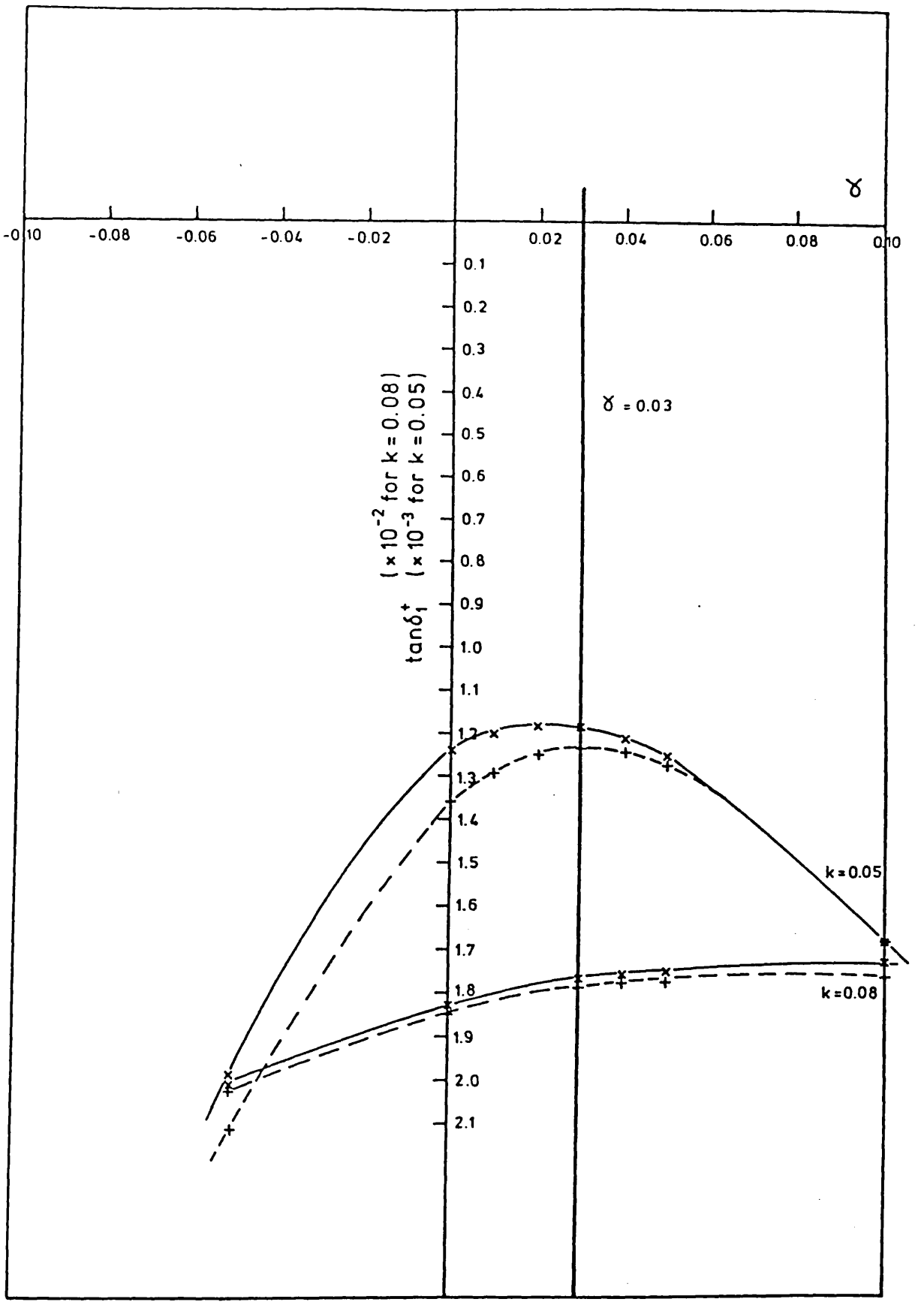

Fig. 4.4 Variation of $\tan\delta_1^+$ with non-linear parameter γ, but fixed α(=0.15) and μ(=0.40) at k = 0.05, 0.08 a_o^{-1}.

———— Kohn results (x)

— — — — Inverse Kohn results (+)

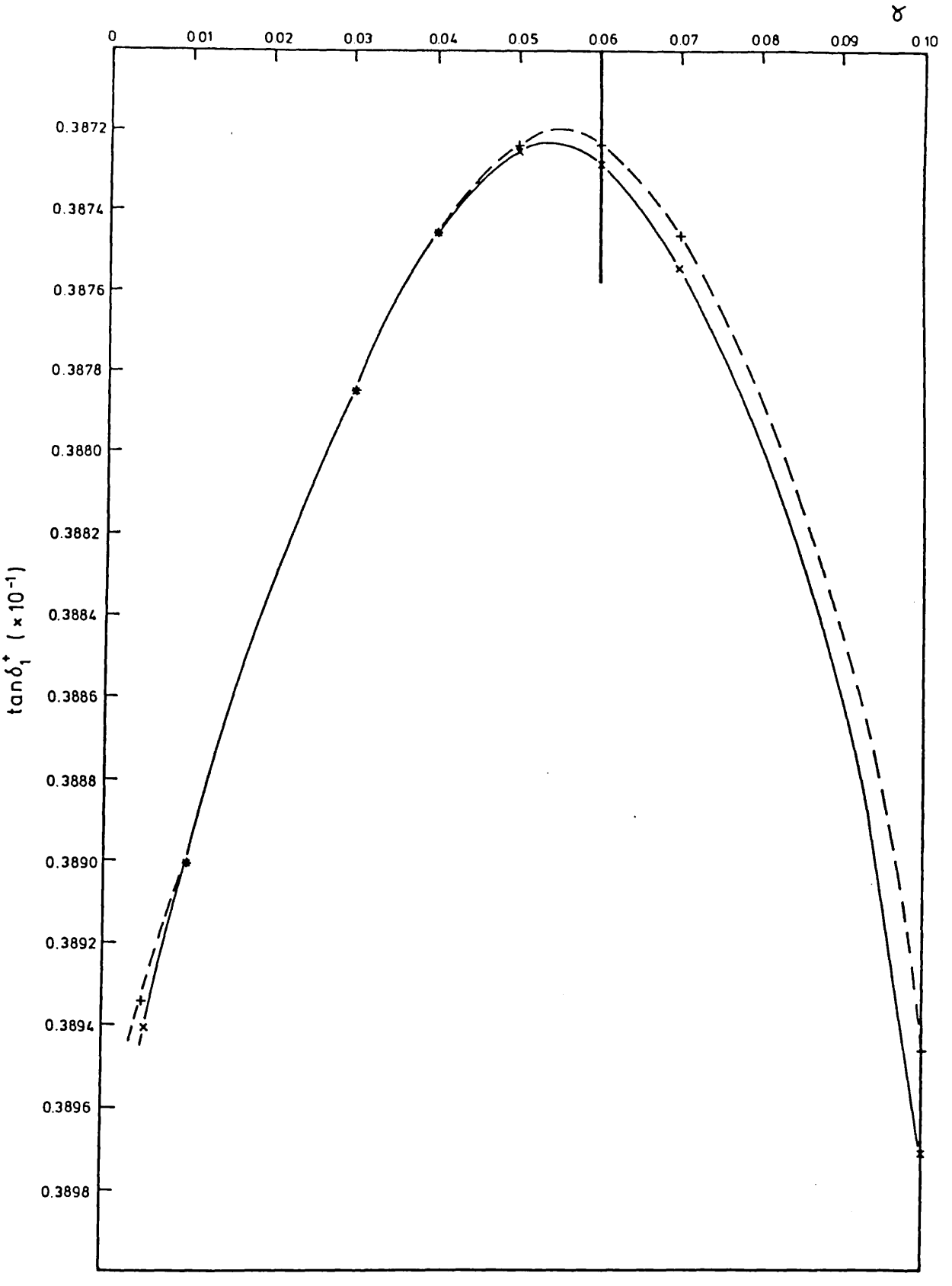

Fig. 4.5 Variation of $\tan\delta_1^+$ with non-linear parameter γ, but fixed α(=0.30) and μ(=0.40), at k = 0.10 a_o^{-1}.

——————Kohn results (x)

— — — —Inverse Kohn results (+)

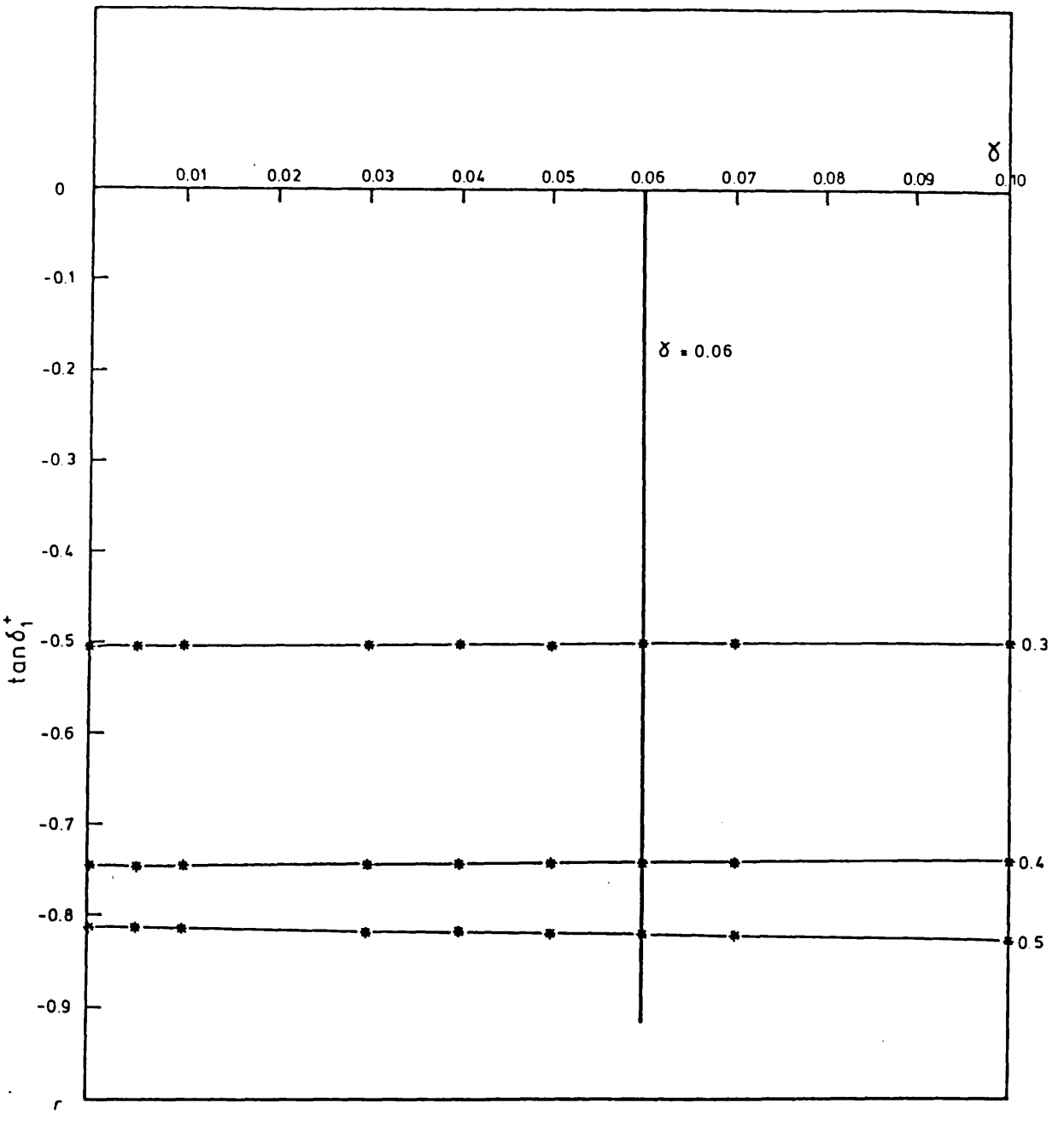

Fig. 4.6 Variation of $\tan\delta_1^+$ with non-linear parameter γ, but fixed α(=0.30) and μ(=0.40) for the range $0.3 \leqslant k(a_o^{-1}) \leqslant 0.5$.

———— Kohn results (x)

— — — — Inverse Kohn results (+)

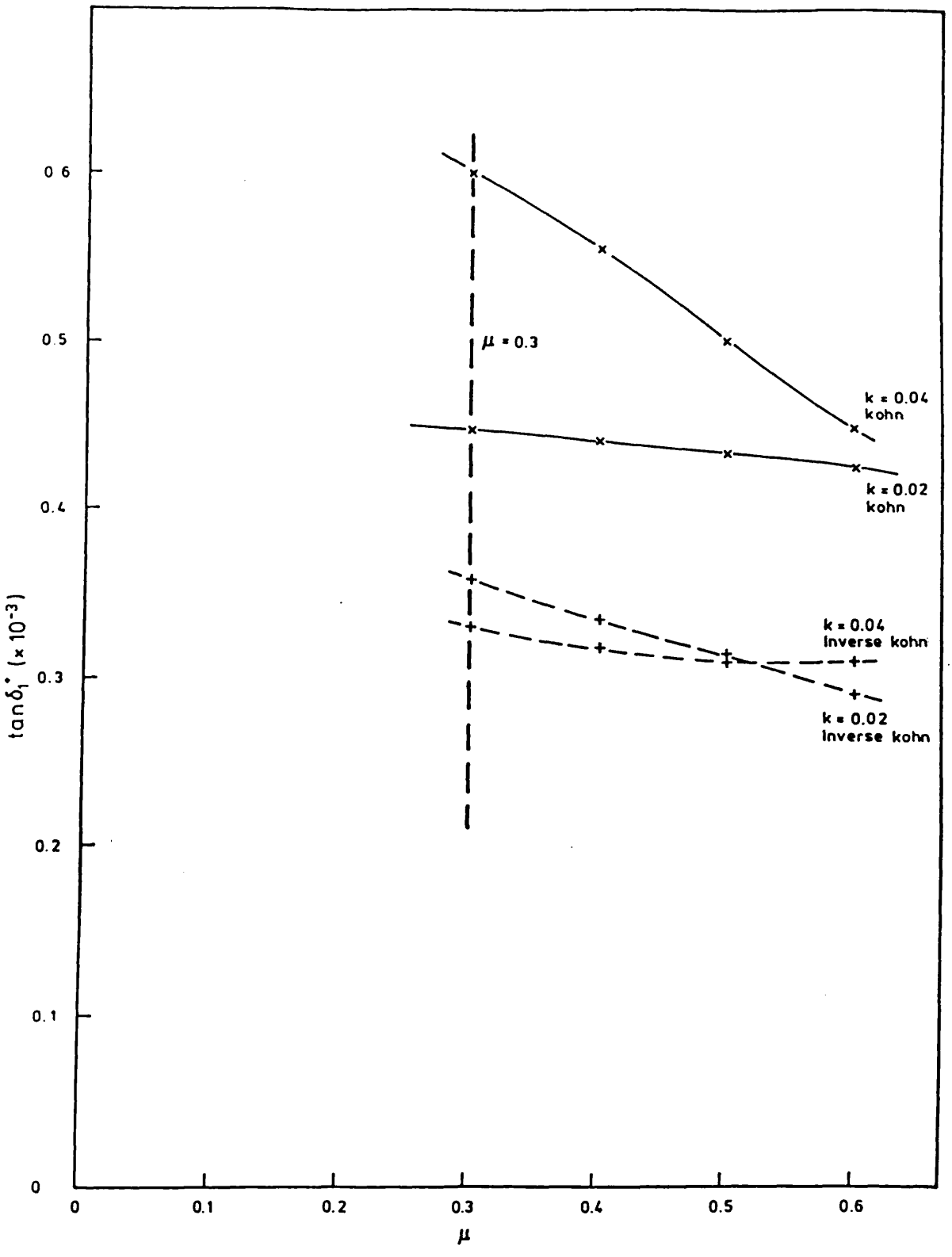

Fig. 4.7 Variation of $\tan\delta_1^+$ with non-linear parameter μ, but fixed α(=0.15) and γ(=0.01), for low values of (k = 0.02, 0.04 a_o^{-1})

———— Kohn results (x)

— — — — Inverse Kohn results (+)

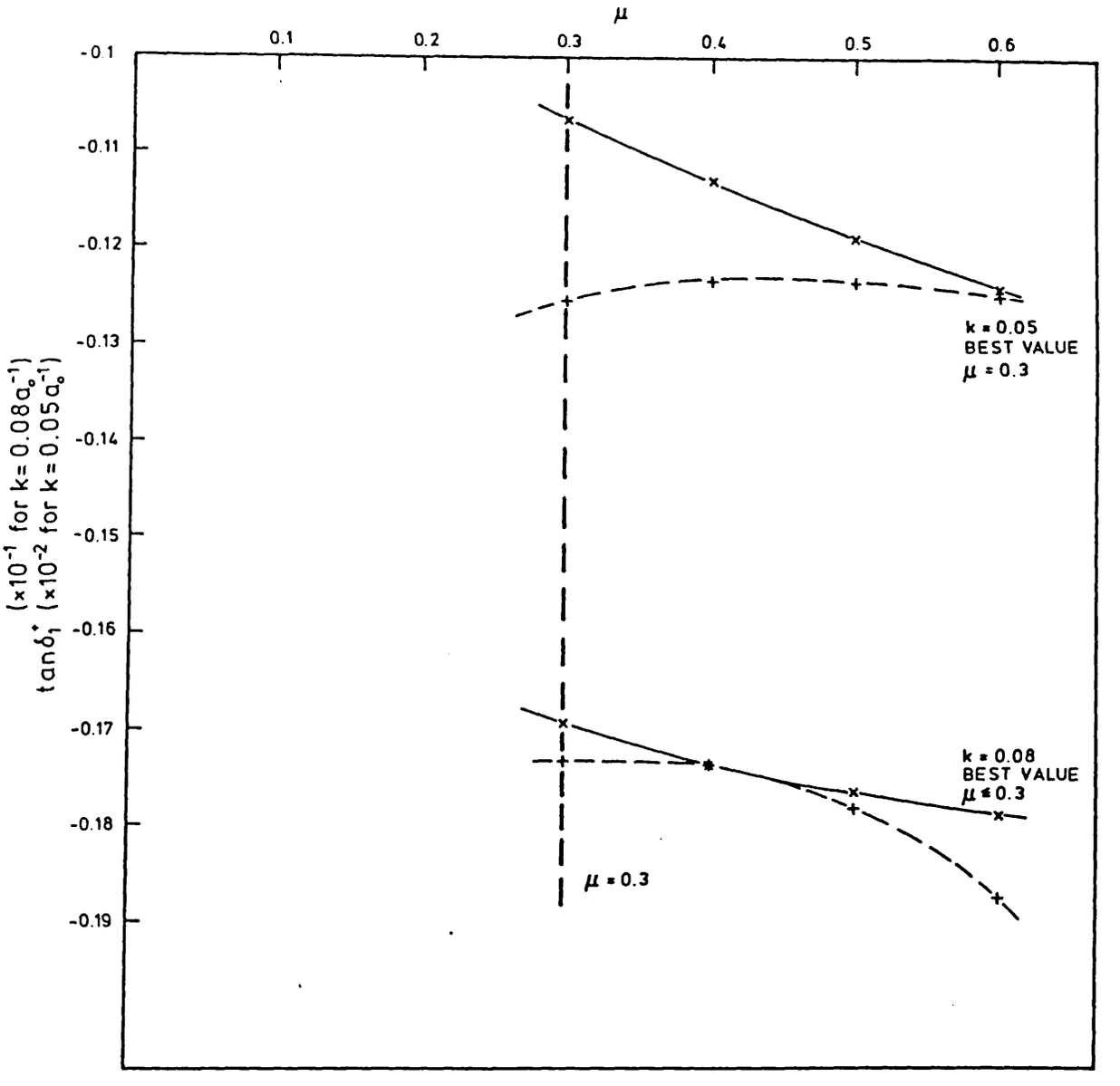

Fig. 4.8 Variation of $\tan\delta_1^+$ with non-linear parameter μ, but fixed α(=0.15) and γ(=0.03) at k = 0.05, 0.08 a_o^{-1}.

———— Kohn results (x)

— — — — Inverse Kohn results (+)

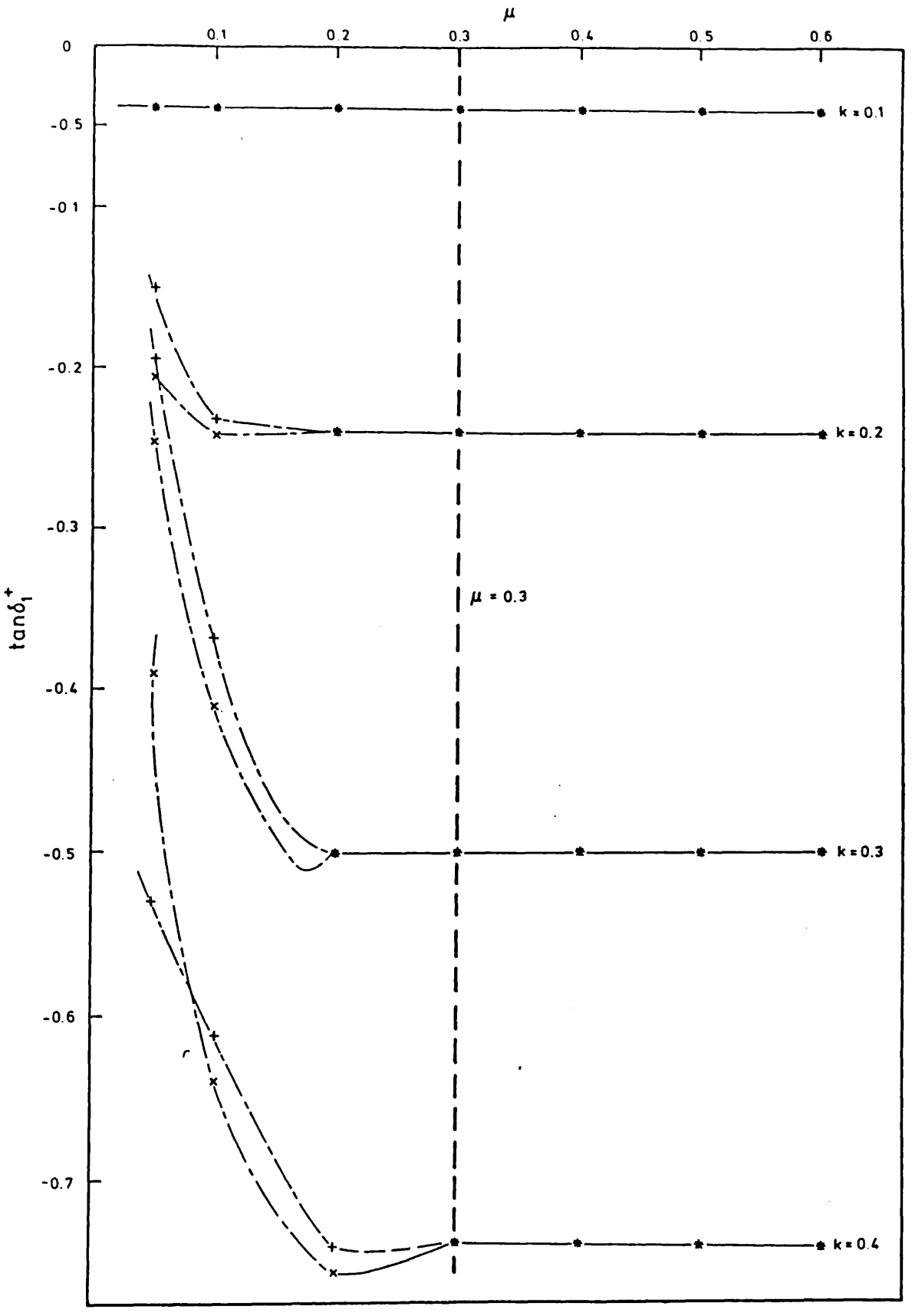

Fig. 4.9 Variation of $\tan\delta_1^+$ with non-linear parameter μ, but fixed α(=0.30) and γ(=0.06) for the range $0.1 \leqslant k(a_o^{-1}) \leqslant 0.5$.

———— Kohn results (x)

— — — — Inverse Kohn results (+)

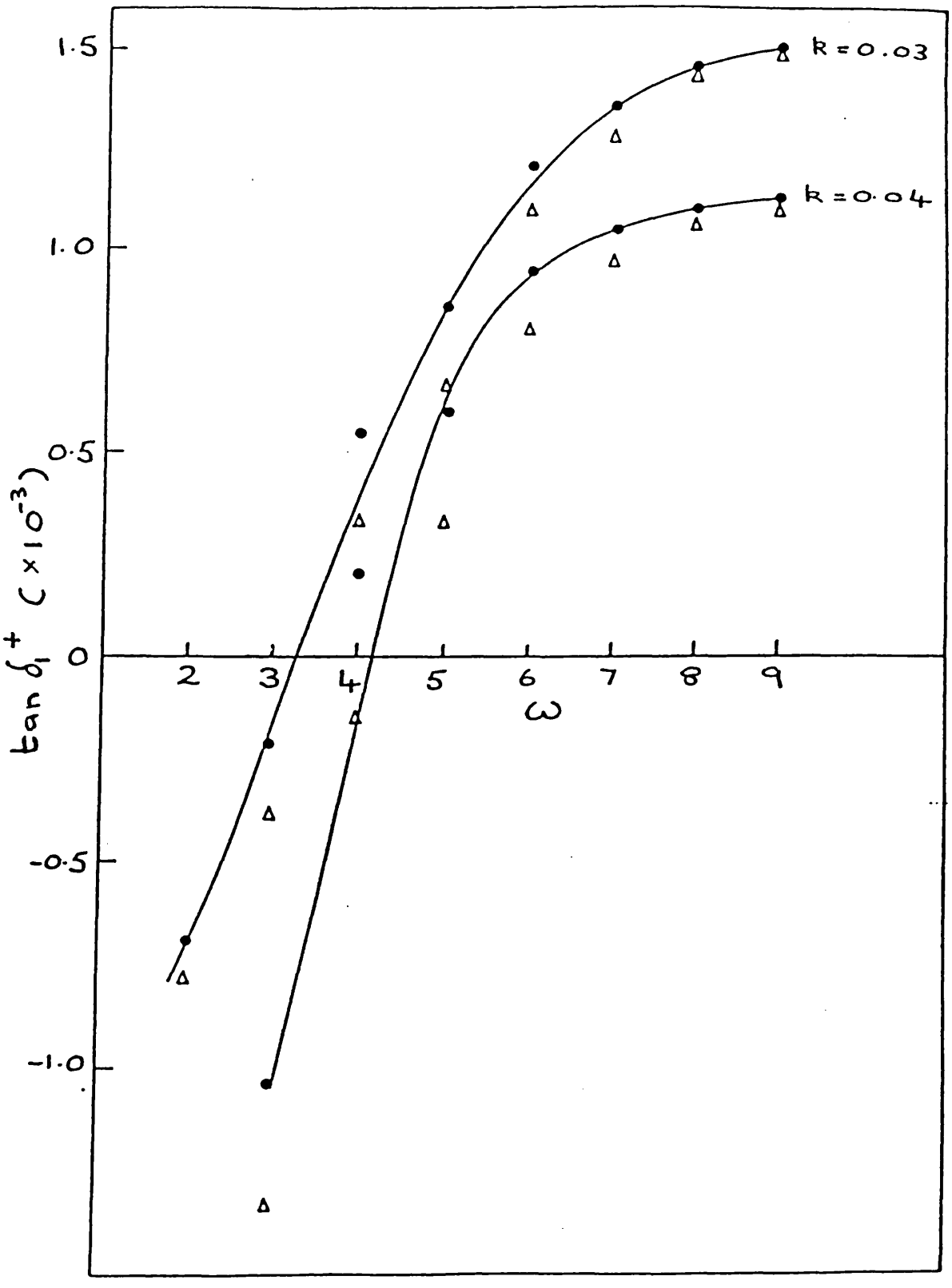

Fig. 4.10 Convergence of tan δ_1^+ as a function of ω at k = 0.03, 0.04 a_o^{-1}.
(The circles represent the Kohn and the triangles the inverse Kohn results.)

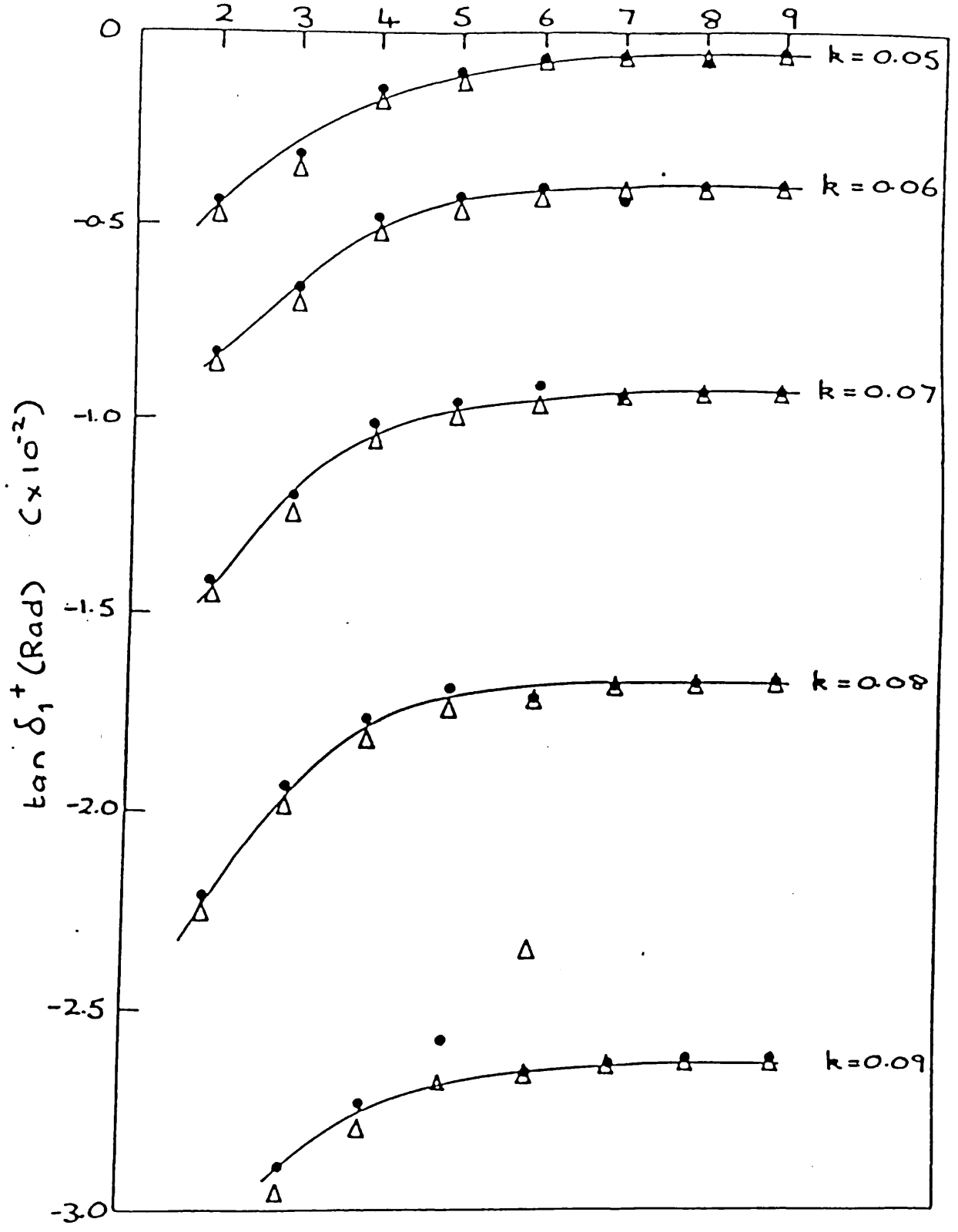

Fig. 4.11 Convergence of tan δ_1^+ as a function of ω for the range $0.05 \leq k\, a_o^{-1}) < 0.1$.
(The circles represent the Kohn and the triangles the Inverse Kohn results.)

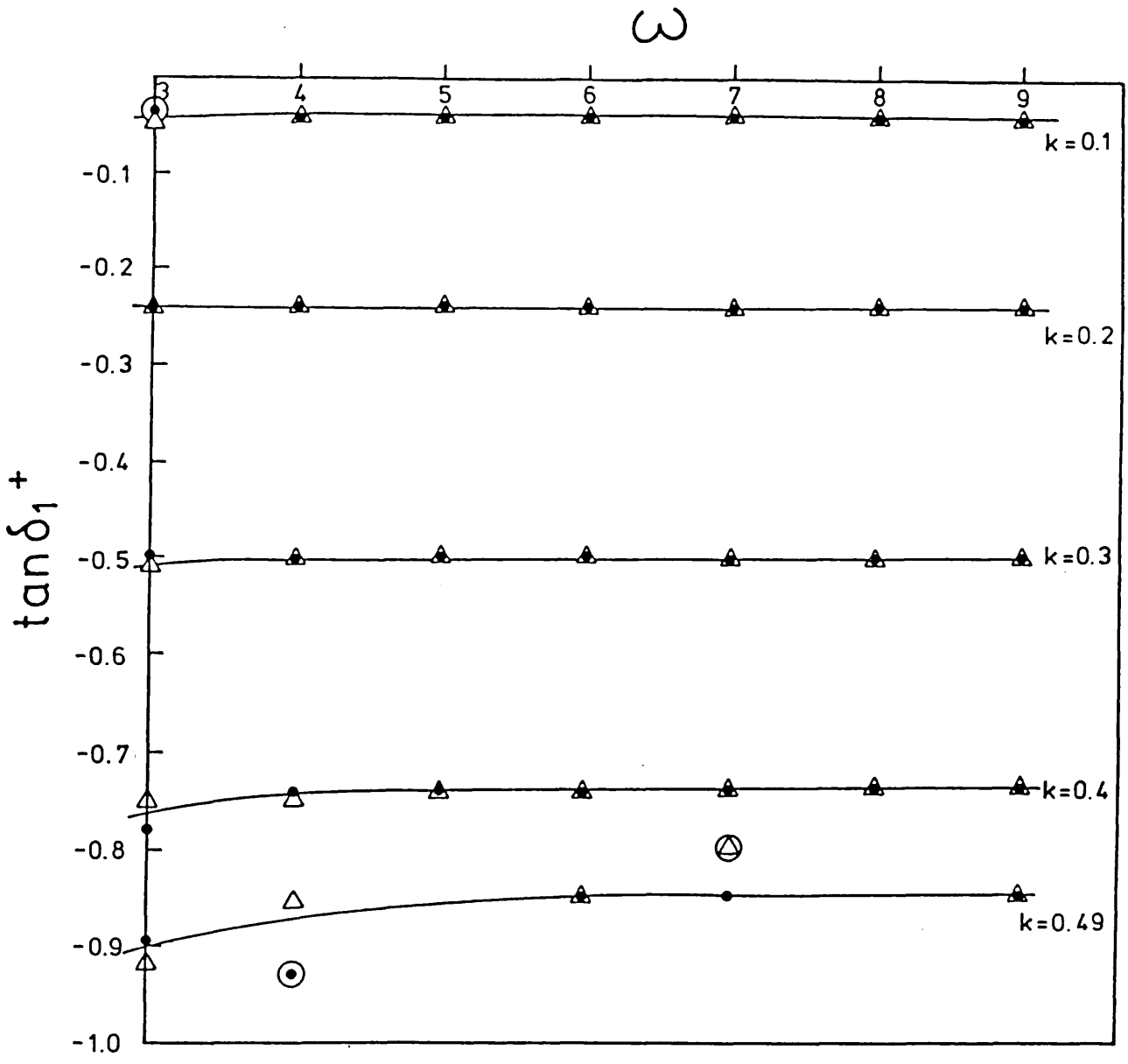

Fig. 4.12 Convergence of $\tan\delta_1^+$ as a function of ω for the range $0.1 \leq k(a_o^{-1}) < 0.5$. Kohn results (●) Inverse Kohn results (Δ).

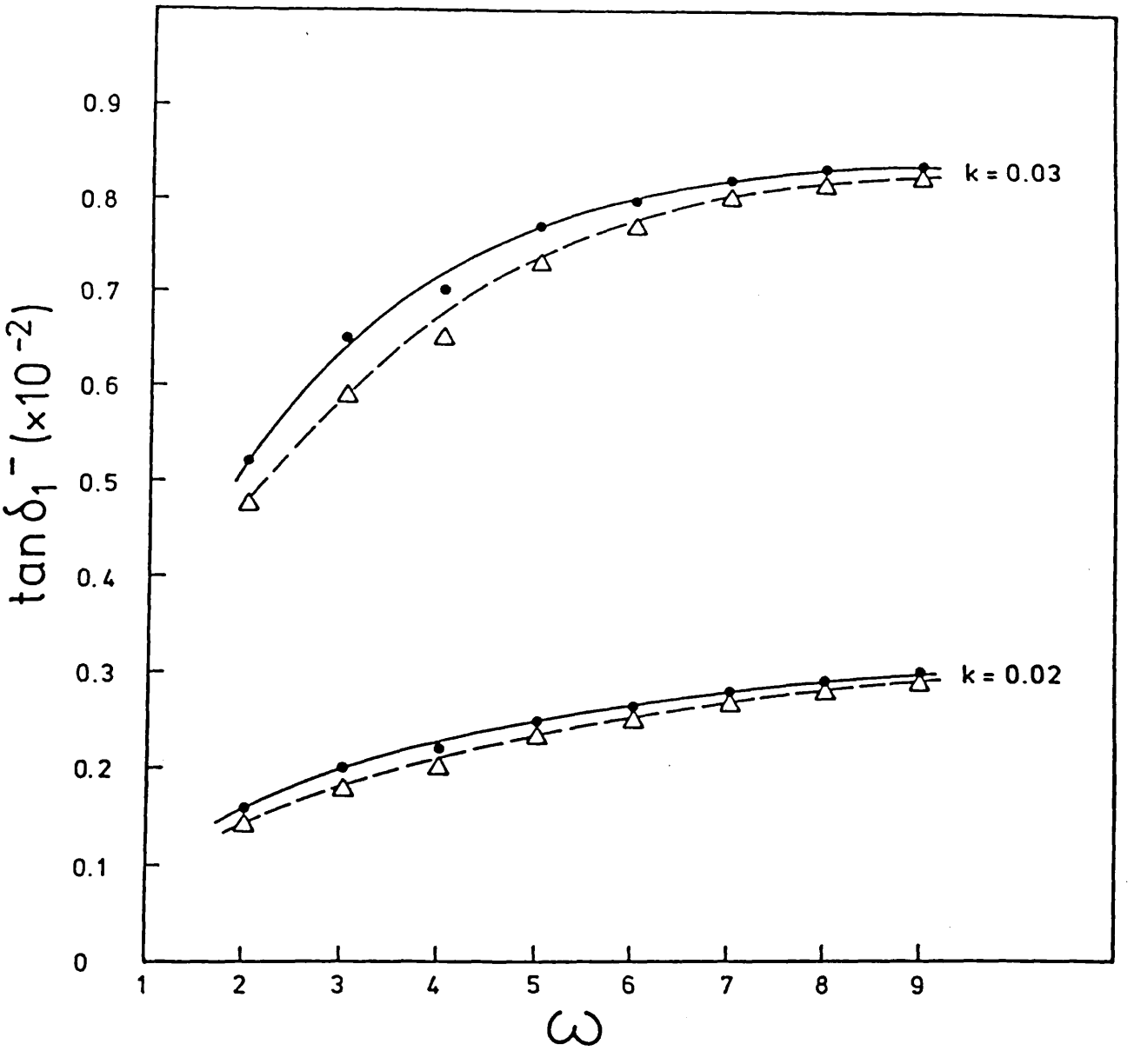

Fig. 4.13 Convergence of $\tan\delta_1^-$ as a function of ω at $k = 0.02, 0.03\ a_o^{-1}$.

——— Kohn results (●)

— — — Inverse Kohn results (Δ)

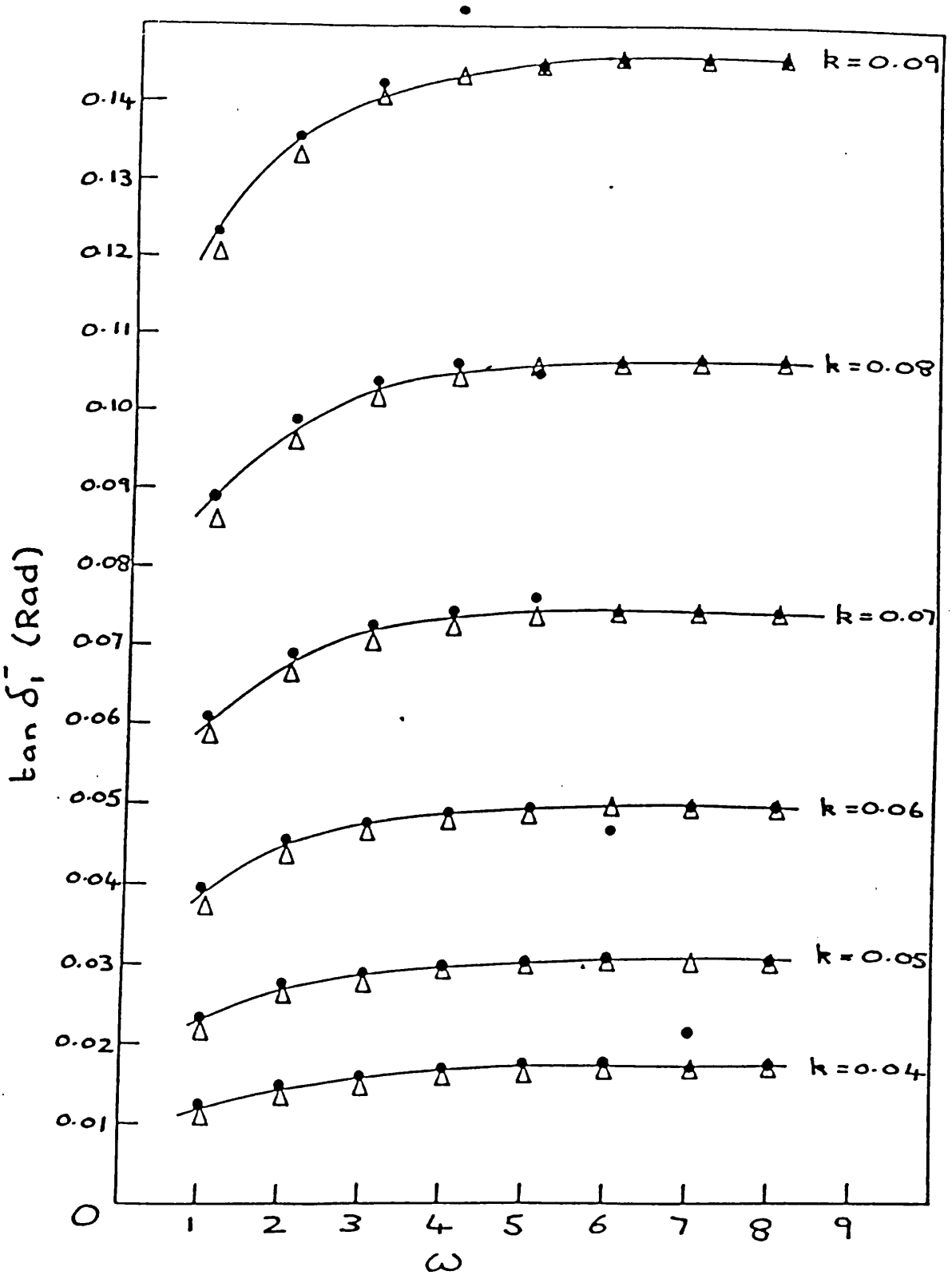

Fig. 4.14 Convergence of $\tan \delta_1^-$ as a function of ω for the range $0.04 \leq k(a_o^{-1}) < 0.1$.
(The circles represent the Kohn and the triangles the Inverse Kohn results.)

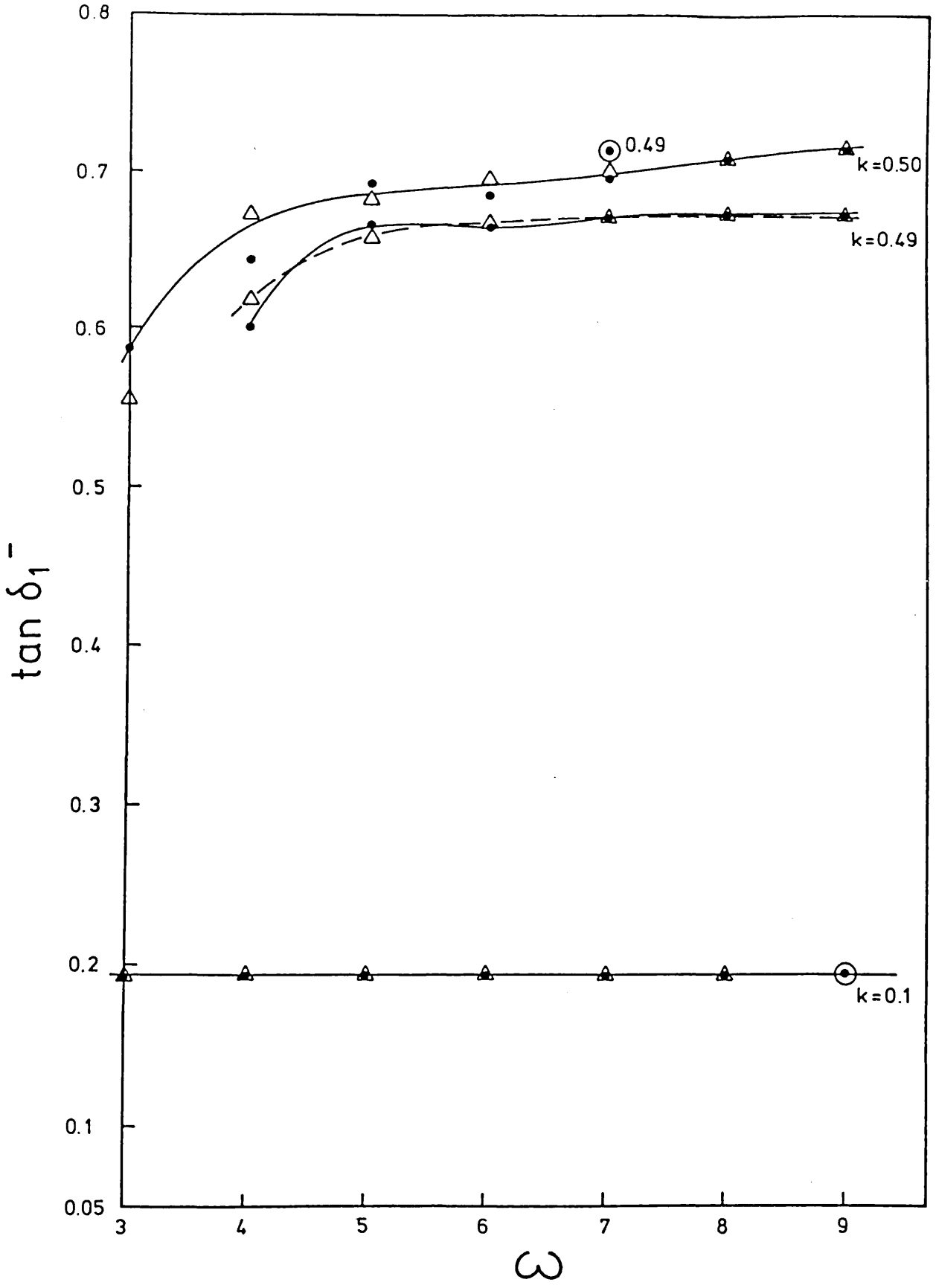

Fig. 4.15 Convergence of $\tan\delta_1^-$ as a function of ω at $k = 0.10, 0.49, 0.50\ a_o^{-1}$.

——————— Kohn results (●)

— — — — Inverse Kohn results (Δ)

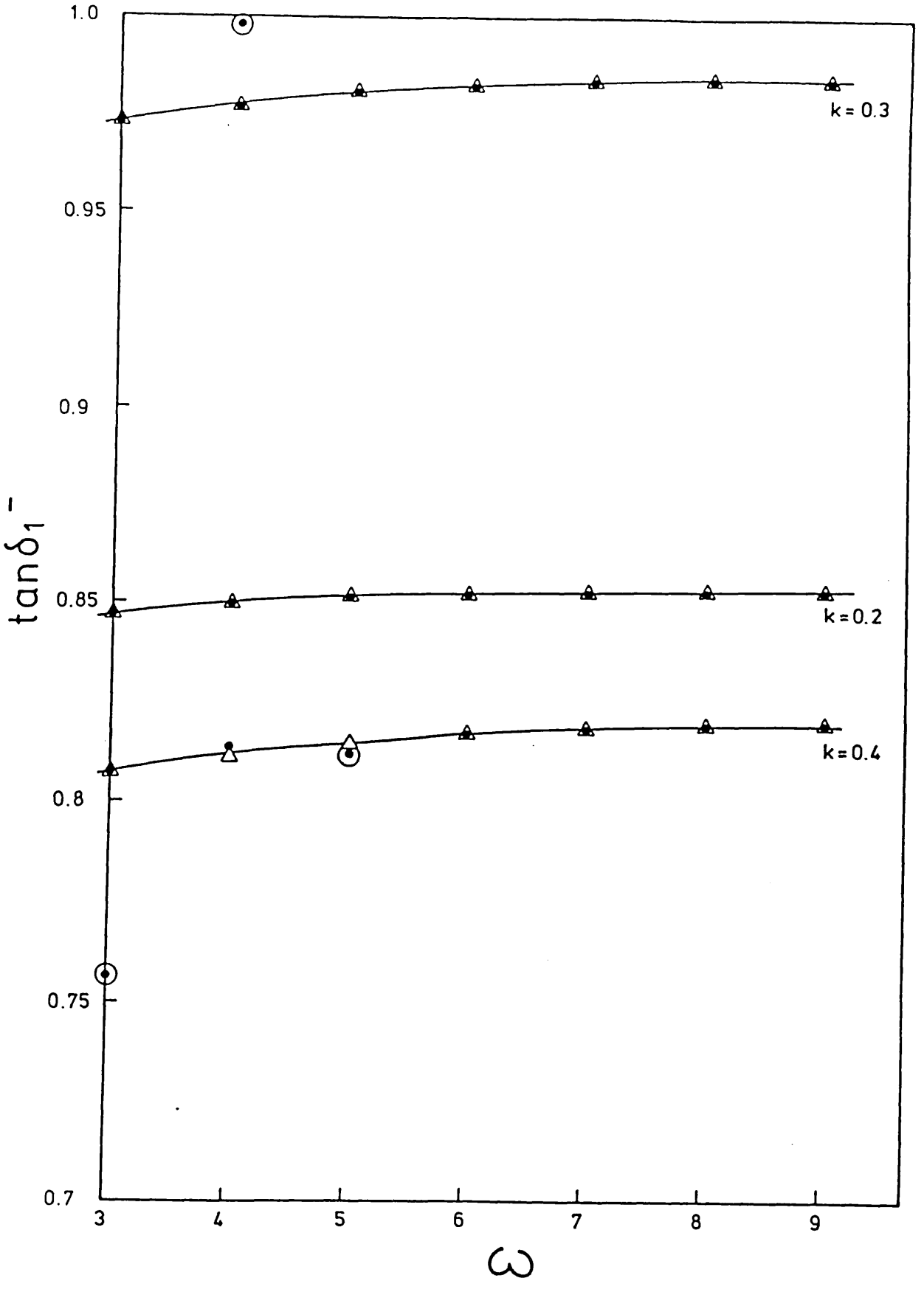

Fig. 4.16 Convergence of $\tan\delta_1^-$ as a function of ω at k = 0.2, 0.3, 0.4 a_o^{-1}.

——— Kohn results (●)

— — — — Inverse Kohn results (Δ)

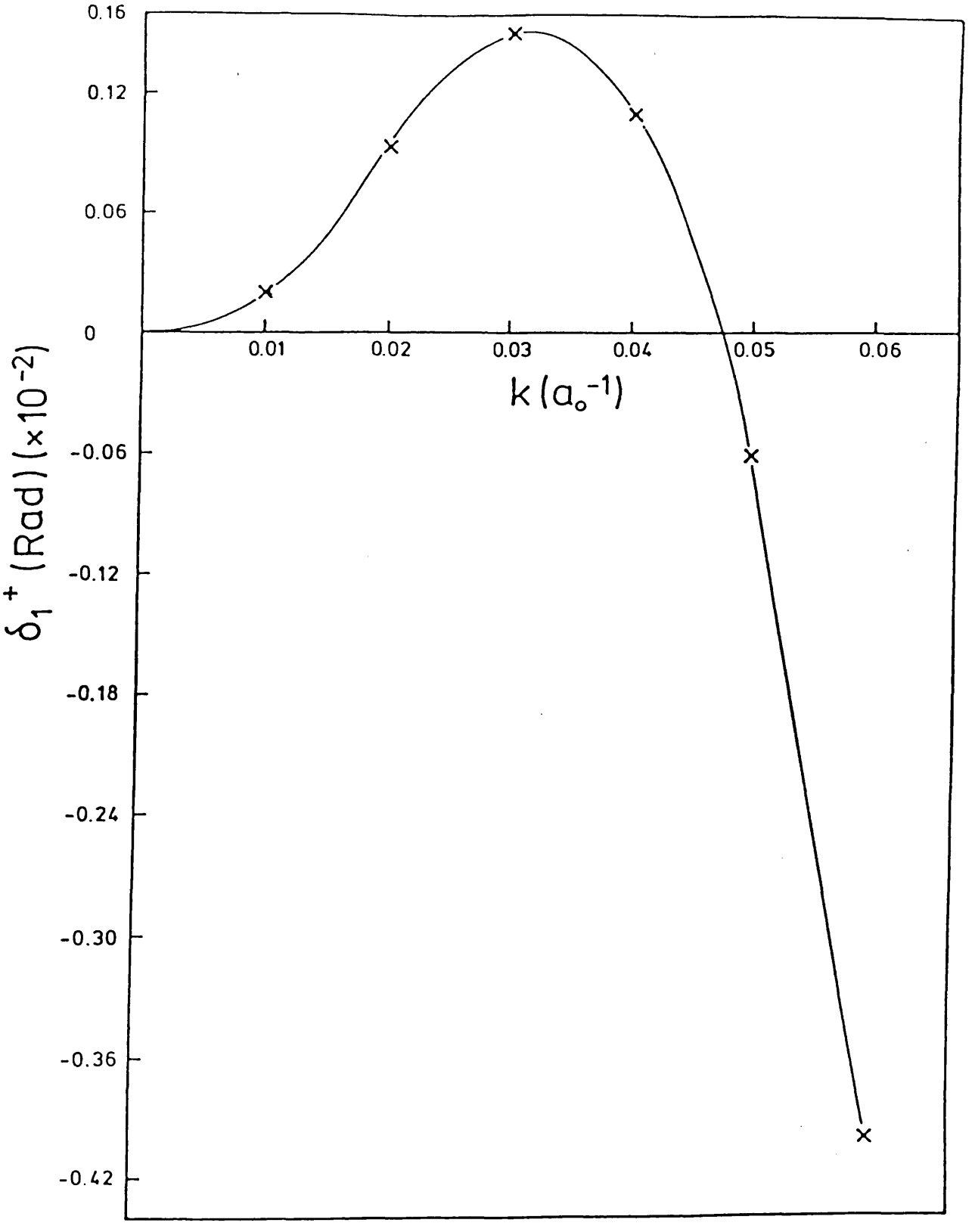

Fig. 4.17 Very low energy ^1P phase shifts as a function of k.

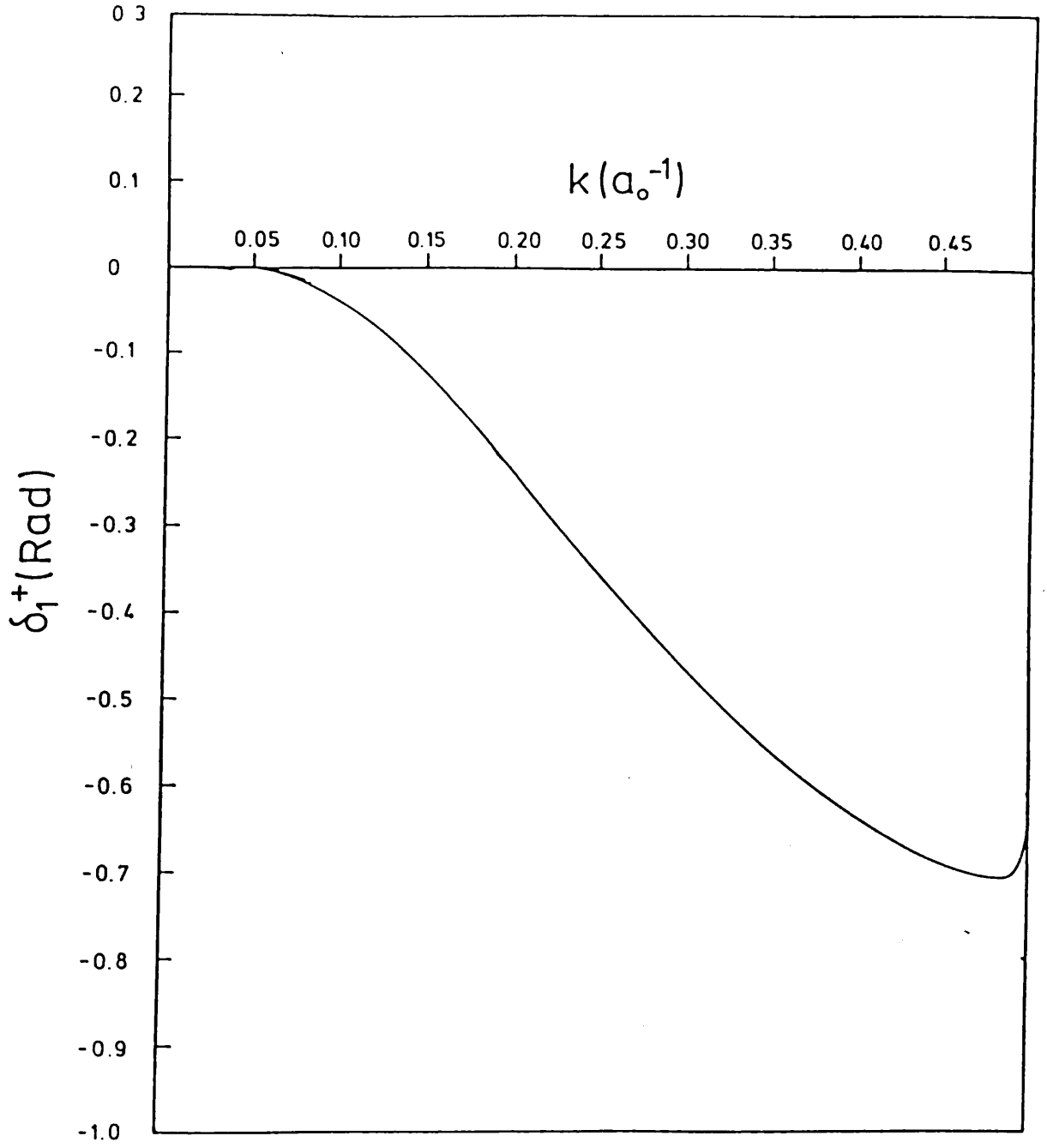

Fig. 4.18 ^1P phase shifts as a function of k.

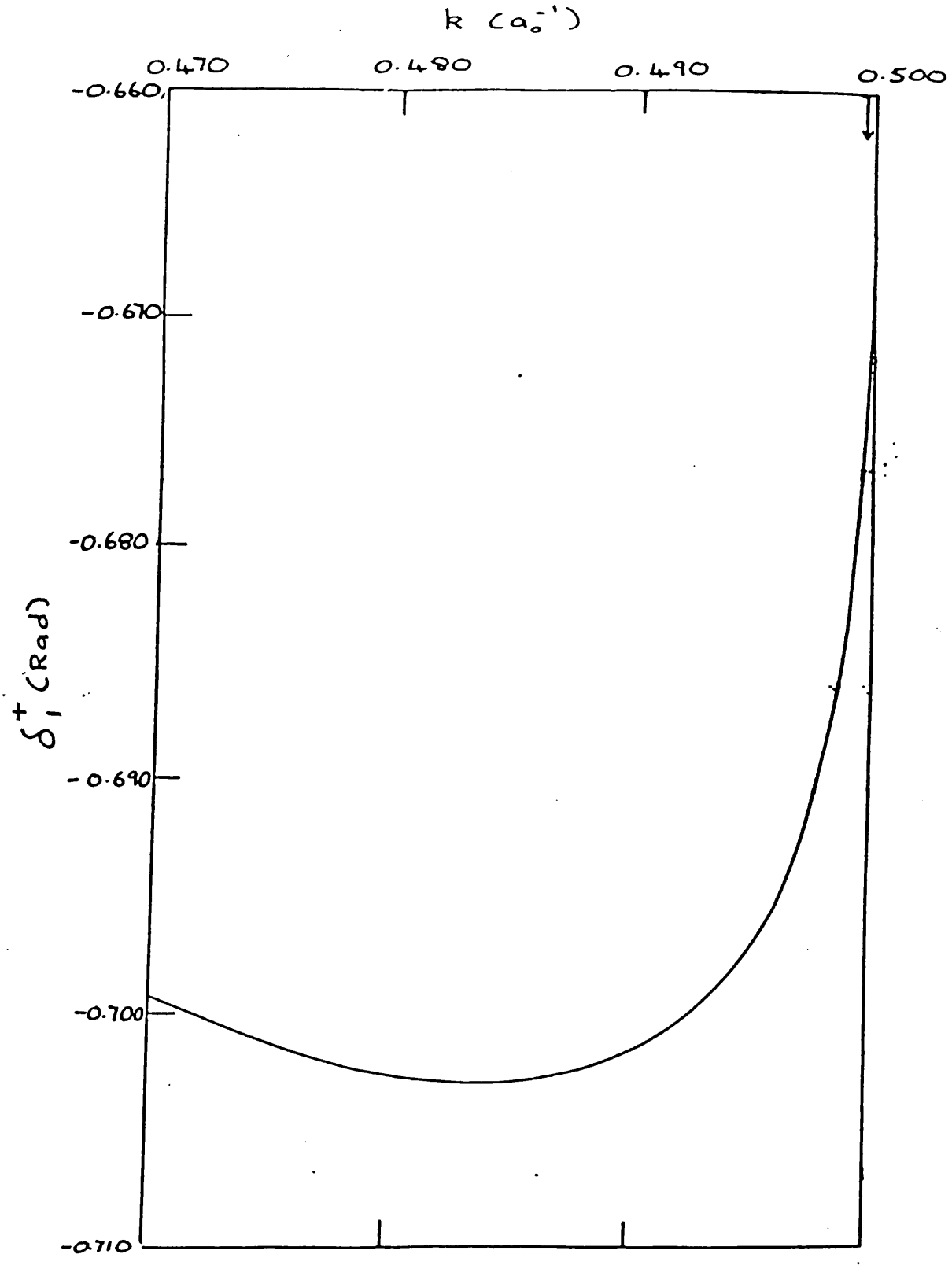

Fig. 4.19 The ^1P phase shift near the n = 2 threshold. (The position of a resonance is indicated by an arrow.)

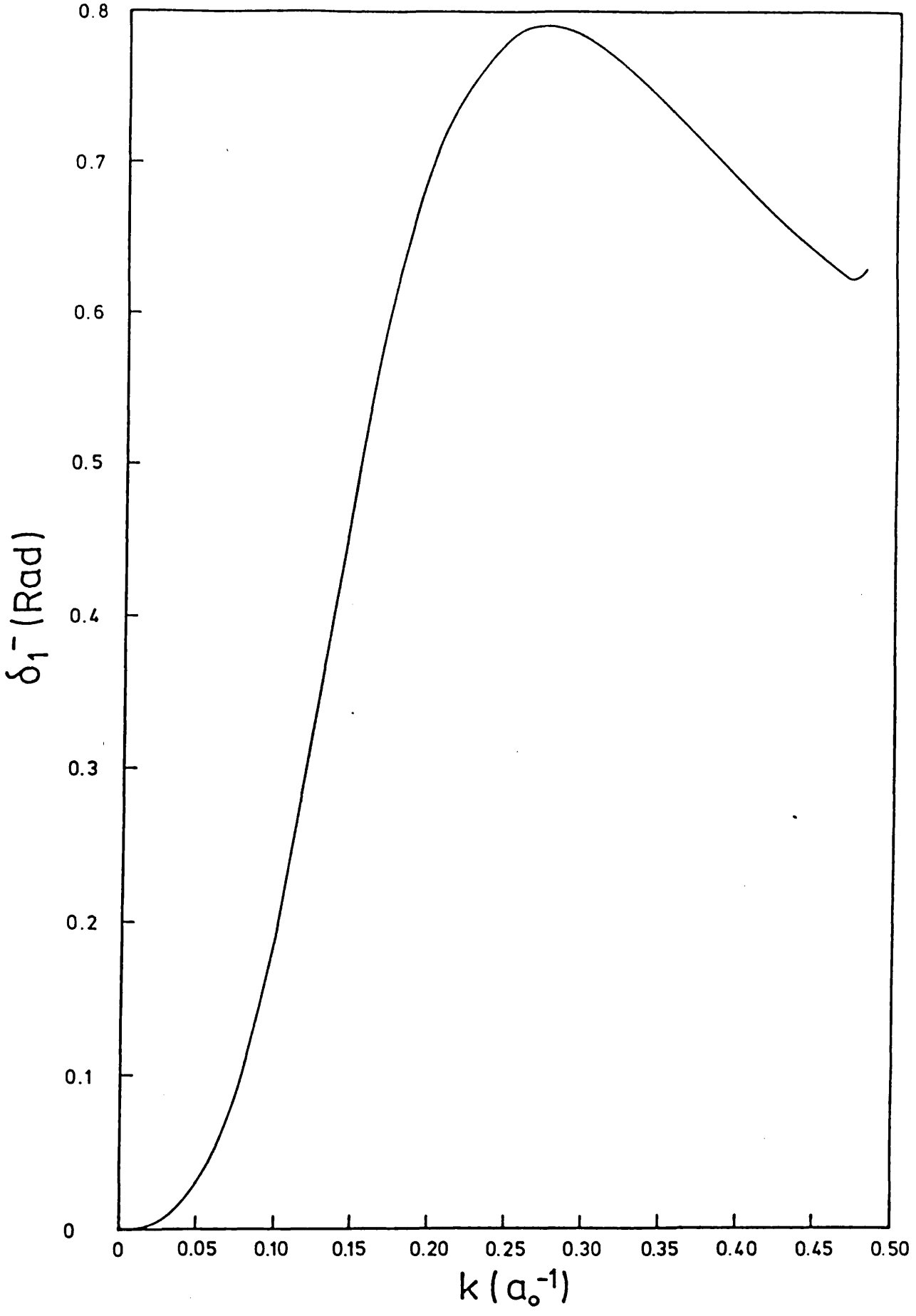

Fig. 4.20 ^3P phase shifts as a function of k.

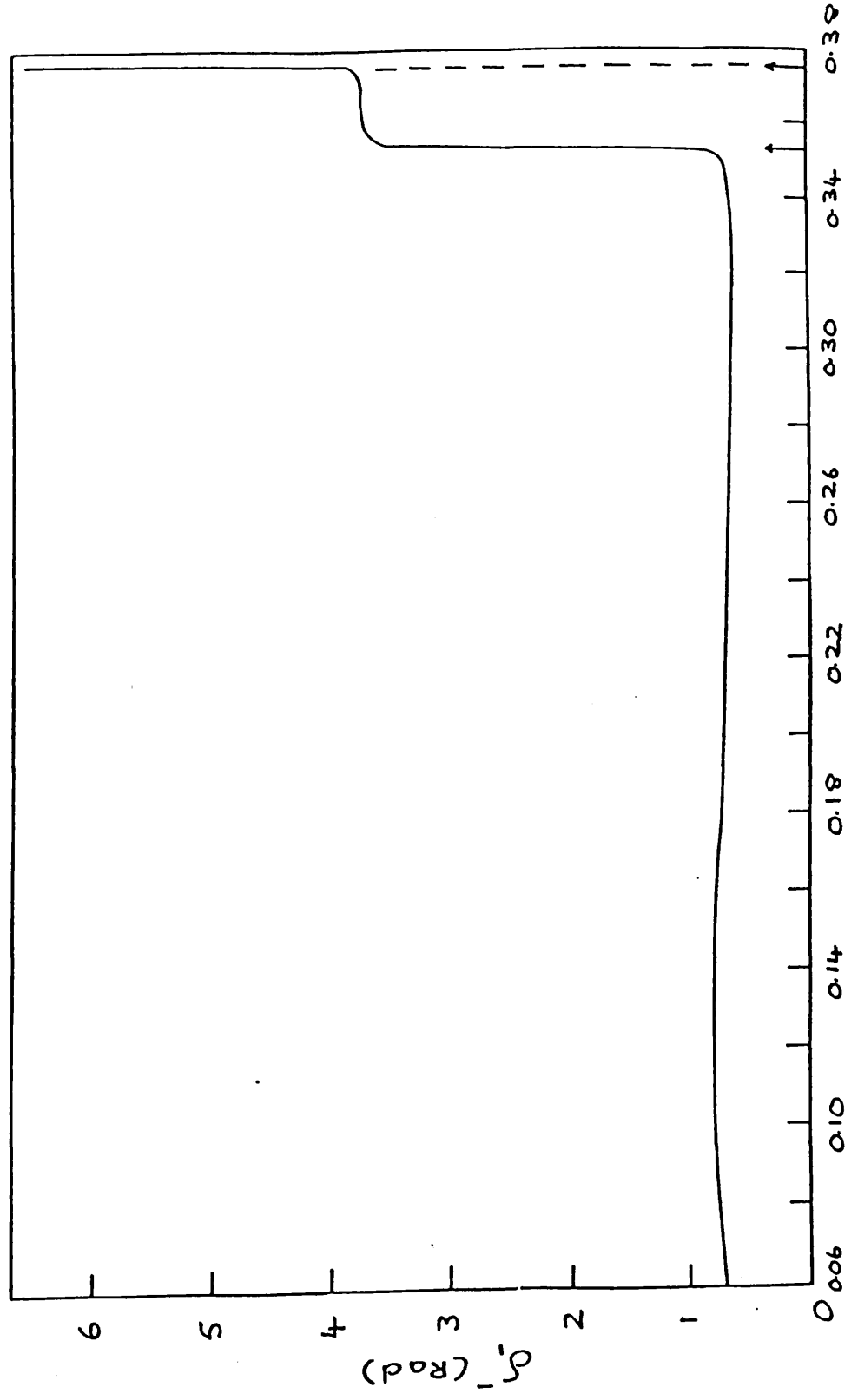

Fig. 4.21 The ^3P resonances below the n = 2 threshold, which are indicated by the arrows. The position of the n = 2 threshold is shown by the vertical dotted line.

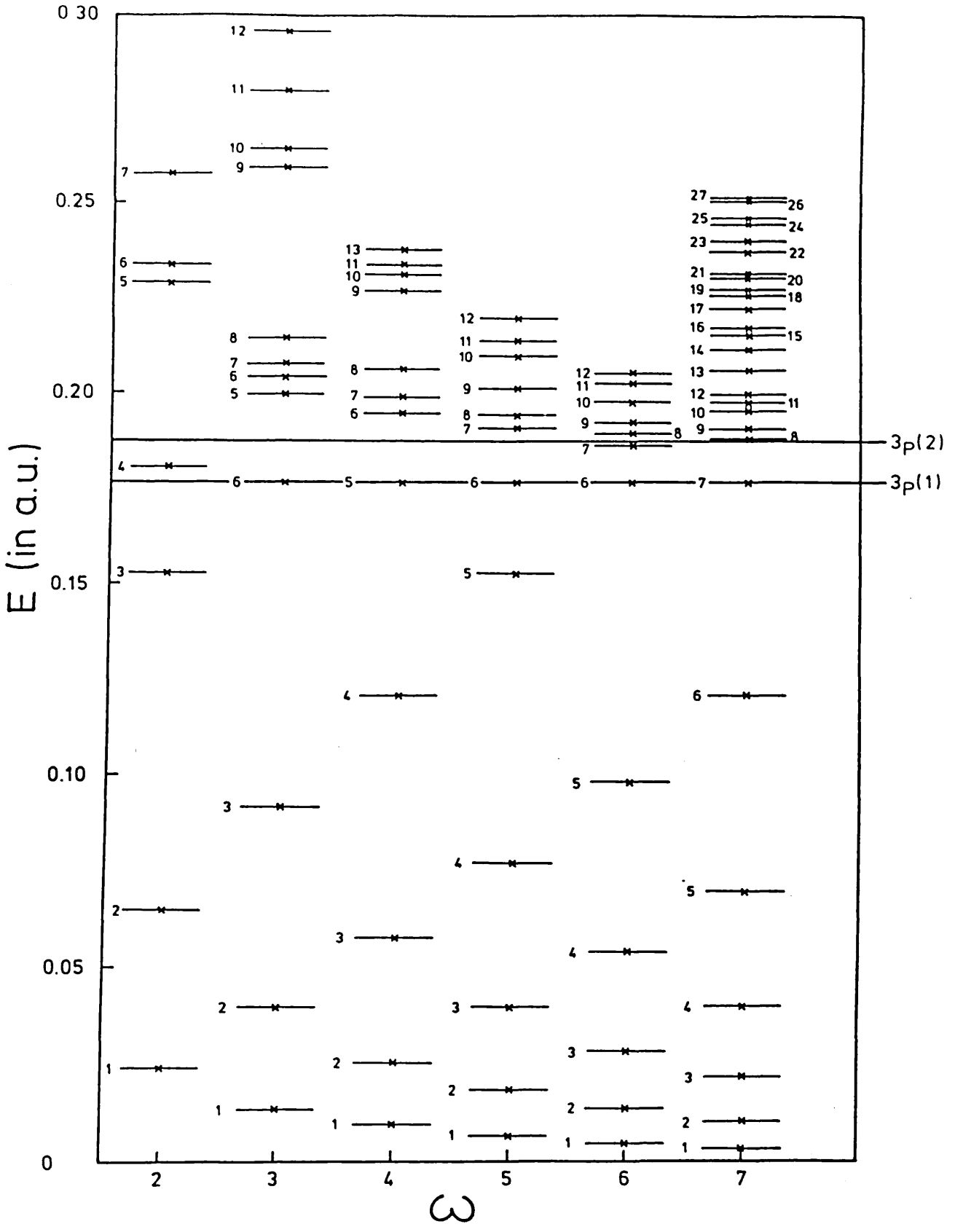

Fig. 4.22 A plot of eigenvalues of the diagonalized hamiltonian for ω = 2,3,4,5,6,7 in search of stabilized eigenvalues (see text).

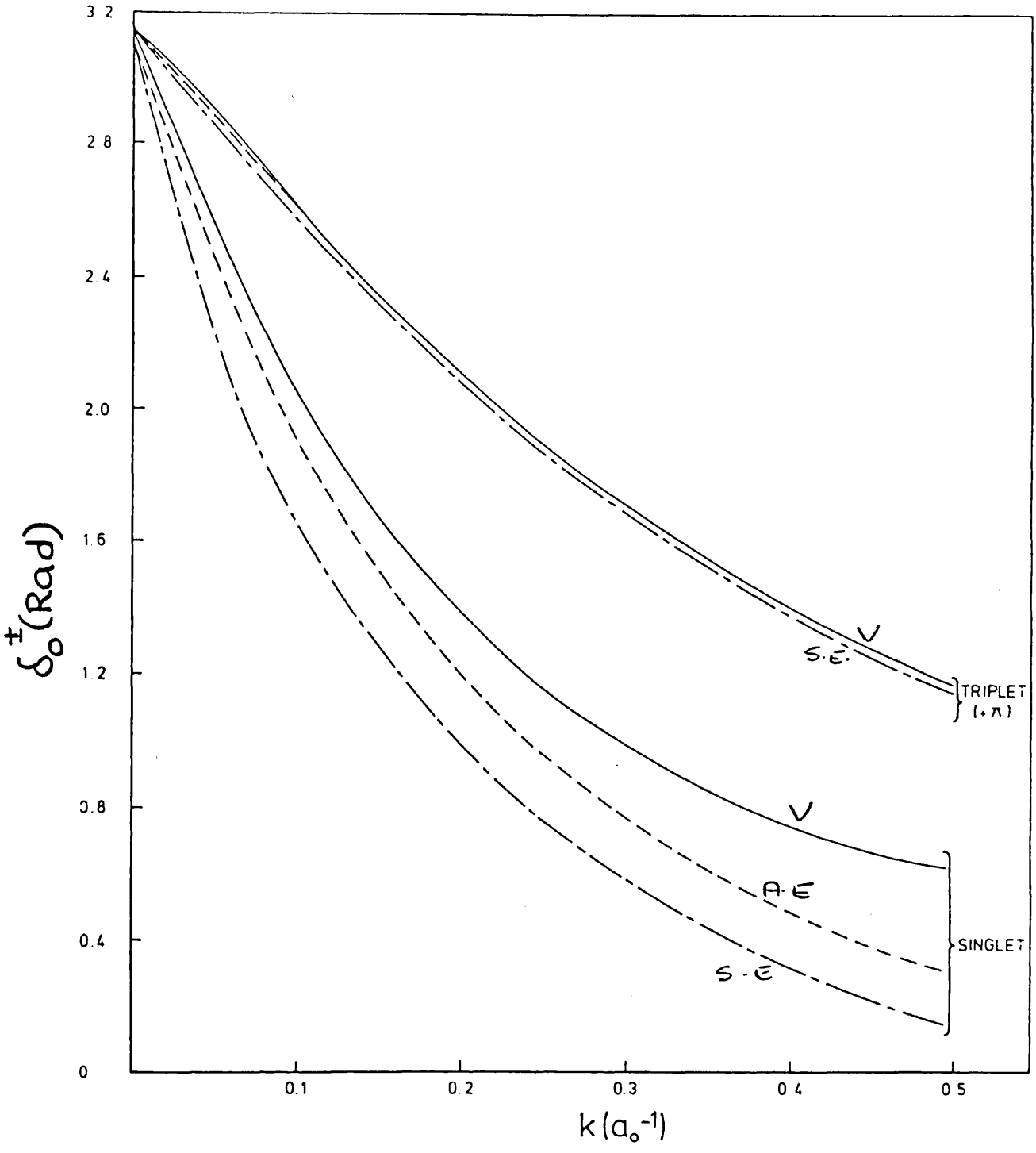

Fig. 5.1 s-wave phase shifts for e^--Ps scattering evaluated by various methods (see text):

——— Variational (V)

— — — — Static-exchange (S·E)

— — — Adiabatic-exchange (A·E.)

(note: π has been added to the triplet results in order to draw the singlet and triplet results on the same graph)

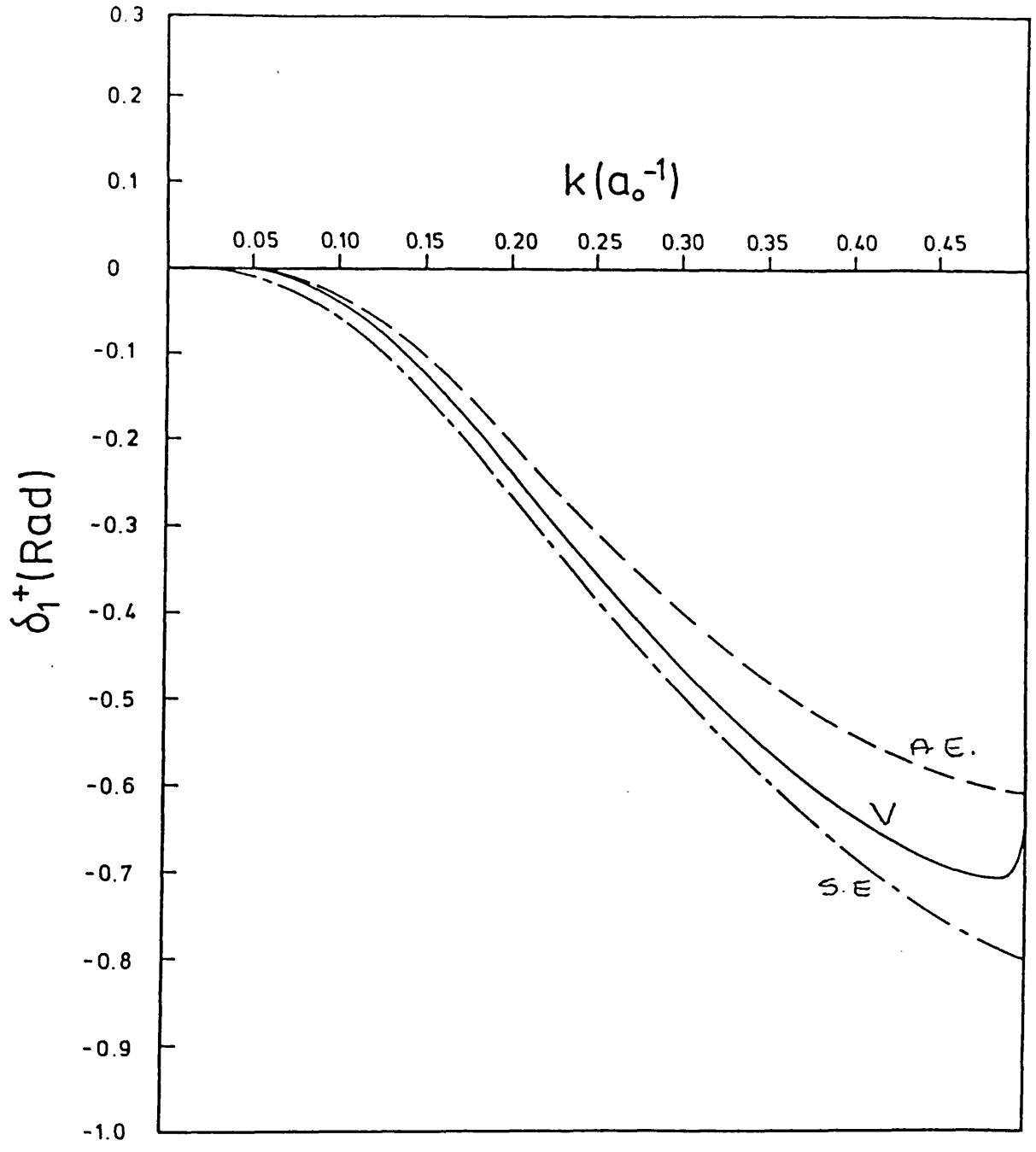

Fig. 5.2 ^1P phase shift for e^--Ps scattering evaluated by various methods (see text):

———— Variational (V)

— — — — — Static-exchange (S.E)

— — — — Adiqbatic-exchange (A.E)

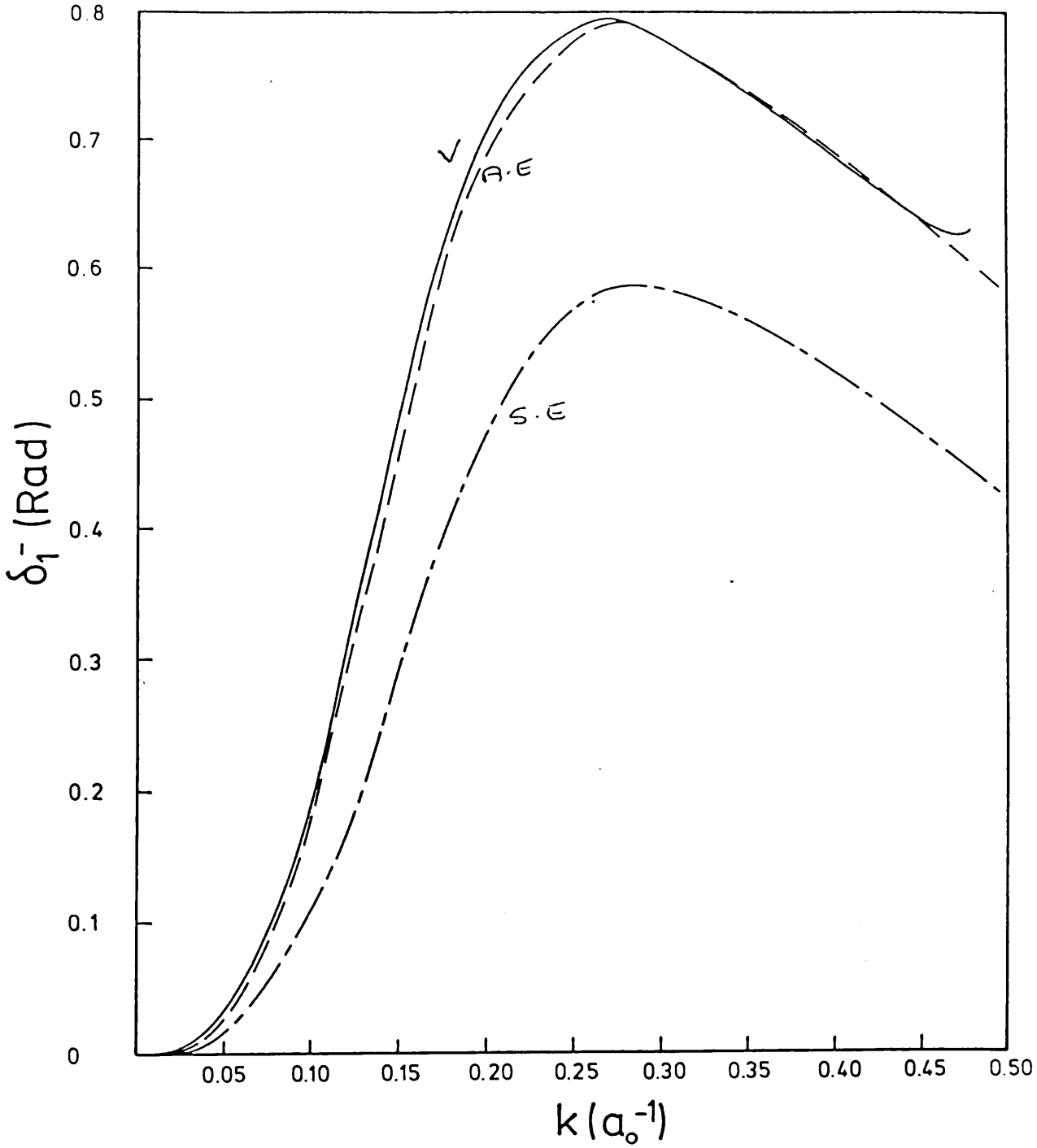

Fig. 5.3 ^3P phase shifts for e^--Ps scattering evaluated by various methods (see text):

———— Variational (V)

— — — — — Static-exchange (S·E)

_ _ _ _ _ Adiqbatic-exchange (A·E)

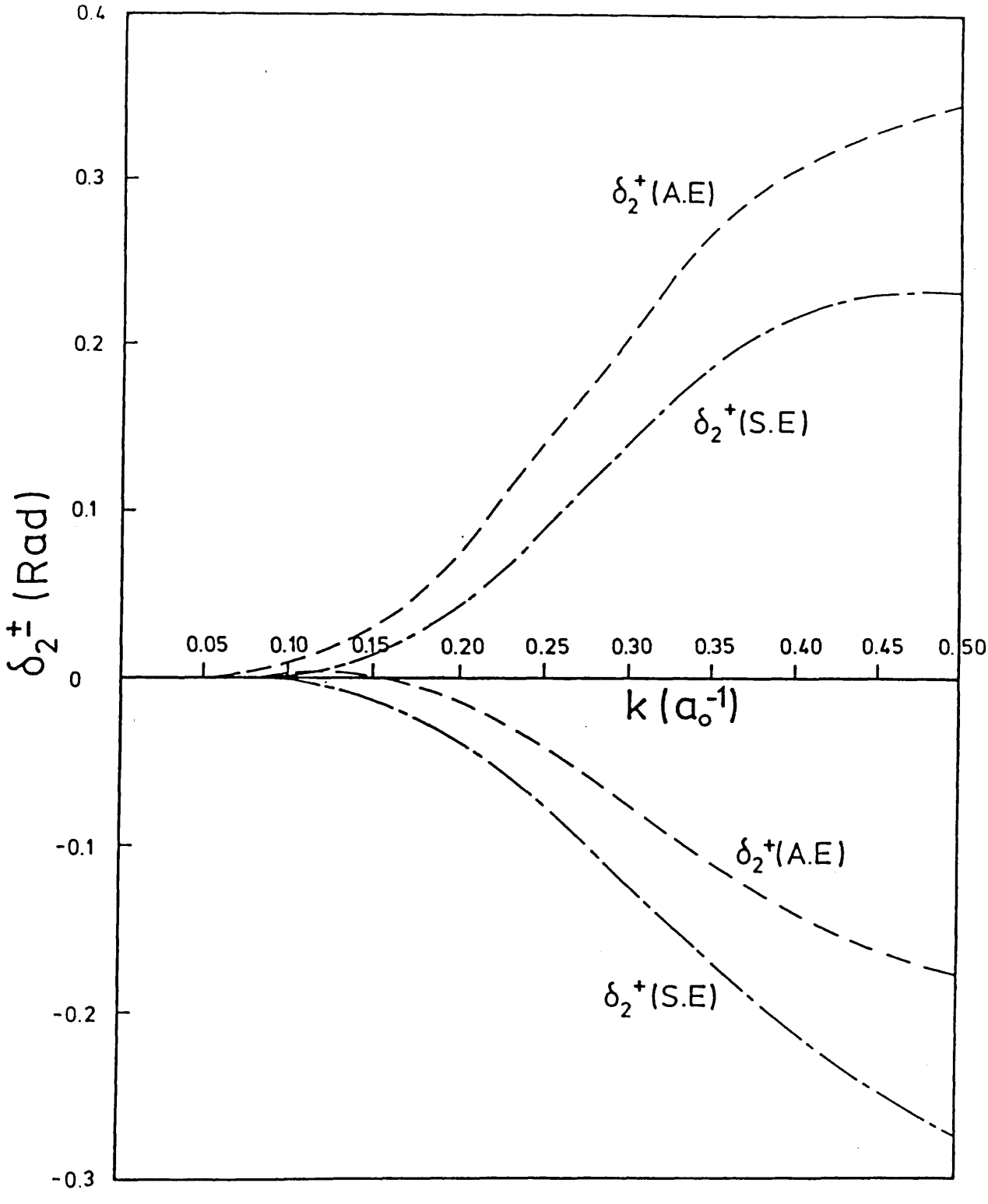

Fig. 5.4 $^{1,3}D$ phase shifts for e^--Ps scattering evaluated by the static-exchange (— - — - - —) and adiabatic-exchange (— — — —) methods.

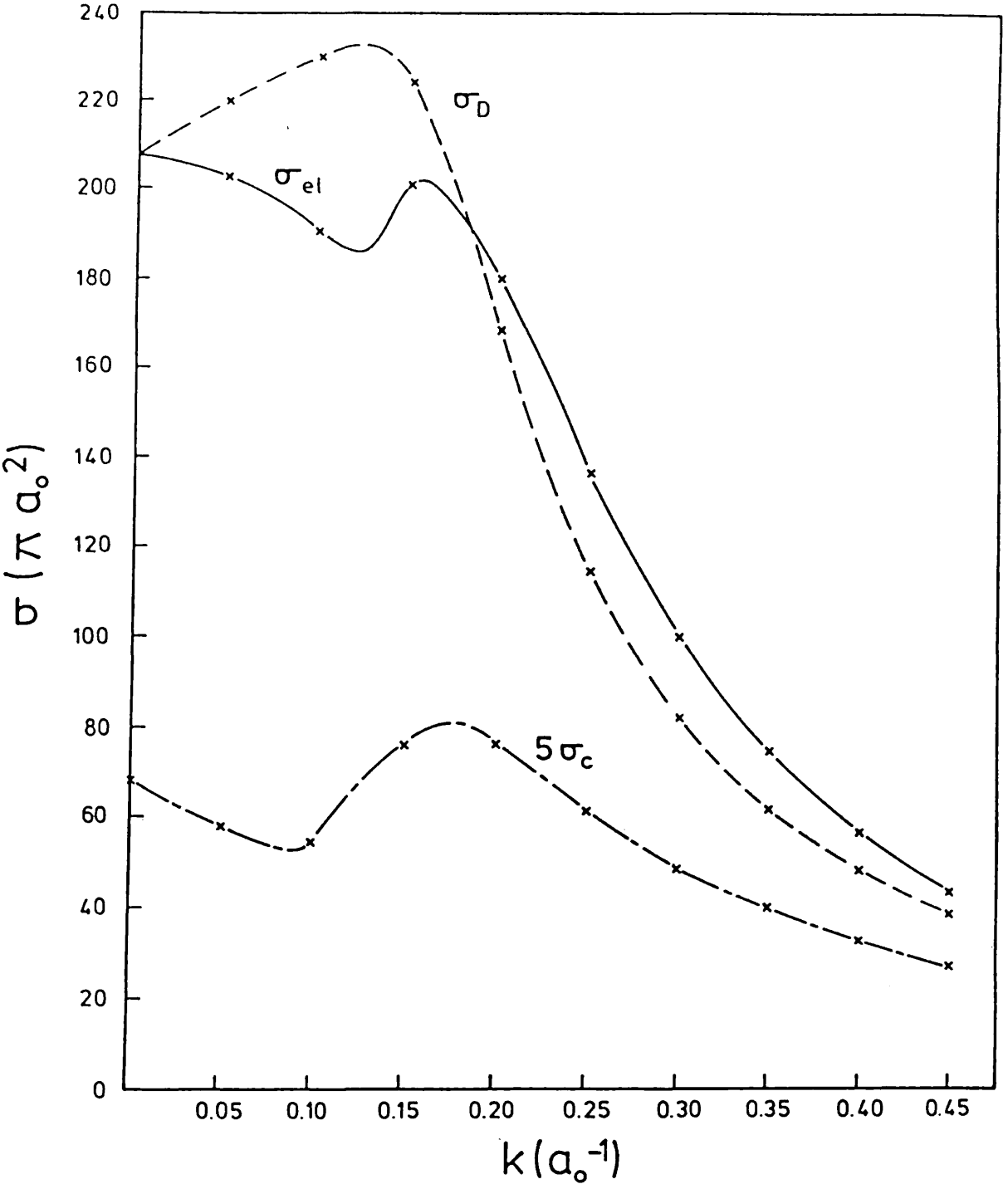

Fig. 5.5 The total elastic cross-section (σ_{el}), the momentum-transfer cross-section (σ_D) and scaled ortho-para conversion cross-section ($5\sigma_c$) for e^--Ps in units of πa_o^2.

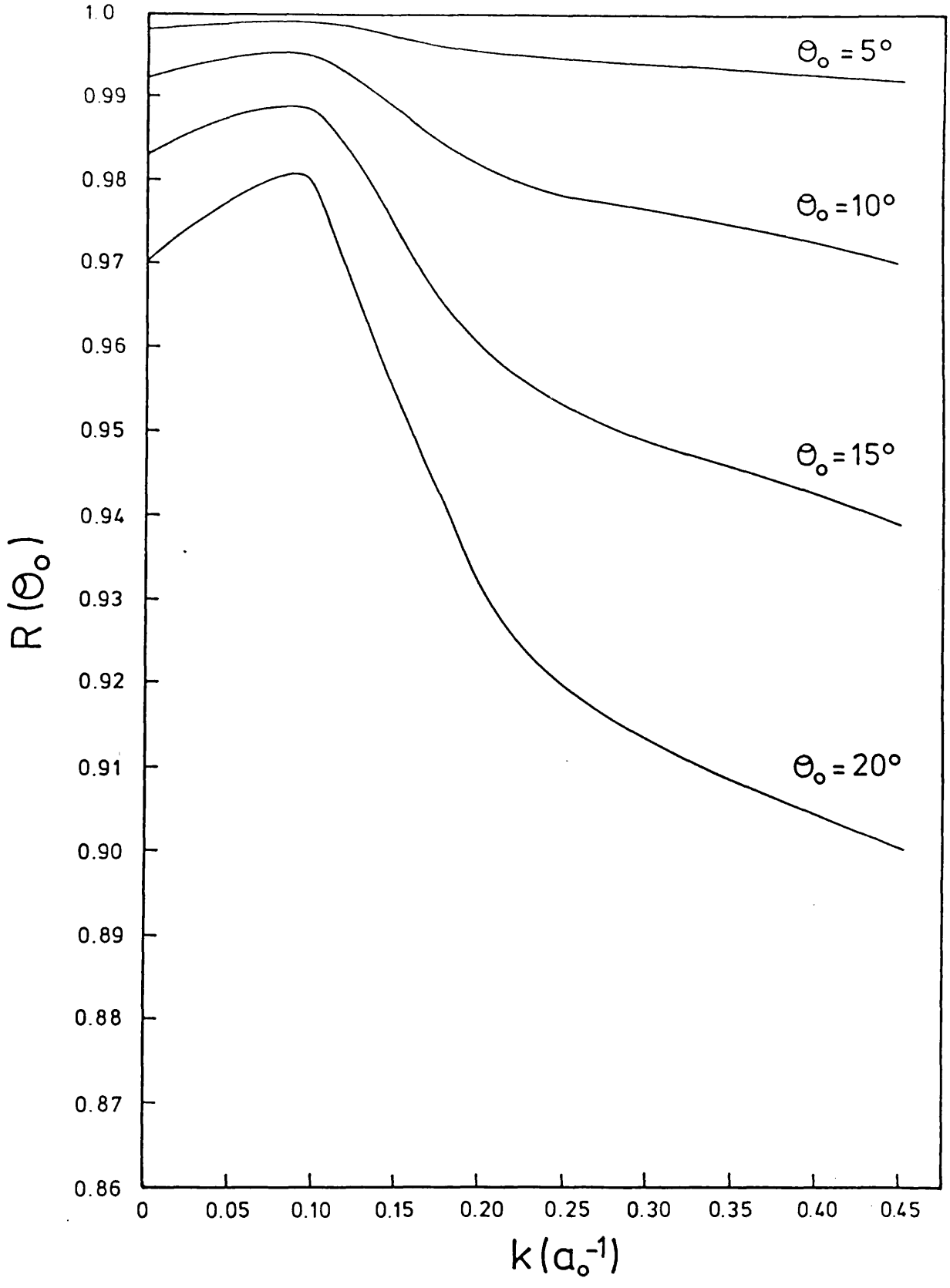

Fig. 5.6 Effective scattering total cross-section, $R(\Theta_o)$, as a function of wave number k.

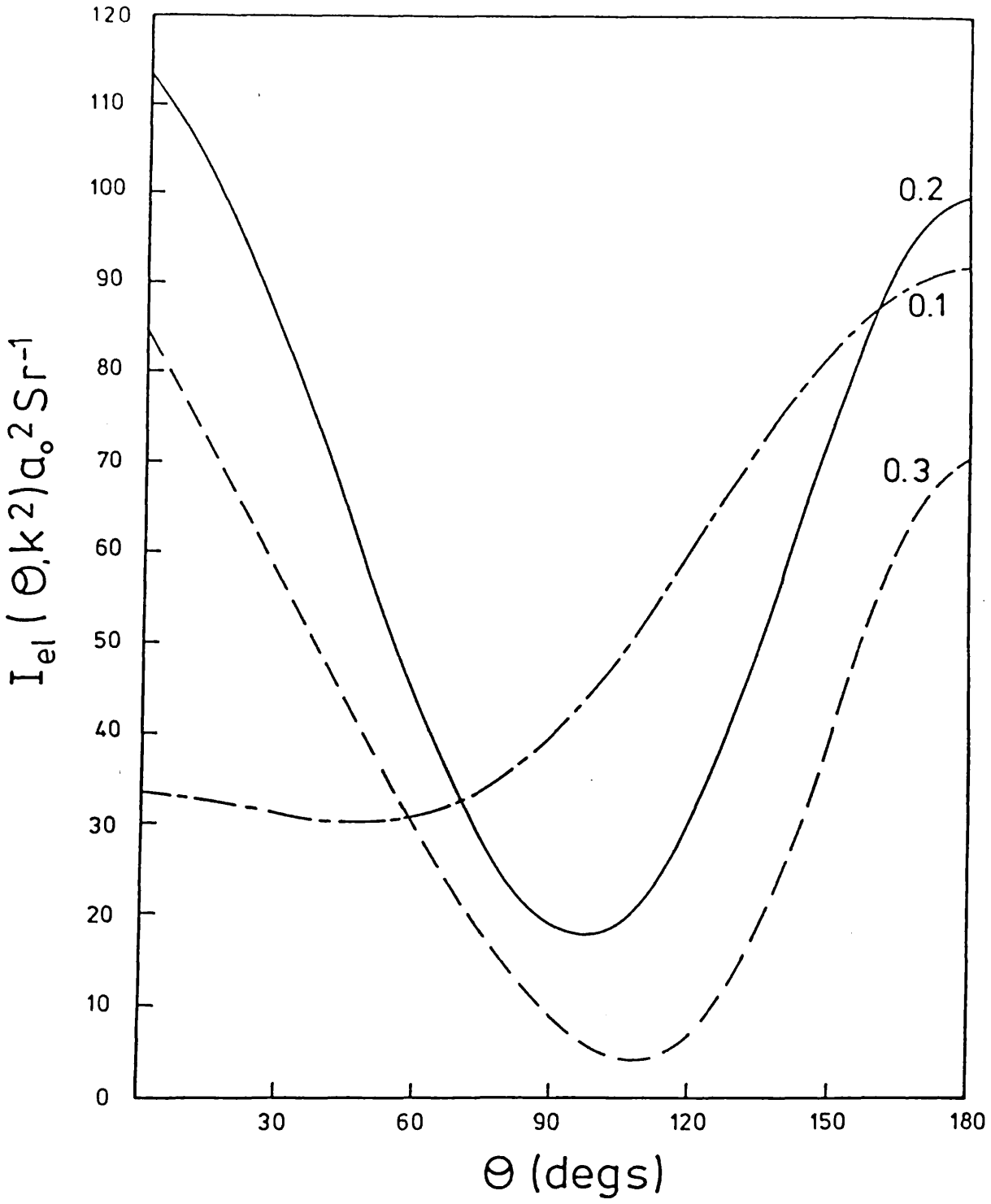

Fig. 5.7 The Elastic differential cross-section $I_{el}(\Theta,k^2)$ for e^--Ps at three values of k (shown on the figure), in units of $a_o^2\ Sr^{-1}$.

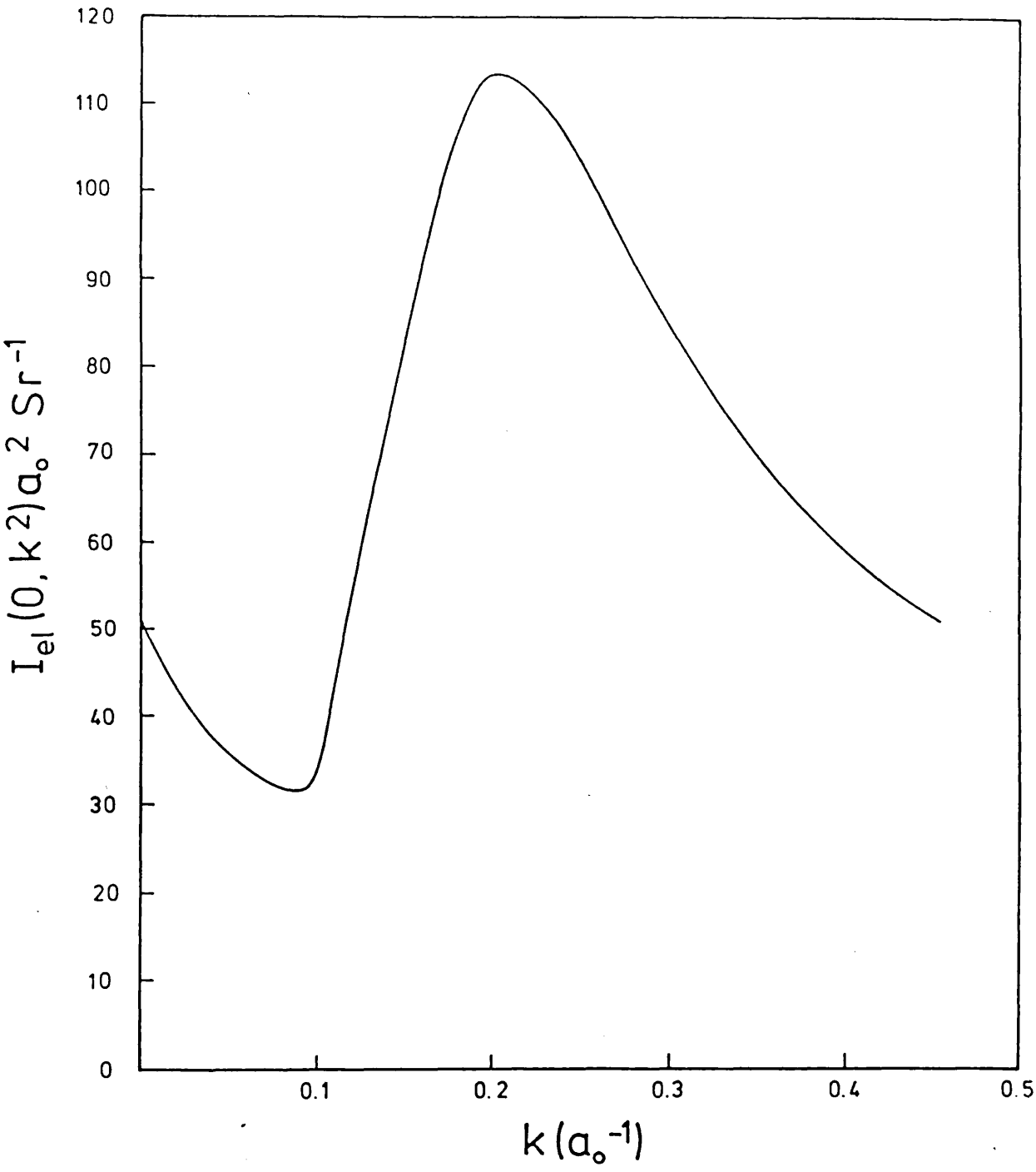

Fig. 5.8 The forward elastic differential cross-section $I_{el}(0,k^2)$ calculated according to equation (5.8).

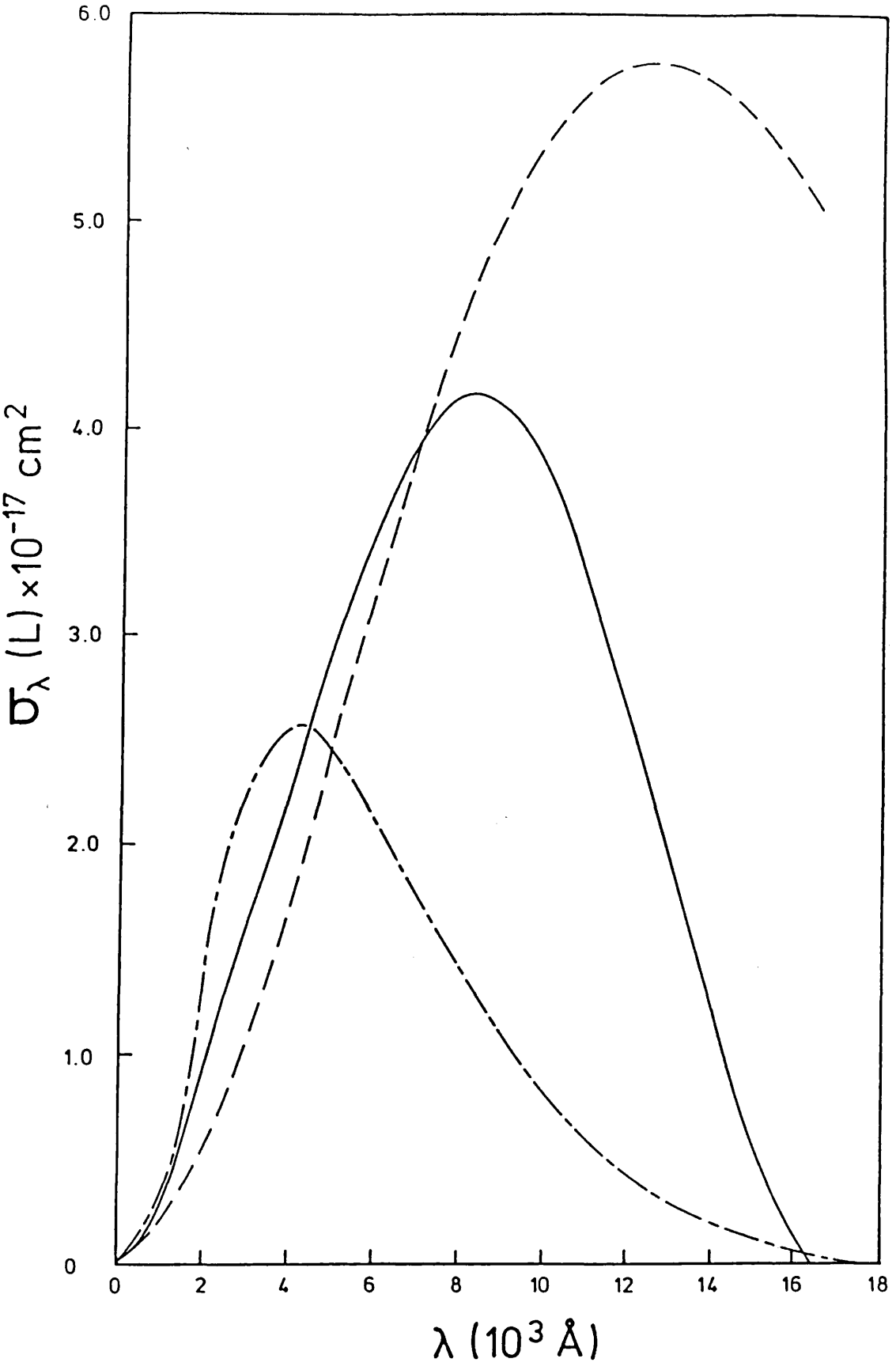

Fig. 6.1 The photodetachment cross-section of H^- in the length formulation evaluated using the plane wave approximation but with different types of bound-state wave functions.

— — — — 2-parameter Chandrasekhar wave function (see Bransden and Joachain, 1983, pg.275

— - — - — 3-parameter Hylleraas-Bethe wave function (Massey and Bates, 1940)

———— 70-parameter Schwartz wave function (Geltman, 1962)

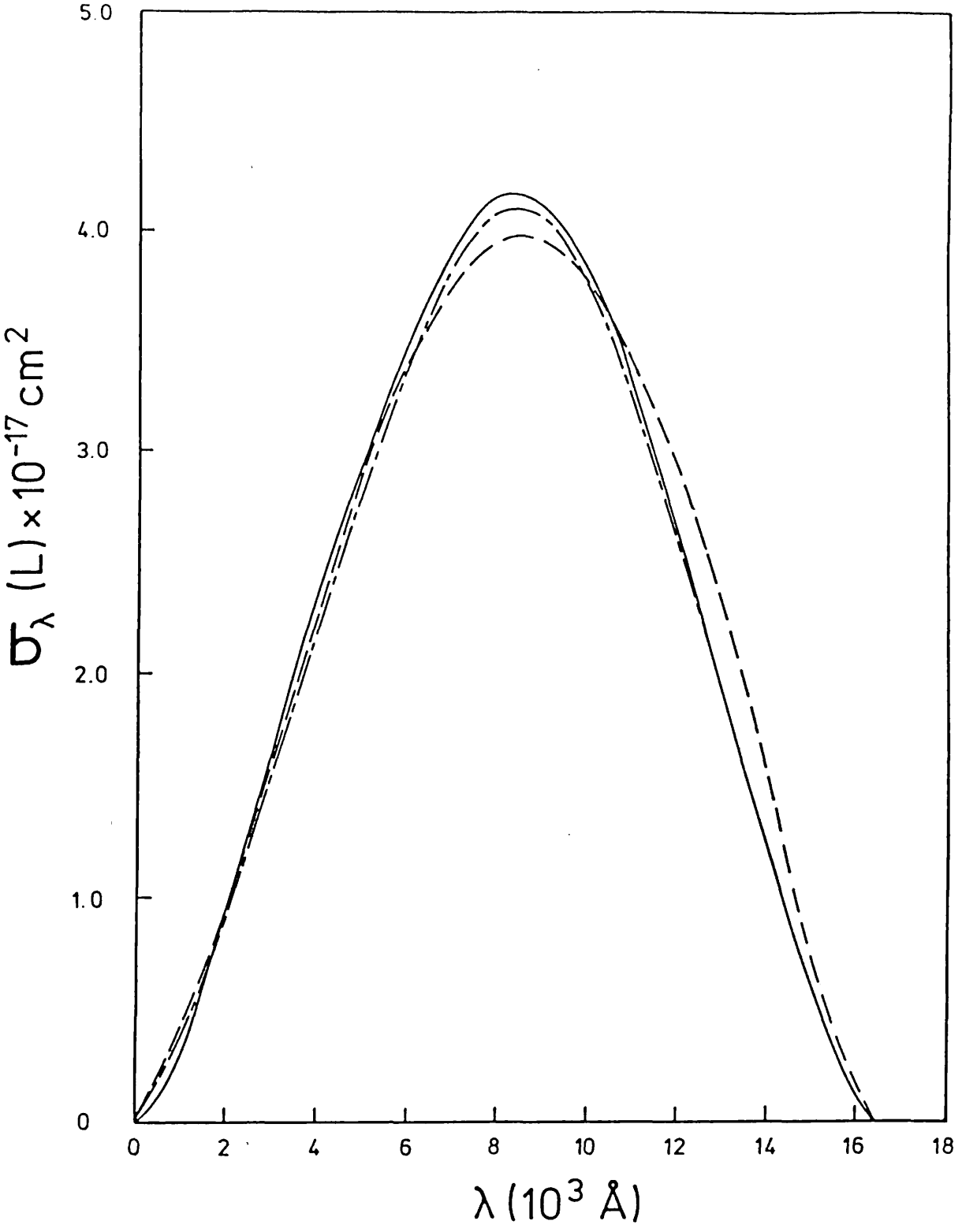

Fig. 6.2 The photodetachment cross-section of H^- in the length formulation to investigate the accuracy of Geltman's (1962) results and the validity of the plane-wave approximation.

——— 70-parameter Schwartz wave function and plane-wave for continuous function (Geltman, 1962)

— - — - 70-parameter Schwartz wave function and a full correlated 6-linear parameter p-wave function (Geltman, 1962)

— — — — 33-parameter wave function of Rotenberg and Stein (1969) for the bound-state and a variational wave function for the continuum state determined by the Kohn-Feshbach method (Ajmera and Chung, 1975)

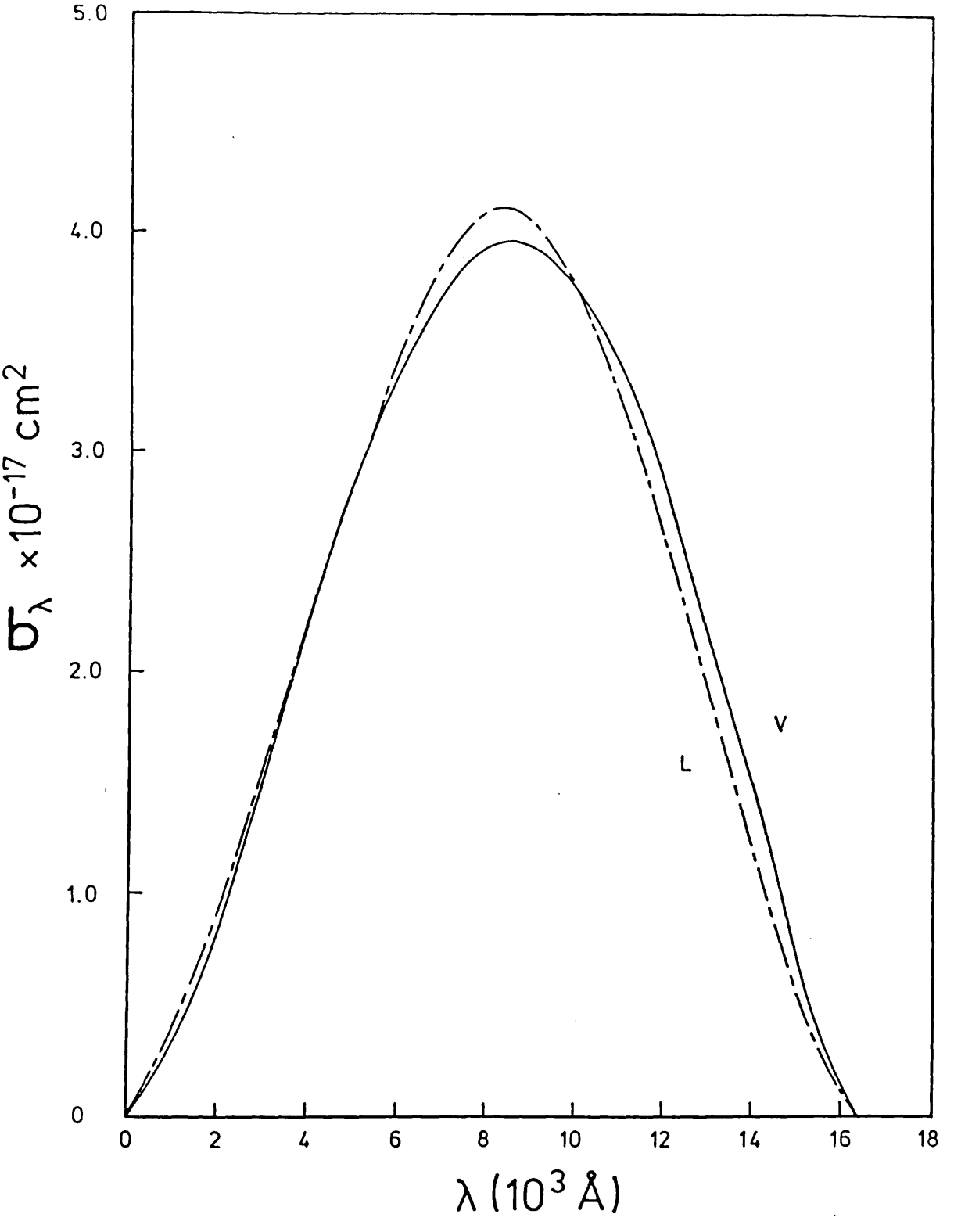

Fig. 6.3 The photodetachment cross-section of H^- determined in the length (L) and velocity (V) formulation using the 70-parameter Schwartz wave function for the bound-state and a full correlated 6-linear parameter p-wave function (Geltman, 1962) for the final state.

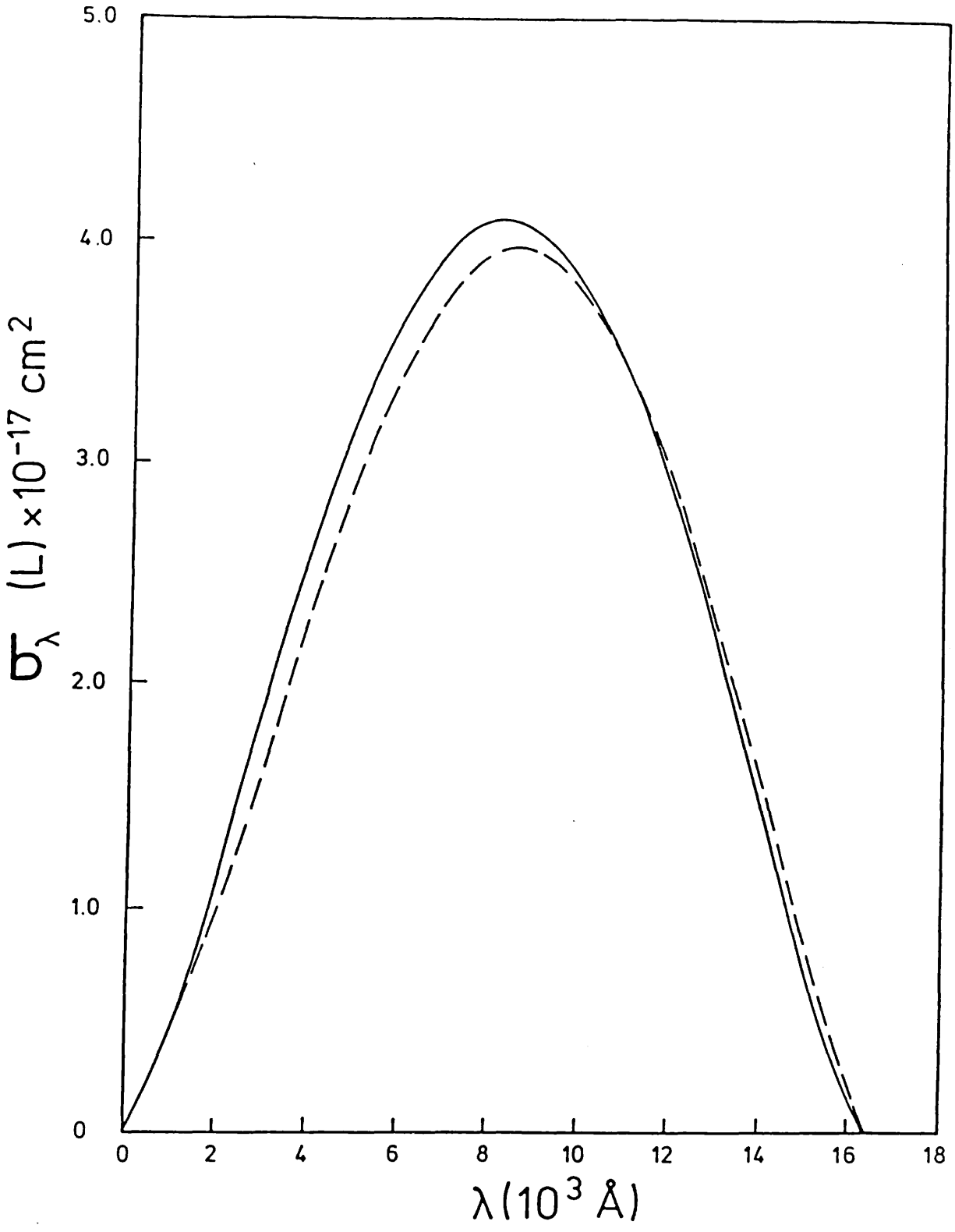

Fig. 6.4 A comparison of Ohmura and Ohmura's (1960) results (_____) in which they used the 'loosely' bound approximation with the accurate length formulation results for the photodetachment of H^- by Ajmera and Chung (1975) (— — — —).

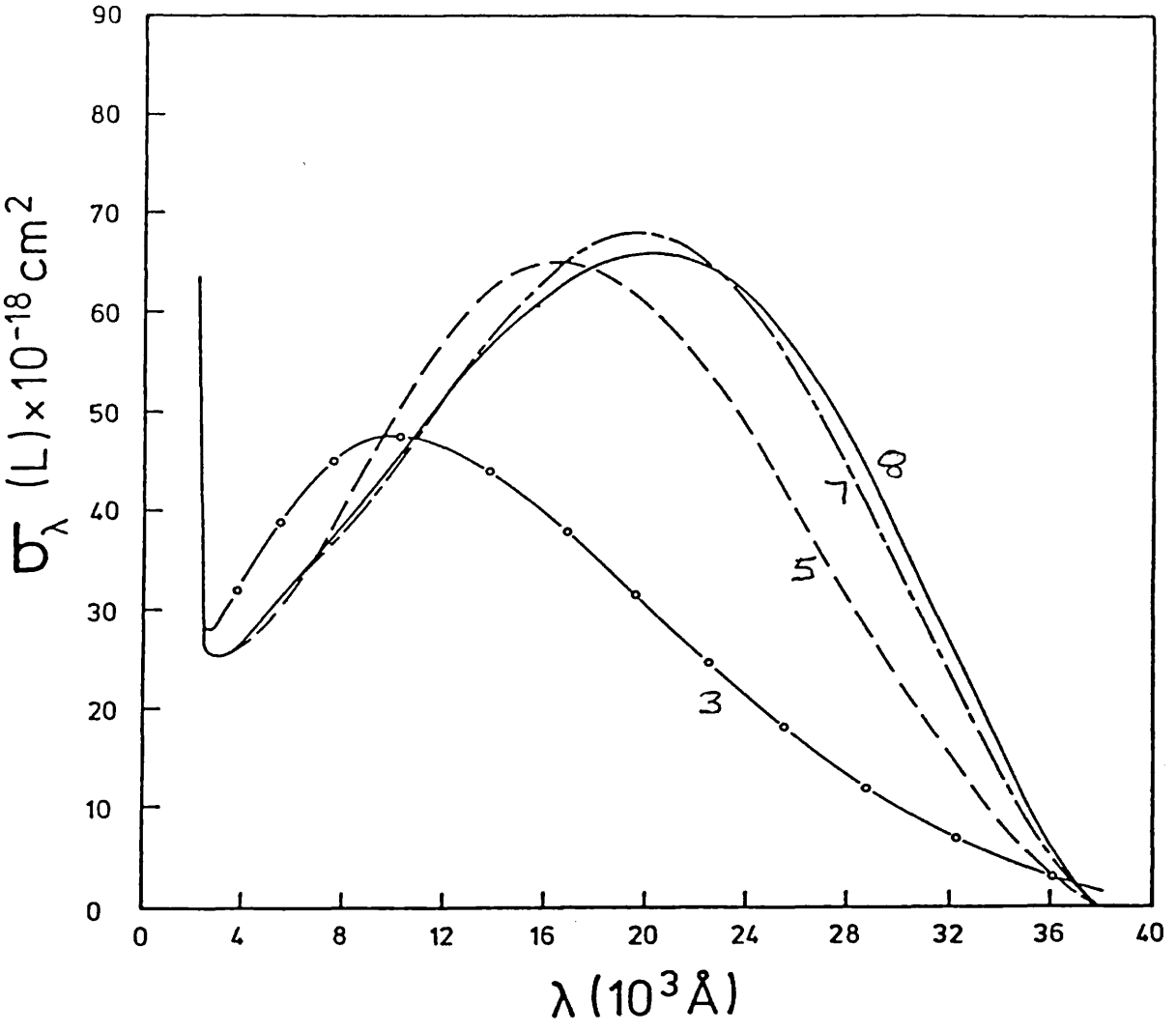

Fig. 6.5 The photodetachment cross-section of Ps^- in the length formulation. Varying ω_b in the bound-state wave function, but using the same continuum wave function (a 220-linear parameter p-wave).

———— ω_b = 8, 95 linear parameters

— — — — ω_b = 7, 70 linear parameters

– – – – – ω_b = 5, 34 linear parameters

–0–0–0–0– ω_b = 3, 13 linear parameters

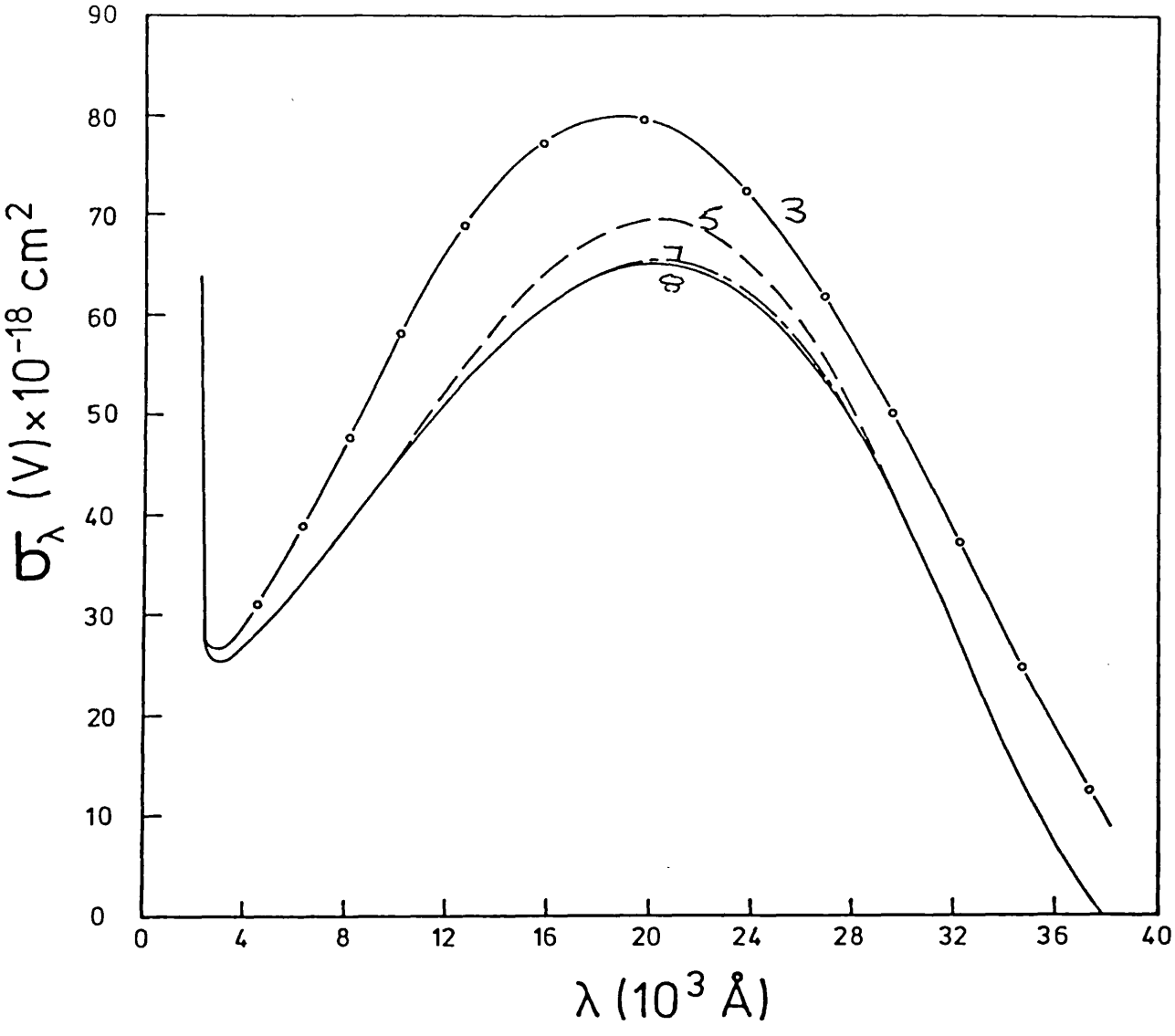

Fig. 6.6 The photodetachment cross-section of Ps^- in the velocity formulation. Varying ω_b in the bound-state wave function but using the same continuum wave function (a 220-linear parameter p-wave).

———— ω_b = 8, 95 linear parameters.
—·—·— ω_b = 7, 70 linear parameters.
— — — ω_b = 5, 34 linear parameters.
—o—o— ω_b = 3, 13 linear parameters.

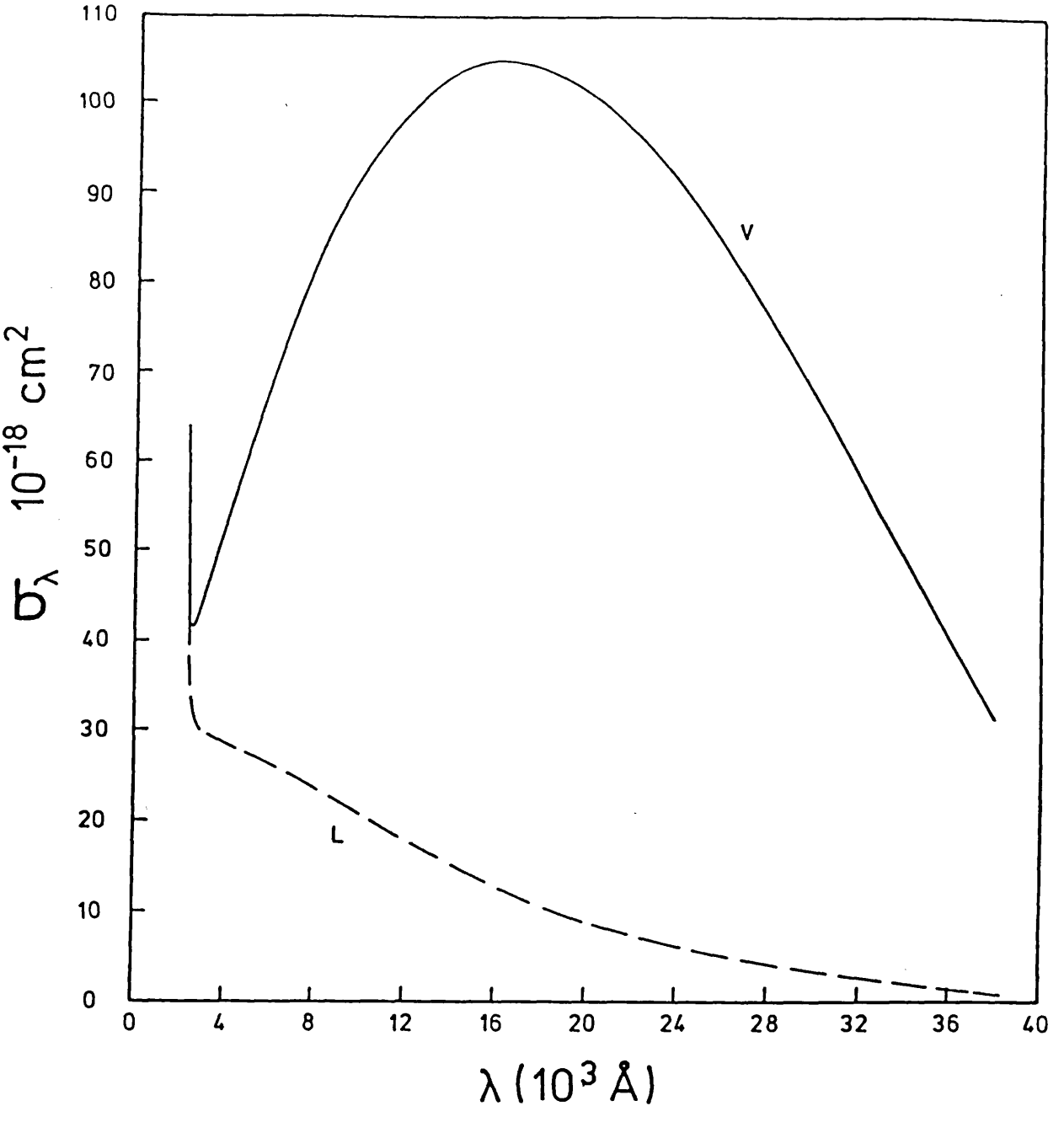

Fig. 6.7 The photodetachment cross-section of Ps^- in the length (L) and velocity (V) formulation using $\omega_b = 1$ in the bound-state wave function (2-linear parameters) and the full 220-linear parameter p-wave function.

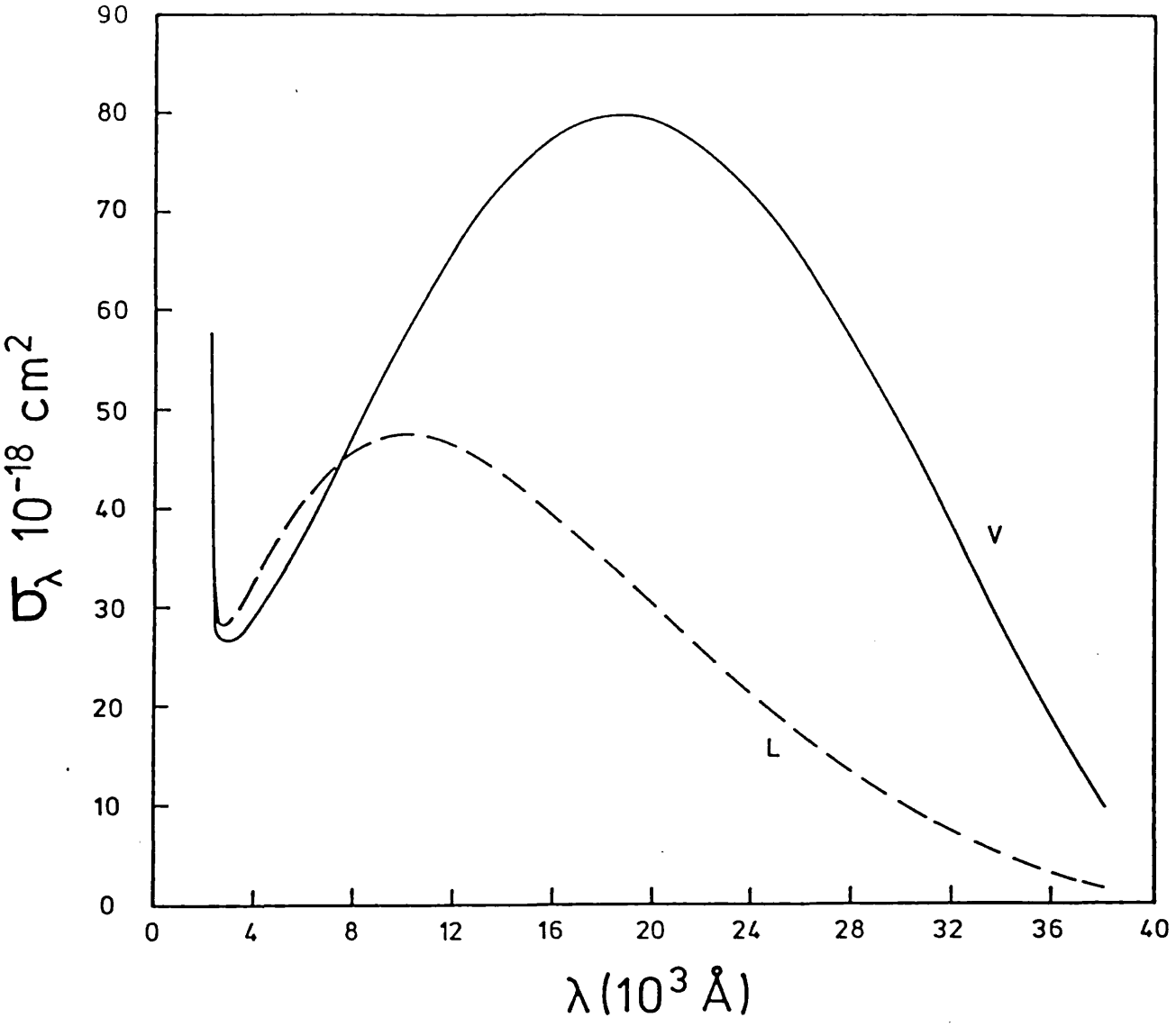

Fig. 6.8 The photodetachment cross-section of Ps^- in the length (L) and velocity (V) formulation using $\omega_b = 3$ in the bound-state wave function (13-linear parameters) and the full 220-linear parameter p-wave function.

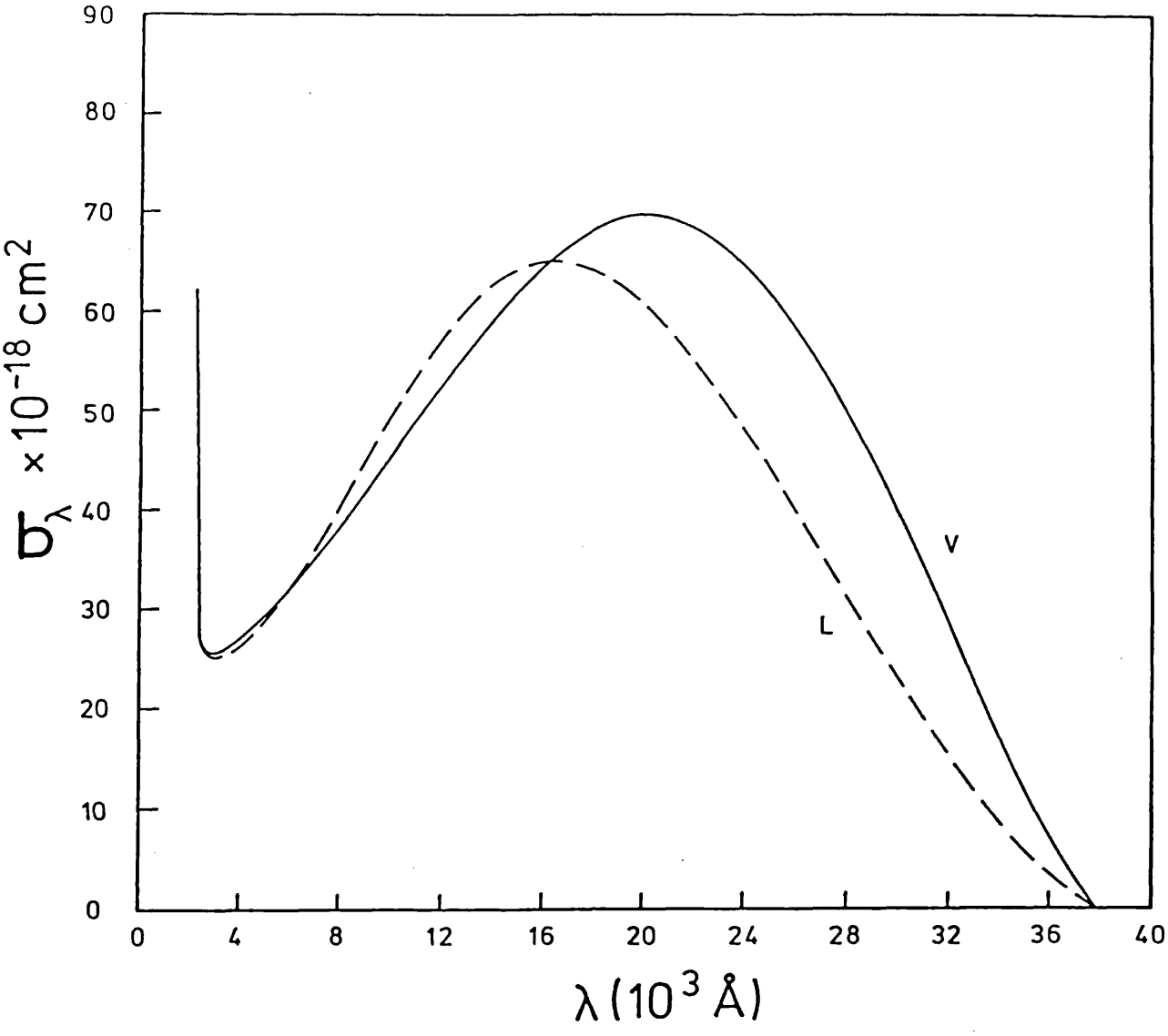

Fig. 6.9 The photodetachment cross-section of Ps^- in the length (L) and velocity (V) formulation using $\omega_b = 5$ in the bound-state wave function (34-linear parameters) and the full 220-linear parameter p-wave function.

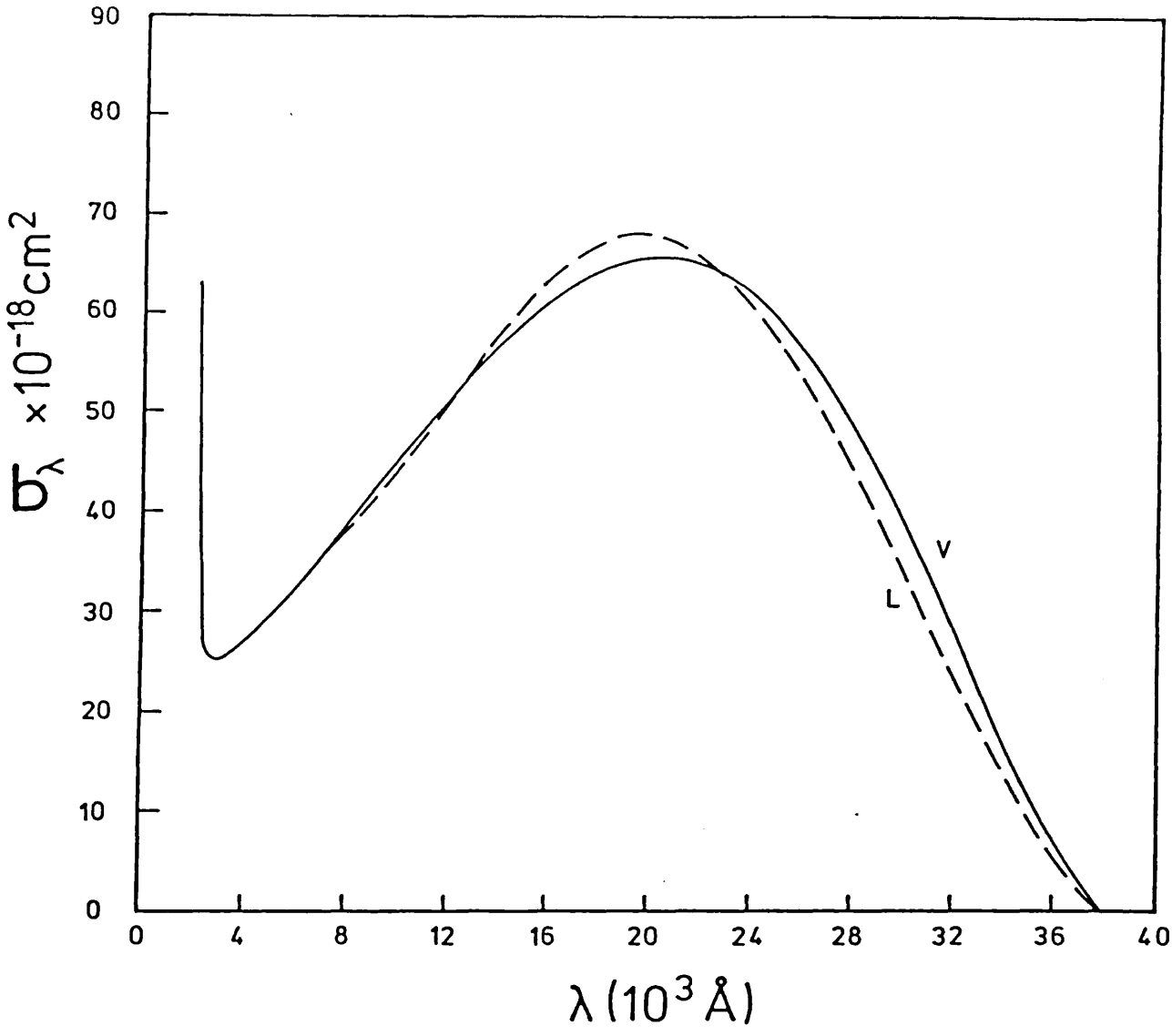

Fig. 6.10 The photodetachment cross-section of Ps^- in the length (L) and velocity (V) formulation using $\omega_b = 7$ in the bound-state wave function (70-linear parameters) and the full 220-linear parameter p-wave function.

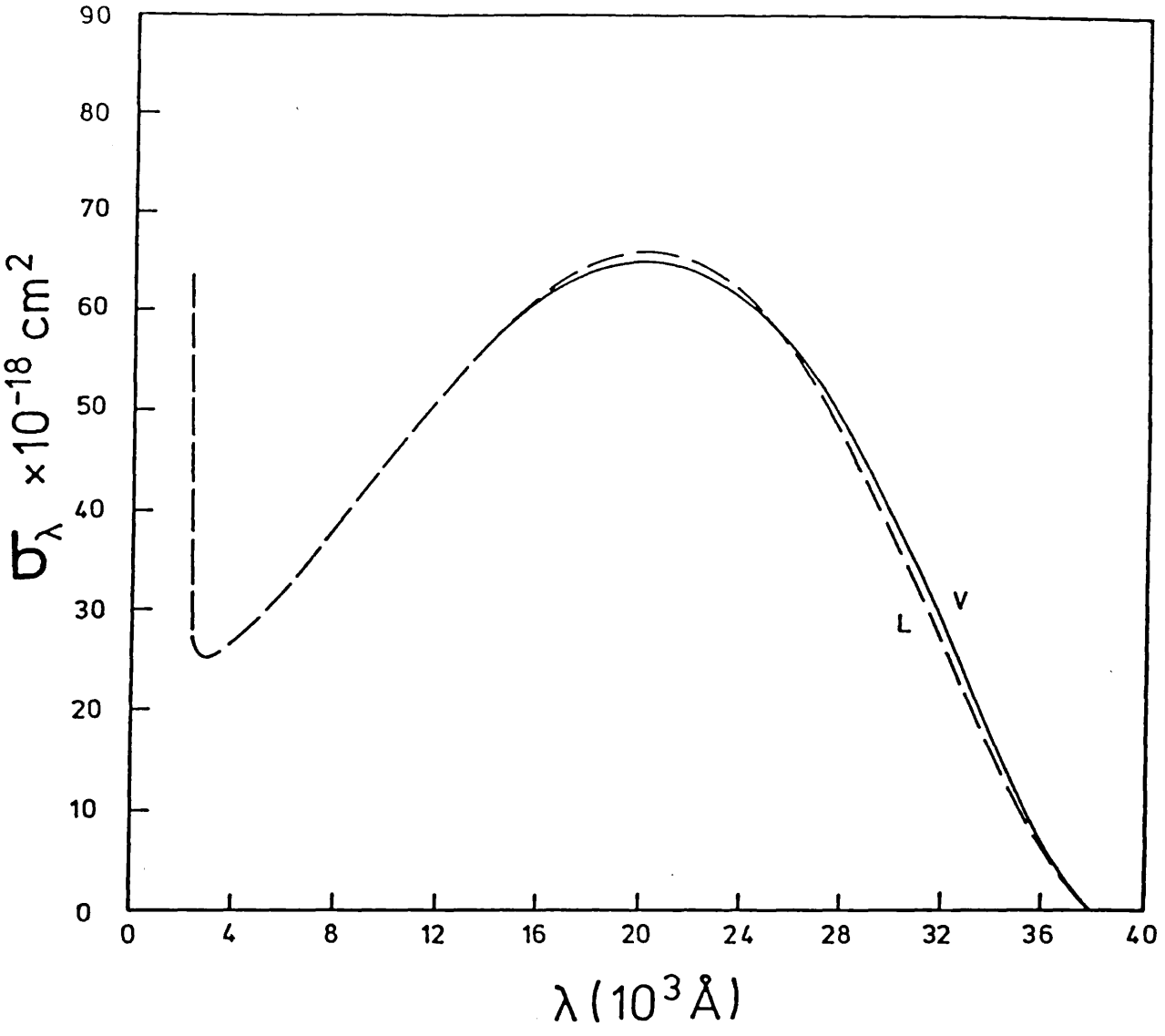

Fig. 6.11 Our most accurate results for the photodetachment cross-section of Ps^- evaluated in the length (L) and velocity (V) formulation in which a 95-linear parameter variational wave function was used for the bound-state (ω_b = 8) and a 220-linear parameter p-wave was used for the continuum-state (ω_c = 9).

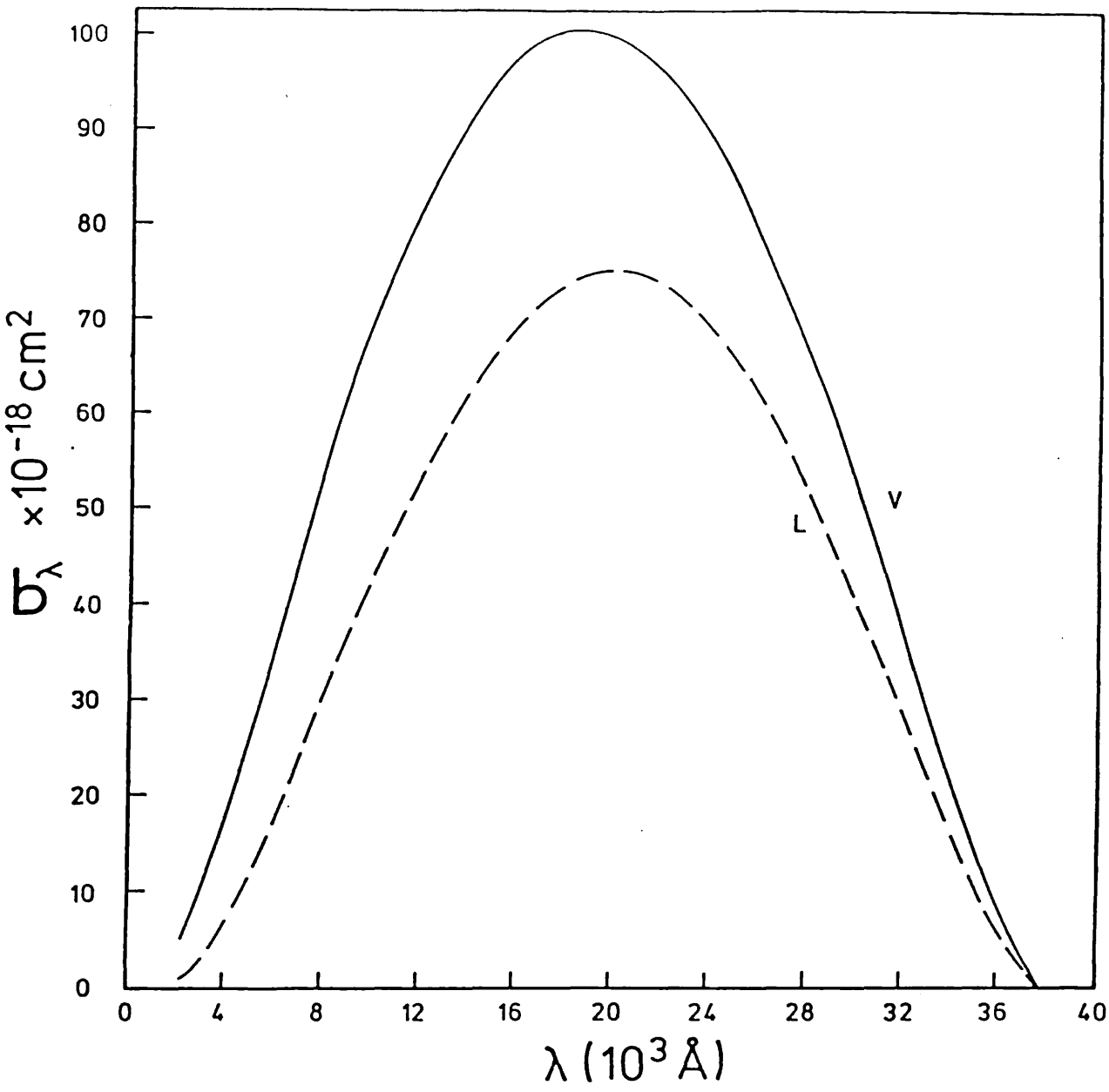

Fig. 6.12 Photodetachment cross-section of Ps^- calculated using the plane wave approximation and the 95-linear parameter bound-state wave function.

— — — — length formulation results

——————velocity formulation results

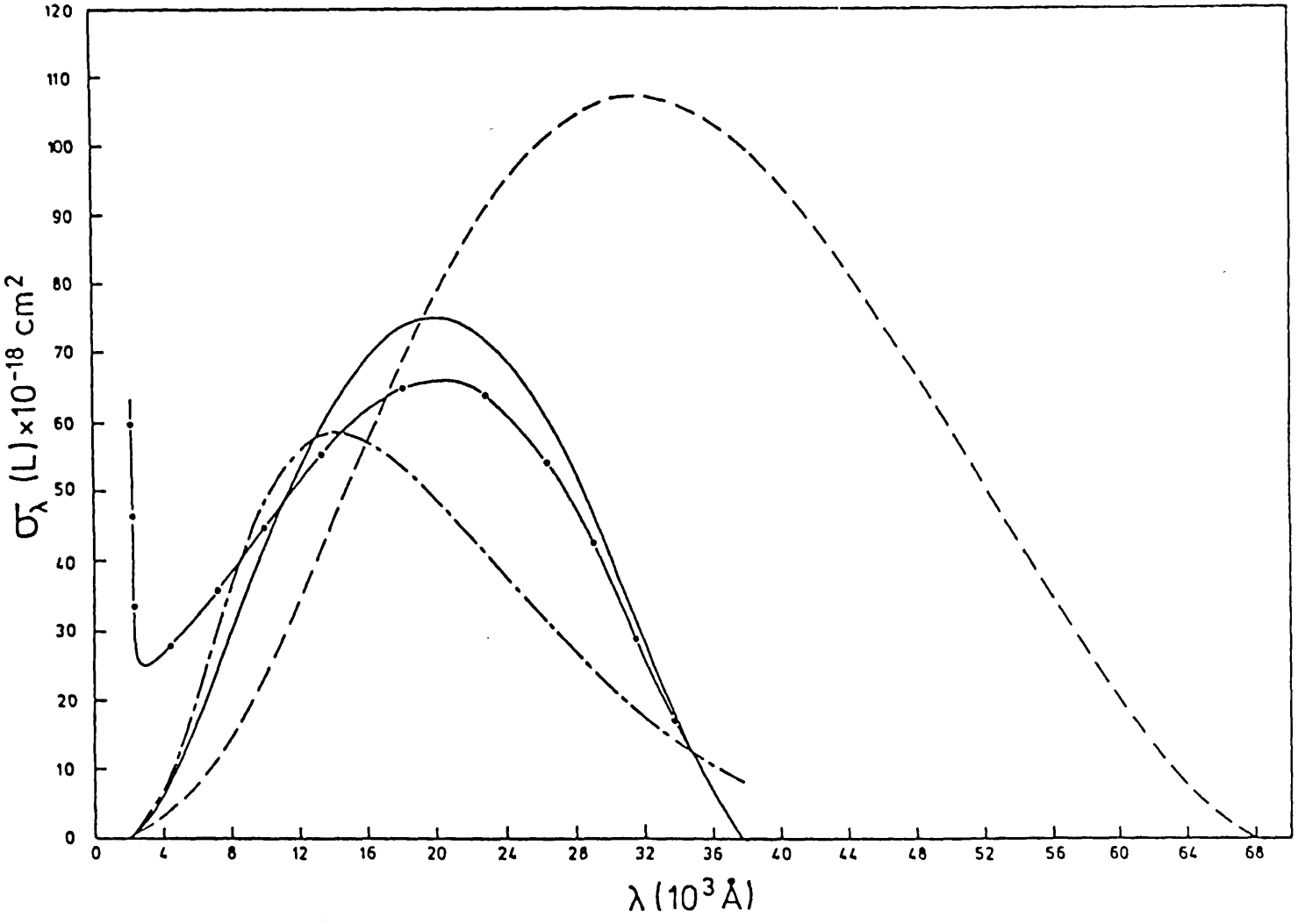

Fig. 6.13 Plane wave treatment of the photodetachment cross-section of Ps^- in the length formulation using different bound-state wave functions, — — — — 2-parameter Ferrantes wave function, — · — — · — 3-parameter Ferrantes wave function, ——— 95-linear parameter. Variational wave function compared with the accurate calculation in which the 95-linear parameter bound-state wave function was used together with the 220-linear parameter p-wave for the continuum state (——•——).

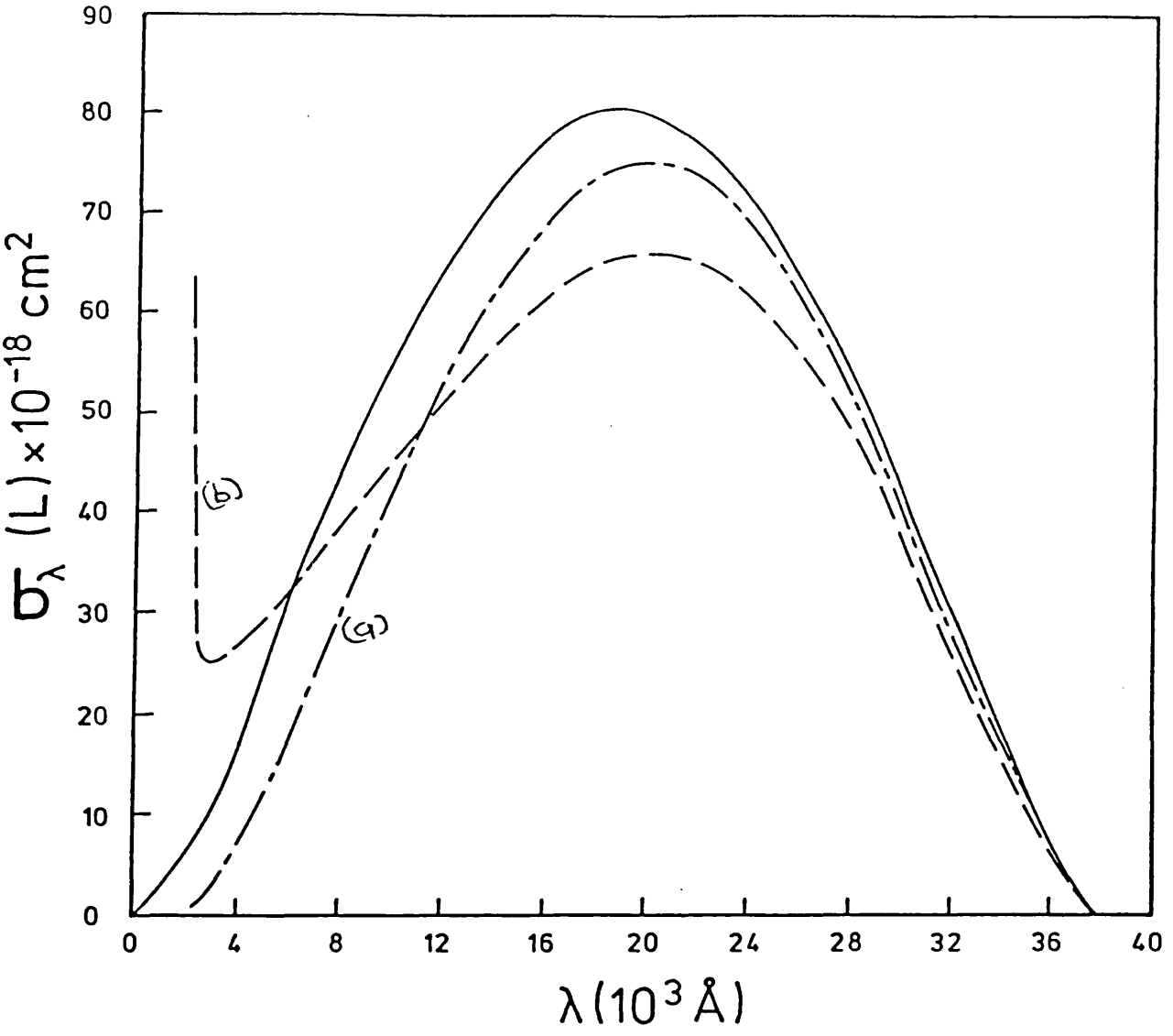

Fig. 6.14 A comparison is made of Bhatia and Drachman's (1985a) results (————) in which they used the 'loosely' bound approximation with our length formulation results in which we used the 95-linear parameter bound-state wave function together with:

(a) a plane wave (—— - —— –)

(b) the 220-linear parameter p-wave (— — –)

for the continuum wave function.

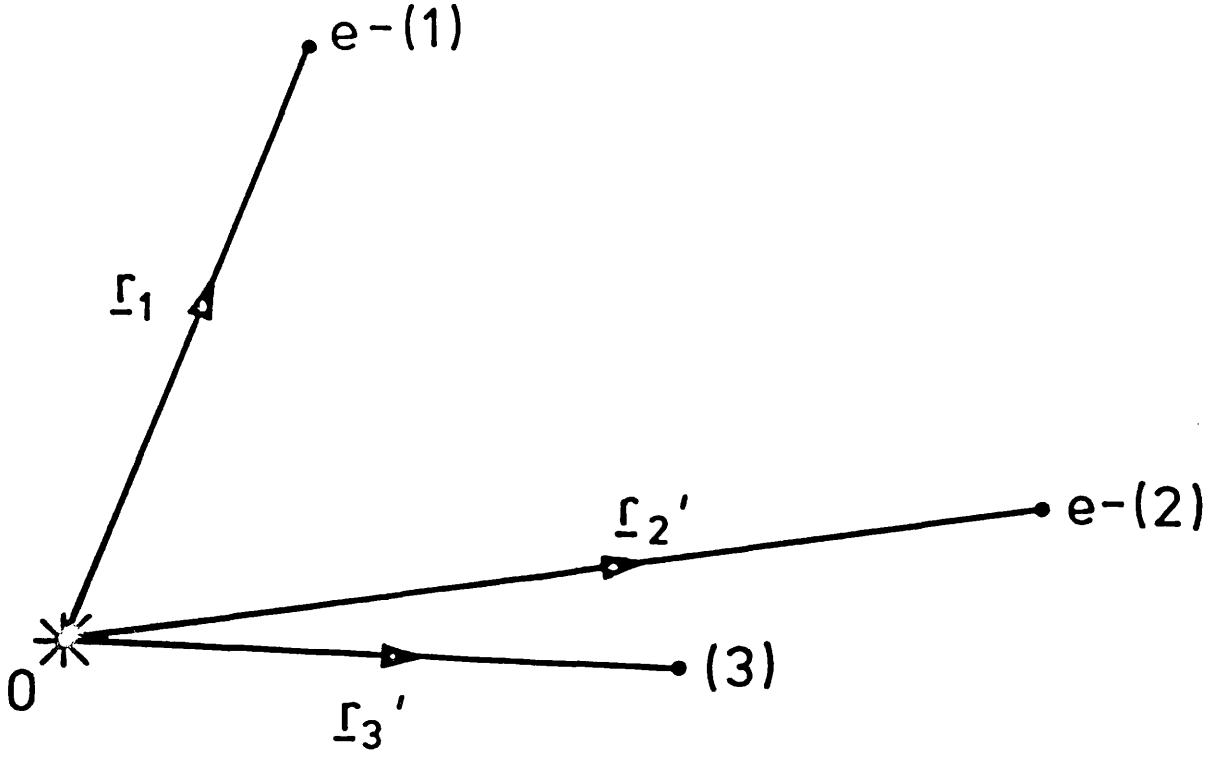

O is a fixed arbitrary origin, Particle (3) is a positron in the case of Ps^-, and a proton in the case of H^-.

Fig. A2.1 Coordinate diagram in the laboratory frame, for a system, such as e^--H, e^--Ps, consisting of two electrons and a positively charged particle.

Published material

J. Phys. B: At. Mol. Phys. 18 (1985) L525-L530. Printed in Great Britain

LETTER TO THE EDITOR

The scattering of low-energy s-wave electrons by positronium

S J Ward†, J W Humberston‡ and M R C McDowell†

† Department of Mathematics, Royal Holloway and Bedford New College, Egham Hill, Egham, Surrey, England

‡ Department of Physics and Astronomy, University College London, Gower Street, London WC1E 6BT, England

Received 28 May 1985

Abstract. Calculations of the s-wave scattering of electrons by positronium with energy less than 7.35 eV are reported in a simple static exchange model based on that for e^--H, the full static exchange model, and an accurate variational model. The pattern of the results is similar to that for scattering by atomic hydrogen. The lowest ^1S resonance is seen at $E_r = 4.768$ eV with a width of 1.6 meV. The zero-energy limit of the elastic cross section is close to 228 πa_0^2.

The first observation of Ps^- was reported by Mills (1981), although its theoretical existence was predicted as long ago as 1946 (Wheeler 1946). In his paper Mills lists a number of interesting experiments which are now, in principle, possible, including photodetachment,

$$h\nu + Ps^- \rightarrow Ps + e^-. \tag{1}$$

A theoretical calculation of the cross section for the process requires a knowledge of the initial bound-state wavefunction and the continuum wavefunction of the final state. This latter is equivalent to a knowledge of the wavefunction for the elastic scattering of slow electrons by Ps, although for the photodetachment problem only the p wave is required. Very good bound-state wavefunctions have already been obtained (see Ho 1983, Bhatia and Drachman 1983 and references therein), but no published work exists on the continuum states.

The elastic scattering of slow electrons by Ps is of interest in itself in view of experiments on the scattering of Ps in gases by e.g. Griffith *et al* at UCL where the existence of a large electron (or positron) scattering cross section might have an important effect (Griffith 1985).

As a first step in a comprehensive investigation of the continuum properties of Ps^- we are using several methods to study the elastic scattering of electrons by Ps and this letter reports the first results of this work.

To obtain an initial comparison with e^--H scattering we first adapt the standard static exchange model to the e^--Ps problem.

The Hamiltonian for the system is (see figure 1)

$$H_1 = -\frac{1}{2\mu(\mathrm{Ps})}\nabla_{r_2}^2 - \frac{1}{2\mu(\mathrm{Ps}^-)}\nabla_{\rho}^2 - \frac{1}{r_2} - \frac{1}{|\boldsymbol{\rho}+\frac{1}{2}\boldsymbol{r}_2|} + \frac{1}{|\boldsymbol{\rho}-\frac{1}{2}\boldsymbol{r}_2|} \tag{2}$$

0022-3700/85/150525+06$02.25

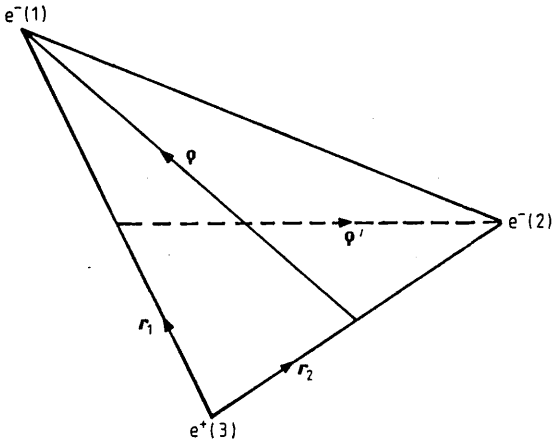

Figure 1. Illustration of the two different coordinate systems used (r_1, r_2 and r_2, ρ) in the e^--Ps problem.

where $\mu(\mathrm{Ps})=\frac{1}{2}$, $\mu(\mathrm{Ps}^-)=\frac{2}{3}$ au, which can be written alternatively as

$$H_2=-\frac{1}{2\mu(\mathrm{Ps})}\nabla^2_{r_1}-\frac{1}{2\mu(\mathrm{Ps})}\nabla^2_{r_2}-\frac{\nabla_{r_1}\cdot\nabla_{r_2}}{m}-\frac{1}{r_1}-\frac{1}{r_2}+\frac{1}{r_3}. \tag{3}$$

The Schrödinger equation is

$$H_2\Psi^{\pm}(\boldsymbol{r}_1,\boldsymbol{r}_2)=(E_{\mathrm{Ps}}+\tfrac{1}{2}\mathcal{K}^2)\Psi^{\pm}(\boldsymbol{r}_1,\boldsymbol{r}_2) \tag{4}$$

where +(−) indicate singlet (triplet) wavefunctions. This differs from the corresponding equation for e^--H scattering by the presence of the mass polarisation term $-\nabla_{r_1}\cdot\nabla_{r_2}/m$ the occurrence of E_{Ps} rather than E_{H} and the replacement of the square of the electron momentum, k^2, by

$$\mathcal{K}^2=k^2/\mu(\mathrm{Ps}^-). \tag{5}$$

We choose a trial function of the same form as the static exchange wavefunction for the electron-hydrogen problem but with $\phi(r)$ the wavefunction of the ground state of positronium,

$$\Psi^{\pm}(\boldsymbol{r}_1,\boldsymbol{r}_2)=2^{-1/2}(\phi(r_2)F^{\pm}(\boldsymbol{r}_1)\pm\phi(r_1)F^{\pm}(\boldsymbol{r}_2)). \tag{6}$$

Inserting this function into (4) and projecting out in the usual way yields the integro-differential equation for each partial wave,

$$\begin{aligned}\left(\frac{\mathrm{d}^2}{\mathrm{d}r_1^2}-\frac{l(l+1)}{r_1^2}+K^2\right)&u_l^{\pm}(K,r_1)\\ &=2\mu(\mathrm{Ps})V_{11}(r_1)u_l^{\pm}(K,r_1)\pm2\mu(\mathrm{Ps})\int_0^{\infty}K_l(r_1,r_2)u_l^{\pm}(K,r_2)\,\mathrm{d}r_2\\ &\pm\tfrac{8}{3}\mu(\mathrm{Ps})z_e^5r_1\exp(-z_er_1)\int_0^{\infty}r_2u_l^{\pm}(K,r_2)\exp(-z_er_2)\,\mathrm{d}r_2\,\delta_{l1}\end{aligned} \tag{7}$$

where

$$K^2=\mu(\mathrm{Ps})\mathcal{K}^2 \qquad z_e=Z\mu(\mathrm{Ps})=\tfrac{1}{2}.$$

This method we refer to as SE1.

The solution has the asymptotic form

$$u_l^{\pm}(K, r_1) \underset{r_1\to\infty}{\sim} K^{-1/2}\sin(Kr_2-\tfrac{1}{2}l\pi+\eta_l^{\pm}) \tag{8}$$

where

$$K=\sqrt{\tfrac{3}{4}}\,k$$

and we note that the true asymptotic form is

$$u_l^{\pm}(k, \rho) \underset{p\to\infty}{\sim} k^{-1/2}\sin(k\rho-\tfrac{1}{2}l\pi+\delta_l^{\pm}) \tag{9}$$

(cf Fels and Mittleman 1967).

Returning to Hamiltonian H_1 we have carried out a full static exchange calculation on the lines of that used for the neutron–deuteron problem (see Buckingham and Massey 1942). Substituting the static-exchange wavefunction

$$\Psi_2^{\pm}(\boldsymbol{r}_2, \boldsymbol{\rho})=2^{-1/2}(\phi(r_2)F^{\pm}(\boldsymbol{\rho})\pm\phi(|\boldsymbol{\rho}+\tfrac{1}{2}\boldsymbol{r}_2|)F^{\pm}(\tfrac{3}{4}\boldsymbol{r}_2-\tfrac{1}{2}\boldsymbol{\rho})) \tag{10}$$

into the Schrödinger equation

$$H_1\Psi_2^{\pm}(\boldsymbol{r}_2, \boldsymbol{\rho})=\left(E_{\mathrm{Ps}}+\frac{k^2}{2\mu(\mathrm{Ps}^-)}\right)\Psi_2^{\pm}(\boldsymbol{r}_2, \boldsymbol{\rho}) \tag{11}$$

yields in the usual way

$$\left(\frac{\mathrm{d}^2}{\mathrm{d}\rho^2}-\frac{l(l+1)}{\rho^2}+k^2\right)u_l^{\pm}(k, \rho)=\int_0^{\infty}K_l^{\pm}(\rho, \rho')u_l^{\pm}(k, \rho')\,\mathrm{d}\rho'. \tag{12}$$

We refer to this method as SE2. We note that unlike the e^-–H system there is no direct potential term. Full details of the analysis and the form of the kernels will be given elsewhere (Ward 1986).

These approximate methods can be tested against a full variational treatment such as that used by Schwartz (1961) for e^-–H scattering. We adopt an s-wave trial function of the form

$$\begin{aligned}\Psi^{\pm}(r_1, r_2, r_3)=\frac{1}{\sqrt{2}}\frac{1}{(4\pi)^{1/2}}\Bigg[&\sqrt{k}\,\phi_{\mathrm{Ps}}(r_2)\left(\frac{\sin k\rho}{k\rho}+\tan\delta^t\frac{\cos k\rho}{k\rho}[1-\exp(-\gamma\rho)]^3\right)\\&\pm\sqrt{k}\,\phi_{\mathrm{Ps}}(r_1)\left(\frac{\sin k\rho'}{k\rho'}+\tan\delta^t\frac{\cos k\rho'}{k\rho'}[1-\exp(-\gamma\rho')]^3\right)\\&+\sum_i c_i\exp(-ar_3)\exp(-bs)s^{k_i}t^{l_i}r_3^{m_i}\Bigg]\end{aligned} \tag{13}$$

where

$$s=r_1+r_2$$

$$t=r_1-r_2$$

and

$$k_i+l_i+m_i\leqslant\omega \qquad k_i, l_i, m_i\geqslant 0.$$

The trial wavefunction was systematically improved by increasing ω. Thus $\omega=2$, 3, 4, 5, 6, 7 correspond to 7, 13, 22, 34, 50, 70 short-range correlation terms for the singlet and 3, 7, 13, 22, 34, 50 for the triplet. Apart from the occurrence of Schwartz

singularities which can be avoided by standard methods (see Nesbet 1980) the variational method is capable of yielding very accurate results. We followed Humberston (1984) in extrapolating to infinite ω.

We investigated the s-wave scattering of electrons by Ps in the energy range 0 to 7.35 eV and in figure 2 we present the singlet and triplet phaseshifts for each of the three methods.

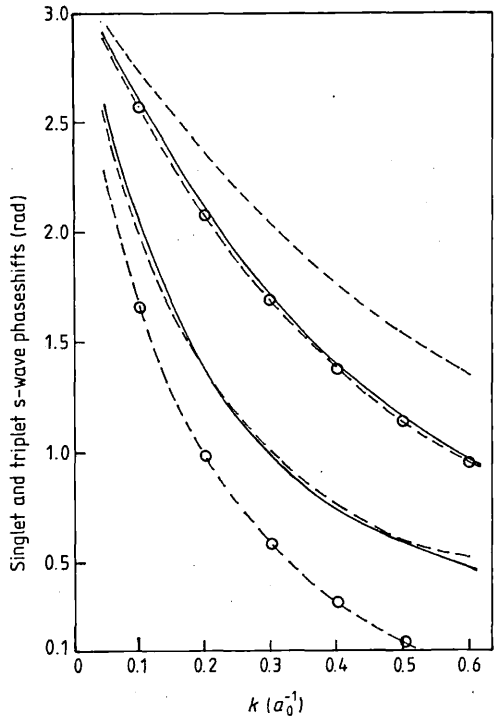

Figure 2. Singlet and triplet s-wave phaseshifts as a function of k (where $k^2/\mu(Ps^-)$ (au) is the energy of the electron in the centre-of-mass frame of e^--Ps) for the various approximations. The upper set of curves are the triplet phaseshifts and the lower set the singlet phaseshifts. ——, phaseshifts obtained by the Kohn variational method ($\omega = 7$); - - O - - O - -, phaseshifts obtained by the full static exchange treatment (SE2); — — —, phaseshifts obtained by the simplified static exchange approximation (SE1).

As an aid to comparison we give the most accurate variational results in table 1 and in table 2 we give the singlet and triplet scattering lengths and the zero-energy cross section for all three methods.

The short-range correlation terms of the variational wavefunction were used to calculate the binding energy of Ps^- and the result with $\omega = 7$ (70 linear parameters) of −0.011 9968 au compares very well with Ho's best result of −0.012 0049 au (Ho 1983). We have not in this letter fully optimised the results with respect to the non-linear parameters in the trial functions.

In the variational calculation convergence with respect to ω is very satisfactory up to just below the $n = 2$ threshold and the Kohn and inverse Kohn results agree extremely well for $\omega \geqslant 3$. A slight deterioration seen in the rate of convergence for $k = 0.5$ drew our attention to the very narrow singlet S resonances found in a complex rotation

Table 1. K-matrix and phaseshifts for the s-wave elastic scattering of electrons by positronium obtained by the variational method.

	Singlet			Triplet		
$k(a_0^{-1})$	$\tan\delta_0^S$ $(\omega=7)^a$	$\tan\delta_0^S$ $(\omega=\infty)^b$	$\delta_0^S(\omega=\infty)^c$	$\tan\delta_0^T$ $(\omega=7)^a$	$\tan\delta_0^T$ $(\omega=\infty)^b$	$\delta_0^T(\omega=\infty)^c$
0.05	−0.681	−0.676 ± 0.005	2.547 ± 0.004	−0.270	−0.256 ± 0.015	−0.25 ± 0.01
0.10	−1.939	−1.930 ± 0.005	2.049 ± 0.001	−0.595	−0.5942 ± 0.0010	−0.5361 ± 0.0008
0.15	−10.58	−10.30 ± 0.15	1.668 ± 0.002	−1.027	−1.023 ± 0.003	−0.7968 ± 0.0015
0.20	5.07	5.13 ± 0.07	1.378 ± 0.002	−1.688	−1.685 ± 0.004	−1.035 ± 0.001
0.25	2.26	2.27 ± 0.01	1.156 ± 0.002	−2.989	−2.981 ± 0.008	−1.247 ± 0.001
0.30	1.503	1.505 ± 0.005	0.984 ± 0.002	−7.27	−7.16 ± 0.10	−1.432 ± 0.002
0.40	0.925	0.928 ± 0.003	0.748 ± 0.002	5.81	5.90 ± 0.08	−1.739 ± 0.002
0.50	0.679	0.71 ± 0.01	0.617 ± 0.007	2.314	2.34 ± 0.02	−1.975 ± 0.003

[a] K matrix calculated by the Kohn variational method at $\omega = 7$.
[b] Fully converged results, K matrix extrapolated to $\omega = \infty$.
[c] Phaseshifts corresponding to the extrapolated K matrix.

Table 2. Singlet and triplet scattering lengths and the zero-energy partial cross section for $l = 0$ calculated by the SE1, SE2 and the Kohn variational method.

Method employed	Singlet scattering length (a_0)	Triplet scattering length (a_0)	Zero-energy s-wave cross section (πa_0^2)
Kohn variational ($\omega = 7$)	12.38 ± 0.07	5.0 ± 0.2	228
SE2	20.5 ± 0.2	5.8 ± 0.2	521
SE1	13.9 ± 0.2	4.04 ± 0.10	242

calculation (Ho 1979, 1984). These lie at 4.734 eV ($k = 0.4816$) and 5.071 eV ($k = 0.4985$) above the ground state, just below the $n = 2$ threshold of the Ps at 5.102 eV ($k = 0.500$). However Ho finds them to be extremely narrow with widths less than 1 meV. Our wavefunction ($\omega = 7$) shows only the lowest $(2s)^2\,{}^1S$ of these resonances and we obtain $E_r = 0.3504$ Ryd compared with $E_r = 0.347\,94$ found by Ho, our width being 1.2×10^{-4} Ryd compared with 8.6×10^{-5} Ryd according to Ho. We intend to increase ω and optimise our non-linear parameters to search for the other resonances below the $n = 2$ threshold.

It can be seen from figure 2 that the triplet phaseshifts from the SE2 method are in close agreement, with, but below, the variational result, and that the singlet phaseshifts from the SE2 method are considerably below. The variational and SE2 triplet phaseshifts actually tend to zero as k tends to zero, and one should therefore subtract π from the results displayed in figure 2. As in the case of atomic hydrogen the spatial antisymmetry of the triplet wavefunction makes the static exchange a better approximation in the triplet case.

The SE1 method shows the correct trends (modulo π) but for the triplet incorrectly overestimates the variational result, which is an upper bound. The singlet SE1 phaseshift

is astonishingly good but orthogonality with the ground state wavefunction of Ps^- has not been imposed, and so the quality of agreement may be misleading. The pattern of agreement of the full static exchange (SE2) and the variational result is reminiscent of that found for atomic hydrogen.

The zero-energy elastic cross section obtained in the variational calculation by extrapolation is 228 πa_0^2 and this confirms preliminary estimates that the elastic cross section remains large out to at least 10 eV: the s-wave contribution in our variational calculation being about 6.3 πa_0^2 at 7.35 eV. Work on higher resonances, higher partial-wave elastic scattering and the photodetachment cross section is continuing.

One of us (SJW) is in receipt of an SERC Research studentship. Discussion with Dr R J Drachman was helpful. We wish to thank Mr C J Brown for help with the variational calculations.

References

Bhatia A K and Drachman R J 1983 *Phys. Rev.* A **28** 2523
Buckingham R A and Massey H S W 1942 *Proc. R. Soc.* A **179** 123-51
Fels M F and Mittleman M H 1967 *Phys. Rev.* **163** 129-34
Griffith T C 1985 private communication
Ho Y K 1979 *Phys. Rev.* A **19** 2347-352
—— 1983 *J. Phys. B: At. Mol. Phys.* **16** 1503-9
—— 1984 *Phys. Lett.* **102A** 348-50
Humberston J W 1984 *J. Phys. B: At. Mol. Phys.* **17** 2353-61
Mills A P Jr 1981 *Phys. Rev. Lett.* **46** 717-20
Nesbet R K 1980 *Variational Methods in Electron-Atom Scattering Theory* Physics of Atoms and Molecules Series, ed P G Burke and H Kleinpoppen (New York, London: Plenum)
Schwartz C 1961 *Phys. Rev.* **124** 1468-71
Ward S J 1986 *PhD Thesis* University of London
Wheeler J A 1946 *Ann. NY Acad. Sci.* **48** 219-24

EUROPHYSICS LETTERS 15 February 1986

Europhys. Lett., **1** (4), pp. 167-171 (1986)

The Photodetachment of the Negative Ion of Positronium (Ps^-).

S. J. WARD and M. R. C. MCDOWELL

Mathematics Department, Royal Holloway and Bedford New College University of London - Egham Hill, Egham, Surrey TW20 OEX

J. W. HUMBERSTON

Department of Physics and Astronomy, University College London, Gower Street, London WC1.

(received 20 November 1985; accepted 18 December 1985)

PACS. 36.90. – Other special atoms and molecules.
PACS. 32.80F. – Photoionization, photodetachment, photoelectron spectra.

Abstract. – Accurate variational calculations of the photodetachment cross-section of Ps^- are reported. Both length and velocity forms are reported. The sum rule S_{-1} is satisfied to within 2%. The cross-section has a maximum of about $68 \cdot 10^{-18}$ cm^2 at a wave-length of between $1.8 \cdot 10^4$ and $2.1 \cdot 10^4$ Å and shows a significant peak just below the threshold for exciting Ps ($n = 2$).

The existence of a bound state of the purely leptonic system ($e^+e^-e^-$) was first demonstrated in a variational calculation by WHEELER [1]. It differs from the negative ion of atomic hydrogen (pe^-e^-)H^-, in the replacement of the proton by a positron. The extra electron is bound to positronium (Ps) to form its negative ion Ps^-.

Among the most recent calculations of its binding energy are those of Ho [2] and of Bhatia and Drachman [3] which differ by one in the fifth figure for the electron affinity, giving

$$\mathrm{EA\,(Ps)} = 0.32668\ \mathrm{eV}. \tag{1}$$

The intense recent interest in Ps^- started with the laboratory demonstration of its existence by MILLS [4], who also measured its decay rate [5]

$$\Gamma = (2.09 \pm 0.09)\ \mathrm{ns}^{-1} \tag{2}$$

in good agreement with theory. Our present knowledge of its properties has been reviewed elsewhere [6].

In this paper announcing the discovery MILLS says «Ps^- has an annihilation lifetime..., a photoionization cross-section..., all of which are sensitive to the details of its wave function and which can now be measured given a sufficiently strong source of slow positrons». It is clear that the Brookhaven facility [7] can provide such a source.

We have, therefore, calculated the photodetachment cross-section of Ps^- from the break-up threshold

$$h\nu + Ps^- \rightarrow e^- + Ps(1s) \tag{3}$$

to just below the $n=2$ threshold

$$h\nu + Ps^- \rightarrow e^- + Ps(n=2), \tag{4}$$

using very accurate variational wave functions for both the initial and the final state.

Previous calculations of (3) have been reported by us [8] and by BĀTHIA and DRACHMAN [9, 10]. BĀTHIA and DRACHMAN used the Ohmura approximation to an accurate ground-state function and a plane wave for the ejected electron, while we used a simple two-parameter bound state [11] together with a plane wave, and both estimates gave a maximum cross-section of about $8 \cdot 10^{-17}$ cm^2 at a wave-length near $2 \cdot 10^4$ Å.

The present letter uses the bound-state function previously reported in our calculation of s-wave scattering [12] which will not be repeated here. The photodetachment cross-section may be written

$$\mathscr{A}_\lambda(\mathrm{V}) = \frac{2k\alpha a_0^2}{9\omega} |\langle \Psi_\mathrm{f} | Q_\mathrm{V} | \Psi_\mathrm{i} \rangle|^2 \tag{5}$$

in the velocity formulation and

$$\mathscr{A}_\lambda(\mathrm{L}) = 2/9 k\omega\alpha a_0^2 |\langle \Psi_\mathrm{f} | Q_\mathrm{L} | \Psi_\mathrm{i} \rangle|^2 \tag{6}$$

in the length formulation, in a usual notation; where α is the fine-structure constant, the ejected electron has energy

$$E = (\omega - E_\mathrm{b}) = \tfrac{3}{2} k^2 \text{ Ryd},$$

where k is its wave number. The transition operators are

$$Q_\mathrm{V} = 4\hat{\boldsymbol{k}} \cdot (\nabla_{r_1} + \nabla_{r_2}) \tag{7}$$

and

$$Q_\mathrm{L} = 2/3 \hat{\boldsymbol{k}} \cdot (\boldsymbol{r}_1 + \boldsymbol{r}_2), \tag{8}$$

where we have taken $\boldsymbol{r}_1$, $\boldsymbol{r}_2$ to be the position vectors of the electrons with respect to the positron.

Writing expressions (5) and (6) in terms of the threshold energy, the corresponding wave-length being

$$\lambda\,(\text{Å}) = \frac{911}{\frac{3}{2}(k^2 + \gamma^2)}, \tag{9}$$

where $E_\mathrm{b} = \frac{3}{2}\gamma^2$ is the binding energy of Ps^- in rydbergs,

$$\mathscr{A}_\lambda(\mathrm{V}) = 3.0274 \cdot 10^{-20} \text{ cm}^2 \frac{k}{(\gamma^2 + k^2)} |M_\mathrm{V}|^2, \tag{10}$$

$$\mathscr{A}_\lambda(\mathrm{L}) = 6.8115 \cdot 10^{-20} \text{ cm}^2 k(\gamma^2 + k^2) |M_\mathrm{L}|^2, \tag{11}$$

where M_V and M_L are the matrix elements of Q_V and Q_L, respectively.

The transition is an allowed dipole transition

$$h\nu + Ps^- ((1s)^2\, {}^1S_0^e) \rightarrow Ps^- (1s\, kp\, {}^1P_0^0), \tag{12}$$

hence only the ^1P wave of the final state is required. This was obtained using the form

$$\begin{aligned}\Psi(k^1P) = \\ = \Psi(\boldsymbol{r}_1, \boldsymbol{r}_2, \boldsymbol{r}_3) = (1 + P_{12}) \left\{ \frac{k^{\frac{1}{2}}}{\sqrt{2}}\, \varphi_{Ps}(\boldsymbol{r}_2)\, Y_{10}(\hat{\boldsymbol{\rho}}) [j_1(k\rho) - \operatorname{tg}\delta_1 n_1(k\rho)][1 - \exp[-\mu\rho]^n] \right\} + \\ + \frac{1}{\sqrt{2}}\, [Y_{10}(\hat{\boldsymbol{\rho}})\rho + Y_{10}(\hat{\boldsymbol{\rho}}')\rho'] \sum_i c_i \exp[-ar_3 - bs] s^{k_i} t^{l_i} r_3^{m_i} + \\ + \frac{1}{\sqrt{2}} [Y_{10}(\hat{\boldsymbol{\rho}})\rho - Y_{10}(\hat{\boldsymbol{\rho}}')\rho'] \sum_j d_j \exp[-ar_3 - bs] s^{k_j} t^{l_j} r_3^{m_j}\end{aligned} \tag{13}$$

with l_i even and l_j odd, and

$$s = r_1 + r_2, \quad t = r_1 - r_2, \quad k_1 + l_1 + m_i \leqslant 9; \tag{14}$$

in a variational calculation, $\boldsymbol{\rho}$ and $\boldsymbol{\rho}'$ being the position vectors of the ejected electron with respect to the centre of mass of the residual Ps in the direct and exchange cases, respectively. We took $n = 5$ and varied μ, a and b independently, the linear parameters c_i, d_j being varied simultaneously. Thus we do not achieve a global maximum on $\operatorname{tg}\delta_1$.

For small values of k ($k \leqslant 0.10$) the convergence of our locally optimized Kohn and inverse Kohn results was not entirely satisfactory, and will be discussed in detail elsewhere [13].

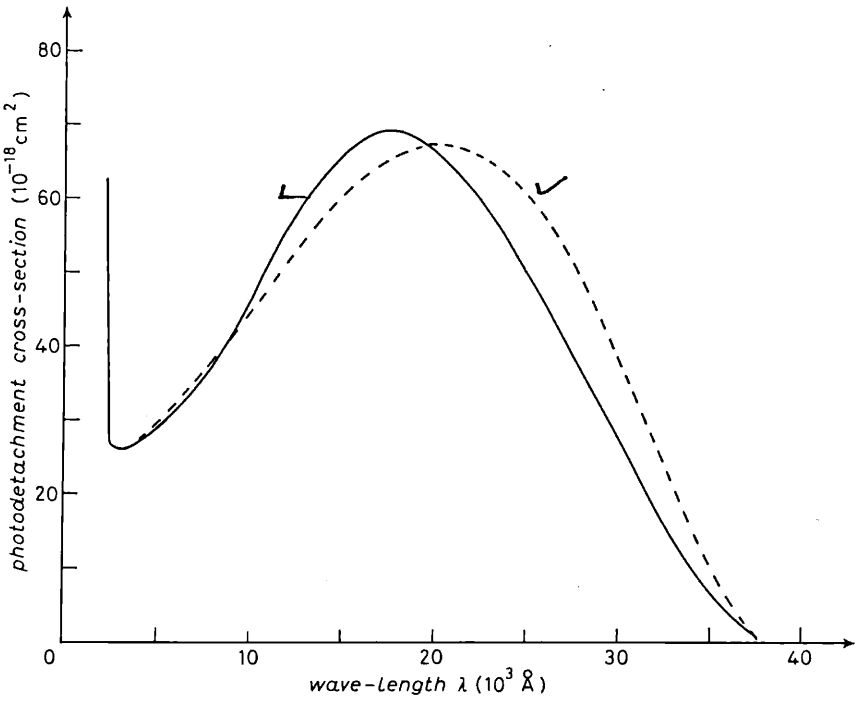

Fig. 1. – The photodetachment cross-section of Ps^- (in units of 10^{-18} cm^2) in length (L) and velocity (V) forms.

For $0.10 < k \leqslant 0.50$, agreement between Kohn and inverse Kohn was to better than 1 part in 10^4 in $\mathrm{tg}\,\delta_1$. For the photodetachment cross-section we need the full expression (11) so use the direct estimate of $\mathrm{tg}\,\delta_1$ consistent with (11) rather than either Kohn or inverse Kohn result.

We find $\delta_1(k)$ first increases through small positive values from threshold and goes negative and is smoothly decreasing to a minimum of -0.70 at $k = 0.484$ after which it increases rapidly to a value close to -0.68 at the $n = 2$ threshold, $k = 0.5$. A full discussion will be given elsewhere, but we remark here that except for $k > 0.484$ the results are in close accord with those of a one-channel treatment. The rapid rise of $\delta_1(k)$ near $k = 0.5$ might be due to a ^1P resonance expected (by analogy to atomic hydrogen) to lie at $k = 0.4994$ a.u., though it appears too broad for that, or to a cusplike behaviour associated with the $n = 2$ threshold. Calculations including $n = 2$ states are at an early stage.

The consequent photodetachment cross-section is displayed in fig. 1, in both length and velocity forms. The sum rule

$$S_{-1} = \frac{1}{2\pi^2 \alpha a_0^2} \int_0^{\lambda_0} a_\lambda \, \mathrm{d}\lambda/\lambda = 8/27 \, \langle (\underline{r}_1 + \underline{r}_2)^2 \rangle \tag{15}$$

(expectation values being taken with respect to the ground state) is well satisfied considering that for $\lambda < \lambda(n = 2)$ we used Bhatia and Drachman's simple closed form expression for $\mathscr{A}_\lambda$.

	S_{-1}		
	LHS (velocity)	LHS (length)	RHS
Our results	29.9	28.9	29.3
Bhatia and Drachman	31.7	31.7	29.78

TABLE I. – *The photodetachment cross-section of* Ps^- *at selected wave-lengths (in units of* 10^{-18} cm^2).

$\lambda(10^3$ Å)	$\mathscr{A}_\lambda$ (V)	$\mathscr{A}_\lambda$ (L)
35	11.11	6.15
30	39.13	26.45
25	60.62	50.11
22.5	66.07	60.08
20	67.48	66.86
19	66.95	68.36
18	65.84	69.04
17	64.23	68.85
15	59.66	65.73
10	44.35	45.65
5.0	29.71	29.09
2.5	26.27	26.49
2.4	28.09	28.23
2.3	39.99	40.02
2.283	62.47	62.33

The Ps ($n = 2$) threshold is at 2283 Å.

Selected values of the cross-section are given in table I. Agreement between length and velocity forms is good, but not yet entirely satisfactory, especially near threshold, the differences reflecting the inadequate convergence of $\mathrm{tg}\,\delta_1(k)$ for $k \leqslant 0.1$ a.u. The marked peak in the cross-section just below the $n = 2$ threshold occurs in both length and velocity forms, which agree there to better than 2 parts in 10^3. It is directly attributable to the similar behaviour of $\delta_1(k)$ and should be detectable experimentally.

* * *

We are indebted to Drs. R. DRACHMAN and A. BHATIA for helpful discussions. One of us (SW) is supported by a SERC studentship. The calculations were carried out on the ULCC CRAY-1S.

REFERENCES

[1] J. A. WHEELER: *Ann. N.Y. Acad. Sci,*, **48**, 219 (1946).
[2] Y. K. HO: *J. Phys. B*, **16**, 1503 (1983).
[3] A. K. BHATIA and R. DRACHMANN: *Phys. Rev. A*, **28**, 2523 (1983).
[4] A. P. MILLS jr.: *Phys. Rev. Lett.*, **46**, 717 (1981).
[5] A. P. MILLS jr.: *Phys. Rev. Lett.* **50**, 671 (1983).
[6] M. R. C. MCDOWELL: to be published in *Positrons (and electrons) in gases*, Edited by A. STEIN and W. KAUPPILA (World Scientific Publishing Co., Singapore).
[7] L. ROELLIG: Invited papers, *XIV ICPEAC Stanford*, to be published by North-Holland, Amsterdam.
[8] S. J. WARD, J. W. HUMBERSTON and M. R. C. MCDOWELL: to be published in *Positrons (and electrons) in gases*, Edited by A. STEIN and W. KUPPILLA (World Scientific Publishing Co., Singapore).
[9] A. K. BHATIA and R. J. DRACHMAN: Preprint and *Phys. Rev. A.*, in press.
[10] A. K. BHATIA and R. J. DRACHMAN: private communication.
[11] G. FERRANTE: *Phys. Rev.*, **170**, 76 (1968).
[12] S. J. WARD, J. W. HUMBERSTON and M. R. C. MCDOWELL: *J. Phys. B*, **18**, L-525 (1985).
[13] S. J. WARD, J. W. HUMBERSTON and M. R. C. MCDOWELL: in preparation for *J. Phys. B.*

Elastic scattering of electrons (or positrons) from positronium and the photodetachment of the negative positronium ion.

S.J. Ward, J.W. Humberston and M.R.C. McDowell

Mathematics Department, Royal Holloway and Bedford New College (University of London), Egham Hill, Egham, Surrey TW20 0EX, England

Department of Physics and Astronomy, University College London, Gower Street, London WC1E 6BT, England

Received 26 March 1986

Abstract. We report accurate variational calculations of the ^{1,3}S and ^{1,3}P phase shifts for elastic scattering of electrons (or positrons) by positronium up to the n=2 threshold. Higher order phase shifts are evaluated both in a static exchange model and in an adiabatic exchange model to give the total elastic, momentum transfer, ortho-para conversion and elastic differential cross sections. The positions of the minima in the elastic differential cross section are given for several values of k^2. New ^{3}P resonances are reported. The ^{1}P continuum wave function is used together with an accurate variational wave function for the ground state of Ps^- to obtain the photodetachment cross section of Ps^-, and both length and velocity results are checked by evaluating the sum-rule S_{-1}.